GREEN-FUNCTION THEORY OF CHEMISORPTION

by
Sydney G. Davison and Kenneth W. Sulston

Springer

GREEN-FUNCTION THEORY OF CHEMISORPTION

Green-Function Theory of Chemisorption

by

SYDNEY GEORGE DAVISON
University of Waterloo, ON, Canada

and

K.W. SULSTON
University of Prince Edward Island, Charlottetown, Canada

Springer

A C.I.P. Catalogue record for this book is available from the Library of Congress.

ISBN-10 1-4020-4404-6 (HB)
ISBN-13 978-1-4020-4404-5 (HB)
ISBN-10 1-4020-4405-4 (e-books)
ISBN-13 978-1-4020-4405-2 (e-books)

Published by Springer,
P.O. Box 17, 3300 AA Dordrecht, The Netherlands.

www.springer.com

Printed on acid-free paper

To our first teachers – our parents:
Sarah and Wilfrid Davison
Madalene and Ward Sulston

How can it be that mathematics, being after all a product of human thought independent of experience, is so admirably adapted to the objects of reality?

— Albert Einstein

Contents

Knowledge is one. Its division into subjects is a concession to human weakness.

— Halford J. Mackinder

Preface

Prefaces are like speeches before the curtain; they make even the most self-forgetful performers seem self-conscious.

— William Allen Neilson

The study of phenomena and processes at the phase boundaries of matter is the realm of the surface scientist. The tools of his trade are drawn from across the spectrum of the various scientific disciplines. It is therefore interesting that, in investigating the properties of such boundaries, the surfacist must transcend the interdisciplinary boundaries between the subjects themselves. In this respect, he harkens back to the days of renaissance man, when knowledge knew no boundaries, and was pursued simply for its own sake, in the spirit of enlightenment.

Chemisorption is a gas-solid interface problem, involving the interaction of a gas atom with a solid surface via a charge-transfer process, during which a chemical bond is formed. Because of its importance in such areas as catalysis and electronic-device fabrication, the subject of chemisorption is of interest to a wide range of surfacists in physics, chemistry, materials science, as well as chemical and electronic engineering. As a result, a vast literature has been created, though, despite this situation, there is a surprising scarcity of books on the subject. Moreover, those that are available tend to be experimentally oriented, such as, *Chemisorption: An Experimental Approach* (Wedler 1976). On the theoretical side, *The Chemisorption Bond* (Clark 1974) provides a good introduction, but is limited in not describing the more advanced techniques presently in use. Other treatments confine the discussion of chemisorption to chapters or sections in works of a more

general nature, for example, *Concepts in Surface Physics* (Desjonquères and Spanjaard 1993). At the advanced level, we have the *Theory of Chemisorption* (Smith 1980), which addresses a set of topics in chapters contributed by recognized authorities. Perhaps the most balanced treatise is *Selected Studies of Adsorption on Metal and Semiconductor Surfaces* (Gumhalter, Milun and Wandelt 1990), where both experimental and theoretical aspects are presented on a variety of different topics. However, the level is again for experts in the field, and lacks pedagogical detail. In contrast, the present work attempts to provide a reasonably self-contained book, to bridge the gap between the introductory and advanced texts that are currently available. In level and style, it mirrors the text *Basic Theory of Surface States* (Davison and Stęślicka 1992). Again, a knowledge of quantum mechanics (Merzbacher 1970) and solid-state theory (Kittel 1986) is assumed, since the material covered is intended for senior undergraduate and junior graduate students.

While there are a number of different theoretical approaches to the problem of chemisorption, only one is adopted here, namely, that of the *tight-binding Green-function method*, which is both powerful and versatile. Moreover, such an approach lends itself well to the pedagogically desirable modellistic treatment of the subject matter in question. Indeed, even with the present-day capabilities of computer simulation and numerical calculation, there is still a need for the model-minded theorists to provide the clarity and insight afforded by analytical solutions of model systems. For, as W. Kohn (1999) stated in his Nobel Prize lecture, "In technological applications, surfaces are generally very imperfect, both structurally and chemically. Nevertheless, concepts developed by idealized surface science have been very important guides for practical applications." A further advantage of the single-method restriction is that it enables attention to be focused on the step-by-step details by which the calculations are performed. In this way, students learn the procedure in a hands-on fashion, and thereby gain confidence to read the current literature on their own. Of course, such a scheme is nothing new, for long ago Aristotle said, "What we have to learn to do, we learn by doing."

Turning to the chapters themselves, the book opens with a brief biographical sketch of George Green, whose famous functions play such a crucial role in exploring the charge-transfer process involved in chemisorption. Chapter 1 provides a straightforward introduction into the research area, by describing the simple molecular-orbital picture, which invokes the tight-binding approximation in explaining the electron localization involved in the formation of the chemisorption states. The foundation of the Green-function method is laid in Chapters 2 and 3, where the aid of projection operators is enlisted in delineating the spaces defining the Green function, whose poles and imaginary part provide the system's eigenenergies and density of states, respectively, within the context of the Dyson equation. The next chapter discusses the very important issue of electron-electron interaction on the adatom, as addressed in the Anderson-Newns-Grimley (ANG) model, and which manifests itself in the self-consistent calculation of the chemisorption energy and adatom charge transfer. Having incorporated the ANG model into the Dyson-equation approach, the power and the versatility of the technique is amply demonstrated by applying it to the calculation of these same quantities in the diverse cases of chemisorption on a variety of widely different substrates. Since the vast majority of chemicals are produced by means of supported catalysts, Chapter 5 deals with the case of metalized semiconductor substrates, which greatly reduce the production costs involved with purely metallic substrates. The success of the coherent-potential approximation, in describing the electronic properties of disordered binary alloys, opens the door to the treatment of chemisorption on these substrates in Chapter 6. Despite its long history, the Stark-ladder effect has only recently received a satisfactory Green-function formulation, which enables the problem of chemisorption on electrified substrates to be investigated in Chapter 7. In contrast to the preceding chapters, Chapter 8 tackles the problem of *two* atoms interacting with a substrate, where the conduction electrons mediate an indirect interaction between the adatoms. The book closes with an extensive set of Appendices, whose additional explanatory details provide further insight into the matters under consideration.

Over the years, we have greatly benefitted from our collaborations with numerous scientists, many of whom have become our good friends, such as, A.T. Amos, S.M. Bose, B.L. Burrows, R.A. English, F. Flores, E. Ilisca, J. Koutecký, W.K. Liu, Z.L. Mišković, D.W. Schrantz and H. Ueba. For the beautifully prepared manuscript, our grateful thanks and admiration go to Ann Puncher. We also thank Karen Critchley for her skillful rendition of our figures. Throughout the course of this work, we were sustained by the constant support and encouragement of Prudence Davison.

Waterloo S.G. Davison
Charlottetown K.W. Sulston
June 2004

ACRONYMS

In science, each new point of view calls forth a revolution in nomenclature.

— Friedrich Engels

ANG	Anderson-Newns-Grimley
AO	atomic orbital
ATA	average t-matrix approximation
BF	Bessel function
CB	conduction band
CF	continued fraction
CNDO	complete neglect of differential overlap
CPA	coherent-potential approximation
DBA	disordered binary alloy
DOS	density of states
FL	Fermi level
GF	Green function
HFA	Hartree-Fock approximation
LDOS	local density of states
LMTO	linear muffin-tin orbital
MO	molecular orbital
NN	nearest neighbour
TBA	tight-binding approximation
VB	valence band
VCA	virtual crystal approximation
WSL	Wannier-Stark ladder

George Green (1793-1841)

Progress in science depends on new techniques, new discoveries and new ideas, probably in that order.

— Sydney Brenner

On the map of the scientific world, the city of Nottingham, England, can justly be regarded as the Mecca of mathematical physics, since not one, but two, of its great prophets hailed from that city's domain. Newton was born in the village of Woolsthorpe, a few miles beyond its eastern precincts, on December 25, 1642 – a fitting day for a Messiah of science. Some 150 years later, in the twilight of the 18th century, George Green arrived on the scene.

He was born into a baker's family on July 14, 1793. Later, his father purchased a windmill in Sneinton, then on the outskirts of Nottingham. Despite the early signs of his exceptional mathematical abilities, he received only a year or so of formal education,when he was eight years old. He then became an apprentice in his father's mill, which he eventually inherited. Though he never married, Green had a family of seven children with his partner, Jane Smith (Cannell 1993).

In those moments, when he could escape from the grind of daily life, having access to the facilities of the Nottingham Subscription Library in Bromley House enabled him to become acquainted with the advanced mathematical concepts embodied in the works of the French school of analytical physics, which was only then being established at Cambridge. In 1828, at the age of thirty-five, he published by subscription the paper that immortalized his name. It was entitled, *An Essay on the Application of Mathematical*

Analysis to the Theories of Electricity and Magnetism, and contained the techniques we now call "Green functions". Being an obscure publication, the article attracted little or no attention, and Green decided he should leave mathematics.

Fortunately, however, one of his subscribers, Sir Edward F. Bromhead, Baronet of Thurlby Hall in Lincolnshire, became his mentor and convinced him to continue his studies. On the death of his father, in 1829, he became comparatively wealthy. Four years later, he sold the business and entered Granville and Caius College, Cambridge, Bromhead's old alma mater. He graduated as the fourth Wrangler in the Tripos of 1837. During his two years of graduate work, he published six more papers on mathematical physics, and was elected a Fellow of Caius College. Sadly, his health now began to fail and he returned to Sneinton, where death overtook him in 1841.

It was only four years later that Lord Kelvin (née William Thomson) came across the Essay. He kindly arranged for it to be reprinted in *Crelle's Journal*, and enthusiastically promoted Green's work in Britain and Europe. The enormous impact of Green's legacy on today's world of science has been clearly assessed by Freeman Dyson (1993).

In light of the lack of recognition he received during his lifetime, the 1993 celebration of the 200th anniversary of his birth afforded a belated opportunity to pay tribute to the genius of this self-taught man. London rendered him due homage with the dedication of a memorial plaque in Westminster Abbey, Cambridge with a stained-glass window in the Granville and Caius College Hall, and Nottingham with special ceremonies at the restored Green's windmill and Science Centre in Sneinton.

Chapter 1

Molecular-Orbital Picture

Order and simplification are the first steps toward the mastery of a subject – the actual enemy is the unknown.

— Thomas Mann

Adsorption is a process whereby an atom, interacting with a solid, *adheres* to its surface to become an adsorbed atom, or, more briefly, an *adatom*. In the language of adsorption, we sometimes call the adatoms the *adsorbate* and the solid the *adsorbent* (or *substrate*). An approximate measure of the *strength* of the adsorbate-adsorbent interaction is provided by the magnitude of the *heat of adsorption* (ΔH). For low $\Delta H \sim 5$ kcal/mole (~ 0.2 eV), say, physical adsorption (*physisorption*) is said to occur, while, for high $\Delta H \sim 50$ kcal/mole (~ 2 eV), say, chemical adsorption (*chemisorption*) arises. The former (latter) is a *weak* (*strong*) interaction involving *no* (*some*) electron transfer. Henceforth, our task will be to study the properties and nature of the chemical bond, formed by the electron charge-transfer process, between the adatom and the substrate.

Although the first quantal studies of atom-surface interactions occurred

in the 1930s (e.g., see Lennard-Jones 1937, Goodwin 1939a), because of World-War II, nearly two decades had to elapse before theoretical surfacists turned their attention to chemisorption again in the latter-half of the 1950s (e.g., see Koutecký 1956, 1957; Grimley 1958). The initial progress, in the post-war years, was reviewed by Grimley (1960), who adopted the straightforward *molecular orbital* (MO)[1] approach, which had proved so successful in discussing atomic binding in molecules. It is therefore appropriate for us to follow in Grimley's footsteps and 'paint' the simplest picture of chemisorption with the MO 'brush'. In doing so, we pave the way for the introduction and development of the Green function theory, in the following chapters.

1.1 Adatom-Substrate Interaction

To find the electronic states of the system, we are interested in solving the Schrödinger equation and obtaining the wave functions (MO's) and the energy levels for the *entire* system, in this case, the adatom and substrate. We model the latter by a chain of identical atoms numbered $0, 1, \ldots, N-1$ (*large*) and denote the former by λ. With each atom, we associate an *atomic orbital* (AO), $\phi(r, m)$, so that $m = \lambda$ is one set and $m = 0, 1, \ldots, N-1$ is the other set, giving a total of $(N+1)$ 1-electron AO's in the chemisorption system (Fig. 1.1).

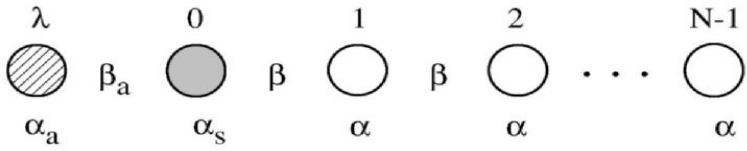

Fig. 1.1. Chemisorption model, where $\alpha_a(\beta_a)$ is adatom site (bond) energy, $\alpha_s(\alpha)$ surface (chain) atom site energy and β chain bond energy.

In MO theory (Coulson 1961), we assume that the wave function of the kth state of the system may be written as a linear combination of the AO's, i.e.,

$$\psi_k(r) = \sum_m c_k(m)\phi(r, m)\,, \tag{1.1}$$

which must satisfy the 1-electron Schrödinger equation

$$H\psi_k(r) = E_k\psi_k(r)\,, \tag{1.2}$$

[1]The name *molecular orbital* was coined by Robert S. Mulliken.

H being the *effective* 1-electron Hamiltonian operator and E_k the energy of the kth state. Inserting (1.1) in (1.2) leads to

$$\sum_m H(n,m)c_k(m) = E_k \sum_m S(n,m)c_k(m)\,, \tag{1.3}$$

where

$$S(n,m) = \int \phi^*(r,n)\phi(r,m)dr \tag{1.4}$$

is the *overlap matrix* between the nth and mth AO's and

$$H(n,m) = \int \phi^*(r,n)H\phi(r,m)dr\,. \tag{1.5}$$

If the AO's are taken to be *orthonormal*, then (1.4) gives[2]

$$S(n,m) = \delta_{n,m}\,, \tag{1.6}$$

which means that overlap is *neglected* and (1.3) reduces to

$$\sum_m H(n,m)c_k(m) = E_k c_k(n) \tag{1.7}$$

for the *wave-function coefficients* $c_k(m)$ and the energies E_k. In order to make (1.7) tractable, we introduce the *tight-binding approximation* (TBA) (Davison and Stęślicka 1996), namely,

$$H(n,m) = \alpha\delta_{n,m} + \beta(\delta_{n+1,m} + \delta_{n-1,m}), \quad m \neq 0, \lambda\,, \tag{1.8}$$

$\alpha\,(\beta)$ being the *site (bond) energy*.[3] Equation (1.7) may now be written as

$$(E_k - \alpha)c_k(n) = \beta[c_k(n+1) + c_k(n-1)], \quad n \neq 0,\ \lambda\,, \tag{1.9}$$

i.e., the Schrödinger equation has been replaced by a *second-order difference equation* with constant coefficients. Because of their different electronic environments, to those of the chain atoms, the adsorbed and surface atoms at $n = \lambda$ and $n = 0$, respectively, are characterized by the different site energies α_a and α_s (Fig. 1.1). Similarly, the bond between them is

[2]The *Kronecker delta-function* $\delta_{n,m} = 1(0)$ for $n = m(n \neq m)$.

[3]Also called the *Coulomb (resonance) integral*.

denoted by β_a instead of β. For these atoms, (1.9) yields the *boundary conditions* for $m = 0$ and λ, viz.,

$$(E_k - \alpha_s)c_k(0) = \beta c_k(1) + \beta_a c_k(\lambda)\,, \tag{1.10}$$

$$(E_k - \alpha_a)c_k(\lambda) = \beta_a c_k(0)\,. \tag{1.11}$$

In addition, we require the wave function to vanish at the chain end ($m = N$), so we put

$$c_k(N) = 0\,. \tag{1.12}$$

Since N is large, this condition does not interfere with those near $m = 0$.

Having completely specified the chemisorption problem, let us now solve (1.9) subject to the above boundary conditions. Utilizing the translational symmetry of a periodic atomic chain, we define the *ladder operators*, $L_\pm$, via

$$L_\pm c_k(n) = c_k(n \pm 1)\,, \tag{1.13}$$

noting that

$$L_+ L_- = 1\,. \tag{1.14}$$

Hence, (1.9) may be expressed in the form

$$(E_k - \alpha)c_k(n) = \beta(L_+ + L_-)c_k(n)\,,$$

which by (1.14) gives

$$L_\pm^2 - 2X_k L_\pm + 1 = 0\,, \tag{1.15}$$

with

$$X_k = (E_k - \alpha)/2\beta \tag{1.16}$$

being the *dimensionless reduced energy*. Solving (1.15), we find

$$L_\pm = X_k \pm (X_k^2 - 1)^{\frac{1}{2}}\,. \tag{1.17}$$

On introducing the unknown parameter θ_k, by setting

$$X_k = \cos\theta_k\,, \tag{1.18}$$

we obtain

$$L_\pm = e^{\pm i\theta_k}\,, \tag{1.19}$$

so that (1.13) becomes

$$c_k(n \pm 1) = e^{\pm i\theta_k} c_k(n)\,, \tag{1.20}$$

where the θ_k-values are determined from the boundary conditions. Repeated operations of $L_\pm$ on $c_k(n)$ leads to the well-known *Bloch theorem* (1928), i.e.,

$$c_k(n \pm \ell) = L_\pm^\ell c_k(n) = e^{\pm i\ell\theta_k} c_k(n)\,, \tag{1.21}$$

by (1.19). Equation (1.21) suggests that we write the *general solution* of (1.9) in the form

$$c_k(n) = (ae^{in\theta_k} + be^{-in\theta_k})c_k(0)$$

or as

$$c_k(n) = A\cos n\theta_k + B\sin n\theta_k\,. \tag{1.22}$$

Imposing (1.12) on (1.22) leads to

$$c_k(n) = A\frac{\sin(N-n)\theta_k}{\sin N\theta_k}, \quad n \neq \lambda\,. \tag{1.23}$$

With the aid of (1.16) and (1.18), inserting (1.23) in (1.11) gives

$$c_k(\lambda) = \eta A(z_a + 2\cos\theta_k)^{-1}\,, \tag{1.24}$$

where

$$\eta = \beta_a/\beta\,, \quad z_a = (\alpha - \alpha_a)/\beta \tag{1.25}$$

are the *dimensionless reduced chemisorption parameters* for the adbond and adatom, respectively. After some manipulation, (1.16), (1.18), (1.23) and (1.24) in (1.10) lead to the *eigenvalue equation* for θ_k, namely,

$$(z_a + 2\cos\theta_k)\left[z_s + \frac{\sin(N+1)\theta_k}{\sin N\theta_k}\right] = \eta^2\,, \tag{1.26}$$

where

$$z_s = (\alpha - \alpha_s)/\beta, \tag{1.27}$$

is the *dimensionless reduced surface parameter*.

For $\beta_a = 0\,(\eta = 0)$, the adatom is *detached* from the surface atom (Fig. 1.1), and θ_k is given by the zeros of the two terms in brackets on the left-hand side of (1.26). The first (second) term represents the single (N) state(s) contributed by the adatom (substrate) for a *total* of $(N+1)$ states. The graphical solution of the [term] is displayed in Fig. 1.2 for several values of z_s (Goodwin 1939b, Davison and Stęślicka 1996). Asymptotes occur at

$\theta_k = k\pi/N \quad (k = 1, 2, \ldots, N)$, while the intercepts on the ordinate axes at $\theta_k = 0$ and π are $\pm(1 + N^{-1})$, which, for $N \to \infty$, become ± 1. Thus, for any horizontal line in the range $\mid z_s \mid \leq 1$, there are N real roots, giving N *real* values of θ_k.

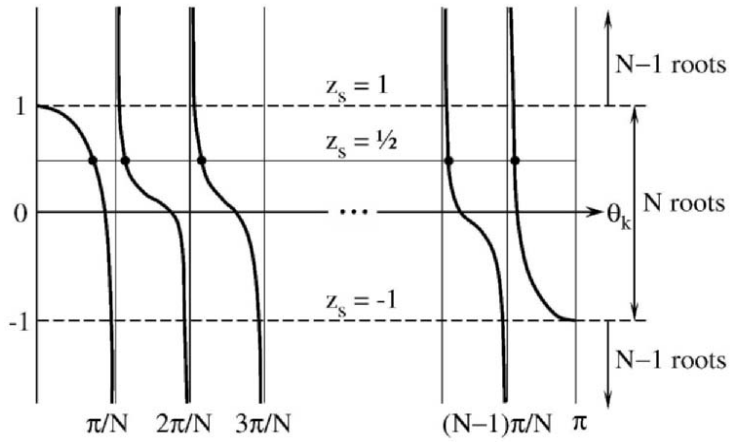

Fig. 1.2. Graphical solutions of $-z_s = \sin(N+1)\theta_k / \sin N\theta_k$.

These real solutions have reduced energies (1.18) lying in the *bulk band* $\mid X_k \mid \leq 1$ (Fig. 1.3), with *delocalized* periodic wave functions (1.23) spread along the chain. When $z_s > 1 (z_s < -1)$, a real root *disappears* at $\theta_k = 0 (\theta_k = \pi)$, and only $(N-1)$ real solutions remain. To account for these lost solutions, it is necessary to take θ_k *complex* and write

$$\theta_k^c = \xi_k + i\mu_k, \quad \mu_k \,\text{real} > 0\,, \tag{1.28}$$

in which case, (1.18) becomes

$$X_k = \cos\xi_k \cosh\mu_k - i \sin\xi_k \sinh\,\mu_k\,. \tag{1.29}$$

However, X_k must *always* be real, so the imaginary part in (1.29) must be zero. Since $\mu_k > 0, \sinh\mu_k \neq 0$, so $\sin\xi_k = 0$, which means

$$\xi_k = j\pi; \quad j = 0, 1, \ldots, \tag{1.30}$$

where, to avoid repeated solutions, only $j = 0$ and 1 are required, so that the two missing solutions are given by

$$\theta_k^c = i\mu_k \quad \text{and} \quad \pi + i\mu_k\,. \tag{1.31}$$

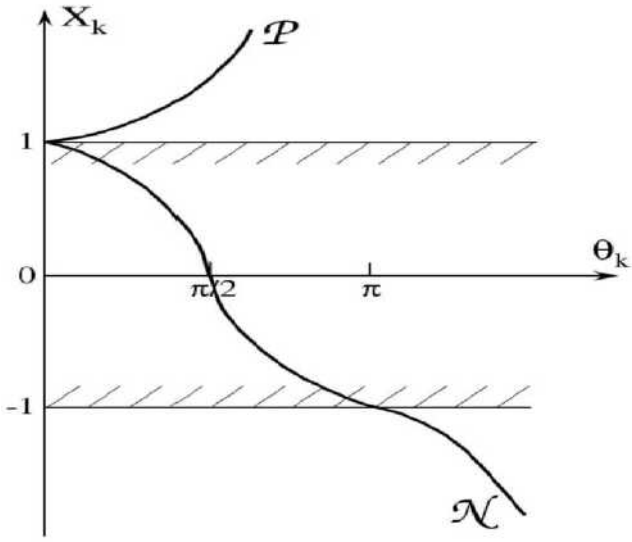

Fig. 1.3. Reduced-energy spectrum showing in-band variation of $X(\theta_k) = \cos\theta_k$ between band edges at $X_k = \pm 1$ for $|z_s| \leq 1$ and θ_k real. $\mathcal{P} - (\mathcal{N}-)$ localized states appear above (below) band for θ_k complex and $|z_s| > 1$.

Returning to (1.26), with $\beta_a \neq 0 (\eta \neq 0)$, we see that it has *at least* $(N-1)$ real roots, whose corresponding wave functions are delocalized and have reduced energies in the bulk band (1.18) of width $\Delta X_k = 2$. The remaining two roots may both be real, so that they too lie in the band, and the system supports only delocalized states. If, however, *one* or *both* of the remaining roots have θ_k-values of the form (1.31), then a new situation arises, which requires further analysis. Inserting (1.31) in (1.18) gives

$$X_k^{\pm} = \pm \cosh \mu_k \gtrless \pm 1 \,, \tag{1.32}$$

which shows that $X_k^+ (X_k^-)$ is *positive* (*negative*) and lies *above* (*below*) the bulk-band edge at $X_k = 1 (X_k = -1)$. Since $X_k > 0 (X_k < 0)$ for $\theta_k^c = i\mu_k (\theta_k^c = \pi + i\mu_k)$, a *$\mathcal{P}$-state* (*$\mathcal{N}$-state*) is said to occur at this θ_k-value, so that $\mathrm{sgn}(X_k)$ provides a useful means of classifying these states. For *N large*, we note that

$$\frac{\sin(N \pm n)\theta_k^c}{\sin N\theta_k^c} \to e^{\mp in\theta_k^c} \,, \tag{1.33}$$

in which case, (1.23) and (1.26) become

$$c_k(n) = Ae^{in\theta_k^c}, \quad n \neq \lambda\,, \tag{1.34}$$

and

$$(z_a + 2\cos\theta_k^c)(z_s + e^{-i\theta_k^c}) = \eta^2\,. \tag{1.35}$$

1.1.1 $\mathcal{P}$-states

When $\theta_k^c = i\mu_k$, the chemisorption system has:

$$X_k = \cosh\mu_k\,, \tag{1.36}$$

$$c_k(n) = Ae^{-n\mu_k}\,, \quad n \neq \lambda\,, \tag{1.37}$$

$$c_k(\lambda) = \eta A(z_a + 2\cosh\mu_k)^{-1}\,, \tag{1.38}$$

$$(z_a + 2\cosh\mu_k)(z_s + e^{\mu_k}) = \eta^2\,, \tag{1.39}$$

by (1.32), (1.34), (1.24) and (1.35), respectively. Equation (1.37) shows that a $\mathcal{P}$-state wave function is exponentially *damped* into the substrate, thus *localizing* the electron near the surface. The wave function of the chemisorption state localized at the adatom is given in (1.38). The μ_k-values for these $\mathcal{P}$-states are determined by the eigenvalue equation (1.39), and their energies X_k (1.36) lie *above* the energy band of the delocalized states. In particular, for $z_s = -2$, $z_a = -4$ and $\eta^2 = 1$, (1.39) reduces to

$$(e^{\mu_k} - 4)(e^{\mu_k} - 2) = 2e^{-\mu_k}\,. \tag{1.40}$$

Plotting the parabola (broken curve) on the left of (1.40) with the rectangular hyperbola (solid curve) on the right (Fig. 1.4) shows that this cubic equation in e^{μ_k} has three roots given by the intersections p_1, p_2 and p_3. However, since $e^{\mu_k} \not> 1$ at p_1, this root is rejected, so (1.40) has *two* real solutions, p_2 and p_3, whose corresponding μ_k-values give rise to *two* $\mathcal{P}$-states.

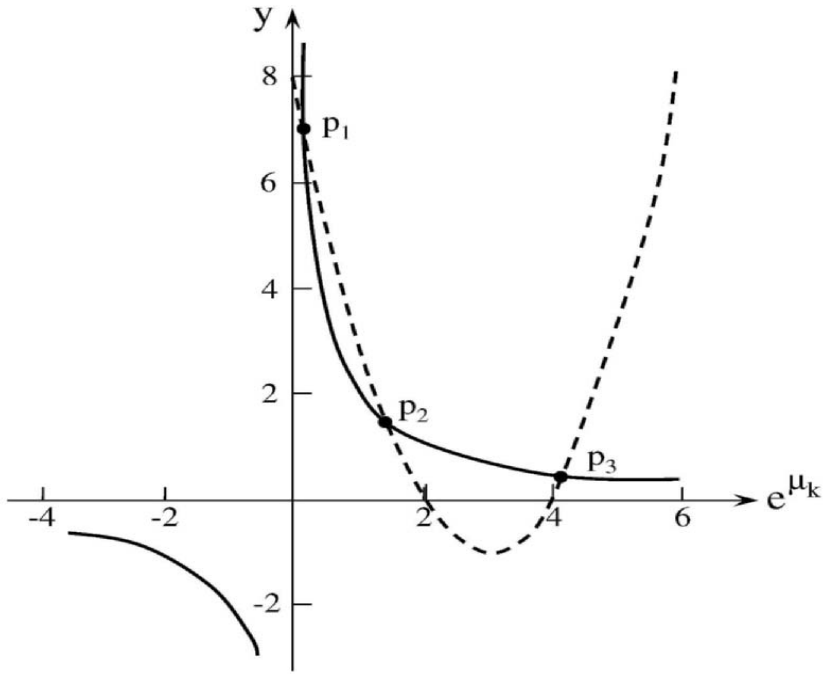

Fig. 1.4. Graphical solutions of (1.40).

1.1.2 $\mathcal{N}$-states

Here, $\theta_k^c = \pi + i\mu_k$, and the chemisorption equations are:

$$X_k = -\cosh\mu_k\,, \tag{1.41}$$

$$c_k(n) = A(-1)^n e^{-n\mu_k}, \quad n \neq \lambda, \tag{1.42}$$

$$c_k(\lambda) = \eta A(z_a - 2\cosh\mu_k)^{-1}, \tag{1.43}$$

$$(z_a - 2\cosh\mu_k)(z_s - e^{\mu_k}) = \eta^2, \tag{1.44}$$

via the same equations as in §1.1.1. We now see that any $\mathcal{N}$-state wave function (1.42) is a damped *oscillatory* one, decaying into the substrate, and has an energy X_k (1.41) *below* the bulk-state band. The $\mathcal{N}$-state μ_k-values are provided by (1.44).

As the μ_k-values increase, the energy levels of the $\mathcal{P}$- and $\mathcal{N}$-states move further from the band edges, while the localization of their wave functions becomes more concentrated.

Since the presence of chemisorption ($\mathcal{P}$ and $\mathcal{N}$) states gives rise to the formation of localized covalent bonds between the adatom and substrate, we are interested in how the *occurrence* of localized states is governed by the values of the parameters z_a, z_s and η, which define the adatom-substrate interaction. Localized states exist, if one or both of (1.39) and (1.44) have real roots μ_k, which, since $\cosh\mu_k \geq 1$ and $e^{\mu_k} \geq 1$, exist for a given η in regions of the $z_a z_s$-plane depicted by the *two hyperbolas*

$$(z_a \pm 2)(z_s \pm 1) = \eta^2 \,. \tag{1.45}$$

The graphs of (1.45) are drawn in Fig. 1.5 for $\eta^2 = 1$. As can be seen, localized $\mathcal{P}$- and $\mathcal{N}$-states occur in the six regions indicated, where $\mathcal{P}^2$ denotes two $\mathcal{P}$-states, $\mathcal{P}\mathcal{N}$ means one $\mathcal{P}$-state and one $\mathcal{N}$-state, etc. The *shaded area* represents the region where there are *no* localized states, i.e., only delocalized bulk states exist, so the effect of the adatom is to introduce an *extra* delocalized state into the band, and any adatom-chain binding is achieved *without* the formation of a *localized* bond. The area of this *forbidden region* decreases as η^2 increases, and is only present if $\eta^2 < 2$, i.e., the intersection points A and B coalesce as $\eta^2 \to 2$. Conversely, as $\eta \to 0$, the curves merge with their asymptotes, $z_a = \pm 2$, $z_s = \pm 1$, and the shaded region attains its maximum size. Figure 1.5 is reminiscent of a *phase diagram* of alloy composition in that the composition of states, in the chemisorption system, varies as one crosses the phase boundary curves (1.45). For example, when the point (z_a, z_s), lying in the shaded area, moves radially outwards, $\mathcal{P}$- and/or $\mathcal{N}$-states *emerge* from the *sea* of $(N+1)$ delocalized bulk states, depleting their number accordingly.

In the present model, a maximum of two localized states arises, which depends on the initial assumptions that only one adatom orbital interacts

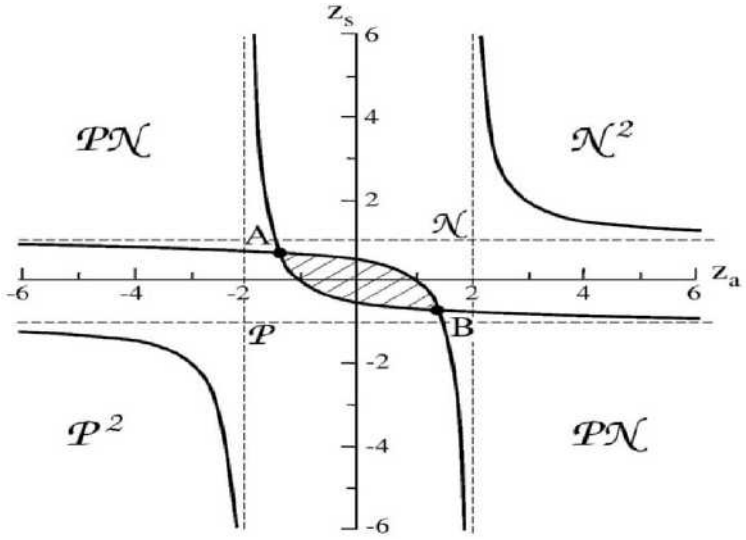

Fig. 1.5. Localized states existence regions for $\eta^2 = 1$. Reprinted from Grimley (1960) with permission from Elsevier.

with only one band of the substrate's orbitals and that the adatom perturbs the substrate only at its first atom. If the perturbation is extended further into the substrate, by modifying the site energies on its first and second atoms, then a maximum of three localized states appear. The generalization of this situation was discussed by Koutecký (1957) and Grimley (1958).

The above 1-dimensional model may be extended to 3-dimensions, in a straightforward manner, and yields a substrate whose surface is *completely covered* by adatoms. The TBA again leads to a difference equation and boundary conditions which can be solved directly (Grimley 1960). We do not intend to discuss the 3-dimensional case here and, instead, direct the reader to the *loc. sit.* articles. However, in passing, we note that, even when there is no *direct* interaction between the atoms *in* the adlayer, an important *indirect* interaction occurs between them *via the substrate* by a delocalization of the bonding electrons in directions parallel to the surface (Koutecký 1957, Grimley 1960). This topic is discussed in Chapter 8.

Before leaving this section, we should also mention that the location of the $\mathcal{P}$- and $\mathcal{N}$-states, relative to the bulk band, depends on the *sign* of the bond energy β. If the AO's in the substrate are of s-(p-)symmetry, then $\beta < 0 (\beta > 0)$ and the $\mathcal{P}$-($\mathcal{N}$-) states lie *below* the bulk s-(p-) band and are

called *bonding* states, while the $\mathcal{N}$-($\mathcal{P}$-) states *above* the band are termed *antibonding* states. Comparing (1.37) with (1.42) shows that the presence of the $(-1)^n$ factor in the latter gives rise to *nodes* between successive substrate atoms. Thus, the wave functions for bonding states are smoother than those for their antibonding counterparts (Grimley 1960).

1.2 Adbond Character

When the combined system of adatom and substrate is in its ground state, so that the lowest energy levels are each doubly occupied with an α- and a β-spin electron, then, if two electrons are in a localized level, a *localized surface bond* will be formed. However, if the localized level is *unoccupied*, then an adbond formation will be achieved *without* localization of the bonding electrons (i.e., only *delocalized* electrons will be involved in the adbond). In the case of electron localization, the *type* of adbond is determined by the *charge order* of the adatom state, namely,

$$R = \mid c_k(\lambda) \mid^2 \left[\mid c_k(\lambda) \mid^2 + \sum_{n=0}^{N} \mid c_k(n) \mid^2 \right]^{-1} . \tag{1.46}$$

Thus, the adbond is classified according to the values of the interaction parameters z_s, z_a and η.

1.2.1 Homopolar bond

If the wave function of a localized state is such that it is *equally* likely to find the electron on the adatom as in the substrate, then a purely *homopolar* adbond exists, when the state in question is doubly occupied. It follows that

$$\mid c_k(\lambda) \mid^2 = \sum_{n=0}^{N} \mid c_k(n) \mid^2 \tag{1.47}$$

in (1.46), so $R = \frac{1}{2}$, for a homopolar state. If we take the $\mathcal{P}$-state to be bonding, so that it lies below the bulk band, then (1.37) and (1.38) in (1.47) lead to

$$\frac{1 - e^{-2(N+1)\mu_k}}{1 - e^{-2\mu_k}} = \frac{\eta^2}{(z_a + 2\cosh\mu_k)^2} ,$$

which, for large N, reduces to

$$(z_a + 2\cosh\mu_k)^2 = \eta^2(1 - e^{-2\mu_k})\,. \tag{1.48}$$

For known values of z_a and η, (1.48) determines μ_k, and hence, the energy (1.36) and wave-function coefficients (1.37) and (1.38), while (1.39) gives the corresponding z_s value.

On taking $\eta^2 = 1$, and putting

$$u = e^{\mu_k} \geq 1, \quad \mu_k \geq 0\,, \tag{1.49}$$

(1.39) and (1.48) may be written as

$$(u + z_s)(u^2 + z_a u + 1) = u\,, \tag{1.50}$$

$$(u^2 + z_a u + 1)^2 = (u^2 - 1)\,, \tag{1.51}$$

respectively. Dividing (1.51) by (1.50), and rearranging terms, yields

$$(z_a - z_s)u^2 + 2u + z_s = 0\,, \tag{1.52}$$

whose roots are

$$u = \{-1 \pm [1 - z_s(z_a - z_s)]^{\frac{1}{2}}\}/(z_a - z_s)\,. \tag{1.53}$$

From (1.52), we have

$$z_s = u(z_a u + 2)/(u^2 - 1)\,, \tag{1.54}$$

so, for *large* z_s, $u \to 1$ and $\mu_k \to 0$ by (1.49). Setting $u = 1$ in (1.53), and performing some straightforward algebra, shows that

$$(z_a - z_s)(z_a + 2) = 0\,, \tag{1.55}$$

i.e., as $\mu_k \to 0$, the *asymptotes* in the $z_s z_a$-plane are

$$z_a = z_s \quad \text{and} \quad z_a = -2\,. \tag{1.56}$$

By the same token, as μ_k increases from zero, u becomes increasingly greater than one, and (1.55) is replaced by the inequality

$$(z_a - z_s)(z_a + 2) < 0\,, \tag{1.57}$$

so that we have two possible situations, viz.,

$$-2 < z_a < z_s \,, \tag{1.58}$$

$$-2 > z_a > z_s \,. \tag{1.59}$$

In order to plot the *existence curve* for the homopolar $\mathcal{P}$-states, in the $z_a z_s$-plane, we use the following 'recipe'. We take $\eta^2 = 1$, and *choose* values of z_a, so that we can obtain the corresponding μ_k-values from (1.48). We then insert these known values of z_a and μ_k in (1.39) and obtain the required z_s-values. With this procedure, the points (z_a, z_s) trace out the curves in Fig. 1.6. As can be seen, the two branches each have the asymptotes (1.56). At the point A, the values of (z_a, z_s) satisfy (1.58), and correspond to a point in the $\mathcal{PN}$-region of Fig. 1.5. Thus, one homopolar $\mathcal{P}$-state exists, whose μ_k-value is very small, so its energy level lies just below the bottom of the bulk band. Moreover, its wave function decays slowly into the solid, giving rise to a *many-centre homopolar state*. As μ_k increases, the sample point A moves down the upper branch, the homopolar $\mathcal{P}$-state energy drops further below the band and the wave function decays more rapidly into the crystal. We now enter the $\mathcal{P}^2$-region of Fig. 1.5, when a second $\mathcal{P}$-state separates from the top of the band, with a many-centre character, but not a purely homopolar nature. Furthermore, for $\eta = 1$, its $c_k(\lambda) < 0$. Continuing the movement of A down the curve, the energy falls steadily and the wave function loses its many-centre character, eventually becoming a *two-centre* homopolar state, involving only the adatom and the crystal's surface atom to any extent. The lower branch of the curves in Fig. 1.6 resides entirely in the $\mathcal{P}^2$-region of Fig. 1.5, so two $\mathcal{P}$-states always exist. However, it is only the one with the higher energy that is purely homopolar. Although it separates from the band with a many-centre character, it becomes an essentially two-centre state for large negative values of z_s and z_a. Such a state satisfies (1.59).

1.2.2 Ionic bond

Since the existence conditions for homopolar localized states are somewhat stringent, most interaction parameters give rise to states with *ionic* character,

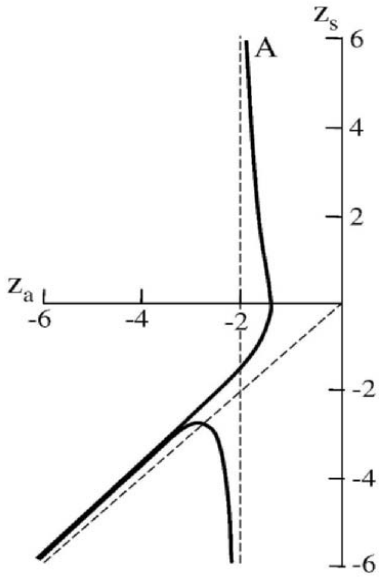

Fig. 1.6. Existence curves of homopolar $\mathcal{P}$-states for $\eta^2 = 1$. Reprinted from Grimley (1960) with permission from Elsevier.

to some degree or other, rather than to a purely homopolar state. Depending on the values $c_k(\lambda)$ and $c_k(n)$ in (1.46), R varies between zero and unity. The extreme cases are:

(a) *Cationic state*, where $c_k(\lambda) = 0$ and $\sum_n |c_k(n)|^2 \neq 0$, so that $R = 0$, and the electron is concentrated entirely in the *crystal*.

(b) *Anionic state*, here $c_k(\lambda) \neq 0$ and $\sum_n |c_k(n)|^2 = 0$, so $R = 1$, and the electron is concentrated completely on the *adatom*.

With the homopolar state $(R = \frac{1}{2})$ being the intermediate case between these two extremes, it is taken as the *reference* state, so that $R < \frac{1}{2}$ $(R > \frac{1}{2})$ indicates a *cationic* (an *anionic*) state. Returning §1.2.1, we see that the left-hand side of the inequalities (1.58) and (1.59), namely, $z_a > -2$ and $z_a < -2$, derived from (1.48), apply to $R < \frac{1}{2}$ and $R > \frac{1}{2}$, respectively, for $\mu_k = 0$. Thus, for any other value of μ_k along the curve (Fig. 1.6),

cationic (*anionic*) states exist in the region to the *right* (*left*) of the curve. Combining Figs. 1.5 and 1.6 yields Fig. 1.7, where the extra information on the ionic character of the states is now provided. For example, $A\mathcal{P}C\mathcal{N}$ means that there is an anionic $\mathcal{P}$-state and a cationic $\mathcal{N}$-state, $A\mathcal{P}C\mathcal{P}$ that there is an anionic $\mathcal{P}$-state and a cationic $\mathcal{P}$-state, etc. If $\mathcal{P}$-states are bonding ($\beta < 0$), then the state written first has the lower energy.

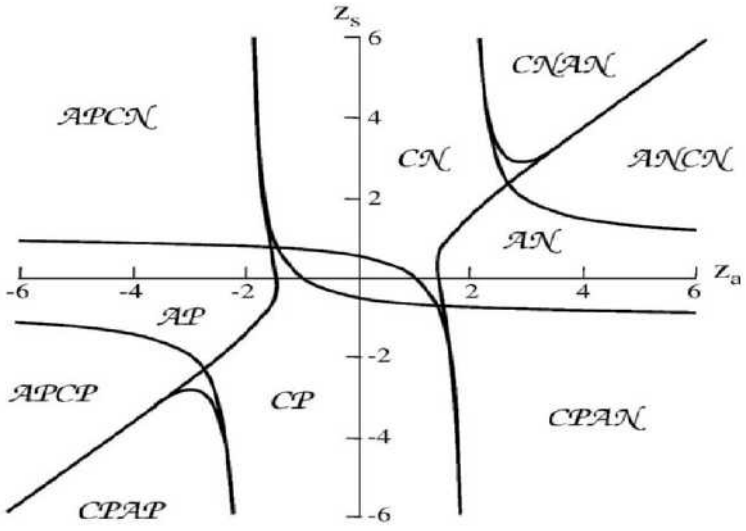

Fig. 1.7. Mapping of anionic (A) and cationic (C) states in $z_a z_s$-plane for $\eta^2 = 1$. Reprinted from Grimley (1960) with permission from Elsevier.

1.2.3 Metallic-like bond

If the point (z_a, z_s) lies in the forbidden region of Fig. 1.5, then the adatom-substrate interaction results in *no* localized states being formed. Here, adbonding occurs because the presence of the adatom changes the boundary conditions at the *free* surface of the solid, in such a way, as to give rise to a general *lowering* of the energies of the electrons in the system. The electrons are now *all* delocalized, so that each one contributes to the creation of the adbond. Such a situation is reminiscent of binding in metals, so, for this reason, such adbonds are termed *metallic-like*.

The change in the *total* electronic energy, due to the interaction of the adatom with the substrate, is called the *chemisorption energy* ΔE. In order

to obtain some *estimate* of ΔE, we return to (1.26), and recall that the zeros of the [term] yields the solutions for the N states in the *substrate*. Thus, the *eigenvalue equation* for θ_k is

$$-z_s = \frac{\sin(M+1)\theta_k}{\sin M\theta_k}. \tag{1.60}$$

We are interested in the *total* electronic energy of the substrate chain in the *pre-adsorption* situation, when $\beta_a = 0$, so that the adatom is isolated from the chain and *no* surface states exist, i.e., $|z_s| < 1$, and we are only concerned with *in-band* states, for which θ_k is *real*.

In Fig. 1.2, a *small increment* ε_s in $-z_s$ causes a correspondingly *small decrement* $-\delta_k$ in θ_k. Thus, (1.60) reads

$$-z_s + \varepsilon_s = \frac{\sin(M+1)(\theta_k - \delta_k)}{\sin M(\theta_k - \delta_k)}, \tag{1.61}$$

which, with the aid of trigonometrical identities, (1.60) and the approximations $\cos\delta_k \simeq 1$ and $\sin\delta_k \simeq \delta_k$, leads to

$$\varepsilon_s = z_s\left[(Z - T^{-1})t + \delta_k(Z + t)\right](1 - tT^{-1})^{-1}, \tag{1.62}$$

where

$$T = \tan M\theta_k, \quad t = \tan M\delta_k, \tag{1.63}$$

and

$$Z = \cot(M+1)\theta_k. \tag{1.64}$$

Equation (1.60), in conjunction with (1.63) and (1.64), enables the following expressions to be derived, viz.,

$$T = -\sin\theta_k(z_s + \cos\theta_k)^{-1}, \tag{1.65}$$

$$Z = z_s^{-1}(\sin\theta_k - T^{-1}\cos\theta_k). \tag{1.66}$$

Inserting (1.65) in (1.66) yields

$$Z = (z_s\cos\theta_k + 1)(z_s\sin\theta_k)^{-1}. \tag{1.67}$$

Another way of obtaining the ε_s-relation is, of course, by straightforward differentiation of (1.60), which results in

$$\varepsilon_s = \delta_k\left[M\sin\theta_k(1 + T^{-2}) - (T^{-1}\cos\theta_k - \sin\theta_k)\right]. \tag{1.68}$$

Thus, (1.62) and (1.68) show that

$$z_s\big[(ZT-1)t+\delta_k T(t+Z)\big](T-t)^{-1} \\ =\delta_k\left[M\sin\theta_k(1+T^{-2})-(T^{-1}\cos\theta_k-\sin\theta_k)\right]. \tag{1.69}$$

Equating the coefficients of like powers of δ_k, we have

$$\delta_k^0: \qquad Z=T^{-1}, \quad T\neq t, \tag{1.70}$$

$$\delta_k^1: \qquad z_sT(t+Z)(T-t)^{-1}=R, \tag{1.71}$$

where, by (1.70),

$$R=M\sin\theta_k(1+Z^2)-(Z\cos\theta_k-\sin\theta_k). \tag{1.72}$$

Eliminating T between (1.70) and (1.71), we arrive at

$$t=Z^{-1}(1-P)(1+Q)^{-1}, \tag{1.73}$$

where, by virtue of (1.72), we find that

$$P=\frac{\cos\theta_k-Z^{-1}\sin\theta_k+z_s}{M\sin\theta_k(Z+Z^{-1})}, \tag{1.74}$$

$$Q=\frac{z_sZ^{-2}-\cos\theta_k+Z^{-1}\sin\theta_k}{M\sin\theta_k(Z+Z^{-1})}. \tag{1.75}$$

Since P and Q are both of $O(M^{-1})$, equation (1.73) reduces to

$$t=Z^{-1}+O(M^{-1}), \tag{1.76}$$

whence, the *phase shift* is (Baldock 1952, 1953)

$$\delta_k=M^{-1}\tan^{-1}\left(\frac{z_s\sin\theta_k}{z_s\cos\theta_k+1}\right)+O(M^{-2}), \tag{1.77}$$

by dint of (1.63) and (1.67).

In the ground state, the $M(=N/2)$ states in the *lower-half* of the bulk band are *doubly occupied*, so the *total reduced energy* for $\theta_k\to(\theta_k-\delta_k)$ is

$$X_t=2\sum_k X_k=2\sum_k\cos(\theta_k-\delta_k), \tag{1.78}$$

by (1.18), the summation being over the *occupied* orbitals. In view of (1.77), equation (1.78) becomes

$$X_t(z_s) = 2\sum_k \left[\cos\theta_k + M^{-1}\sin\theta_k \tan^{-1}\left(\frac{z_s \sin\theta_k}{z_s\cos\theta_k + 1}\right)\right]. \tag{1.79}$$

The *first* summation in (1.79) represents the total reduced energy, $X_t^{(1)}$ of the N-chain electrons, whose *mean reduced energy* of the M-levels in the lower-half band is given by

$$\overline{X}_1 = \frac{2}{\pi}\int_{\pi/2}^{\pi} \cos\theta\, d\theta = -2\pi^{-1}, \tag{1.80}$$

whence,

$$X_t^{(1)} = 2M\overline{X}_1 = -2N\pi^{-1}. \tag{1.81}$$

In the *second* summation, the θ_k-values occur at π/N intervals in the range $\pi/2 \le \theta_k \le \pi$, so the sum can be converted into an integral, namely,

$$X_t^{(2)}(z_s) = \frac{2N}{M\pi}\int_{\pi/2}^{\pi} \sin\theta \tan^{-1}\left(\frac{z_s\sin\theta}{z_s\cos\theta + 1}\right) d\theta. \tag{1.82}$$

Integration by parts, leads to

$$\begin{aligned} X_t^{(2)}(z_s) = \frac{4}{\pi}\Bigg\{ &\left[-\cos\theta\tan^{-1}\left(\frac{z_s\sin\theta}{1 + z_s\cos\theta}\right)\right]_{\pi/2}^{\pi} \\ &+ \int_{\pi/2}^{\pi} \frac{\cos\theta(z_s + \cos\theta)}{(z_s + z_s^{-1}) + 2\cos\theta} d\theta\Bigg\}, \end{aligned} \tag{1.83}$$

where the first term on the right is equal to zero. Equation (1.83) can be cast in the form

$$X_t^{(2)}(b) = b(J_0 + 2z_s J_1 + J_2)/\pi, \tag{1.84}$$

where

$$b = 2(z_s + z_s^{-1})^{-1} \le 1, \tag{1.85}$$

and

$$J_n(b) = \int_{\pi/2}^{\pi} \frac{\cos n\theta}{1 + b\cos\theta} d\theta. \tag{1.86}$$

On evaluating $J_n(b)$, as in the *Appendices* (App. A), (1.84) becomes

$$X_t^{(2)}(b) = 2\pi^{-1}\left\{(b^{-1} - z_s)\left[J_0(b) - \pi/2\right] - 1\right\}, \tag{1.87}$$

via (A.9) and (A.10). With the aid of (1.85), (A.3) and (A.8), we can express (1.87) as

$$X_t^{(2)}(z_s) = 2\pi^{-1}\left[(z_s^{-1} + z_s)\tan^{-1} z_s + z_s\pi/2 - 1\right]. \tag{1.88}$$

Hence, (1.81) and (1.88) in (1.79) yield

$$X_t(z_s) = 2\pi^{-1}\left[(z_s^{-1} + z_s)\tan^{-1} z_s + \pi z_s/2 - 1 - N\right], \tag{1.89}$$

which is somewhat different from the Grimley (1960) finding, which was derived for an *odd* number of electrons (as opposed to the *even* number here), and where β was taken *negative*, so that $z_s \to -z_s$ by (1.27). The latter point is the reason for the range of integration in (1.82) being $\pi/2 \leq \theta \leq \pi$, rather than Baldock's $0 \leq \theta \leq \pi/2$, to correspond to the occupied lower-half of the energy band. Note also that the factor of "2", inadvertently omitted by Grimley, has been replaced in (1.89).

Having analyzed the pre-chemisorption situation, we now address the *post-chemisorption* one, in which the foreign atom is brought up to the chain end atom at $n = 0$. For simplicity, we assume that $\beta_a = \beta$ and $\alpha_s = \alpha$ (Fig. 1.1), whence, $\eta = 1$ (1.25) and $z_s = 0$ (1.27), so that the interaction parameters lie on the z_a-axis in Fig. 1.5. In the case where *no* localized states are occupied, the total electronic reduced energy of the system is

$$X_t(z_a) = 2\pi^{-1}\left[(z_a^{-1} + z_a)\tan^{-1} z_a + \pi z_a/2 - 1 - (N+1)\right], \tag{1.90}$$

i.e., (1.89) with $z_s \to z_a$ and $N \to (N+1)$, as a result of the additional electron from the adatom in the chemisorption system. If γ denotes the reduced energy of the valence electron in the isolated foreign atom, then

$$\Delta X = X_t(z_a) - X_t(z_s) - \gamma \tag{1.91}$$

represents the *change* in the total electronic reduced energy as a result of the interaction of the foreign atom with the chain, i.e., the so-called *chemisorption energy*. From (1.89), (1.90) and (1.91), we have

$$\Delta X = -(2\pi^{-1} + \gamma) + \Delta X_s, \tag{1.92}$$

where

$$\Delta X_s = 2\pi^{-1}\left[F(z_a) - F(z_s)\right] + (z_a - z_s), \tag{1.93}$$

with

$$F(z) = (z + z^{-1}) \tan^{-1} z. \tag{1.94}$$

The chemisorption reduced energy in (1.92) appears as the sum of two terms. The first term, being associated with the crystal's mean electron energy and the foreign atom's valence electron energy, represents the energy change arising from the *delocalization* of the valence electron on the foreign atom. The second term in (1.92) is the *surface-energy change* caused by the presence of the foreign atom.. Apparently, for chemisorption involving a metallic-like surface bond, the form of (1.92) is quite general. Finally, it should be mentioned that, for a *stable* adbond to be formed, the chemisorption process must result in a lowering of the electronic energy of the system, thus, $\Delta X < 0$. If $\Delta X > 0$, *no* chemisorption occurs.

Chapter 2

Resolvent Technique

Practical sciences proceed by building up; theoretical sciences by resolving into components.

— Thomas Aquinas

In the previous chapter, we used the MO approach to cast the Schrödinger equation in the form of a second-order finite-difference equation with constant coefficients (1.9). We were able to solve this equation straightforwardly for the boundary conditions pertaining to a single adatom interacting with a chain-like substrate. We also mentioned that the 3-dimensional situation of a substrate *completely covered* with adatoms (i.e., an *adlayer*) could be treated in the same manner, being a direct extension of the single-adatom case (Grimley 1960). However, should we wish to study the problem of a *single* (or *group* of) adatom(s) interacting with the free surface of a 3-dimensional crystal, then (1.9), and its attending boundary conditions, *cannot* be solved directly. In this case, it is necessary to describe the limited interaction region by means of *projection operators* (Löwdin 1962; Yao and Shi 2000) as Koutecký (1965, 1976) did in his *resolvent formalism* (Davison

and Stęślicka 1996). Thus, this chapter introduces us to the powerful and versatile *Green-function methods*, which are employed henceforward.

2.1 Projection Operators

As the name implies, the *projection operator* P projects onto some *space* p, where P of the system consists of operators P_i of the subsystems, so that

$$P = \sum_i P_i. \tag{2.1}$$

For a *non-interacting* system, the space p^o is composed of subspaces p_i^0, whose associated operators are assumed to satisfy

$$P^0 = \sum_i P_i^0 = I, \tag{2.2}$$

I being the *identity* operator, whence, the projection capacity of P^0 is said to be *complete*. In addition, if

$$P_i^0 P_j^0 = 0, \quad i \neq j, \tag{2.3}$$

then subspaces p_i^0 and p_j^0 will have *zero overlap*.

In terms of the $\langle bra|\mathrm{c}|ket\rangle$ notation of Dirac (1958), the Schrödinger equation (1.2) takes the form

$$H_0|\psi_0\rangle = E_0|\psi_0\rangle, \tag{2.4}$$

in which

$$|\psi_0\rangle = \sum_n c_n^0 |\phi_n^0\rangle, \tag{2.5}$$

as in (1.1). From (2.5), we have

$$\langle\phi_m^0|\psi_0\rangle = \sum_n c_n^0 \langle\phi_m^0|\phi_n^0\rangle,$$

i.e.,

$$\langle\phi_m^0|\psi_0\rangle = \sum_n c_n^0 \delta_{mn} = c_m^0, \tag{2.6}$$

via the *orthonormality* of $|\phi_n^0\rangle$. In view of (2.6), we can write (2.5) as

$$|\psi_0\rangle = \sum_n |\phi_n^0\rangle\langle\phi_n^0|\psi_0\rangle, \tag{2.7}$$

whence,

$$\sum_n |\phi_n^0\rangle\langle\phi_n^0| = I. \tag{2.8}$$

Comparison of (2.2) and (2.8), shows that

$$P_n^0 = |\phi_n^0\rangle\langle\phi_n^0| \tag{2.9}$$

is the *representation* of the projection operator P_n^0 for the subspace p_n^0.

2.2 Perturbation Formulation

Turning to the question of an *interacting* system, we define the perturbed Hamiltonian as

$$H = H_0 + V, \tag{2.10}$$

where the *interaction potential* V is viewed as a *small perturbation*. If E and $|\psi\rangle$ are the corresponding *perturbed* eigenvalues and eigenfunctions, then (1.2) becomes

$$H|\psi\rangle = (H_0 + V)|\psi\rangle = E|\psi\rangle. \tag{2.11}$$

The perturbed space p falls naturally into two *complementary* subspaces q and $\bar{q}$, such that

$$p = q + \bar{q}, \tag{2.12}$$

q being the space over which V *acts* and $\bar{q}$ that where it does not. For calculating purposes, it is useful to express p as a subspace of p^0, by writing

$$p = p^0 - s, \tag{2.13}$$

where s denotes a space *removed* from p^0 to form p. In operator language, we now have

$$\bar{Q}V = V\bar{Q} = 0, \tag{2.14}$$

and (Davison and Stęślicka 1996)

$$S + Q + \bar{Q} = I, \tag{2.15}$$

by dint of (2.2), (2.12) and (2.13). Moreover, removal of the space s implies that

$$S|\psi\rangle = 0, \tag{2.16}$$

while (2.10) gives

$$SH|\psi\rangle = (SH_0 + SV)|\psi\rangle = 0,$$

i.e.,

$$SV = -SH_0. \tag{2.17}$$

On rearranging, (2.11) can be written as

$$|\psi\rangle = GV|\psi\rangle, \tag{2.18}$$

where the operator

$$G = (E - H_0)^{-1} \tag{2.19}$$

is known as the *resolvent*. For analysis purposes, let us now insert the identity operator in (2.18), so that

$$|\psi\rangle = GIVI\,|\psi\rangle. \tag{2.20}$$

Substituting (2.15) into (2.20), and using (2.14), (2.16) and (2.17), leads to

$$|\psi\rangle = G(QV - SH_0)Q|\psi\rangle. \tag{2.21}$$

As in (2.6), the coefficients are given by

$$\langle\phi_m^0|\psi\rangle = \langle\phi_m^0|G(QV - SH_0)Q|\psi\rangle, \tag{2.22}$$

where

$$\begin{aligned} \langle\phi_m^0|\psi\rangle \neq 0, \quad |\phi_m^0\rangle \in p, \\ = 0, \quad |\phi_m^0\rangle \in s. \end{aligned} \tag{2.23}$$

Utilizing (2.5), the non-trivial solutions of (2.22) (i.e., $Q|\psi\rangle \neq 0$) require that

$$\det_Q \left[\langle\phi_m^0|G(QV - SH_0)Q - I|\phi_n^0\rangle\right] = 0, \tag{2.24}$$

where $m \leq$ order (q). Note that the presence of the S-term in the above enables the initial system to be larger and simpler than the system being studied. Solutions of the secular equation (2.24) provide the perturbed eigenvalues E, whence, $|\psi\rangle$ can be obtained from the linear algebraic equation (2.21).

2.3 Chemisorption on Cyclic Crystal

In order to become acquainted with the resolvent technique, and the use of projection operators, we re-examine the problem treated in §1.1. In doing so, we employ the *cyclic crystal*, which lends itself well to modelling a non-interacting (or unperturbed) substrate (Davison and Steślicka 1996).

2.3.1 Cyclic crystal

A cyclic crystal[1] consists of a ring of equally spaced atoms formed by joining the ends of a chain of N atoms numbered $n \in [0, N-1]$. Thus, for the kth state, the wave function (2.5) becomes

$$|\psi_k^0\rangle = \sum_{n=0}^{N-1} c_{nk}^0 |\phi_n^0\rangle, \tag{2.25}$$

where the coefficients satisfy (1.9), whose solution can be written as (cf. (1.22))

$$c_{nk}^0 = A e^{in\theta_k^0}. \tag{2.26}$$

The constant A is obtained by means of the normalization condition

$$\langle \psi_k^0 | \psi_k^0 \rangle = 1, \tag{2.27}$$

which, since $\langle \phi_n^0 | \phi_n^0 \rangle = 1$, yields

$$\sum_{n=0}^{N-1} A^2 = 1,$$

via (2.25) and (2.26), whence,

$$A = N^{-\frac{1}{2}}, \tag{2.28}$$

so that (2.25) now reads

$$|\psi_k^0\rangle = N^{-\frac{1}{2}} \sum_{n=0}^{N-1} e^{in\theta_k^0} |\phi_n^0\rangle. \tag{2.29}$$

[1] An infinite crystal can be represented by a finite one, by either allowing $N \to \infty$, or by imposing periodic boundary conditions at each end. Another way is to construct a *cyclic crystal*.

The values of θ_k^0 are found by means of the *cyclic* boundary condition (Ziman 1965)

$$c_{0k}^0 = c_{Nk}^0. \tag{2.30}$$

Inserting (2.26) in (2.30), and equating real and imaginary parts, we find

$$\cos N\theta_k^0 = 1, \quad \sin N\theta_k^0 = 0,$$

thus,

$$\theta_k^0 = 2\pi k/N, \quad k = 0, 1, \ldots, N-1. \tag{2.31}$$

From (1.16) and (1.18), we see that each θ_k^0-value has a corresponding energy level

$$E_k^0 = \alpha + 2\beta \cos\theta_k^0. \tag{2.32}$$

2.3.2 Cyclic Green function

By virtue of (2.8) and (2.19), we can write the resolvent (or *Greenian*) for k-space as

$$G(E^0) = (E - H_0)^{-1} \sum_k |\psi_k^0\rangle\langle\psi_k^0| = \sum_k |\psi_k^0\rangle\langle\psi_k^0|(E - E_k^0)^{-1}, \tag{2.33}$$

via (2.4). Hence, we have the Greenian *matrix element*

$$G_{m,N-n} = \sum_k \langle\phi_m^0|\psi_k^0\rangle\langle\psi_k^0|\phi_{N-n}^0\rangle(E - E_k^0)^{-1},$$

which, by dint of (2.29) and (2.6), reduces to

$$G_{m,N-n} = N^{-1} \sum_k e^{i(m+n)\theta_k^0}(E - E_k^0)^{-1} = G_{m+n} \tag{2.34}$$

since $e^{-iN\theta_k^0} = 1$ by (2.31), which also shows that

$$\delta\theta_k^0 = \theta_{k+1}^0 - \theta_k^0 = 2\pi N^{-1}. \tag{2.35}$$

Consequently, in the limit of $N \to \infty$, (2.34) leads to the *Green function* (GF)

$$G_\ell = (4\pi\beta)^{-1} \int_0^{2\pi} e^{i\ell\theta}(X - X^0)^{-1} d\theta, \tag{2.36}$$

by (1.16), where $\ell = (m + n)$.

Evaluation of (2.36) proceeds via *complex integration* (Mathews and Walker 1965). With the aid of (1.18), putting (cf. (1.19))

$$t = e^{i\theta} \tag{2.37}$$

transforms (2.36) into an integral around a unit circle in the complex plane, viz.,

$$G_\ell = i(2\pi\beta)^{-1} \oint \left[t^\ell / F(t)\right] dt, \tag{2.38}$$

where (cf. (1.15))

$$F(t) = t^2 - 2Xt + 1, \tag{2.39}$$

whose roots are

$$t_{1,2} = X \pm (X^2 - 1)^{1/2}, \quad t_1 t_2 = 1. \tag{2.40}$$

Invoking the theory of residues, (2.38) can be expressed as

$$\beta G_\ell = -(R_1 + R_2), \tag{2.41}$$

where each residue

$$R_j = \left[(t - t_j)t^\ell (t - t_1)^{-1}(t - t_2)^{-1}\right]_{t=t_j} \tag{2.42}$$

is at a *pole inside* the unit circle. Since $X \neq X_0$ in (2.36), θ must be *complex*, i.e.[2],

$$\theta \equiv \theta^\pm = \xi \pm i\mu, \tag{2.43}$$

which with (1.18) enables (2.40) to be expressed as

$$t_{1,2}^\pm = e^{\pm i(\xi \pm i\mu)}, \tag{2.44}$$

whence,

$$|t_{1,2}^+| = e^{\mp\mu} \lesseqgtr 1, \tag{2.45}$$

$$|t_{1,2}^-| = e^{\pm\mu} \gtreqless 1. \tag{2.46}$$

[2] In (2.43), μ must be small, because a cyclic crystal supports only delocalized states, so the poles at $X \neq X^0$ are located close to the unit-circle contour. This observation is connected with the notion of *complex energy* (§3.2), since, for μ small, (2.43) in (1.18) shows that $X^\pm \sim X \mp i\mu$.

These conditions show that R_2 and R_1, respectively,lies *outside* the unit-circle contour and is excluded. Thus, (2.41) and (2.42) give

$$\beta G_\ell^+ = -R_1 = t_1^\ell (t_2 - t_1)^{-1} \quad \text{for} \quad \theta^+, \tag{2.47}$$

$$\beta G_\ell^- = -R_2 = t_2^\ell (t_1 - t_2)^{-1} \quad \text{for} \quad \theta^-, \tag{2.48}$$

which lead to

$$2\beta G_\ell^\pm = \pm i e^{\pm i\ell\theta} csc\theta, \tag{2.49}$$

via (1.18) and (2.40).

2.3.3 Model representation

Let us now consider the interaction of an atom A with the zeroth atom of a monatomic cyclic crystal C, as depicted in Fig. 2.1. If the site energy of $A(C)$ is $\alpha_a(\alpha)$ and the bond energy of C is β, then in the *pre-* (*post-*) *chemisorption* situation the adbond energy $\beta_a = 0(\beta_a \neq 0)$.

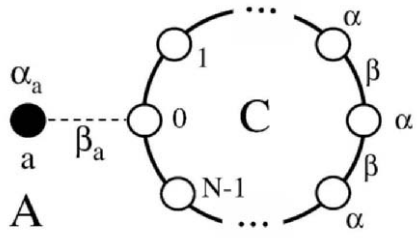

Fig. 2.1. Atom (A) and cyclic crystal (C) before and after interaction.

Prior to interaction, the unperturbed system consists of its isolated A and C parts, whence, its *total* k-state wave function is (cf. (2.25))

$$|\psi_k\rangle = c_{ak}|\phi_a\rangle + \sum_{n=0}^{N-1} c_{nk}|\phi_n\rangle = \sum_t c_{tk}|\phi_t\rangle, \quad t = a \quad \text{and} \quad n, \tag{2.50}$$

where

$$\langle\phi_a|\phi_t\rangle = \delta_{at}. \tag{2.51}$$

Likewise, we have (Koutecký 1976)

$$G_{AC} = G_A + G_C, \tag{2.52}$$

in which G_C is given by (2.33), and

$$G_A = |\phi_a\rangle\langle\phi_a|(E - \alpha_a)^{-1}. \tag{2.53}$$

Returning to (2.22), we see that

$$\langle\phi_r|\psi\rangle = \langle\phi_r|G_{AC}QVQ|\psi\rangle, \quad r = a \quad \text{or} \quad n, \tag{2.54}$$

since $S = 0$. Moreover, V acts over the space q between A and C, whose corresponding projection operator is defined by

$$Q = |\phi_a\rangle\langle\phi_0| + |\phi_0\rangle\langle\phi_a|. \tag{2.55}$$

Thus, (2.50), (2.52) and (2.55) in (2.54) result in

$$\langle\phi_r|\sum_t c_t|\phi_t\rangle = \langle\phi_r|(G_A + G_C) \times (|\phi_a\rangle\langle\phi_0| + |\phi_0\rangle\langle\phi_a|)V(|\phi_a\rangle\langle\phi_0| + |\phi_0\rangle\langle\phi_a\rangle)\sum_t c_t|\phi_t\rangle, \tag{2.56}$$

After some algebra, using (2.50) and (2.52), we find

$$\langle\phi_r|\sum_t c_t|\phi_t\rangle = \beta_a(G^{AC}_{ra}\langle\phi_0| + G^{AC}_{r0}\langle\phi_a|)\sum_t c_t|\phi_t\rangle, \tag{2.57}$$

where $\langle\phi_a|V|\phi_a\rangle = \langle\phi_0|V|\phi_0\rangle = 0$,

$$\beta_a = \langle\phi_0|V|\phi_a\rangle = \langle\phi_a|V|\phi_0\rangle, \tag{2.58}$$

and

$$G^{AC}_{ra(0)} = \langle\phi_r|G^{AC}|\phi_{a(0)}\rangle. \tag{2.59}$$

Consequently, in view of (2.50) and (2.51), equation (2.57) gives

$$c_a\delta_{ra} + c_n\delta_{rn} = \beta_a(G^{AC}_{ra}c_0 + G^{AC}_{r0}c_a), \tag{2.60}$$

which, for $r = n$ and $r = a$, yields the simultaneous equations

$$c_n = \beta_a(G^{AC}_{na}c_0 + G^{AC}_{n0}c_a), \tag{2.61}$$

$$c_a = \beta_a(G^{AC}_{aa}c_0 + G^{AC}_{a0}c_a), \tag{2.62}$$

respectively. From (2.62), we have

$$c_a = \beta_a G^{AC}_{aa}(1 - \beta_a G^{AC}_{a0})^{-1} c_0, \tag{2.63}$$

whereby (2.61) becomes

$$c_n = \beta_a \left(G^{AC}_{na} + \frac{G^{AC}_{n0} G^{AC}_{aa}}{\beta_a^{-1} - G^{AC}_{a0}} \right) c_0. \tag{2.64}$$

However, from (2.33) and (2.50) to (2.53), we see that

$$G^{AC}_{na} = G^{AC}_{a0} = 0, \tag{2.65}$$

so that (2.63) and (2.64) reduce to

$$c_a = \beta_a G^{AC}_{aa} c_0, \tag{2.66}$$

and

$$c_n = \beta_a^2 G^{AC}_{n0} G^{AC}_{aa} c_0. \tag{2.67}$$

Moreover, because

$$G^{C}_{aa} = G^{A}_{n0} = 0 \tag{2.68}$$

also, we eventually obtain

$$c_a = \beta_a G^{A}_{aa} c_0, \tag{2.69}$$

and

$$c_n = \beta_a^2 G^{C}_{n0} G^{A}_{aa} c_0, \tag{2.70}$$

which, for $n = 0$ and $c_0 \neq 0$, yields

$$\beta_a^2 G^{A}_{aa} G^{C}_{00} = 1. \tag{2.71}$$

Utilizing (1.16), (1.18), (1.25) and (2.53) in (2.69), enables us to reclaim (1.24), viz.,

$$c_a = \eta c_0 (z_a + 2\cos\theta)^{-1}. \tag{2.72}$$

Meanwhile, from (2.70) we have

$$c_n = \pm i\eta c_a (2\sin\theta)^{-1} e^{\pm in\theta}, \tag{2.73}$$

via (2.49) and (2.69). We note that (2.73) has the same exponential behaviour with n as (1.34), and that (2.71) is the same *eigenvalue equation* as that derived from (2.24), and leads to

$$(z_a + 2\cos\theta)(e^{-i\theta} - e^{i\theta}) = \eta^2, \tag{2.74}$$

which is close to (1.35), when $z_s = 0$, as required for cyclic crystal substrate.

Clearly, the incorporation of the "cut and stick" tailoring feature of projection operators into the resolvent-technique formulation, makes it a particularly adaptable modelling tool. Moreover, it enables the atomic structure of the geometric space to be reflected in the so-called *site representation* of the GF.

Chapter 3

Dyson-Equation Approach

The aim of research is the discovery of the equations which subsist between the elements of phenomena.

— Ernst Mach

Having introduced GFs into the analysis, let us now proceed to explore ways by which we might exploit their properties to gain further insight into the charge-transfer process involved in chemisorption. Of particular interest, in this regard, is the *density of states* (DOS), which is accessed by adopting the concept of *complex energy* in the GF, as was footnoted in §2.3.2.

However, before addressing this issue, we must first develop a means whereby a perturbed GF is expressed in terms of an unperturbed one.

3.1 Dyson Equation

Consider an unperturbed system, whose Hamiltonian (Greenian) is $H_0(G_0)$, which is perturbed by a *small* potential (V), so that the perturbed system Hamiltonian (Greenian) is $H(G)$. As in (2.19), the Greenian operators are defined as

$$G_0 = (E - H_0)^{-1}, \quad G = (E - H)^{-1}, \tag{3.1}$$

where

$$H = H_0 + V, \tag{3.2}$$

V being the *scattering (or perturbation) potential*. With the aid of (3.2), we can write (3.1) as

$$G = (E - H_0 - V)^{-1} = (G_0^{-1} - V)^{-1},$$

which, on rearranging, gives the *Dyson equation* (Dyson 1949, Taylor 1970)

$$G = G_0 + G_0 V G. \tag{3.3}$$

By iteration, we see that (3.3) leads to the perturbation expansion

$$G = G_0 + G_0 V G_0 + G_0 V G_0 V G_0 + \cdots, \tag{3.4}$$

while in matrix form (3.3) reads

$$G(m,n) = G_0(m,n) + \sum_{k\ell} G_0(m,k) V(k,\ell) G(\ell,n), \tag{3.5}$$

which relates the perturbed and unperturbed GFs via the scattering-potential matrix.

3.2 Density of States

The expression for the DOS is derived by taking the *trace* of the Greenian $G(E)$ in (3.1), i.e.,

$$TrG(E) = \sum_j \langle \psi_j | G | \psi_j \rangle = \sum_j (E - E_j)^{-1} \tag{3.6}$$

ψ_j being the orthonormal eigenfunctions of H and E_j their corresponding eigenvalues. We see that the presence of the *pole* at $E = E_j$ gives rise to a singularity in the integration path of the GF in (3.6), which is avoided by introducing the idea of complex energy (Haken 1976) and taking

$$E \longrightarrow E + is, \tag{3.7}$$

where $s = 0^+$, the *positive infinitesimal*, is eventually taken to zero.[1] In view of (3.7), we set $\xi_j = E - E_j$ in the summand of (3.6), and write it as

$$\frac{1}{\xi_j + is} = \frac{\xi_j}{\xi_j^2 + s^2} - \frac{is}{\xi_j^2 + s^2},$$

whereby (3.6) shows that

$$Im\ Tr\ G(E) = -\sum_j s(\xi_j^2 + s^2)^{-1}, \tag{3.8}$$

whose summand has the properties

$$\lim_{s\to 0} \frac{s}{\xi_j^2 + s^2} = 0, \quad \xi_j \neq 0,$$

and

$$\lim_{s\to 0} \int_{-c}^{c} \frac{s d\xi_j}{\xi_j^2 + s^2} = \lim_{s\to 0} \left[\tan^{-1}\left(\frac{\xi_j}{s}\right)\right]_{-c}^{c} = \pi. \tag{3.9}$$

Comparing (3.9) with the Dirac δ-function definition, viz.,

$$\int_{-\infty}^{\infty} \delta(\xi_j) d\xi_j = 1, \tag{3.10}$$

shows that

$$\lim_{s\to 0} \frac{s}{\xi_j^2 + s^2} = \pi\delta(\xi_j),$$

whereby (3.8) provides the definition

$$\rho(E) = \sum_j \delta(E - E_j) = -\pi^{-1} Im\ Tr\ G(E), \tag{3.11}$$

for the *total energy DOS* (Raimes 1972). In the site representation, (3.11) becomes

$$\rho(E) = -\pi^{-1} Im \sum_m G(m, m), \tag{3.12}$$

whence,

$$\rho_m(E) = -\pi^{-1} Im\ G(m, m) \tag{3.13}$$

is the *local density of states* (LDOS) at the mth site.

[1] More precisely, $s = 0^+$ is understood as the $\lim_{s\to 0^+}$.

3.3 Chemisorption on Monatomic Substrate

The system we wish to investigate consists of a single atom a interacting with a semi-infinite monatomic chain. The site (bond) energy of the chain is $\alpha(\beta)$, while that of the a-atom is $\alpha_a(\beta_a)$. Initially, the substrate is represented by a *cyclic* chain of N atoms, whose GF is given by (2.49). A *semi-infinite* chain is then formed by breaking the bond between the $n = 0$ and $N - 1$ atoms (Fig. 3.1).

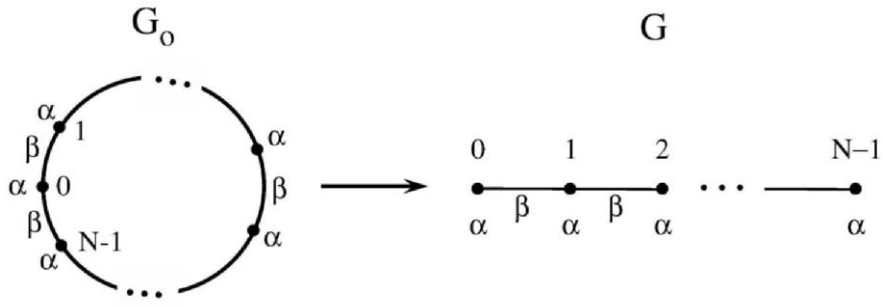

Fig. 3.1. Formation of N-atom chain from cyclic chain by breaking bond between $n = 0$ and $N - 1$ atoms.

Mathematically, this is achieved by means of the Dyson operator equation (3.3), in which $G_0(G)$ denotes the Greenian of the cyclic (semi-infinite) chain, and the bond-breaking potential operator is given by

$$V = -\beta(|0\rangle\langle N-1| + |N-1\rangle\langle 0|). \tag{3.14}$$

Thus, inserting (3.14) in (3.3), gives

$$G(0,0) = G_0(0,0) - \beta[G_0(0,0)G(N-1,0) + G_0(0,N-1)G(0,0)], \tag{3.15}$$

for the GF at the $n = 0$ atom of the semi-infinite chain, where, for example, $G(0,0) = \langle 0|G|0\rangle$. We observe that $G(N-1,0) = 0$, since it is *not* contained in space over which G operates (Fig. 3.1), so on rearranging, (3.15) yields

$$G(0) = G_0(0)\left[1 + \beta G_0(0,N-1)\right]^{-1}, \tag{3.16}$$

where, e.g., $G(0) \equiv G(0,0)$. Inserting $G^{-}_{\ell=1}$ of (2.49) in (3.16) leads to

$$\beta G(0) = -i(2\sin\theta - ie^{-i\theta})^{-1}, \tag{3.17}$$

which reduces to

$$\beta G(0) = e^{-i\theta}. \tag{3.18}$$

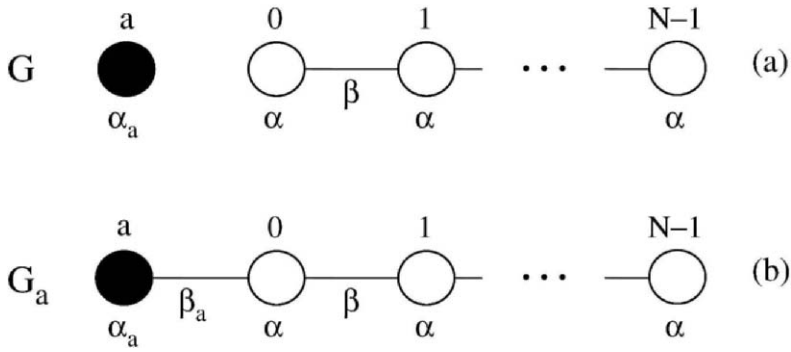

Fig. 3.2. Schematic representation of chemisorption. (a) Before and (b) after formation of β_a-bond between a-atom and $n = 0$ atom of N-atom chain.

3.3.1 Adatom Green function

Turning to the *chemisorption situation* portrayed in Fig. 3.2, we require the potential-bond operator

$$V = \beta_a(|0\rangle\langle a| + |a\rangle\langle 0|), \tag{3.19}$$

to attach the a-atom to the $n = 0$ atom of the semi-infinite chain. In this case, inserting (3.19) in (3.3), we find the *adatom GF* is given by

$$G_a(a) = G(a) + \beta_a[G(a,0)G_a(a) + G(a)G_a(0,a)],$$

which reduces to

$$G_a(a) = [1 + \beta_a G_a(0,a)]G(a), \tag{3.20}$$

since

$$G(0,a) = G(a,0) = 0, \tag{3.21}$$

via Fig. 3.2(a). Likewise, we have

$$G_a(0,a) = G(0,a) + \beta_a \left[G(0)G_a(a) + G(0,a)G_a(0,a)\right],$$

which by (3.21) results in

$$G_a(0,a) = \beta_a G(0) G_a(a). \tag{3.22}$$

Thus, substituting (3.22) into (3.20), and collecting terms, we have

$$G_a(a) = \left[G^{-1}(a) - \beta_a^2 G(0)\right]^{-1}, \tag{3.23}$$

where the GF for the *isolated* a-atom in Fig. 3.2(a) is

$$G(a) = (E - \alpha_a)^{-1}. \tag{3.24}$$

On using (3.18) and (3.24), we can write (3.23) as

$$2\beta G_a(a) = \left\{(X - z_a) - 2\eta^2[X - i(1-X^2)^{1/2}]\right\}^{-1}, \tag{3.25}$$

where the *adatom parameters*

$$z_a = (\alpha_a - \alpha)/2\beta, \quad \eta = \beta_a/2\beta, \tag{3.26}$$

and

$$X = (E - \alpha)/2\beta = \cos\theta, \tag{3.27}$$

by dint of (1.16) and (1.18).

3.3.2 Adatom self-energy and density of states

Alternately, by introducing the so-called reduced *self-energy*

$$\Sigma(X) = \Lambda(X) - i\Delta(X), \tag{3.28}$$

we can express (3.25) in the concise form

$$2\beta G_a(a) = \left[X - \Sigma(X)\right]^{-1}, \tag{3.29}$$

where

$$\Lambda(X) = z_a + 2\eta^2 X, \tag{3.30}$$

and

$$\Delta(X) = 2\eta^2(1 - X^2)^{1/2}, \tag{3.31}$$

are referred to as the *chemical shift* and *line broadening*, respectively, both of which result from the effect of the atom-substrate interaction on the discrete level (i.e., $X = z_a$) of the a-atom, as it approaches the substrate surface.

With the aid of (3.28) and (3.29), equation (3.13) gives the *adatom DOS* as

$$\rho_a(X) = (2\pi\beta)^{-1} \left\{ \Delta[(X - \Lambda)^2 + \Delta^2]^{-1} \right\}. \tag{3.32}$$

For the system in question, inserting (3.30) and (3.31) in (3.32), and taking $2\pi\beta = 1$, we find

$$\rho_a^b(X) = \frac{2\eta^2(1 - X^2)^{1/2}}{[(1 - 2\eta^2)X - z_a]^2 + 4\eta^4(1 - X^2)}, \tag{3.33}$$

for $|X| < 1$, i.e., states lying *inside* the band of reduced energies defined by (3.27). The graphs of the adatom DOS curves are drawn in Fig. 3.3 for $z_a = 0.1$, with $\eta = 0.25$ and 0.5, which are depicted by the solid and dashed lines, respectively. We note that $\rho_a^b(X) = 0$ at the $X = \pm 1$ band edges. When $\eta = 0.25$, $\beta_a < \beta$, so the adbond is weaker than the substrate one, and the $\rho_a^b(X)$-curve assumes a typical Lorentzian-shape with a high, narrow central peak. On increasing η to 0.5, so that $\beta_a = \beta$, the peak broadens and shrinks in height until it vanishes, and the $\rho_a^b(X)$-curve becomes a low, wide "plateau", which is indicative of the increasing strength of the adatom-substrate interaction. Note that the changing shape of the DOS curves always proceeds in an *area-preserving* manner, since

$$2\beta \int_{-1}^{1} \rho_a^b(X) dX = 1, \tag{3.34}$$

for the total number of states on the adatom to be unity (Davison and Stęślicka 1992).

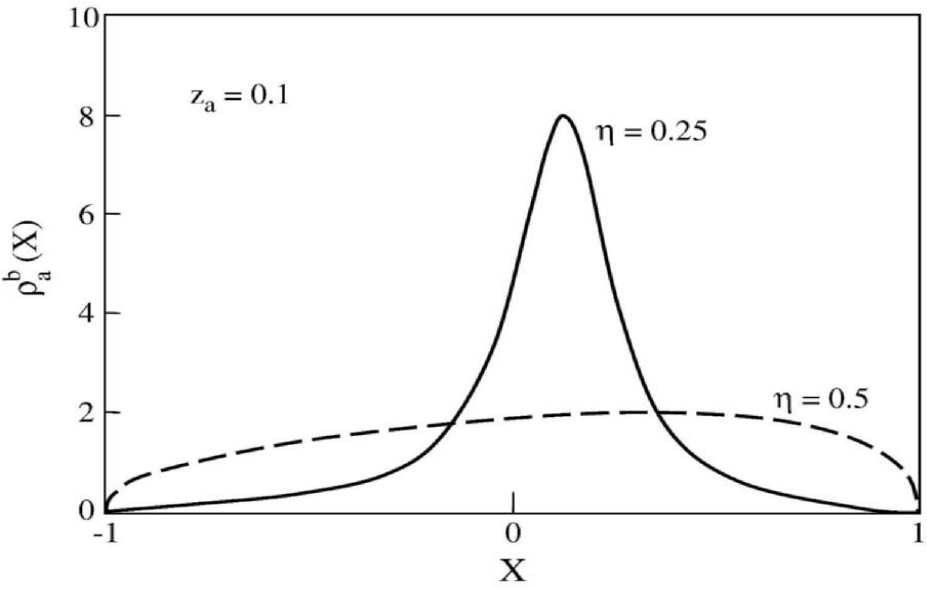

Fig. 3.3. Adatom DOS inside the band for the parameter values specified.

Let us now explore the DOS situation *outside* the band (i.e., $|X| > 1$), where the reduced energy X_a of the localized adstate is given by the *zeros* of the denominator of the GF (3.25), which is written as

$$2\beta G_a(a) = \left\{(X - z_a) - 2\eta^2[X - sgn\ X(X^2-1)^{1/2}]\right\}^{-1}, \tag{3.35}$$

for $|X| > 1$. For illustration purposes, we consider an adstate *above* the band, and choose $\eta = 0.5$. In this case, we find

$$X_a = z_a + (4z_a)^{-1}, \tag{3.36}$$

whence, $z_a > \frac{1}{2}$ for $X_a > 1$.

With the aid of (3.36), we can express (3.25) in the form

$$G_a(a) = (4\beta z_a)^{-1}(X_a - X)^{-1}\left[(X - 2z_a) - i(1-X^2)^{1/2}\right], \tag{3.37}$$

whose corresponding DOS via (3.13) is

$$\rho_a^b(X) = (4\pi\beta z_a)^{-1}(X_a - X)^{-1}(1-X^2)^{1/2}, \quad |X| < 1. \tag{3.38}$$

If X in (3.37) is replaced by $X + is$, then in the *adstate region*, we have to $O(s)$ that

$$G_a(a) = (4\beta z_a)^{-1}(P + isQ)\left[(X_a - X) - is\right]^{-1}, \tag{3.39}$$

where

$$P = (X - 2z_a) - (X^2 - 1)^{1/2}, \tag{3.40}$$

and

$$Q = 1 - X(X^2 - 1)^{-1/2}. \tag{3.41}$$

To $O(s)$, equation (3.39) shows that

$$Im\, G_a(a) = \frac{s[P + Q(X_a - X)]}{4\beta z_a[(X_a - X)^2 + s^2]}, \tag{3.42}$$

which, in the limit as $s \to 0^+$, reduces to

$$Im\, G_a(a) = 0, \qquad X \neq X_a, \tag{3.43}$$

and

$$Im\, G_a(a) = P/4\beta z_a s, \qquad X = X_a. \tag{3.44}$$

On using (3.36) and (3.40), inserting (3.44) in (3.13) gives

$$\rho_a^b(X_a) = \left[1 - (4z_a^2)^{-1}\right]/2\pi\beta s. \tag{3.45}$$

To proceed, we consider the function

$$f(X, s) = \pi^{-1} s \left[(X - X_a)^2 + s^2\right]^{-1}, \tag{3.46}$$

which has the properties

$$\begin{aligned} \lim_{s\to 0^+} f(X, s) &= 0, \quad X \neq X_a \\ &= (\pi s)^{-1}, \quad X = X_a \end{aligned} \tag{3.47}$$

of the Dirac δ-function. Thus, the adatom DOS (3.45), *above* the band, can be written as

$$\rho_a^a(X) = (2\beta)^{-1} I_a \delta(X - X_a), \tag{3.48}$$

where

$$I_a = 1 - (4z_a^2)^{-1}, \quad |z_a| > \tfrac{1}{2} \tag{3.49}$$

is the *intensity* of the adstate at $X = X_a$. The same analysis for $X < 1$, $z_a < -\frac{1}{2}$ reproduces (3.48) and (3.49) for the adstate at $X = -X_a$ *below* the band.

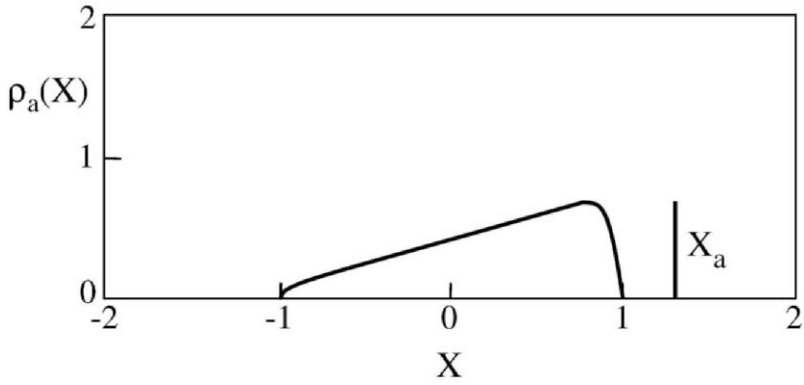

Fig. 3.4. Adatom DOS showing band and adstate contributions for $\eta = 0.5$ and $z_a = 1$ with $X_a = 1.25$.

Equations (3.38) and (3.48) are the analytical expressions for the band and adstate contributions to the total reduced-energy spectrum of the adatom DOS, $\rho_a(x)$, respectively. Their graphs are displayed in Fig. 3.4 for $2\beta = 1$ and the parameter values indicated. As can be seen, the presence of the large adstate "spike" at $X = X_a$ markedly reduces the area under the in-band portion of the DOS, in accordance with the sum rule (cf. (3.34))

$$2\beta \int_{-\infty}^{\infty} (\rho_a^b + \rho_a^a) dX = 1. \tag{3.50}$$

We note that the $\rho_a^b(X)$-curve attains its maximum value at $X = X_a^{-1}$, being given by

$$\hat{\rho}_a^b(X_a^{-1}) = (2z_a)^{-1} \left[X_a - (2z_a)^{-1} \right]^{-1}. \tag{3.51}$$

Moreover, the dichotomy in the adatom DOS distribution provides the ad-charge with access to a state localized mainly on the adatom and also to delocalized band states that are spread throughout the whole system.

Chapter 4

Anderson-Newns-Grimley Model

The purpose of models is not to fit the data, but to sharpen the questions.

— Samuel Karlin

One of the problems encountered in formulating a theory of chemisorption is that of *overcompleteness* (and thus *nonorthogonality*), which arises because the isolated substrate itself is described by a *complete set* of states, so that the combined system of substrate and adatom forms an *overcomplete* set. This issue has been addressed by various authors (Grimley 1970, 1975, Gomer and Schrieffer 1971, Bagchi and Cohen 1974, Paulson and Schrieffer 1975, Bell and Madhukar 1976). The easiest way to handle the difficulty is to incorporate the effect by employing renormalized matrix elements and 1-electron energies. Henceforth, we assume orthogonalization has been carried out, so that the effect is not treated explicitly (Kranz 1978).

Another fundamental deficiency in the 1-electron theory is its failure to account for the significant role played by *electron-electron interaction* in the charge-transfer process. An *approximate* solution to this difficult many-electron problem appeared towards the end of the sixties (Edwards and Newns 1967, Grimley 1967, Newns 1969), which tackled it by adopting a modified version of the work of Anderson (1961) on dilute magnetic impurities

in metals. The resulting *Anderson-Newns-Grimley* (ANG) model introduces a new ingredient into the 1-electron Hamiltonian, namely, the *intra-atomic electron Coulomb repulsion term* on the adatom, which is visualized as an impurity residing on the surface. As a consequence, the chemisorption energy can be calculated in a *self-consistent* manner.

In order to proceed further, we now introduce the language of many-electron theory, and the concept of occupation number.

4.1 Second Quantization Formalism

The wave function of a many-electron system can be written as a *Slater determinant* (see App. B). However, a more convenient notation is provided by using the *occupation number* representation, whereby the N-electron determinantal function takes the form (March et al. 1967, Raimes 1972)

$$\Psi_N(n_1 \dots n_k \dots) = |n_1 \dots n_k \dots\rangle, \tag{4.1}$$

where n_k is the number of electrons in the level k, whose value is either 0 or 1 and

$$\sum_k n_k = N. \tag{4.2}$$

Equation (4.1) is sometimes referred to as a *state vector in Fock space* and its use requires that the Hamiltonian be expressed in terms of operators that can act on such vectors.

4.1.1 Creation and annihilation operators

Assuming that all the 1-electron levels are arranged in some definite *order*, then, since n_k is 1 or 0, we can define the *annihilation* operator c_k by

$$c_k|\dots 1_k \dots\rangle = \theta_k|\dots 0_k \dots\rangle, \tag{4.3}$$

$$c_k|\dots 0_k \dots\rangle = 0. \tag{4.4}$$

In (4.3), all the occupation numbers remain unchanged, except n_k. Likewise, the *creation* operator $c_k^\dagger$ is defined by

$$c_k^\dagger|\dots 0_k \dots\rangle = \theta_k|\dots 1_k \dots\rangle, \tag{4.5}$$

$$c_k^\dagger|\ldots 1_k\ldots\rangle = 0. \tag{4.6}$$

Note that the c-operation in (4.4) (or (4.6)) yields a *null* result, because an electron can not be destroyed (created), where the k-state is already empty (occupied). In the above equations,

$$\theta_k = (-1)^{\nu_k}, \quad \nu_k = \sum_{j<k} n_j, \tag{4.7}$$

since, if an even (odd) number of states, with $n_k = 1$, precede the k-level, the sum is an even (odd) number and $\theta_k = 1(\theta_k = -1)$[1]. Of course, this reflects the antisymmetric nature of the Slater determinant wave function (App. B).

The above definitions can be expressed more succinctly as:

$$c_k|\ldots n_k\ldots\rangle = \theta_k n_k|\ldots 0_k\ldots\rangle, \tag{4.8}$$

$$c_k^\dagger|\ldots n_k\ldots\rangle = \theta_k(1-n_k)|\ldots 1_k\ldots\rangle. \tag{4.9}$$

As shown in App. C, the c-operators satisfy the following set of *anticommutation relations*:

$$[c_\ell, c_k]_+ = 0, \tag{4.10}$$

$$[c_\ell^\dagger, c_k^\dagger]_+ = 0, \tag{4.11}$$

$$[c_\ell^\dagger, c_k]_+ = \delta_{\ell k}, \tag{4.12}$$

where

$$[a, b]_+ = ab + ba. \tag{4.13}$$

Moreover, as in (C.5),

$$c_k^\dagger c_k = n_k \tag{4.14}$$

is known as the *number operator* for the 1-electron state function $|k\rangle$. Equations (4.12) and (4.14) yield the result

$$c_k c_k^\dagger = 1 - n_k. \tag{4.15}$$

[1]The adopted sign convention is simply that which leaves the sign of the determinant unchanged when a 1-electron function is destroyed or created *in the first position* (i.e.,first row). The plus or minus sign arises from moving a given 1-electron function *to* the first position to be *destroyed*, or *from* the first position to its correctly ordered one when it has been *created*.

Recalling §2.1, we observe that the operator $|i\rangle\langle j|$ gives zero, when it acts on any of the states $|k\rangle$, except that for which $k = j$, when it gives the state $|i\rangle$. Consequently, $|i\rangle\langle j|$ *removes* an electron from a state whose wave function is $|j\rangle$,and *puts* it in the state $|i\rangle$. In other words, $|i\rangle\langle j|$ *annihilates* an electron in the state $|j\rangle$ and *creates* one in the state $|i\rangle$ (Taylor 1970), which means it is equivalent to the c-operator $c_i^\dagger c_j$.

If we now introduce the *vacuum state* $|0\rangle$, for which

$$\langle 0|0\rangle = 1, \quad \langle k|0\rangle = 0, \tag{4.16}$$

then we can write

$$\begin{aligned} |i\rangle\langle j| &= |i\rangle\langle 0|0\rangle\langle j| \\ &= (|i\rangle\langle 0|)\,(|0\rangle\langle j|) \\ &= c_i^\dagger c_j, \end{aligned} \tag{4.17}$$

whereby we obtain

$$c_j = |0\rangle\langle j|, \quad c_i^\dagger = |i\rangle\langle 0|. \tag{4.18}$$

4.1.2 Hamiltonian in c-operator form

For a *free-electron*, the Schrödinger equation takes the form

$$T|\psi\rangle = E|\psi\rangle, \tag{4.19}$$

where

$$T = p^2/2m \tag{4.20}$$

is the *kinetic energy* operator, with

$$\mathbf{p} = -i\hbar\boldsymbol{\nabla}. \tag{4.21}$$

Now (4.19) has solutions for an infinite number of energies $E_u (u = 1, 2, \ldots)$, whose corresponding state functions $|u\rangle$, which satisfy

$$T|u\rangle = E_u|u\rangle \tag{4.22}$$

and

$$\langle u|v\rangle = \delta_{uv}, \tag{4.23}$$

form a complete set, so that any other function can be expressed in terms of $|u\rangle$.

In view of (2.8), we can write

$$\begin{aligned} T &= \sum_u |u\rangle\langle u|T\sum_v |v\rangle\langle v| \\ &= \sum_{u,v}\langle u|T|v\rangle|u\rangle\langle v|, \end{aligned} \tag{4.24}$$

which by (4.17) becomes

$$T = \sum_{u,v} T_{uv}c_u^\dagger c_v. \tag{4.25}$$

It is convenient to choose $|u\rangle$, so that T_{uv} has only *diagonal* elements. One such choice is the *plane-wave* $e^{i\mathbf{k}_u\cdot\mathbf{r}}$, for which (4.20) and (4.21) yield (Taylor 1970)

$$T_{uv} = \int e^{-i\mathbf{k}_u\cdot\mathbf{r}}(-\hbar^2\nabla^2/2m)e^{i\mathbf{k}_v\cdot\mathbf{r}}d\mathbf{r},$$

i.e., the diagonal form

$$T_{uv} = (\hbar^2 k_u^2/2m)\delta_{uv} = E_u\delta_{uv}, \tag{4.26}$$

via (4.22).

A similar derivation for the *potential energy* operator V leads to the result

$$V = \sum_{u,v} V_{uv}c_u^\dagger c_v, \tag{4.27}$$

so the c-operator form of the 1-electron Hamiltonian is

$$H = \sum_u E_u c_u^\dagger c_u + \sum_{u,v} V_{uv}c_u^\dagger c_v \tag{4.28}$$

by (4.25)-(4.27). Note that the annihilation and creation operators always appear in *pairs*, since a potential cannot remove an electron from one state without putting it back in another.

Turning to the situation where the electrons *interact*, requires we add to (4.28) a 2-electron repulsion term

$$W = \tfrac{1}{2}{\sum_{u,v}}' w(\mathbf{r}_u, \mathbf{r}_v), \tag{4.29}$$

where the prime on the summation sign indicates $u \neq v$ and the $\frac{1}{2}$ factor eliminates doubly-counted summands. To express (4.29) in c-operator language, we have to perform some lengthy analysis. Since this is available in the loc. cit. texts, we omit it here, in the interest of brevity, and merely quote the result, viz.,

$$W = \tfrac{1}{2} \sum_{i,j,k,\ell} w_{ijk\ell} c_i^\dagger c_j^\dagger c_k c_\ell, \tag{4.30}$$

which, being a 2-electron term, contains *two pairs* of $c_u^\dagger c_v$ operators, as expected.

In (4.28) and (4.30), we have achieved our aim of expressing the Hamiltonian in the appropriate *second quantized* form for acting on the state vectors in Fock space.

4.2 ANG Hamiltonian

At this point, we have reached the stage where we can describe the adatom-substrate system in terms of the ANG Hamiltonian (Muscat and Newns 1978, Grimley 1983). We consider the case of *anionic* chemisorption (§1.2.2), where a $\downarrow$-spin electron in the substrate level ε_k, below the *Fermi level* (FL) ε_F, "hops over" into the *affinity level* (A) of the adatom, whose $\uparrow$-spin electron resides in the lower *ionization level* (I), as in Fig. 4.1. Thus, the *intra-atomic electron Coulomb repulsion energy* on the adatom (a) is

$$U = |I - A|, \tag{4.31}$$

and (4.30) reduces to

$$W = \tfrac{1}{2} U n_{a\sigma} n_{a,-\sigma} \tag{4.32}$$

via (4.14), where $\sigma = +(-)$ labels the $\uparrow$ ($\downarrow$) electron spin.

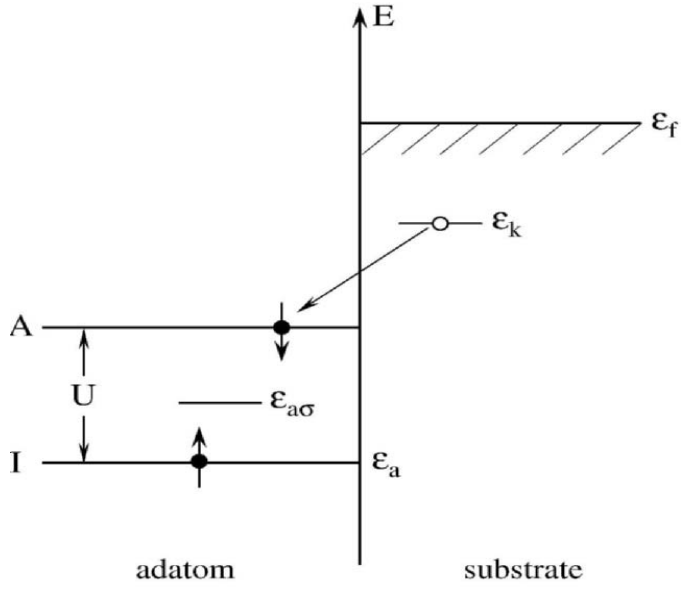

Fig. 4.1. Anionic chemisorption energy-level diagram showing transfer of $\downarrow$-spin electron from substrate level ε_k to affinity level A on adatom, while experiencing Coulomb repulsion U from $\uparrow$-spin electron in ionization level I. ε_f is the substrate Fermi level.

Using (4.28) and (4.32) with (4.14), we can now write the ANG Hamiltonian of the combined adatom-substrate system as

$$H = \sum_{\sigma} \Big\{ [\varepsilon_a n_{a\sigma} + \tfrac{1}{2} U n_{a\sigma} n_{a,-\sigma}] + \sum_{k} [\varepsilon_k n_{k\sigma} + (V_{ak} c^{\dagger}_{a\sigma} c_{k\sigma} + V^{*}_{ka} c^{\dagger}_{k\sigma} c_{a\sigma})] \Big\}, \tag{4.33}$$

where $\varepsilon_a (= I)$ is the adatom site energy and k labels the substrate energy levels. The last term in (4.33) is the "hopping term" coupling the adatom states $a\sigma$ with the substrate states $k\sigma$.

Invoking the *Hartree-Fock approximation* (HFA) (Salem 1966), means that we can replace $U n_{a,-\sigma}$ in (4.33) by an "averaged" *self-energy* $U\langle n_{a,-\sigma}\rangle$, whereby an *effective* adatom level of spin σ is defined by[2]

[2]Equation (4.34) is sometimes called the *spin-unrestricted* HFA, because it allows solutions in which self-consistent adatom orbitals of opposite spin have *different* energies

$$\varepsilon_{a\sigma} = \varepsilon_a + U\langle n_{a,-\sigma}\rangle, \tag{4.34}$$

$\langle n_{a,-\sigma}\rangle$ being the *adoccupancy* of the $-\sigma$ spin state, so (4.33) can be approximated by

$$H = \sum_\sigma H^\sigma = \sum_\sigma \Big\{ \varepsilon_{a\sigma} n_{a\sigma} + \sum_k [\varepsilon_k n_{k\sigma} + (V_{ak} c^\dagger_{a\sigma} c_{k\sigma} + V^*_{ka} c^\dagger_{k\sigma} c_{a\sigma})] \Big\}. \tag{4.35}$$

4.3 Hartree-Fock Treatment

4.3.1 Perturbed energy

In the HFA, the Schrödinger equation for the σ-spin *ground state* is

$$H^\sigma \Phi^\sigma_0 = \varepsilon_0 \Phi^\sigma_0, \tag{4.36}$$

where the wave function Φ^σ_0 is written as the antisymmetric product (Anderson 1961)

$$\Phi^\sigma_0 = \prod_{\varepsilon_{m\sigma} < \varepsilon_F} c^\dagger_{m\sigma} |0\rangle, \tag{4.37}$$

$\varepsilon_{m\sigma}$ being the perturbed 1-electron energy.

If the operator $c^\dagger_{m\sigma}$ creates an excitation of energy $\varepsilon_0 + \varepsilon_{m\sigma}$, then

$$H^\sigma c^\dagger_{m\sigma} \Phi^\sigma_0 = (\varepsilon_0 + \varepsilon_{m\sigma}) c^\dagger_{m\sigma} \Phi^\sigma_0, \tag{4.38}$$

since the excited state $c^\dagger_{m\sigma}\Phi^\sigma_0$ is also an eigenfunction of the spin-dependent Fock Hamiltonian H^σ. With the aid of (4.36), equation (4.38) can be expressed as

$$[H^\sigma, c^\dagger_{m\sigma}]\Phi^\sigma_0 = \varepsilon_{m\sigma} c^\dagger_{m\sigma} \Phi^\sigma_0, \tag{4.39}$$

in which [,] denotes the *commutator* defined by

$$[a, b] = ab - ba. \tag{4.40}$$

($\varepsilon_{a+} \neq \varepsilon_{a-}$, i.e., $\langle n_{a+}\rangle \neq \langle n_{a-}\rangle$), as opposed to the *spin-restricted* HFA, where orbitals are restricted to the *same* energy (i.e., $\varepsilon_{a+} = \varepsilon_{a-}$, $\langle n_{a+}\rangle = \langle n_{a-}\rangle$).

The solution of (4.39) is sought by putting (cf. (2.50))

$$c^\dagger_{m\sigma} = \langle m|a\rangle_\sigma c^\dagger_{a\sigma} + \sum_k \langle m|k\rangle_\sigma c^\dagger_{k\sigma} \tag{4.41}$$

and commuting it with H^σ in (4.35) to give

$$\begin{aligned}[H^\sigma, c^\dagger_{m\sigma}] = \varepsilon_{a\sigma}[n_{a\sigma}, c^\dagger_{m\sigma}] + \sum_k \Big\{ & \varepsilon_k [n_{k\sigma}, c^\dagger_{m\sigma}] \\ & + (V_{ak}[c^\dagger_{a\sigma} c_{k\sigma}, c^\dagger_{m\sigma}] + V^*_{ka}[c^\dagger_{k\sigma} c_{a\sigma}, c^\dagger_{m\sigma}]) \Big\}\end{aligned} \tag{4.42}$$

Now, in general, using (4.12) shows that

$$\left[c^\dagger_{p\sigma} c_{q\sigma}, c^\dagger_{m\sigma}\right] = c^\dagger_{p\sigma}\delta_{qm}, \tag{4.43}$$

which in (4.42) leads to

$$\begin{aligned}[H^\sigma, c^\dagger_{k\sigma}] &= \varepsilon_k c^\dagger_{k\sigma} + V_{ak} c^\dagger_{a\sigma}\,;\; m = k, \\ [H^\sigma, c^\dagger_{a\sigma}] &= \varepsilon_{a\sigma} c^\dagger_{a\sigma} + \sum_k V^*_{ka} c^\dagger_{k\sigma}\,;\; m = a.\end{aligned} \tag{4.44}$$

Meanwhile, (4.41) in (4.39) gives

$$\begin{aligned}\Big\{ \langle m|a\rangle_\sigma [H^\sigma, c^\dagger_{a\sigma}] + \sum_k \langle m|k\rangle_\sigma [H^\sigma, c^\dagger_{k\sigma}] \Big\} \Phi_0 \\ = \varepsilon_{m\sigma} \left(\langle m|a\rangle_\sigma c^\dagger_{a\sigma} + \sum_k \langle m|k\rangle_\sigma c^\dagger_{k\sigma} \right) \Phi_0,\end{aligned} \tag{4.45}$$

which by (4.44) yields

$$\begin{aligned}\Big(\langle m|a\rangle_\sigma \varepsilon_{a\sigma} + \sum_k \langle m|k\rangle_\sigma V_{ak} \Big) c^\dagger_{a\sigma} \\ + \sum_k \left(\langle m|a\rangle_\sigma V^*_{ka} + \langle m|k\rangle_\sigma \varepsilon_k \right) c^\dagger_{k\sigma} \\ = \left(\langle m|a\rangle_\sigma c^\dagger_{a\sigma} + \sum_k \langle m|k\rangle_\sigma c^\dagger_{k\sigma} \right) \varepsilon_{m\sigma}.\end{aligned} \tag{4.46}$$

On equating the coefficients of $c^\dagger_{a\sigma}$ and $c^\dagger_{k\sigma}$, we arrive at

$$\varepsilon_{m\sigma}\langle m|a\rangle_\sigma = \varepsilon_{a\sigma}\langle m|a\rangle_\sigma + \sum_k V_{ak}\langle m|k\rangle_\sigma, \tag{4.47}$$

$$\varepsilon_{m\sigma}\langle m|k\rangle_\sigma = \varepsilon_k\langle m|k\rangle_\sigma + V^*_{ka}\langle m|a\rangle_\sigma, \tag{4.48}$$

which are the *equations of motion* for $\langle m|a\rangle_\sigma$ and $\langle m|k\rangle_\sigma$, respectively (Anderson 1961).

Forming (4.47) $\langle a|m\rangle_\sigma$ and $\sum_k$ (4.48) $\langle k|m\rangle_\sigma$ yields

$$\varepsilon_{m\sigma}\left|\langle m|a\rangle_\sigma\right|^2 = \varepsilon_{a\sigma}\left|\langle m|a\rangle_\sigma\right|^2 + \sum_k V_{ak}\langle m|k\rangle_\sigma\langle a|m\rangle_\sigma, \tag{4.49}$$

$$\sum_k \varepsilon_{m\sigma}\left|\langle m|k\rangle_\sigma\right|^2 = \sum_k \left(\varepsilon_k\left|\langle m|k\rangle_\sigma\right|^2 + V^*_{ka}\langle m|a\rangle_\sigma\langle k|m\rangle_\sigma\right), \tag{4.50}$$

respectively. However, since

$$\left|\langle m|a\rangle_\sigma\right|^2 + \sum_k \left|\langle m|k\rangle_\sigma\right|^2 = 1, \tag{4.51}$$

adding (4.49) and (4.50) gives

$$\varepsilon_{m\sigma} = \varepsilon_{a\sigma}\left|\langle m|a\rangle_\sigma\right|^2 + \sum_k \left[\varepsilon_k\left|\langle m|k\rangle_\sigma\right|^2 + \left(V_{ak}\langle m|k\rangle_\sigma\langle a|m\rangle_\sigma + h.c.\right)\right], \tag{4.52}$$

where h.c. stands for the *hermitian conjugate* of the preceding term. Inserting (4.34), and summing over all *occupied* levels, we obtain

$$\begin{aligned}\sum_{m,\sigma}\varepsilon_{m\sigma} = \sum_{m,\sigma}\Bigg[&\sum_q \varepsilon_q\left|\langle m|q\rangle_\sigma\right|^2 \\ &+ \sum_k \left(V_{ak}\langle m|k\rangle_\sigma\langle a|m\rangle_\sigma + h.c.\right)\Bigg] \\ &+ U\sum_\sigma\langle n_{a,-\sigma}\rangle\sum_m\left|\langle m|a\rangle_\sigma\right|^2,\end{aligned} \tag{4.53}$$

in which q runs over a and k. Taking a closer look at the last summation, we observe that

$$\begin{aligned}\sum_m\left|\langle m|a\rangle_\sigma\right|^2 &= \sum_m\langle m|a\rangle_\sigma\langle a|m\rangle_\sigma = \sum_m\langle m|a\rangle_\sigma\langle 0|0\rangle\langle a|m\rangle_\sigma \\ &= \sum_m\langle m\sigma|c^\dagger_{a\sigma}c_{a\sigma}|m\sigma\rangle = \sum_m\langle m\sigma|n_{a\sigma}|m\sigma\rangle = \langle n_{a\sigma}\rangle,\end{aligned} \tag{4.54}$$

where we have used (4.16) and (4.18). Thus, (4.53) becomes

$$\sum_{m,\sigma}\varepsilon_{m\sigma}=\sum_{m,\sigma}\left[\sum_{q}\varepsilon_{q}\left|\langle m|q\rangle_{\sigma}\right|^{2}+\sum_{k}\left(V_{ak}\langle m|k\rangle_{\sigma}\langle a|m\rangle_{\sigma}+h.c.\right)\right]$$
$$+2U\langle n_{a+}\rangle\langle n_{a-}\rangle, \tag{4.55}$$

via (4.54).

From (4.33) and (4.34), we see that the ANG Hamiltonian can be written as

$$H=\sum_{\sigma}\left[\sum_{q}\varepsilon_{q}n_{q\sigma}+\sum_{k}\left(V_{ak}c_{a\sigma}^{\dagger}c_{k\sigma}+h.c.\right)\right]+U\langle n_{a-}\rangle n_{a+}. \tag{4.56}$$

Hence, in the HF ground-state Φ_0, the energy expectation value of the *perturbed* system is

$$E=\langle\Phi_{0}|H|\Phi_{0}\rangle=\sum_{n,\sigma}\left[\sum_{q}\varepsilon_{q}\left|\langle n|q\rangle_{\sigma}\right|^{2}+\sum_{k}\left(V_{ak}\langle n|k\rangle_{\sigma}\langle a|n\rangle_{\sigma}+h.c.\right)\right]$$
$$+U\langle n_{a+}\rangle\langle n_{a-}\rangle, \tag{4.57}$$

by (4.54). Comparing (4.55) with (4.57), reveals that the *perturbed energy*

$$E=\sum_{\substack{m,\sigma\\ occ}}\varepsilon_{m\sigma}-U\langle n_{a+}\rangle\langle n_{a-}\rangle, \tag{4.58}$$

where the U-term appears negatively, because it is counted twice in the preceding Fock eigenvalues summation.

4.3.2 Adatom Green function and density of states

In matrix notation, the GF, $G_{q\ell}^{\sigma}$, is defined by

$$\sum_{q}(E-H^{\sigma})_{pq}G_{q\ell}^{\sigma}=\delta_{p\ell}, \tag{4.59}$$

where, as in (3.7), we have introduced the concept of complex energy, viz.,

$$E=\varepsilon+is,\qquad s=0^{+} \tag{4.60}$$

to handle the singularity in the GF matrix $\mathbf{G}^\sigma(\varepsilon)$ at the eigenvalue of $\mathbf{H}^\sigma$.

For $p = \ell = a$, (4.59) becomes

$$\sum_q (E - H^\sigma)_{aq} G^\sigma_{qa} = 1,$$

i.e., since $q = a$ or k,

$$(E - H^\sigma)_{aa} G^\sigma_{aa} + \sum_k (E - H^\sigma)_{ak} G^\sigma_{ka} = 1. \tag{4.61}$$

With the aid of (4.35), we find

$$\begin{aligned} (E - H^\sigma)_{aa} &= \langle a|E - H^\sigma|a\rangle \\ &= E\langle a|a\rangle - \langle a|H^\sigma|a\rangle \\ &= E - \varepsilon_{a\sigma}. \end{aligned} \tag{4.62}$$

Similarly,

$$\begin{aligned} (E - H^\sigma)_{ak} &= E\langle a|k\rangle - \langle a|H^\sigma|k\rangle \\ &= -V_{ak}. \end{aligned} \tag{4.63}$$

Thus, (4.62) and (4.63) in (4.61) give

$$(E - \varepsilon_{a\sigma}) G^\sigma_{aa} - \sum_k V_{ak} G^\sigma_{ka} = 1. \tag{4.64}$$

For $p = k$ and $\ell = a$, (4.59) yields

$$(E - H^\sigma)_{ka} G^\sigma_{aa} + \sum_{k'} (E - H^\sigma)_{kk'} G^\sigma_{k'a} = 0,$$

which by (4.35) leads to

$$-V^*_{ka} G^\sigma_{aa} + \sum_{k'} (E - \varepsilon_{k'}) \delta_{kk'} G^\sigma_{k'a} = 0,$$

whence,

$$G^\sigma_{ka} = V^*_{ka} G^\sigma_{aa} (E - \varepsilon_k)^{-1}. \tag{4.65}$$

Inserting (4.65) in (4.64), we arrive at

$$G^{\sigma}_{aa}(E) = \left[E - \varepsilon_{a\sigma} - \sum_k |V_{ak}|^2 (E - \varepsilon_k)^{-1} \right]^{-1}. \tag{4.66}$$

In view of (4.60) and the *Plemelj formula* (D.9), the summation in (4.66) can be evaluated by writing

$$\begin{aligned} \sum_k |V_{ak}|^2 (\varepsilon - \varepsilon_k + is)^{-1} &= \sum_k |V_{ak}|^2 \int_{-\infty}^{\infty} (\varepsilon - \varepsilon' + is)^{-1} \delta(\varepsilon' - \varepsilon_k) d\varepsilon' \\ &= P \int_{-\infty}^{\infty} \sum_k |V_{ak}|^2 (\varepsilon - \varepsilon')^{-1} \delta(\varepsilon' - \varepsilon_k) d\varepsilon' \\ &\quad - i\pi \int_{-\infty}^{\infty} \sum_k |V_{ak}|^2 \delta(\varepsilon' - \varepsilon_k) \delta(\varepsilon - \varepsilon') d\varepsilon', \end{aligned}$$

i.e.,

$$\sum_k |V_{ak}|^2 (\varepsilon - \varepsilon_k + is)^{-1} = \Lambda(\varepsilon) - i\Delta(\varepsilon), \tag{4.67}$$

where the so-called *chemisorption functions*

$$\Delta(\varepsilon) = \pi \sum_k |V_{ak}|^2 \delta(\varepsilon - \varepsilon_k), \tag{4.68}$$

$$\Lambda(\varepsilon) = \pi^{-1} P \int_{-\infty}^{\infty} (\varepsilon - \varepsilon')^{-1} \Delta(\varepsilon') d\varepsilon', \tag{4.69}$$

the latter being the *Hilbert transform of the spectral density* $\Delta(\varepsilon)$. Hence, from (4.66) and (4.67), we see that the *adatom GF* is

$$G^{\sigma}_{aa}(\varepsilon) = \left[\varepsilon - \varepsilon_{a\sigma} - \Lambda(\varepsilon) + i\Delta(\varepsilon) \right]^{-1}. \tag{4.70}$$

Noting that the Greenian operator

$$G^{\sigma}(\varepsilon + is) = (\varepsilon + is - H^{\sigma})^{-1}, \tag{4.71}$$

we have

$$\begin{aligned} \operatorname{Tr} G^{\sigma}(\varepsilon + is) &= \sum_m \langle m | G^{\sigma} | m \rangle_{\sigma} \\ &= \sum_m (\varepsilon + is - \varepsilon_{m\sigma})^{-1}, \end{aligned} \tag{4.72}$$

$\varepsilon_{m\sigma}$ being given by (4.52). Equations (D.1), (D.9) and (4.72) show that the *energy* DOS

$$\rho^{\sigma}(\varepsilon) = \sum_{m} \delta(\varepsilon - \varepsilon_{m\sigma}) = -\pi^{-1}\mathrm{Im}\ \left[Tr\, G^{\sigma}(\varepsilon + is)\right]. \tag{4.73}$$

However, using (2.8), we obtain

$$\begin{aligned} G^{\sigma}_{aa} &= \sum_{m,n} \langle a|m\sigma\rangle\langle m\sigma|G^{\sigma}|n\sigma\rangle\langle n\sigma|a\rangle \\ &= \sum_{m} |\langle a|m\sigma\rangle|^2 (\varepsilon + is - \varepsilon_{m\sigma})^{-1}, \end{aligned} \tag{4.74}$$

so the *projected* DOS for the adatom orbital, in terms of the Fock eigenfunctions $|m\sigma\rangle$, is

$$\begin{aligned} \rho^{\sigma}_{aa}(\varepsilon) &= \sum_{m} |\langle m\sigma|a\rangle|^2 \delta(\varepsilon - \varepsilon_{m\sigma}) \\ &= -\pi^{-1}\mathrm{Im}\, G^{\sigma}_{aa}(\varepsilon) \\ &= \frac{\pi^{-1}\Delta(\varepsilon)}{[\varepsilon - \varepsilon_{a\sigma} - \Lambda(\varepsilon)]^2 + \Delta^2(\varepsilon)}, \end{aligned} \tag{4.75}$$

via (4.72) to (4.74) and (4.70).

4.3.3 Adoccupancy and self-consistency

In order to evaluate the energies $\varepsilon_{a\sigma}$ (4.34) and $\varepsilon_{m\sigma}$ (4.52), it is necessary to know the *adoccupancy*, which is given by

$$\langle n_{a\sigma}\rangle = \int_{B} \rho^{\sigma}_{aa}(\varepsilon) d\varepsilon + \sum_{\ell} \langle n_{a\sigma}\rangle_{\ell}, \tag{4.76}$$

where the integration is over the occupied bulk band B and the summation is over any *localized* state below the FL. The summand in (4.76) can be written as

$$\begin{aligned} \langle n_{a\sigma}\rangle_{\ell} &= \langle \ell\sigma|n_{a\sigma}|\ell\sigma\rangle = \langle \ell\sigma|c^{\dagger}_{a\sigma}c_{a\sigma}|\ell\sigma\rangle \\ &= \langle \ell\sigma|a\rangle\langle 0|0\rangle\langle a|\ell\sigma\rangle \\ &= \langle \ell\sigma|a\rangle\langle a|\ell\sigma\rangle = |\langle \ell\sigma|a\rangle|^2, \end{aligned} \tag{4.77}$$

via (4.14), (4.16) and (4.18). From (4.74) and (4.77), we note that

$$\operatorname{Res} G^{\sigma}_{aa}(\varepsilon_{\ell\sigma}) = |\langle \ell\sigma|a\rangle|^2 = \langle n_{a\sigma}\rangle_{\ell}, \tag{4.78}$$

whence, the adoccupancy derives from the perturbed Greenian matrix G^{σ}_{aa}. Furthermore, since $\Delta(\varepsilon) = 0$ outside B, (4.70) yields[3]

$$\operatorname{Res} G^{\sigma}_{aa}(\varepsilon_{\ell\sigma}) = \left[1 - \Lambda'(\varepsilon_{\ell\sigma})\right]^{-1}, \tag{4.79}$$

the prime denoting differentiation. Thus, (4.78) and (4.79) show that (Newns 1969)

$$\langle n_{a\sigma}\rangle_{\ell} = \left[1 - \Lambda'(\varepsilon_{\ell\sigma})\right]^{-1}. \tag{4.80}$$

Returning to (4.76), we see that the right-hand side depends on $\varepsilon_{a\sigma}$, which in turn is a function of $\langle n_{a,-\sigma}\rangle$ (4.34). We can express this dependence via the *self-consistent equations*

$$\begin{aligned} \langle n_{a\sigma}\rangle &= N\left(\langle n_{a,-\sigma}\rangle\right), \\ \langle n_{a,-\sigma}\rangle &= N\left(\langle n_{a\sigma}\rangle\right), \end{aligned} \tag{4.81}$$

which can be combined into the single equation

$$\langle n_{a\sigma}\rangle - N\left[N(\langle n_{a\sigma}\rangle)\right] = 0, \tag{4.82}$$

[3]From complex variable theory (Marsden 1973), for $f(z) = g(z)/h(z)$, $\operatorname{Res}_{z=a} f(z) = g(a)/h'(a)$.

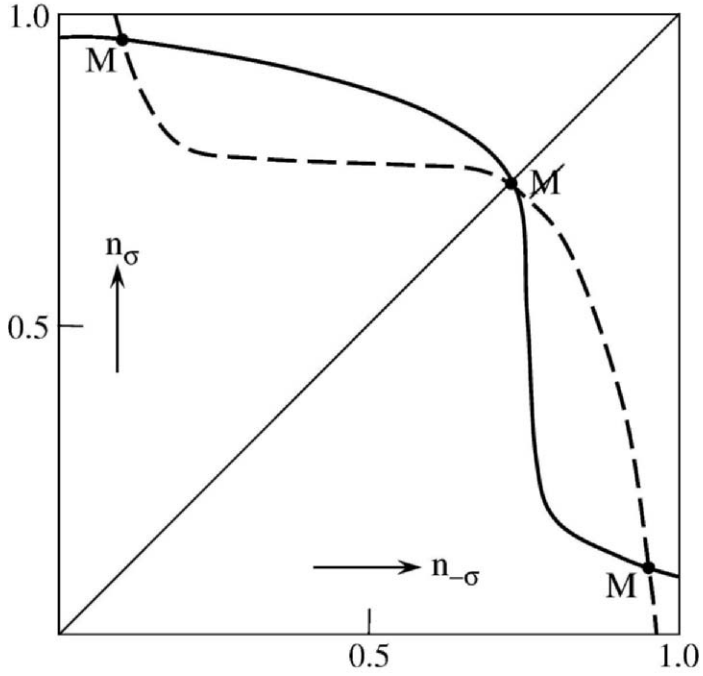

Fig. 4.2. Self-consistency plots of $n_{-\sigma} = N(n_{-\sigma})$ (solid line) and $n_\sigma = N(n_\sigma)$ (broken line), showing $\not{M}$ - and M-solutions at intersections. $n_\sigma = n_{-\sigma} = 0.73$.

whose numerical solution determines the adoccupancy $\langle n_{a\sigma}\rangle$. Equation (4.82) always has a *non-magnetic* ($\not{M}$) solution at $\langle n_{a\sigma}\rangle = \langle n_{a,-\sigma}\rangle$ and may (or may not) have *magnetic* (M) ones for which $\langle n_{a\sigma}\rangle \neq \langle n_{a,-\sigma}\rangle$. Typical self-consistency plots of (4.82) are portrayed in Fig. 4.2.

4.3.4 Chemisorption energy and charge transfer

If a single electron is in AO $|a\rangle$, the *unperturbed* ground-state energy of the *non-interacting* adatom and substrate is

$$E_0 = 2\sum_{\substack{k\\ occ}} \varepsilon_k + \varepsilon_a, \tag{4.83}$$

the factor 2 arising because of spin degeneracy.

As in (1.92), the *chemisorption energy* is the difference between the electronic energy of the adatom-substrate system *before* and *after* the interaction occurs, i.e.,

$$\Delta E = E - E_0, \tag{4.84}$$

which by (4.58) and (4.83) leads to

$$\Delta E = \sum_{\sigma} \Delta E^{\sigma} - \varepsilon_a + \varepsilon_f - U\langle n_{a+}\rangle\langle n_{a-}\rangle, \tag{4.85}$$

where

$$\Delta E^{\sigma} = \sum_{\substack{m\\ occ}} \varepsilon_{m\sigma} - \sum_{\substack{k\\ occ}} \varepsilon_k. \tag{4.86}$$

Since $\langle n_{a\sigma}\rangle$ is given by (4.76), the problem of finding ΔE reduces to that of calculating ΔE^{σ}.

In order to perform this task, we introduce the function (Newns 1967)

$$g(\varepsilon) = f'(\varepsilon)/f(\varepsilon) = d\left[\ln f(\varepsilon)\right]/d\varepsilon, \tag{4.87}$$

where $f(\varepsilon)$ is a *meromorphic function*, which is analytic in a contour C, except at a finite number of poles (Marsden 1973). If $\omega_+(\omega_-)$ are the zeros (poles) of $f(\varepsilon)$ in the contour C, which are of order r, then, for $\varepsilon \simeq \omega_{\pm}$, (4.87) gives (App. E)

$$g(\varepsilon)\Big|_{\varepsilon=\omega_+} \simeq +r(\varepsilon-\omega_+)^{-1}, \tag{4.88}$$

$$g(\varepsilon)\Big|_{\varepsilon=\omega_-} \simeq r(\varepsilon-\omega_-)^{-1}, \tag{4.89}$$

whence,[3]

$$\operatorname{Res} g(\varepsilon)\Big|_{\varepsilon=\omega_\pm} = \pm r. \tag{4.90}$$

Now the function

$$f(\varepsilon) = \varepsilon - \varepsilon_{a\sigma} - \sum_k |V_{ak}|^2 (\varepsilon - \varepsilon_k)^{-1} \tag{4.91}$$

in (4.66) has a zero (pole) of order r at an r-fold degenerate perturbed (unperturbed) eigenvalue $\varepsilon_{m\sigma}(\varepsilon_k)$. The graph showing the solutions of $f(\varepsilon) = 0$ is drawn in Fig. 4.3 for the *1-band system*. The interpolative property of the perturbed eigenvalues lying between the unperturbed ones is observed; the perturbation merely causing a small shift in all the eigenvalues within the unperturbed bands. Addition of the adatom orbital $|a\rangle$ gives rise to eigenvalues outside the bands.

By setting

$$\Delta E^\sigma = (2\pi i)^{-1} \int_C \varepsilon g(\varepsilon) d\varepsilon, \tag{4.92}$$

where the contour C contains all the *occupied* eigenvalues in the complex plane (Fig. 4.4), each occupied unperturbed (perturbed) eigenvalue $\varepsilon_k(\varepsilon_{m\sigma})$ with degeneracy r contributes $-2\pi i r \varepsilon_k$ $(2\pi i r \varepsilon_{m\sigma})$ to the integral, so the *whole integral* equals the value of ΔE^σ in (4.86) (Whittaker and Watson 1965). To a good approximation, it is immaterial where the right-hand side of C crosses the real axis, since eigenvalues in this region make only a very small contribution.

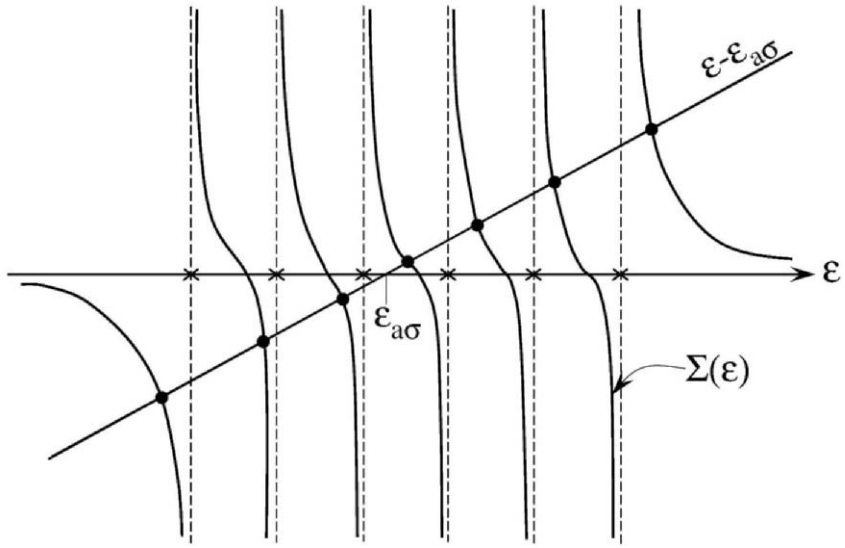

Fig. 4.3. Graphical solution of $f(\varepsilon) = 0$, where $\times(\bullet)$ is unperturbed (perturbed) eigenvalue and $\Sigma(\varepsilon) = \sum_k |V_{ak}|^2(\varepsilon - \varepsilon_k)^{-1}$.

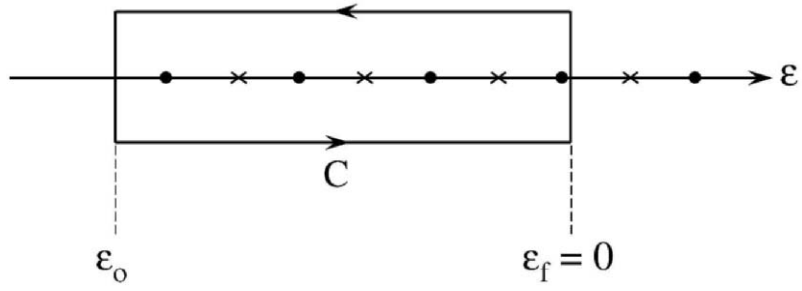

Fig. 4.4. Contour C containing occupied unperturbed $(\times)$ and perturbed $(\bullet)$ eigenvalues. $\varepsilon_0(\varepsilon_f)$ denotes lower band edge (Fermi Level).

Integrating (4.92) by parts, using (4.87), gives

$$\Delta E^{\sigma} = (2\pi i)^{-1} \left[\varepsilon \ln f(\varepsilon)\big|_c - \int_C \ln f(\varepsilon) d\varepsilon \right], \tag{4.93}$$

whose first term can be reduced to zero, without affecting the value of (4.93) appreciably, by distorting the high-energy end of C, so that it contains an even number of poles and zeros (Whittaker and Watson 1965). Hence, (4.60), (4.91) and (4.93) yield

$$\Delta E^{\sigma} = -(2\pi i)^{-1} \int_C \ln \left[\varepsilon + is - \varepsilon_{a\sigma} - \Sigma_+(\varepsilon) \right] d\varepsilon, \tag{4.94}$$

where

$$\Sigma_{\pm}(\varepsilon) = \sum_k |V_{ak}|^2 (\varepsilon \pm is - \varepsilon_k)^{-1}. \tag{4.95}$$

Following Newns (1969), if we take C (Fig. 4.4) to be the rectangular contour defined by the points $\varepsilon_0 \pm is$ and $\pm is$, then the end portions may be neglected as $s \to 0^+$, and (4.94) becomes[4]

$$\begin{aligned} \Delta E^{\sigma} = -(2\pi i)^{-1} \Bigg\{ & \int_{\varepsilon_0}^{0} \ln[\varepsilon - is - \varepsilon_{a\sigma} - \Sigma_-(\varepsilon)] d\varepsilon \\ & + \int_{0}^{\varepsilon_0} \ln[\varepsilon + is - \varepsilon_{a\sigma} - \Sigma_+(\varepsilon)] d\varepsilon \Bigg\}, \end{aligned} \tag{4.96}$$

which, on taking $s \to 0^+$ and utilizing (D.9) and (4.67), leads to

$$\begin{aligned} \Delta E^{\sigma} = -(2\pi i)^{-1} \Bigg\{ & \int_{\varepsilon_0}^{0} \ln[\varepsilon - \varepsilon_{a\sigma} - \Lambda(\varepsilon) - i\Delta(\varepsilon)] d\varepsilon \\ & - \int_{\varepsilon_0}^{0} \ln[\varepsilon - \varepsilon_{a\sigma} - \Lambda(\varepsilon) + i\Delta(\varepsilon)] d\varepsilon \Bigg\}. \end{aligned} \tag{4.97}$$

However, from (F.8), we have

$$\ln(x \pm iy) = \ln|x \pm iy| \pm i \tan^{-1}(y/x). \tag{4.98}$$

Inserting (4.98) in (4.97), we see that the logarithmic functions cancel out, so that

$$\Delta E^{\sigma} = \pi^{-1} \int_{\varepsilon_0}^{0} \tan^{-1} \left[\frac{\Delta(\varepsilon)}{\varepsilon - \varepsilon_{a\sigma} - \Lambda(\varepsilon)} \right] d\varepsilon, \tag{4.99}$$

[4]Note also, when $\alpha = \varepsilon_f = 0$ in (1.16) and (1.18), $\varepsilon_\theta = 2\beta \cos\theta$, so $\varepsilon_0 = 2\beta (< 0)$.

where we take $-\pi < \tan^{-1} < 0$ (App. G). If an occupied localized state $\varepsilon_{\ell\sigma}$ exists below the band B, say, then the contour C should include both the occupied B levels and the isolated pole at $\varepsilon_{\ell\sigma}$. In this case, it is convenient to split C into two parts C_1 and C_2, where C_1 encloses $\varepsilon_{\ell\sigma}$ and the lowest unperturbed B level at ε_0, and C_2 the remaining occupied B levels $\varepsilon_{m\sigma}$ and ε_k. The contribution from C_1 is $\varepsilon_{\ell\sigma} - \varepsilon_0$. The removal of one perturbed and one unperturbed level from the bottom of B does not affect the C_2 contribution. Thus, (4.99) now becomes

$$\Delta E^{\sigma} = \varepsilon_{\ell\sigma} - \varepsilon_0 + \pi^{-1} \int_{\varepsilon_0}^{0} \tan^{-1} \left[\frac{\Delta(\varepsilon)}{\varepsilon - \varepsilon_{a\sigma} - \Lambda(\varepsilon)} \right] d\varepsilon, \tag{4.100}$$

which in (4.85) provides the *chemisorption energy* expression

$$\begin{aligned} \Delta E = \sum_{\sigma} \left\{ \varepsilon_{\ell\sigma} + \pi^{-1} \int_{\varepsilon_0}^{0} \tan^{-1} \left[\frac{\Delta(\varepsilon)}{\varepsilon - \varepsilon_{a\sigma} - \Lambda(\varepsilon)} \right] d\varepsilon \right\} \\ - \varepsilon_a - U \langle n_{a+} \rangle \langle n_{a-} \rangle, \end{aligned} \tag{4.101}$$

where $0 < \tan^{-1} < \pi$,[5] when an occupied localized state exists at $\varepsilon_{\ell\sigma}$, but $-\pi < \tan^{-1} < 0$ and $\varepsilon_{\ell\sigma} = 0$, if not. It is interesting to note that (4.101) is the same functional form as (1.93), but now contains the adatom *electron-electron interaction* features.

Lastly, we come to the *adatom charge transfer*, which is obtained from

$$\Delta q = \left(\sum_{\sigma} \langle n_{a\sigma} \rangle - 1 \right) e, \tag{4.102}$$

where e is the electronic charge. When $\Delta q > 0 (\Delta q < 0)$ the transfer is to (from) the adatom from (to) the substrate.

Having formulated the ANG model, in terms of a 1-band metallic substrate, we now apply it to a 2-band semiconductor.

4.4 Oxygen on III-V Semiconductors

For atomic oxygen, $I = -13.6eV$ (Day and Selbin 1962), while $A = -1.48eV$ is below the vacuum level of the isolated oxygen atom. Since image-charge

[5] This amounts to introducing a contribution of $-\pi^{-1} \int_{\varepsilon_0}^{0} \pi d\varepsilon$ into (4.100), which removes the $-\varepsilon_0$ term (Newns 1974).

effects push the A-level below the substrate's FL, in the chemisorbed state (Engel and Gomer 1970), *both* I and A lie below ε_f, so the adsorbate is negatively charged, and we have the *anionic* chemisorption situation of Fig. 4.1 (Kranz 1978).

4.4.1 Electronic properties of AB-type semiconductor

We can represent a III-V semiconductor substrate by a binary chain of $2N$ A and B atoms with s- and p-orbitals associated with them, respectively (Fig. 4.5). The site energy at an $A(B)$ atom is $\varepsilon_A(\varepsilon_B)$, and the $A-B(B-A)$ bond energy is $-\beta(\beta)$. The adatom a is characterized by the site energy ε_a and interacts with the semiconductor surface A-atom at $n=1$ via the bond of energy β' (Davison and Huang 1974).

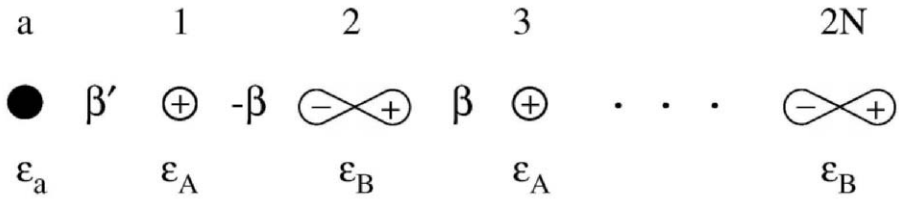

Fig. 4.5. *sp*-orbital model of AB-binary semiconductor of $2N$ atoms interacting with adatom a. Reprinted from Davison and Huang (1974) with permission from Elsevier.

Within the framework of the MO-TBA method (§1.1), the Schrödinger equation for an AB-chain can be written as a pair of coupled difference equations, namely, (Davison and Levine 1970)

$$(X-z)c_n = c_{n-1} - c_{n+1}, \quad n \quad \text{odd}, \tag{4.103}$$

$$(X+z)c_n = c_{n+1} - c_{n-1}, \quad n \quad \text{even}, \tag{4.104}$$

where, in reduced notation,

$$X = (\varepsilon_k - \bar{\varepsilon})/\beta, \quad \bar{\varepsilon} = (\varepsilon_A + \varepsilon_B)/2, \quad z = (\varepsilon_A - \varepsilon_B)/2\beta, \tag{4.105}$$

ε_k being the energy of the electron in the kth state and z the *composition parameter*. On taking the *zero of energy* at $\bar{\varepsilon} = \varepsilon_f = 0$, so that

$$\varepsilon_A = -\varepsilon_B = \lambda, \tag{4.106}$$

the solutions of (4.103) and (4.104) become (App. H)

$$\varepsilon_k^{\pm} = \pm(\lambda^2 + 4\beta^2 \sin^2 k)^{1/2}, \tag{4.107}$$

for a chain of *unit* atomic spacing, and

$$|k\rangle = R(k) \left(\sum_{\substack{n \\ \text{odd}}} \sin nk|n\rangle + K \sum_{\substack{n \\ \text{even}}} \cos nk|n\rangle \right), \tag{4.108}$$

where the normalization factor (App. I)

$$R(k) = 2\left[(1 + |K|^2)(2N - 1) + 2\right]^{-1/2}, \tag{4.109}$$

with

$$K = 2i\beta \sin k/(\varepsilon_k^{\pm} + \lambda), \tag{4.110}$$

from (4.104) and (4.108), and

$$k = j\pi/(2N + 1); \quad j = 1, 2, \ldots, N, \tag{4.111}$$

via the condition that $c_{2N+1} = 0$. For N *large*, we note that $k \simeq 0$ when $j = 1$, and $k \simeq \pi/2$ when $j = N$. Moreover, we have

$$dk = \frac{(j+1)\pi}{2N+1} - \frac{j\pi}{2N+1} = \frac{\pi}{2N+1},$$

whence, in converting a summation into an integral we write

$$(2N + 1)^{-1} \sum_k \underset{N\to\infty}{=} \pi^{-1} \int dk. \tag{4.112}$$

Turning to the question of the energy DOS, (4.73) gives

$$\rho(\varepsilon) = \sum_k \delta(\varepsilon - \varepsilon_k^{\pm}), \tag{4.113}$$

which, with the aid of (4.107) and (4.112), can be written as

$$\rho(\varepsilon) = \pi^{-1}(2N + 1) \int_0^{\pi/2} \delta\left[\varepsilon \pm (\lambda^2 + 4\beta^2 \sin^2 k)^{1/2}\right] dk. \tag{4.114}$$

To evaluate this integral of the *Dirac δ-functional*, we note that

$$\int_0^{\pi/2} F(k)\delta[f(k)]dk = \int_0^{\pi/2} [F(k)/f'(k)]\,\delta[f(k)]f'(k)dk$$
$$= [F(k)/f'(k)]_{f(k)=0}\,. \tag{4.115}$$

Comparing (4.114) and (4.115), we see that

$$\left.\begin{aligned} F(k) &= 1, \quad f(k) = \varepsilon \pm (\lambda^2 + 4\beta^2 \sin^2 k)^{1/2}, \\ f(k) &= 0 \Rightarrow \varepsilon^2 - \lambda^2 = 4\beta^2 \sin^2 k, \\ f'(k) &= \pm 2\beta^2 \sin 2k(\lambda^2 + 4\beta^2 \sin^2 k)^{-1/2}. \end{aligned}\right\} \tag{4.116}$$

Hence, (4.116) in (4.115) in (4.114) gives

$$\rho(\varepsilon) = \pm\pi^{-1}(2N+1)\left[(\lambda^2 + 4\beta^2 \sin^2 k)^{1/2}/2\beta^2 \sin 2k\right]_{f(k)=0}$$
$$= \pm(2N+1)\varepsilon/\pi\left[(\varepsilon^2 - \lambda^2)(4\beta^2 + \lambda^2 - \varepsilon^2)\right]^{1/2}, \tag{4.117}$$

which is *real* for $\lambda^2 \le \varepsilon^2 \le \lambda^2 + 4\beta^2$. Figure 4.6 displays the familiar behaviour of $\rho(\varepsilon)$ in the *2-band* diagram of a binary semiconductor, the band edges being given by

$$\varepsilon_1^{\pm} = \pm(\lambda^2 + 4\beta^2)^{1/2}, \quad \varepsilon_2^{\pm} = \pm\lambda, \tag{4.118}$$

which correspond to $k = \pi/2$ and $k = 0$ in (4.107), respectively.

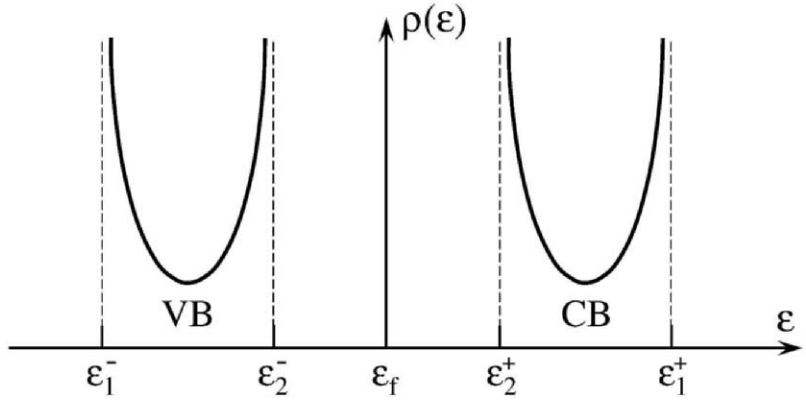

Fig. 4.6. Variation of energy DOS curves in valence (VB) and conduction (CB) bands.

4.4.2 Chemisorption functions

(a) Spectral density $\Delta(\varepsilon)$[6]
Since the adatom a is attached to the substrate A-atom at $j = 1$ by the bond β' (Fig. 4.5), we have (Newns 1969)

$$\langle a|H^\sigma|j\rangle = \beta'\delta_{1j}, \tag{4.119}$$

i.e., only the matrix element connecting the AO $|a\rangle$ with the AO $|1\rangle$ is non-zero. Moreover,

$$V_{ak} = \langle a|H^\sigma|k\rangle = \sum_j \langle a|H^\sigma|j\rangle\langle j|k\rangle, \tag{4.120}$$

by (2.8), so we obtain

$$V_{ak} = \sum_j \beta'\delta_{1j}\langle j|k\rangle = R(k)\beta' \sin k, \tag{4.121}$$

via (4.119) and (4.108). Thus, (4.68) becomes

$$\Delta(\varepsilon) = \pi\beta'^2 \sum_k R^2(k) \sin^2 k\, \delta(\varepsilon - \varepsilon_k^\pm), \tag{4.122}$$

or

$$\Delta(\varepsilon) = (2N+1)\beta'^2 \int_0^{\pi/2} R^2(k) \sin^2 k\, \delta(\varepsilon - \varepsilon_k^\pm) dk, \tag{4.123}$$

by dint of (4.112).

Inserting (4.109) in (4.123), and using (4.110), we find

$$\Delta(\varepsilon) = 4\beta'^2 \int_0^{\pi/2} \frac{(\varepsilon_k^\pm + \lambda)^2 \sin^2 k\, \delta(\varepsilon - \varepsilon_k^\pm)}{(\varepsilon_k^\pm + \lambda)^2 + 4\beta^2 \sin^2 k} dk, \tag{4.124}$$

for N large. Comparing this with (4.115), reveals

$$F(k) = (\varepsilon_k^\pm + \lambda)^2 \sin^2 k \left[(\varepsilon_k^\pm + \lambda)^2 + 4\beta^2 \sin^2 k\right]^{-1},$$

[6]Sometimes called the "weighted DOS".

which, with (4.116) for $f'(k)$, yields

$$\frac{F(k)}{f'(k)} = \frac{(\varepsilon_k^{\pm} + \lambda)^2 \sin^2 k(\lambda^2 + 4\beta^2 \sin^2 k)^{1/2}}{2\beta^2 \sin 2k[(\varepsilon_k^{\pm} + \lambda)^2 + 4\beta^2 \sin^2 k]},$$

i.e.,

$$\left.\frac{F(k)}{f'(k)}\right|_{f(k)=0} = \frac{|\varepsilon + \lambda|}{8\beta^2} \left(\frac{\varepsilon^2 - \lambda^2}{4\beta^2 + \lambda^2 - \varepsilon^2}\right)^{1/2}, \tag{4.125}$$

via (4.116). Hence, (4.124) reduces to (Davison and Huang 1974)

$$\Delta(\varepsilon) = \frac{\beta'^2 |\varepsilon + \lambda|}{2\beta^2} \left(\frac{\varepsilon^2 - \lambda^2}{4\beta^2 + \lambda^2 - \varepsilon^2}\right)^{1/2}, \tag{4.126}$$

by virtue of (4.115) and (4.125). In contrast to Fig. 4.6, the graph of $\Delta(\varepsilon)$ is as depicted in Fig. 4.7.

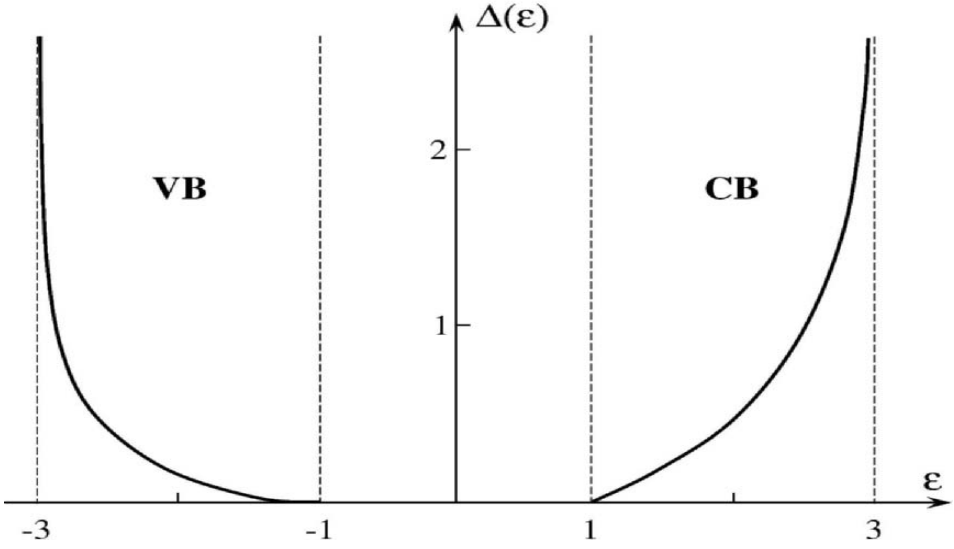

Fig. 4.7. Spectral density curves in VB and CB with $\varepsilon_f = 0$. Reprinted from Davison and Huang (1974) with permission from Elsevier.

(b) Hilbert transform $\Lambda(\varepsilon)$
For our 2-band system, (4.69) can be written as

$$\Lambda(\varepsilon) = \pi^{-1} P \left[\int_{\varepsilon_1^-}^{\varepsilon_2^-} \frac{\Delta(\varepsilon_-)}{\varepsilon - \varepsilon_-} d\varepsilon_- + \int_{\varepsilon_2^+}^{\varepsilon_1^+} \frac{\Delta(\varepsilon_+)}{\varepsilon - \varepsilon_+} d\varepsilon_+\right], \tag{4.127}$$

P indicating the *Cauchy principal value*. Utilizing (4.107), (4.116), (4.118) and (4.126), we obtain

$$\Lambda(\varepsilon) = \frac{\beta'^2}{2\pi\beta^2} P \left[\int_0^{\pi/2} I_+ dk' - \int_{\pi/2}^{0} I_- dk' \right], \tag{4.128}$$

where

$$\begin{aligned} I_\pm &= \frac{|\varepsilon_\pm + \lambda|}{(\varepsilon - \varepsilon_\pm)} \frac{(\varepsilon_\pm^2 - \lambda^2)^{1/2}}{(4\beta^2 + \lambda^2 - \varepsilon_\pm^2)^{1/2}} \frac{2\beta^2 \sin 2k'}{(\lambda^2 + 4\beta^2 \sin^2 k')^{1/2}} \\ &= \frac{|\varepsilon_\pm + \lambda|}{(\varepsilon - \varepsilon_\pm)} \frac{4\beta^2 \sin^2 k'}{(\lambda^2 + 4\beta^2 \sin^2 k')^{1/2}}. \end{aligned} \tag{4.129}$$

Substituting (4.129) in (4.128) leads to

$$\Lambda(\varepsilon) = \frac{2\beta'^2}{\pi} P \int_0^{\pi/2} \frac{A(\varepsilon, \varepsilon_\pm) \sin^2 k'}{(\lambda^2 + 4\beta^2 \sin^2 k')^{1/2}} dk', \tag{4.130}$$

where

$$\begin{aligned} A(\varepsilon, \varepsilon_\pm) &= \frac{|\varepsilon_+ + \lambda|}{\varepsilon - \varepsilon_+} + \frac{|\varepsilon_- + \lambda|}{\varepsilon - \varepsilon_-} \\ &= \frac{(\varepsilon + \lambda)(\varepsilon_+ - \varepsilon_-)}{\varepsilon^2 + \varepsilon_+ \varepsilon_-} \\ &= \frac{2(\varepsilon + \lambda)(\lambda^2 + 4\beta^2 \sin^2 k')^{1/2}}{\varepsilon^2 - (\lambda^2 + 4\beta^2 \sin^2 k')}, \end{aligned} \tag{4.131}$$

since $\varepsilon_+ = -\varepsilon_-$ by (4.107). Hence, (4.131) in (4.130) gives

$$\Lambda(\varepsilon) = \frac{4\beta'^2(q+1)}{\pi\lambda} P \int_0^{\pi/2} \frac{\sin^2 k'}{q^2 - \Gamma^2} dk', \tag{4.132}$$

where

$$\begin{aligned} &\Gamma = (1 + p^2 \sin^2 k')^{1/2}, \\ &p = 2\beta/\lambda, \quad q = \varepsilon/\lambda. \end{aligned} \tag{4.133}$$

After some rearranging, (4.132) gives

$$\Lambda(\varepsilon) = \frac{\beta'^2(\varepsilon + \lambda)}{\pi\beta^2} \left[\Phi(\varepsilon) - \pi/2 \right], \tag{4.134}$$

where

$$\Phi(\varepsilon) = P\int_0^{\pi/2}(1 - m\sin^2 k')^{-1}dk', \tag{4.135}$$

with

$$m = p^2(q^2 - 1)^{-1/2}. \tag{4.136}$$

If we let

$$t = \tan k',$$

then

$$dt = (1 + t^2)dk', \quad \sin^2 k' = t^2(1 + t^2)^{-1},$$

and (4.135) becomes

$$\Phi(\varepsilon) = P\int_0^{\infty}\left[1 + (1 - m)t^2\right]^{-1}dt,$$

i.e.,

$$\Phi(\varepsilon) = P\Big\{(1 - m)^{-1/2}\tan^{-1}\left[(1 - m)^{1/2}t\right]\Big\}_0^{\infty},$$

or

$$\Phi(\varepsilon) = P\big[\pi/2(1 - m)^{1/2}\big]. \tag{4.137}$$

Thus, on inserting (4.137) in (4.134), using (4.136) and (4.133), we arrive at

$$\Lambda(\varepsilon) = \begin{cases} \dfrac{\beta'^2(\varepsilon + \lambda)}{2\beta^2}\left[\dfrac{(\varepsilon^2 - \lambda^2)^{1/2}}{(\varepsilon^2 - \lambda^2 - 4\beta^2)^{1/2}} - 1\right], & \varepsilon^2 > \lambda^2 + 4\beta^2, \\ -\dfrac{\beta'^2(\varepsilon + \lambda)}{2\beta^2}, & \lambda^2 < \varepsilon^2 < \lambda^2 + 4\beta^2, . \\ \dfrac{\beta'^2(\varepsilon + \lambda)}{2\beta^2}\left[\dfrac{(\lambda^2 - \varepsilon^2)^{1/2}}{(\lambda^2 + 4\beta^2 - \varepsilon^2)^{1/2}} - 1\right], & \varepsilon^2 < \lambda^2 \end{cases} \tag{4.138}$$

The graph of $\Lambda(\varepsilon)$, in these various ε-regions, is presented in Fig. 4.8.

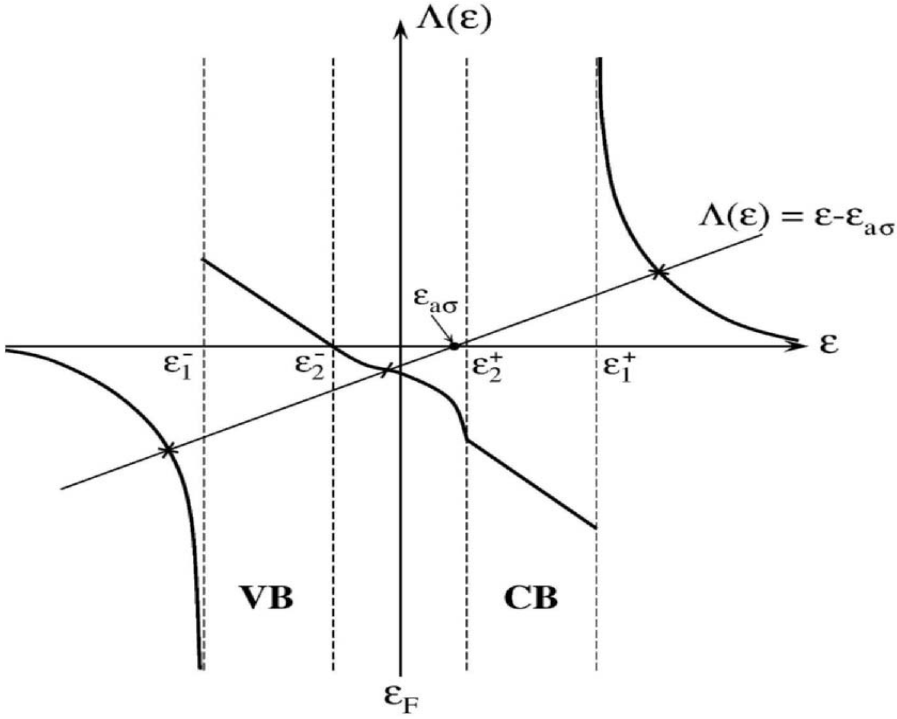

Fig. 4.8. Graph of Hilbert transform $\Lambda(\varepsilon)$. Solutions ($\times$) of $\Lambda(\varepsilon) = \varepsilon - \varepsilon_{a\sigma}$ locate localized-state energies $\varepsilon_{\ell\sigma}$. Reprinted from Davison and Huang (1974) with permission from Elsevier.

Since $\Delta(\varepsilon) = 0$ outside the bands (Fig. 4.7), the poles of $G^{\sigma}_{aa}(\varepsilon)$ in (4.70) are given by

$$\varepsilon - \varepsilon_{a\sigma} - \Lambda(\varepsilon) = 0, \tag{4.139}$$

whose roots are the *localized-state energies* $\varepsilon_{\ell\sigma}$ (Fig. 4.8). The intercept of the straight line with the ε-axis provides the value of $\varepsilon_{a\sigma}$. From (4.139) and Fig. 4.8, we see that the *existence condition* for a localized state *above* or *below* the bands or in the *gap* between them is:

$$\varepsilon_{\ell\sigma} > \varepsilon_1^+, \quad \varepsilon_1^+ - \varepsilon_{a\sigma} < \Lambda(\varepsilon_1^+), \tag{4.140}$$

$$\varepsilon_{\ell\sigma} < \varepsilon_1^-, \quad \varepsilon_1^- - \varepsilon_{a\sigma} > \Lambda(\varepsilon_1^-), \tag{4.141}$$

$$\begin{aligned} &\varepsilon_{\ell\sigma} > \varepsilon_2^-, \quad \varepsilon_2^- - \varepsilon_{a\sigma} < \Lambda(\varepsilon_2^-), \\ &\varepsilon_{\ell\sigma} < \varepsilon_2^+, \quad \varepsilon_2^+ - \varepsilon_{a\sigma} > \Lambda(\varepsilon_2^+), \end{aligned} \tag{4.142}$$

respectively.

4.4.3 Results and discussion

Having established the expressions for the chemisorption functions of an AB-type chain, we can now employ them in calculating ΔE (4.101) and Δq (4.102) for oxygen on *narrow-gap* III-V semiconductors. Specifically, we are interested in GaSb, InAs and InSb. The choice of narrow-gap substrates ensures that the approximation made regarding the contour C in (4.92) remains valid. Results are presented for the $\not{M}$-case only.

The systems' parameters, used in the numerical calculations, are provided in Table 4.1, where the values of ΔE and Δq for oxygen on the (100) and (111) planes of the various semiconductors are also listed. As can be seen from the table, $|\Delta E(111)| < |\Delta E(100)|$, and larger ΔE are usually associated with wider energy gaps. Thus, the decrease in the energy gap with increasing temperature should, in general, lead to a reduction in ΔE. The positive values of ΔE indicate that chemisorption is not possible on these planes for $\beta' = 1.2$ (-2β units). The values of Δq are also given in Table 4.1. On increasing β', both ΔE and Δq are found to decrease for the (100) and (111) planes.

Table 4.1. All energies are in eV. EG_0 = Energy gap width at 0^0K, VB = Valence band width, ϕ = Work function. $\beta' = 1.2$ (in -2β units), $\varepsilon_a = -8.78$ and $U = 12.14$.

Substrate	EG_0^a	VB^b		ϕ^c	-2β		ΔE		Δq	
		(100)	(111)		(100)	(111)	(100)	(111)	(100)	(111)
GaSb	0.81	3.2	1.2	4.76	3.58	1.55	-2.46	-0.58	0.38	0.40
InAs	0.42	3.2	1.1	4.90	3.40	1.29	-2.02	+0.37	0.36	0.40
InSb	0.24	3.2	1.1	4.75	3.32	1.21	-2.00	+0.90	0.37	0.40

[a]Long (1968). [b]Hilsum (1966) [c]Gobeli and Allen (1966)

Chapter 5

Supported-Metal Catalysts

Chemistry without catalysis would be a sword without a handle, a light without brilliance, a bell without sound.

— Alwyn Mittasch

Among the various types of composite systems, that of the *metal-support* ranks as one of the most important, because of its crucial role in catalysis. The situation under consideration is that of chemisorption on a thin metal film (the *catalyst*), which sits on the surface of a semiconductor (the *support*). The fundamental question concerns the thickness of the film needed to accurately mimic the chemisorption properties of the bulk metal, because *metallization* of inexpensive semiconductor materials provides a means of fabricating catalysts economically, even from such precious metals as Pt, Au and Ag.

5.1 Metal-Support Greenian

The substrate being modelled is a metal with a semiconductor support, illustrated schematically in Fig. 5.1 (Davison et al 1988). The system has two components: metal and semiconductor. The metal part consists of a finite $(n+1)$-atom chain (or film), occupying atomic sites $m = 0$ to $m = n$

inclusive. The atoms have site energy α_1 and bond energy β_1, giving rise to a single d-like energy band. The binary semiconductor support is semi-infinite, occupying atomic sites $m \geq n+1$. The site energies alternate between α_A and α_B, corresponding to the s- and p-orbitals, respectively, the one at the metal-semiconductor interface being taken as α_A, to be specific. The bond energies in the semiconductor are $\pm\beta_2$, while that at the interface is γ.

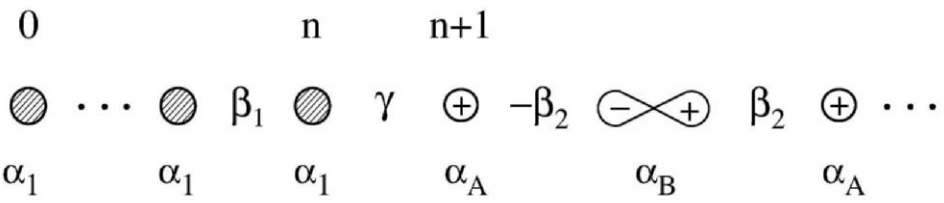

Fig. 5.1. Schematic representation of Ni/ZnO system. Ni film, lying between $0 \leq m \leq n$, contains atoms of site energy α_1 and bond energy β_1. Bond of energy γ attaches film to first ($m = n+1$) Zn atom in semi-infinite ZnO support, depicted by chain of alternating s- and p-orbitals with corresponding site energies α_A and α_B, and bond energies $\pm\beta_2$. Reprinted from Davison et al (1988) with permission from Elsevier.

To construct the Greenian for the metal-support system described above, we start from the infinite Greenians for the metal and the semiconductor. Dyson's equation is used to obtain the Greenians for the finite or semi-infinite components, and again to "glue" the two components together to produce the Greenian for the composite system.

For convenience, we summarize here the list of Greenians to be employed in the following discussion:

G_1: Greenian for infinite metal
g_1: Greenian for finite metal
G_2: Greenian for infinite semiconductor
g_2: Greenian for semi-infinite semiconductor
g_{12}: composite Greenian for metal-semiconductor system

Turning first to the metal film, we let G_1 be the Greenian for the infinite, one-dimensional metal, and g_1 its finite counterpart. These two Greenians are connected by the Dyson equation (3.3)

$$g_1 = G_1 + G_1 V_1 g_1, \tag{5.1}$$

where the potential

$$\begin{aligned} V_1 = &- \beta_1 \left(|0\rangle\langle -1| + |-1\rangle\langle 0| + |n\rangle\langle n+1| + |n+1\rangle\langle n| \right) \\ &+ (\alpha_1' - \alpha_1) \left(|0\rangle\langle 0| + |n\rangle\langle n| \right). \end{aligned} \tag{5.2}$$

creates a finite chain (of length $n+1$) by cutting the bonds (of energy β_1) between the $m=-1$ and $m=0$ atoms, and between the $m=n$ and $m=n+1$ atoms. The potential also modifies the site energies, on the end atoms of the film, from α_1 to α_1'. In principle, the α_1' at $m=0$ may be different from that at $m=n$, but for simplicity we take them to be the same.

The matrix elements of g_1 are derived in the next section, as required, while those of the infinite Greenian G_1 are already known (from (2.49) with (2.37) and (2.40)), and can be written as (App. J)

$$G_1(n,m) = t^{|n-m|} G_1(0,0), \tag{5.3}$$

where

$$G_1(0,0) = t/\beta_1(1-t^2), \tag{5.4}$$

with

$$t = \begin{cases} X \pm (X^2-1)^{1/2}, & X \lessgtr \mp 1, \\ X - i(1-X^2)^{1/2}, & |X| < 1, \end{cases} \tag{5.5}$$

and

$$X = (E - \alpha_1)/2\beta_1. \tag{5.6}$$

The semiconductor support can be treated in a similar manner (Bose and Foo 1974), since the Greenians G_2 and g_2 of the infinite and semi-infinite solids, respectively, are also linked by the Dyson equation, i.e.,

$$g_2 = G_2 + G_2 V_2 g_2, \tag{5.7}$$

where

$$V_2 = -\beta_2 \left(|n\rangle\langle n+1| + |n+1\rangle\langle n| \right) + (\alpha_A' - \alpha_A)|n+1\rangle\langle n+1|. \tag{5.8}$$

The first term in (5.8) cuts the bond between the atoms n and $n+1$, thereby creating a surface at $m = n+1$, the second term perturbs the site energy on the surface atom from α_A to α'_A.

The only element of g_2 needed here is that at the surface site, namely

$$\begin{aligned} g_2(n+1,n+1) = {} & G_2(n+1,n+1) - \beta_2 G_2(n+1,n) g_2(n+1,n+1) \\ & - \beta_2 G_2(n+1,n+1) g_2(n,n+1) \\ & + (\alpha'_A - \alpha_A) G_2(n+1,n+1) g_2(n+1,n+1), \end{aligned} \tag{5.9}$$

which derives from (5.7). However, $g_2(n,n+1) = 0$, because the sites n and $n+1$ lie on *opposite sides* of the cleaved interface (Kalkenstein and Soven 1971). Thus, (5.9) leads to the desired matrix element at the interface site, viz.,

$$\begin{aligned} g_2(n+1,n+1) = G_2(n+1,n+1) \Big[& 1 + \beta_2 G_2(n+1,n) \\ & - (\alpha'_A - \alpha_A) G_2(n+1,n+1) \Big]^{-1}. \end{aligned} \tag{5.10}$$

The elements of G_2 required in (5.10) are (App. K)

$$G_2(n+1,n+1) = (E - \alpha_B)/\beta_2^2 (2z_\pm - p), \tag{5.11}$$

and

$$G_2(n+1,n) = \beta_2 (1 - z_\pm) G_2(n+1,n+1)/(E - \alpha_B), \tag{5.12}$$

where

$$|z_\pm| = \frac{1}{2} |p \pm (p^2 - 4)^{1/2}| < 1, \tag{5.13}$$

and

$$p = 2 - (E - \alpha_A)(E - \alpha_B)/\beta_2^2. \tag{5.14}$$

Knowing g_1 and g_2, the Greenian g_{12} for the composite metal-support system is given by the Dyson equation

$$g_{12} = g + g V g_{12}, \tag{5.15}$$

where

$$g(\ell,m) = \begin{cases} g_1(\ell,m), & 0 \le \ell, m \le n, \\ g_2(\ell,m), & \ell, m > n, \\ 0, & \text{otherwise}, \end{cases} \tag{5.16}$$

and

$$V = \gamma(|n\rangle\langle n+1| + |n+1\rangle\langle n|), \tag{5.17}$$

the potential V connecting the metal film to the semiconductor support by the bond of energy γ.

5.2 Substrate Surface Green Function

In this section, we utilize the Dyson equation (5.15) to develop the surface GF of the composite system. Inserting (5.17) in (5.15), the matrix element

$$g_{12}(0,0) = g_1(0,0) + \gamma g_1(0,n) g_{12}(n+1,0), \tag{5.18}$$

for the surface GF, since $g(0,n+1) = 0$ from (5.16). The $g_{12}(n+1,0)$ in (5.18) is found from (5.15), i.e.,

$$\begin{aligned} g_{12}(n+1,0) = g(n+1,0) + \gamma g(n+1,n) g_{12}(n+1,0) \\ + \gamma g(n+1,n+1) g_{12}(n,0), \end{aligned}$$

which reduces to

$$g_{12}(n+1,0) = \gamma g_2(n+1,n+1) g_{12}(n,0), \tag{5.19}$$

again via (5.16). Another application of (5.15) reveals that

$$g_{12}(n,0) = g_1(n,0) + \gamma g_1(n,n) g_{12}(n+1,0). \tag{5.20}$$

Equations (5.19) and (5.20) are a pair of coupled equations, whose solution yields

$$g_{12}(n+1,0) = \gamma g_1(n,0) \left[g_2^{-1}(n+1,n+1) - \gamma^2 g_1(n,n) \right]^{-1}. \tag{5.21}$$

Substituting (5.21) into (5.18), we arrive at

$$\begin{aligned} g_{12}(0,0) = g_1(0,0) + \gamma^2 g_1(0,n) g_1(n,0) \\ \times \left[g_2^{-1}(n+1,n+1) - \gamma^2 g_1(n,n) \right]^{-1}, \end{aligned} \tag{5.22}$$

$g_2(n+1,n+1)$ being given by (5.10). It now remains to use (5.1) to obtain the 4 elements of g_1 needed in (5.22).

Using (5.1) and (5.2), the matrix elements of the Greenian g_1 can be obtained. Specifically,

$$g_1(0,n) = G_1(0,n) - \beta_1\Big[G_1(0,-1)g_1(0,n) + G_1(0,n+1)g_1(n,n)\Big] + (\alpha_1' - \alpha)\Big[G_1(0,0)g_1(0,n) + G_1(0,n)g_1(n,n)\Big], \tag{5.23}$$

where

$$g_1(-1,n) = 0 = g_1(n+1,n), \tag{5.24}$$

because these matrix elements connect sites on opposite sides of broken bonds. Rearranging (5.23) in terms of the unknown GFs $g_1(0,n)$ and $g_1(n,n)$, we can write

$$Ag_1(0,n) + Bg_1(n,n) = G_1(0,n), \tag{5.25}$$

where

$$A = 1 + \beta_1 G_1(0,-1) - (\alpha_1' - \alpha_1)G_1(0,0), \tag{5.26}$$

and

$$B = \beta_1 G_1(0,n+1) - (\alpha_1' - \alpha_1)G_1(0,n). \tag{5.27}$$

Employing (5.1) again, we find

$$g_1(n,n) = G_1(n,n) - \beta_1\left[G_1(n,-1)g_1(0,n) + G_1(n,n+1)g_1(n,n)\right] + (\alpha_1' - \alpha_1)\left[G_1(n,0)g_1(0,n) + G_1(n,n)g_1(n,n)\right], \tag{5.28}$$

by virtue of (5.24). In the infinite solid, translational symmetry implies that

$$G_1(n,m) = G_1\left(|n-m|\right), \tag{5.29}$$

so (5.28) can be expressed in the form

$$Bg_1(0,n) + Ag_1(n,n) = G_1(n,n). \tag{5.30}$$

The pair of linear equations (5.25) and (5.30) has the solution

$$g_1(0,n) = \left[AG_1(0,n) - BG_1(n,n)\right](A^2 - B^2)^{-1}, \tag{5.31}$$

and

$$g_1(n,n) = \left[AG_1(n,n) - BG_1(0,n)\right](A^2 - B^2)^{-1}. \tag{5.32}$$

A parallel application of (5.1) gives rise to the pair of equations

$$g_1(0,0) = [AG_1(0,0) - BG_1(n,0)]\,(A^2 - B^2)^{-1}, \tag{5.33}$$

and

$$g_1(n,0) = [AG_1(n,0) - BG_1(0,0)]\,(A^2 - B^2)^{-1}, \tag{5.34}$$

which are very similar to (5.31) and (5.32). Examining (5.31)-(5.34), with reference to (5.29), shows that

$$g_1(0,0) = g_1(n,n), \tag{5.35}$$

and

$$g_1(n,0) = g_1(0,n), \tag{5.36}$$

which are not unexpected results, in light of the fact that g_1 represents an $(n+1)$-atom chain, with reflectional symmetry about its center. In other words, the two end sites ($m = 0$ and $m = n$) are physically indistinguishable, so the corresponding GFs relating them should be equal.

Substituting (5.35) and (5.36) into (5.22) gives

$$g_{12}(0,0) = g_1(0,0) + \gamma^2 (g_1(n,0))^2 \left[g_2^{-1}(n+1,n+1) - \gamma^2 g_1(0,0)\right]^{-1}, \tag{5.37}$$

which, on inserting (5.33) and (5.34), becomes

$$\begin{aligned} g_{12}(0,0) = {} & [AG_1(0,0) - BG_1(n,0)]\,(A^2 - B^2)^{-1} \\ & + \gamma^2 \left[AG_1(n,0) - BG_1(0,0)\right]^2 (A^2 - B^2)^{-1} \\ & \times \left\{ g_2^{-1}(n+1,n+1)(A^2 - B^2) - \gamma^2 \left[AG_1(0,0) - BG_1(n,0)\right] \right\}^{-1}. \end{aligned} \tag{5.38}$$

With the aid of (5.10), some rearrangement of (5.38) produces an explicit expression for the surface GF, in terms of the infinite GFs, viz.,

$$\begin{aligned} g_{12}(0,0) = {} & [AG_1(0,0) - BG_1(n,0)]\,(A^2 - B^2)^{-1} \\ & + \gamma^2 G_2(n+1,n+1) \left[AG_1(n,0) - BG_1(0,0)\right]^2 (A^2 - B^2)^{-1} \\ & \times \Big\{ (A^2 - B^2) \left[1 + \beta_2 G_2(n+1,n) - (\alpha'_A - \alpha_A) G_2(n+1,n+1)\right] \\ & - \gamma^2 G_2(n+1,n+1) \left[AG_1(0,0) - BG_1(n,0)\right] \Big\}^{-1}. \end{aligned} \tag{5.39}$$

For present purposes, the surface and interface perturbations are neglected, so that $\alpha_1' = \alpha_1$ and $\alpha_A' = \alpha_A$, thereby reducing (5.26) and (5.27) to

$$A = 1 + \beta_1 G_1(0, -1), \tag{5.40}$$

and

$$B = \beta_1 G_1(0, n+1). \tag{5.41}$$

On setting

$$P = 1 + \beta_2 G_2(n+1, n), \tag{5.42}$$
$$Q = A G_1(0,0) - B G_1(n, 0), \tag{5.43}$$
$$R = \gamma^2 G_2(n+1, n+1), \tag{5.44}$$
$$S = A G_1(n, 0) - B G_1(0, 0), \tag{5.45}$$

(5.39) can be rewritten as

$$g_{12}(0,0) = \frac{PQ(A^2 - B^2) + R(S^2 - Q^2)}{(A^2 - B^2)[P(A^2 - B^2) - RQ]}. \tag{5.46}$$

After some algebra, we find that

$$S^2 - Q^2 = (A^2 - B^2)\left[G_1^2(n,0) - G_1^2(0,0)\right], \tag{5.47}$$

so (5.46) simplifies to

$$g_{12}(0,0) = \frac{PQ + R[G_1^2(n,0) - G_1^2(0,0)]}{P(A^2 - B^2) - RQ}. \tag{5.48}$$

It should be noted that (5.48), like the more general (5.39), expresses the surface GF in terms of the infinite GFs G_i of the two components (the metal and semiconductor support). Since G_1 and G_2 have already been derived in (5.3)-(5.4) and (5.11)-(5.12), respectively, our knowledge of the surface GF is now complete.

5.3 Chemisorption Properties

At this point, we can undertake the study of chemisorption on a supported metal. Despite the importance of this process to catalysis, quantum-mechanical studies have been somewhat scarce. The problem was first investigated by Ruckenstein and Huang (1973), who formulated a general MO

approach to the chemisorption process and demonstrated the effect of the support in modifying the energies of both localized and nonlocalized states. A decade later, Haberlandt and Ritschl (1983) used a semi-empirical complete neglect of differential overlap (CNDO/2) cluster calculation to study the H-Ni/SiO_2 system. The charge transfer was found to be directed *into* the support, and to increase with increasing electron affinity of the surface site and with the number of interface bonds. The chemisorption energy of a H atom on a single Ni atom was found to be decreased (in absolute value) by up to 26%, due to the influence of the support.

A few years later, Davison et al (1988) applied the ANG model of chemisorption to supported-metal catalysts. The key parameters were found to be the metal film thickness and the metal-support bond strength. Related papers followed, studying impurity effects (Zhang and Wei (1991), Sun et al (1994b)) and variation with metal substrate (Xie et al (1992)).

Parallel studies were performed by Liu and Davison (1988), who investigated the process of chemisorption on inverse-supported catalysts, where the surface film is a semiconductor and the underlying support is a metal. Again a key parameter was found to be film thickness, and the substrate was observed to behave as either an acceptor or a donor, depending upon that thickness. The lack of charge self-consistency in this work was addressed by Sun et al (1994a), who also studied the effects of thickness and different metal constituents.

A different approach was taken by Hao and Cooper (1994), who used a combination of the film linear muffin-tin orbital (LMTO) method and an ab initio molecular quantum cluster method, to investigate SO_2 adsorption on a Cu monolayer supported by $\gamma-Al_2O_3$. Emphasis here was on the geometry of adsorption sites, with the conclusion that the preferred adsorption site is the Al−Al bridging one.

The problem at hand is the application of the ANG model (Chap. 4) to the adatom-metal-support system, which is shown schematically in Fig. 5.2. The adatom (H) at site $m = a$, has electronic energy, $\varepsilon_{a\sigma}$ (4.34) and is connected by a bond of energy β to the surface atom (Ni), at site $m = 0$. The support is ZnO, with a Zn atom at the interface site $m = n+1$ (Davison et al 1988).

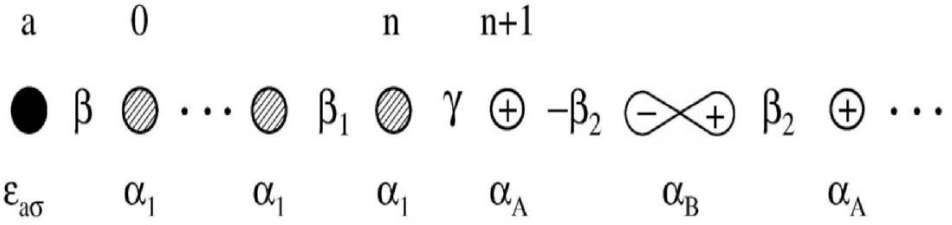

Fig. 5.2. Schematic representation of H-Ni/ZnO system showing hydrogen adatom a of electronic energy $\varepsilon_{a\sigma}$ with bond energy β attached to Ni surface atom at $m = 0$. Reprinted from Davison et al (1988) with permission from Elsevier.

The adatom and surface Greenians are linked, once again, by the Dyson equation

$$g_a = g_{12} + g_{12} V_a g_a, \tag{5.49}$$

where

$$V_a = U\langle n_{a,-\sigma}\rangle |a\rangle\langle a| + \beta\left(|a\rangle\langle 0| + |0\rangle\langle a|\right), \tag{5.50}$$

$U\langle n_{a,-\sigma}\rangle$ being the averaged self-energy of the adatom, within the HFA. From (5.49), we have

$$\begin{aligned} g_a(a,a) = {} & g_{12}(a,a) + U\langle n_{a,-\sigma}\rangle g_{12}(a,a) g_a(a,a) \\ & + \beta g_{12}(a,a) g_a(0,a), \end{aligned} \tag{5.51}$$

where $g_{12}(a,0) = 0$, and also

$$g_a(0,a) = \beta g_{12}(0,0) g_a(a,a). \tag{5.52}$$

Substituting (5.52) into (5.51) and rearranging yields

$$g_a(a,a)\left[g_{12}^{-1}(a,a) - U\langle n_{a,-\sigma}\rangle - \beta^2 g_{12}(0,0)\right] = 1. \tag{5.53}$$

Noting that the isolated adatom GF is

$$g_{12}(a,a) = (E - \varepsilon_a)^{-1}, \tag{5.54}$$

and putting

$$\varepsilon_{a\sigma} = \varepsilon_a + U\langle n_{a,-\sigma}\rangle, \tag{5.55}$$

as in (4.34), reduces (5.53) to the adatom expression

$$g_a(E) \equiv g_a(a,a) = \left[E - \varepsilon_{a\sigma} - \beta^2 g_{12}(0,0)\right]^{-1}. \tag{5.56}$$

The general theory of §4.3 can now be applied, with some modification, due to the fact that the substrate electronic structure consists of discrete states arising from the metal film, in addition to the delocalized band states of the semiconductor. The adatom GF (5.56) can be written as (cf. (4.70))

$$g_a(E) = \left[E - \varepsilon_{a\sigma} - \Lambda(E) + i\Delta(E)\right]^{-1}, \tag{5.57}$$

by means of the chemisorption functions

$$\Lambda(E) = \beta^2 \mathrm{Re}\left[g_{12}(0,0)\right], \quad \Delta(E) = -\beta^2 \mathrm{Im}\left[g_{12}(0,0)\right]. \tag{5.58}$$

The adatom occupancy is now given by (cf. (4.76) and (4.80))

$$\langle n_{a\sigma}\rangle = \int_{\varepsilon_\ell}^{\varepsilon_u} \rho_a(E)dE + \sum_i \left[1 - \Lambda'(E_i)\right]^{-1}, \tag{5.59}$$

where the adatom DOS is (cf. (4.75))

$$\begin{aligned}\rho_a(E) &= -\pi^{-1}\mathrm{Im}\left[g_a(E)\right] \\ &= \pi^{-1}\Delta(E)\left[(E - \varepsilon_{a\sigma} - \Lambda(E))^2 + \Delta^2(E)\right]^{-1}.\end{aligned} \tag{5.60}$$

Furthermore, the summation in the second term of (5.59) is over all discrete states with energies below the FL ε_f, and the integration in the first term is over the VB of the semiconductor.

Here, we examine only the non-magnetic case, so we have

$$\langle n_{a+}\rangle = \langle n_{a-}\rangle \equiv \langle n_a\rangle, \tag{5.61}$$

on dropping the subscript σ, for convenience. The charge transfer from the substrate to the adatom is now given by (cf. (4.102))

$$\Delta q = (2\langle n_a\rangle - 1)\, e. \tag{5.62}$$

The chemisorption energy expression (4.101) now takes the form

$$\Delta E = 2\sum_{j=0}^{n}\left[E_a(j) - E_b(j)\right] + 2\pi^{-1}\int_{\varepsilon_\ell}^{\varepsilon_u}\tan^{-1}\left[\Delta(E)/(E-\varepsilon_{a\sigma}-\Lambda(E))\right]dE - \varepsilon_a - U\langle n_a\rangle^2, \tag{5.63}$$

with $-\pi < \tan^{-1} < 0$ (App. G). In (5.63), $E_b(j)$ and $E_a(j)$ represent the energy of the jth discrete state of the metal film, before and after chemisorption, respectively. Thus the quantity $E_a(j) - E_b(j)$ is the energy shift in that state as induced by the chemisorption process. It is noted that, for the parameter values used here, the energy ε_a^* of the adatom level after chemisorption lies in the semiconductor VB and, hence, its contribution to ΔE is automatically included in the integrated term, and does not require explicit inclusion as in (4.101). With these considerations, the numerical calculations of ΔE and Δq are straightforward.

5.4 H-Ni/ZnO System

Results are presented for the case of a H adatom interacting with a Ni film on a ZnO support. The band structure of the composite system is shown schematically in Fig. 5.3. Relative to the FL as energy zero, the principal parameters have values (in eV): $\alpha_1 = -1.7$, $\beta_1 = 0.95$, $\alpha_A = 0$, $\alpha_B = -3.4$ and $\beta_2 = 3.755$. The interface interaction parameter γ is approximated as the average of β_1 and β_2 for a value of 2.35, although variation of the results with γ is examined later. With this set of parameters, the Ni d-band lies between 0.2 and -3.6. For thin Ni films (e.g., $n+1 = 6$, as shown in Fig. 5.3), all Ni energies fall within the ZnO band gap, while, for thicker films, some Ni energies lie in either the VB or CB of ZnO.[1]

[1]Note, as successive Ni atoms are added to the film, their energy levels gradually fill up the semiconductor band gap. Thus, eventually the 2-band support appears as a 1-band metal to the H adatom, and *metallization* of the semiconductor has been achieved.

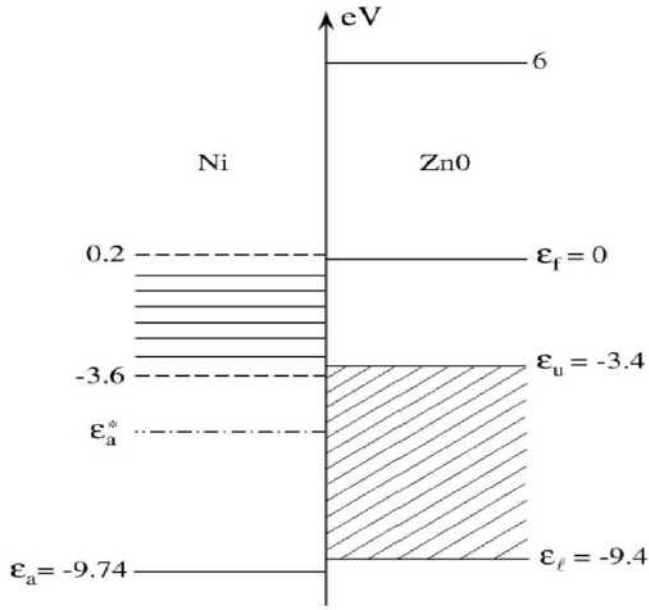

Fig. 5.3. Energy band-structure diagram (in eV) of Ni/ZnO support and pre-(post-)chemisorbed hydrogen adatom level at $\varepsilon_a(\varepsilon_a^*)$. VB (shaded) and CB of ZnO are of width 6. Fermi level (ε_f), which coincides with lower edge of CB, is taken as zero of energy. 6-layer Ni film has 6 localized levels lying between band edges (dashed lines), which just overlap ZnO energy gap. Reprinted from Davison et al (1988) with permission from Elsevier.

The H atom has parameters $\varepsilon_a = -9.74$ and $U = 12.9$, with bond energy $\beta = 3.75$. The isolated adatom energy ε_a is shifted upwards upon chemisorption to ε_a^*, which is a solution to (cf. (4.139))

$$E - \varepsilon_{a\sigma} - \Lambda(E) = 0, \tag{5.64}$$

i.e., it is the chemisorption state, which arises mathematically as a pole of the adatom GF (5.57). As the energy ε_a^* overlaps the ZnO valence band, it appears as a broadened spike in the DOS, rather than the more familiar δ-function that occurs when such a state is isolated from the bands.

Using the "reference" value of $\gamma = 2.35$ eV for the Ni-ZnO interface parameter, the charge transfer Δq and chemisorption energy ΔE were calculated for a Ni film of thickness varying from 1 to 6 layers, as listed in Table 5.1. For the case of a single Ni layer, Δq is quite small (0.08), and $\Delta E = -1.166$ has a value about two-fifths of that for pure Ni ($\Delta E = -2.975$ eV). Such

behaviour is not surprising, as the thinness of the Ni film allows some charge to be drained away from the surface into the ZnO support, thus weakening the adsorption process.

Table 5.1. Adatom charge transfer Δq and chemisorption energy ΔE for atomic hydrogen on Ni film of $(n+1)$-layers thickness on ZnO support.

$n+1$	$\Delta q(e)$	ΔE (eV)
1	0.08	-1.166
2	0.14	-2.730
3	0.16	-2.933
4	0.16	-2.963
5	0.16	-2.969
6	0.16	-2.974

Increasing the thickness of the Ni film to just 2 layers produces marked changes in the values (increasing Δq to 0.14 and lowering ΔE to -2.730), making them much closer to the values for pure Ni. A 3-layer film leads to Δq having the pure-Ni value of 0.16 and a marginally lower value of ΔE ($= -2.933$ eV). Further increases in the thickness of the film produce no significant change in Δq and only very small changes in ΔE. The Ni film completely reflects the chemisorption properties of pure Ni, when the film thickness reaches 6 layers.

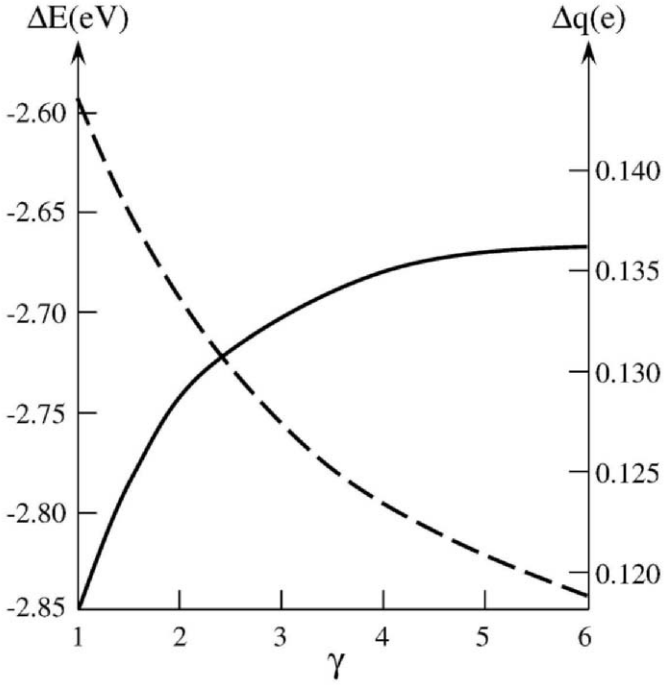

Fig. 5.4. Dependence of hydrogen chemisorption energy ΔE (solid line) and adatom charge transfer Δq (dashed line) of 2-layer Ni film on interaction parameter γ. Reprinted from Davison et al (1988) with permission from Elsevier.

Since the value of the Ni-ZnO interface interaction parameter γ was estimated to be the average of β_1 and β_2, further calculations were done to assess the sensitivity of the results to changes in the value of γ. Fig. 5.4 shows the variation of Δq and ΔE, with γ in the range from 1 to 6 eV for a 2-layer film. (The reference value of γ is 2.35 eV.) In the low-γ region ($1 \leq \gamma \leq 3$), ΔE increases quite quickly with increasing γ, while for higher γ (> 3 eV) the rate of increase in ΔE is much smaller. The decrease of Δq with increasing γ is similar, although the difference in the rate of change between the low- and high-γ regimes is less pronounced. It is significant that, for low γ, the chemisorption properties are closest to those for a pure (semi-infinite) Ni substrate. Increasing the metal-support interface bond γ from 1 eV to 6 eV results in a 6% increase (17% decrease) in ΔE (Δq), indicating that the effect of the support, in this case, is to draw charge from the Ni film into the ZnO support, resulting in less charge being available

for transfer to the adatom, thereby weakening the chemisorption process. It should be noted that these findings are qualitatively in accord with those of Haberlandt and Ritschl (1983). As mentioned earlier, the results of Fig. 5.4 are for a 2-layer film. For a thicker film, the variation in the chemisorption properties with γ should be smaller, due to the fact that the metal-support interface is physically located farther away from the adsorption site.

In conclusion, metal-support substrates provide good examples of composite systems that can be studied efficiently by GF techniques. The key parameter is clearly seen to be the film thickness: it controls the extent to which the metal-support system mimics the chemisorption properties of the pure metal. Also important is the bond strength (γ) between the metal and the support, as it governs the flow of charge between the metal and the support, thus determining the amount of charge available at the surface to partake in chemisorption.

Chapter 6

Disordered Binary Alloys

One of the advantages of being disorderly is that one is constantly making exciting discoveries.

— A.A. Milne

So far, the solids that we have studied have been ordered, in the sense that they possess perfect translational symmetry. However, this "perfection" is really an idealization and, in reality, an actual crystal can be expected to have some sort of *disorder*, which breaks the long-range periodicity of the lattice. There are a number of ways in which disorder can arise. For instance, *interstitial* disorder occurs when an impurity atom is placed in the vacant space between two substrate atoms, which remain at their original locations in the lattice. Another situation is that of *structural* disorder, where the substrate atoms move away from their positions on the perfect lattice. However, the situation of interest in this chapter is that of *substitutional* disorder. Here, a perfect lattice of one type of atoms (say, A) has some of its members randomly replaced by another type (B). The result is a structurally periodic lattice, but with the constituent atoms A and B randomly placed on the lattice sites. The relative numbers of A and B atoms can be represented by the concentrations c_A and c_B, with $c_A + c_B = 1$. The randomness of this type of solid introduces a level of difficulty into the theory, that we have not yet encountered.

6.1 Coherent-Potential Approximation

In this section, we consider how to model a bulk (i.e., infinite) substitutionally *disordered binary alloy* (DBA), in light of its intrinsic randomness. The fact that the DBA lacks periodicity means that the key tool of Bloch's theorem is inapplicable, so specialized methods (Ehrenreich and Schwartz 1976, Faulkner 1982, Yonezawa 1982, Turek et al 1996) must be used.

One early and simple concept is the *rigid-band model* (Friedel 1958), wherein a fixed DOS is taken to represent an entire class of alloys (such as those composed of 3d transition metals). Individual alloys are distinguished solely by assigning to each a Fermi level, determined by the concentration of valence electrons. Unfortunately, this model is too much of an oversimplification, because, for example, the DOS is chosen empirically, and may not be clearly related to that for any of the constituent metals.

In the *virtual-crystal approximation* (VCA) (Nordheim 1931), the site energy of an alloy atom is taken to be

$$\alpha_v = c_A \varepsilon_A + c_B \varepsilon_B, \tag{6.1}$$

where $\varepsilon_A(\varepsilon_B)$ is the electronic energy of component $A(B)$. Therefore, α_v is the average of the site energies for the constituent atoms, weighted by the corresponding concentrations. Thus, the basic idea of the VCA (6.1) is to replace the random energy at each site by an average one, thereby making the lattice periodic and the calculation of the DOS straightforward. Although this approach may sound reasonable, in principle, it is in fact inadequate in its implementation. The VCA treats the randomness of the alloy too simplistically, and in effect models the solid as if it were ordered. The failure of the VCA is perhaps illustrated most obviously by the fact that it always gives rise to a single energy band (termed the *amalgamated* band structure). Although some alloys do possess this structure, others do not. For example, Cu-Zn alloy (Ehrenreich and Schwartz 1976) maintains two separate bands, associated with the Cu and Zn 3d-bands, respectively. This type of band structure is termed *persistent*, and cannot be produced using the VCA. So, although the VCA might prove satisfactory for some amalgamated-type alloys, it certainly fails as a more comprehensive theory.

A better method is the *average t-matrix approximation* (ATA) (Korringa 1958), in which the alloy is characterized by an *effective medium*, which is determined by a non-Hermitean (or "effective") Hamiltonian with complex-energy eigenvalues. The corresponding self-energy is calculated (non-self-

consistently) by means of an average t-matrix, which represents the average scattering of an electron at each site. One fundamental approximation that is made in this approach is the so-called *single-site approximation*, wherein the scattering from a particular site is assumed to be independent of that from other sites. The ATA is certainly an improvement over the VCA, because, it can predict either the persistent or amalgamated bands. However, the ATA does possess deficiencies, largely due to the lack of self-consistency in the effective potential. For instance, the ATA does not always fix the band edges correctly, and calculated results are also dependent upon the choice of the reference system with respect to which the electron scattering is considered to take place. Consequently, a better approximation was sought.

The improvement came in the form of the *coherent-potential approximation* (CPA) (Soven 1967, Taylor 1967, Velický et al 1968), which remedied the lack of self-consistency exhibited by the ATA. The crux of this approach is that each lattice site has associated with it a complex self-consistent potential, called a *coherent potential* (CP). The CP gives rise to an effective medium with the important property that removing that part of the medium belonging to a particular site, and replacing it by the true potential, produces, on average, no further scattering. Because the CPA is used for our discussion of chemisorption on DBA's, its mathematical formulation is given below.

The CPA has proved to be an enormously successful tool in the study of alloys, and has been implemented within various frameworks, such as the TB, linear muffin-tin orbital and Korringa-Kohn-Rostoker (Kumar et al 1992, Turek et al 1996), and is still considered to be the most satisfactory single-site approximation. Efforts to do better than the single-site CPA have focused on multi-site (or cluster) CPA's (see, e.g., Gonis et al 1984, Turek et al 1996), in which a central site and its set of nearest neighbours are embedded in an effective medium. Still, for present purposes, the single-site version of the CPA suffices, and we derive the necessary equations here, within the framework of the TB model.

The derivation of the single-site CPA involves the calculation of an average GF G_e for a corresponding effective Hamiltonian H_e, with the key requirement being that there is zero average scattering from any particular site. It should be noted that, because H_e is non-Hermitean with complex eigenenergies, any putative "average" wave function would necessarily lead to unphysical predictions. Fortunately, an average GF does not suffer from this drawback.

The exact 1-electron Hamiltonian for a DBA can be written as the sum of the Hamiltonian for a translationally invariant solid plus that for the random perturbations, i.e.,

$$H = \sum_{i,j} w_{ij}|i\rangle\langle j| + \sum_i v_i|i\rangle\langle i|. \tag{6.2}$$

The first summation incorporates the (non-random) translational invariance, while the second includes random deviations from the lattice on a site-by-site basis. Note that the second summation explicitly indicates that all randomness or disorder is *diagonal*, not off-diagonal. The corresponding exact GF $G = (\omega - H)^{-1}$ satisfies the matrix equation

$$\sum_\ell \left[(\omega - v_i)\delta_{i\ell} - w_{i\ell}\right] G(\omega; \ell, j) = \delta_{ij}, \tag{6.3}$$

where $\omega = E + i0$. Since the Hamiltonian

$$H_0 = \sum_{i,j} w_{ij}|i\rangle\langle j| \tag{6.4}$$

represents a translationally invariant crystal (which we term the "unperturbed" system), it can be assumed that the corresponding unperturbed GF, satisfying

$$\sum_\ell (\omega\delta_{i\ell} - w_{i\ell}) G_0(\omega; \ell, j) = \delta_{ij}, \tag{6.5}$$

is known. The two GF's are linked by the Dyson equation (3.3), viz.,

$$G = G_0 + G_0 V G, \tag{6.6}$$

where

$$V = \sum_i v_i|i\rangle\langle i| = H - H_0. \tag{6.7}$$

Successive substitution of (6.6) into itself produces

$$G = G_0 + G_0VG_0 + G_0VG_0VG_0 + \cdots + G_0(VG_0)^n + \cdots \tag{6.8a}$$

$$= G_0 + G_0TG_0 \tag{6.8b}$$

where the *t-matrix* is

$$T = V + VG_0V + \cdots + V(G_0V)^n + \cdots = V + VG_0T. \tag{6.9}$$

Since G is the exact GF for one of the many possible configurations of the alloy, what we would like to do is to obtain an "average" GF $\langle G \rangle$, where the averaging is over all possible configurations. Performing such a configurational average on (6.8b) gives

$$\langle G \rangle = G_0 + G_0 \langle T \rangle G_0, \tag{6.10}$$

where $\langle G_0 \rangle = G_0$, because this GF represents a translationally invariant crystal. Thus, the problem is reduced to evaluating $\langle T \rangle$.

To determine $\langle T \rangle$, let $V_n = v_n |n\rangle\langle n|$, so that

$$V = \sum_n V_n, \tag{6.11}$$

from which (6.8a) becomes

$$G = G_0 + G_0 \sum_n V_n G_0 + G_0 \sum_n V_n G_0 \sum_m V_m G_0 + \cdots . \tag{6.12}$$

If we let t_n be the single-site scatterers, with $T_n = t_n |n\rangle\langle n|$, then we can rearrange G in (6.12) as

$$\begin{aligned} G = G_0 &+ G_0 \sum_n T_n G_0 + G_0 \sum_n T_n G_0 \sum_{m \neq n} T_m G_0 \\ &+ G_0 \sum_n T_n G_0 \sum_{m \neq n} T_m G_0 \sum_{r \neq m} T_r G_0 + \cdots , \end{aligned} \tag{6.13}$$

where it can be seen that

$$\begin{aligned} t_n &= v_n + v_n G_0(n,n) v_n + v_n G_0(n,n) v_n G_0(n,n) v_n + \cdots \\ &= v_n \left[1 - v_n G_0(n,n) \right]^{-1} . \end{aligned} \tag{6.14}$$

Comparing (6.13) with (6.8b), we see that

$$T = \sum_n T_n + \sum_n T_n G_0 \sum_{m \neq n} T_m + \sum_n T_n G_0 \sum_{m \neq n} T_m G_0 \sum_{r \neq m} T_r + \cdots \tag{6.15}$$

so taking averages gives

$$\langle T \rangle = \sum_n \langle T_n \rangle + \sum_n \sum_{m \neq n} \langle T_n G_0 T_m \rangle + \cdots . \tag{6.16}$$

In the *single-site approximation*, scattering from different sites are taken to be independent, so (6.16) becomes

$$\langle T\rangle = \sum_n \langle T_n\rangle + \sum_n \sum_{m\neq n} \langle T_n\rangle G_0 \langle T_m\rangle + \cdots ; \quad \langle T_n\rangle = \langle t_n\rangle |n\rangle\langle n|. \tag{6.17}$$

Note that

$$\langle t_n\rangle = c_A t_n^A + c_B t_n^B \tag{6.18}$$

since each scatterer must be of type A or B, with respective concentrations c_A and c_B. Taking all A or all B scatterers to be equivalent, (6.18) simplifies to

$$\langle t_n\rangle = c_A t_A + c_B t_B, \tag{6.19}$$

where from (6.14),

$$t_X \equiv t_n^X = v_n^X \left[1 - v_n^X G_0(n,n)\right]^{-1} \tag{6.20}$$

with $X = A$ or B.

To this point, the formalism has been quite general, and from here we could proceed to derive any one of several *single-site* approximations (such as the ATA, for example). However, we wish to focus on the desired approach, the CPA. To do so, we recall that our aim is to produce a (translationally invariant) *effective* Hamiltonian H_e, which reflects the properties of the exact Hamiltonian H (6.2) as closely as possible. With that in mind, we notice that the closer the choice of unperturbed Hamiltonian H_0 (6.4) is to H_e, then the smaller are the effects of the perturbation term in (6.7), and hence in (6.10). Clearly, then, the optimal choice for H_0 is H_e. Thus, we have

$$G_0 = G_e \equiv \langle G\rangle, \tag{6.21}$$

where

$$G_e = (\omega - H_e)^{-1}. \tag{6.22}$$

In light of the choice giving (6.21), we see that (6.10) implies

$$\langle T\rangle = 0, \tag{6.23}$$

from which (6.17) gives

$$\langle t_n\rangle = 0, \quad \forall \quad n. \tag{6.24}$$

Equation (6.24) is the *crucial condition* of the CPA, whose physical interpretation is that the scattering from a single site of the effective medium is, on average, the same as that for the exact medium. In view of (6.19), the condition (6.24) reduces to

$$c_A t_A + c_B t_B = 0, \tag{6.25}$$

with t_A and t_B given by (6.20), and v_n^A, v_n^B yet to be determined.

We are now at the stage where we can specify the Hamiltonians and thus calculate the GF's. Firstly, we take the exact Hamiltonian to be

$$H = \sum_n \varepsilon_n |n\rangle\langle n| - \sum_n J(|n\rangle\langle n+1| + |n+1\rangle\langle n|), \tag{6.26}$$

where $J = -\beta$ in the notation of Chap. 1, and

$$\varepsilon_n = \begin{cases} \varepsilon_A, & \text{site } n \text{ occupied by } A, \\ \varepsilon_B, & \text{site } n \text{ occupied by } B, \end{cases} \tag{6.27}$$

with the choice of occupant of site n being *random*. Secondly, the form for the unperturbed, effective Hamiltonian is taken to be

$$H_0 = H_e = \sum_n \left[\alpha_v + \sigma_n(E)\right] |n\rangle\langle n| - \sum_n J\left(|n\rangle\langle n+1| + |n+1\rangle\langle n|\right), \tag{6.28}$$

where α_v is the VC site energy (6.1) and $\sigma_n(E)$ is the complex, energy-dependent *coherent potential* (as yet unknown) on site n. For an infinite (cyclic) alloy, the CP is a site-independent *bulk CP*, i.e., $\sigma_n = \sigma_b(E)$, and the corresponding effective GF is found to be (App. J, with $J = -\beta$)

$$G_e(n,m) = t^{|n-m|}[2Js(\xi^2-1)^{1/2}]^{-1}, \tag{6.29}$$

from (2.49), (2.40) and (2.37), where

$$t = \xi + s(\xi^2-1)^{1/2}, \tag{6.30}$$

$$\xi = [\alpha_v + \sigma_b(E) - E]/2J, \tag{6.31}$$

$$s = \pm 1 \quad \text{so that} \quad |t| < 1. \tag{6.32}$$

In light of (6.26) and (6.28), we see that the perturbation $V = H - H_0$, from (6.7), can be expressed as

$$\begin{aligned} V &= \sum_n \left[\varepsilon_n - \alpha_v - \sigma_n(E)\right] |n\rangle\langle n| \\ &= \sum_n \left[\Delta\eta_n - \sigma_n(E)\right] |n\rangle\langle n|, \end{aligned} \tag{6.33}$$

where, using (6.1) and (6.27), we see that

$$\Delta = \varepsilon_A - \varepsilon_B \tag{6.34}$$

and

$$\eta_n = \begin{cases} 1-c, & \text{site } n \text{ occupied by } A, \\ -c, & \text{site } n \text{ occupied by } B, \end{cases} \tag{6.35}$$

with $c = c_A = 1 - c_B$. In other words, we have

$$v_n = \Delta\eta_n - \sigma_n(E), \tag{6.36}$$

or, more explicitly,

$$v_n^A = \Delta(1-c) - \sigma_n(E), \tag{6.37a}$$

$$v_n^B = -\Delta c - \sigma_n(E), \tag{6.37b}$$

Thus, the single-site scatterers (6.20) can be written as

$$t_A = [\Delta(1-c) - \sigma_n]\left\{1 - [\Delta(1-c) - \sigma_n]G_e(n,n)\right\}^{-1}, \tag{6.38a}$$

$$t_B = (-\Delta c - \sigma_n)\left[1 - (-\Delta c - \sigma_n)G_e(n,n)\right]^{-1}. \tag{6.38b}$$

Inserting (6.38) into (6.25) and rearranging produces

$$\sigma_n = (\Delta c + \sigma_n)G_e(n,n)[\Delta(1-c) - \sigma_n], \tag{6.39}$$

which is the *self-consistency condition* for the complex, energy-dependent CP $\sigma_n(E)$. In principle, both σ_n and c can be taken to vary from site to site, but for a bulk, infinite alloy they should be taken to be site-independent. It is within the context of surface properties that the site dependence becomes important (§6.2).

It should be kept in mind that any GF, and specifically G_e, is complex within the energy bands, but is purely real outside them. Equation (6.39) then implies that the same property is attached to the CP, namely, that $\sigma_n(E)$ is complex (real) for energies E inside (outside) the bands.

We note that G_e in (6.39) depends on σ_n through (6.29)-(6.32), so (6.39) is actually quite a complicated relationship for σ_n as a function of E. $\sigma_n(E)$ can be calculated numerically, by defining the function

$$f(u) = u - (\Delta c + u)G_e(n,n)[\Delta(1-c) - u], \tag{6.40}$$

and then noting that the zeroes $u = \sigma_n(E)$ of (6.40) are solutions of (6.39). A technique, such as quadratic interpolation, can be used to find that zero of f satisfying Im $\sigma_n(E) \leq 0$, a condition needed to give a positive DOS.

6.2 Alloy Surface Green Function

In this section, we extend the above formalism to that for an alloy surface within the CPA, which serves as the model for the pre-chemisorption substrate. The model discussed here is based on that of Ueba and Ichimura (1979a,b) and Parent et al (1980). For a comprehensive introduction to alloy surfaces see Turek et al (1996). A feature of surface-alloy models, which is different from bulk ones, is that the CP in layers near the surface is different from that in the bulk, due to the surface perturbation. Moreover, the alloy concentration in the surface layers may be quite different from that in the bulk, a feature known as *surface segregation*. (See Ducastelle et al 1990 and Modrak 1995 for recent reviews.) We assume that both of these surface effects are confined to the first surface layer only.

The system under consideration consists of an isolated hydrogen-like atom and a DBA with a surface, as shown in Fig. 6.1. Following (6.28), the effective Hamiltonian for this system is

$$H_s = \varepsilon_a|0\rangle\langle 0| + \sum_{n=1}^{\infty}[\alpha_n + \sigma_n(E)]|n\rangle\langle n| - \sum_{n=1}^{\infty} J(|n\rangle\langle n+1| + |n+1\rangle\langle n|), \quad (6.41)$$

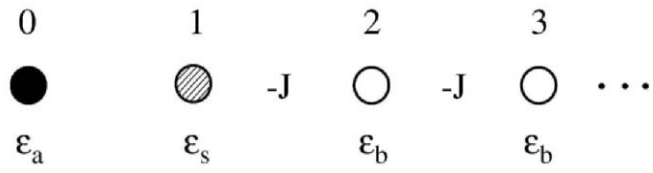

Fig. 6.1. One-dimensional model depicting pre-chemisorption, where $\varepsilon_m = \alpha_m + \sigma_m$, with $m = b$ or s. Reprinted with permission from Sulston et al (1986). Copyright 1986 by the American Physical Society.

where ε_a is the electronic energy of the pre-adsorbed atom, α_n is the VC electronic energy on the nth substrate atom, $\sigma_n(E)$ the CP, and $-J$, the bond strength between *nearest-neighbour* (NN) atoms in the alloy. In light of the comments in the preceding paragraph, σ_n is taken to have its bulk

value σ_b at all lattice sites, except the surface one ($n = 1$), where it has the value σ_s. Similarly, the alloy concentration is assumed to be the same, namely, $c = c_b$ in all layers, except the surface one, where it has the value c_s. Consequently, the VC electronic energy (6.1) has the values

$$\alpha_n = \begin{cases} c_s^A \varepsilon_A + c_s^B \varepsilon_B = c_s \Delta + \varepsilon_B, & n = 1, \\ c_b^A \varepsilon_A + c_b^B \varepsilon_B = c_b \Delta + \varepsilon_B, & n > 1, \end{cases} \tag{6.42}$$

with Δ given by (6.34). In addition, an extension of the VCA (Foo et al 1971) introduces a concentration dependence into the bond energy, so that

$$J = c_b^2 J_A + 2c_b(1 - c_b)J_{AB} + (1 - c_b)^2 J_B, \tag{6.43}$$

where J_A, J_{AB} and J_B are the $A-A$, $A-B$ and $B-B$ negative bond energies, respectively.

The Greenian corresponding to the semi-infinite Hamiltonian (6.41), viz.,

$$G_s(E) = (E + i0^+ - H_s)^{-1}, \tag{6.44}$$

is connected to the infinite Greenian G_e (6.29) via the Dyson equation (6.6), i.e.,

$$G_s = G_e + G_e V_s G_s, \tag{6.45}$$

where

$$V_s = J\left(|0\rangle\langle 1| + |1\rangle\langle 0|\right) + (\alpha_s + \sigma_s - \alpha_b - \sigma_b)|1\rangle\langle 1|. \tag{6.46}$$

The first term in (6.46) severs the bonds between the $n = 0$ and $n = 1$ sites, thereby creating a surface at the $n = 1$ site, while the second term perturbs the electronic environment on the surface atom, compared to that in the bulk. Substituting (6.46) into (6.45) and evaluating the matrix element $\langle 1|G_s|1\rangle = G_s(1,1)$ leads to

$$\begin{aligned} G_s(1,1) = G_e(1,1) + JG_e(1,0)G_s(1,1) + JG_e(1,1)G_s(0,1) \\ + (\alpha_s + \sigma_s - \alpha_b - \sigma_b)G_e(1,1)G_s(1,1). \end{aligned} \tag{6.47}$$

However, $G_s(0,1) = 0$, since sites 0 and 1 are on opposite sides of the cleaved solid. Moreover, from (6.29) we see that $G_e(1,0) = tG_e(1,1)$, so (6.47) reduces to

$$\begin{aligned} G_s(1,1) = G_e(1,1) + JtG_e(1,1)G_s(1,1) \\ + (\alpha_s + \sigma_s - \alpha_b - \sigma_b)G_e(1,1)G_s(1,1), \end{aligned}$$

which can be rearranged to give

$$G_s(1,1) = \left[G_e^{-1}(1,1) - Jt - (\alpha_s + \sigma_s - \alpha_b - \sigma_b)\right]^{-1}. \tag{6.48}$$

Inserting (6.29), (6.30), (6.42) and simplifying yields the *surface GF*

$$g_s(E) = G_s(1,1) = \left[Js(\xi^2-1)^{1/2} - (c_s - c_b)\Delta - \sigma_s + \sigma_b - J\xi\right]^{-1}. \tag{6.49}$$

The surface CP σ_s is found by putting g_s in place of G_e in the CPA self-consistency equation (6.39), whence

$$\sigma_s = (\Delta c_s + \sigma_s) g_s(E) \left[\Delta(1-c_s) - \sigma_s\right]. \tag{6.50}$$

Substituting (6.49) into (6.50) and rearranging gives an explicit form for σ_s:

$$\sigma_s(E) = \frac{2\Delta^2 c_s(1-c_s)}{2Js(\xi^2-1)^{1/2} - 2\Delta(1-2c_s) + \sigma_b - 2c_s\Delta + c_b\Delta - \varepsilon_B + E}. \tag{6.51}$$

Note that the evaluation of (6.51) does *not* require a self-consistency calculation. The bulk CP $\sigma_b(E)$ is, as we have seen, calculated self-consistently in (6.39), but once that has been done, the computation of the surface CP $\sigma_s(E)$ via (6.51) is straightforward.

The energies E_s of any localized surface states (Davison and Stęślicka 1996) are given by the (real) poles of $g_s(E)$ in (6.49); i.e., by the solutions $E = E_s$ of

$$Js(\xi^2-1)^{1/2} - (c_s - c_b)\Delta - \sigma_s + \sigma_b - J\xi = 0, \tag{6.52}$$

which can be calculated numerically. Since the CP's are real outside the bands (as noted earlier), the surface-state energies E_s from (6.52) do turn out to be real. The existence condition for the surface states can be obtained from (6.52), whose rearrangement gives

$$s(\xi^2-1)^{1/2} = J^{-1}\left[(c_s - c_b)\Delta + \sigma_s - \sigma_b\right] + \xi, \tag{6.53}$$

which, upon squaring and solving for ξ, shows that

$$\xi = -\frac{J}{2}\left[(c_s - c_b)\Delta + \sigma_s - \sigma_b\right]^{-1} - \frac{1}{2J}\left[(c_s - c_b)\Delta + \sigma_s - \sigma_b\right]. \tag{6.54}$$

With the aid of (6.30), adding (6.53) and (6.54) leads to

$$t = -J\left[(c_s - c_b)\Delta + \sigma_s - \sigma_b\right]^{-1}, \tag{6.55}$$

which, by dint of (6.32), provides the *surface-state existence condition*

$$|(c_s - c_b)\Delta + \sigma_s(E) - \sigma_b(E)| > |J|. \tag{6.56}$$

Thus, any solution $E = E_s$ to (6.52) must satisfy (6.56) to be a valid surface-state energy.

The last surface property to consider is the surface DOS, which has the form (Davison and Stęślicka 1996)

$$\rho_s(E) = -\pi^{-1}\text{Im } g_s(E), \tag{6.57}$$

g_s being given by (6.49). With the surface properties now known, via the GF, they can be used to study those of the chemisorbed system.

6.3 Adatom Green Function

The literature on the theory of DBA chemisorption has been rather sporadic over the years, perhaps because of the complexity of treating a disordered substrate. Van Santen (1975, 1982) and van Santen and Sachtler (1977) used a cluster model to study the effects of alloying two metals on a chemisorption bond. It was noted that modification of the d-band structure is a key consideration in determining the impact on chemisorption properties. In another early paper, Moran-Lopez et al (1975) used a TB model with the Bethe-Peierls approximation (an extension of the CPA) to model Ni atoms on Cu/Ni alloys. Important factors in the chemisorption process were found to be the alloy concentration, the adatom's position and the strength of the adatom-substrate bond. In the paper, upon which the current section is based, Sulston et al (1986) modelled the chemisorption process by using the ANG theory in conjunction with the CPA. An extension of this work, by Sulston and Bose (1988), incorporated the effects of long-range order. Cong (1994) used a similar model to look at the effects of multi-layer segregation, concluding that these are indeed non-negligible. Closely related work by Zhang (1992a,b), using both the ATA and the CPA, confirmed the importance of surface segregation as a factor in the chemisorption process, and that, in fact, the chemisorption itself may change the surface segregation, the consequence being to stabilize the chemisorption.

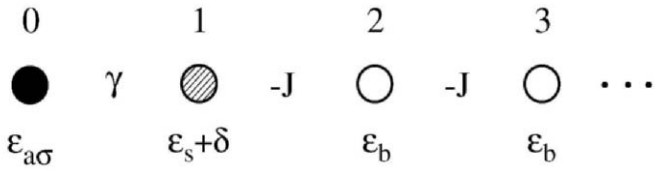

Fig. 6.2. One-dimensional model depicting post-chemisorption. Reprinted with permission from Sulston et al (1986). Copyright 1986 by the American Physical Society.

We now investigate a model of the chemisorbed system, consisting of a semi-infinite DBA and a hydrogen-like adatom, as depicted in Fig. 6.2. The adatom, with initial electronic site energy ε_a, is attached to the surface atom (at site $n = 1$) by a bond of energy γ. Using the HF approximation to the ANG model (§4.3), the effective adatom level of spin σ is shifted to (4.34)

$$\varepsilon_{a\sigma} = \varepsilon_a + U\langle n_{a,-\sigma}\rangle, \quad \sigma = + \quad \text{or} \quad - . \tag{6.58}$$

Here, we consider only the non-magnetic case, so the subscript σ can be omitted, i.e.,

$$\langle n_{a_+}\rangle = \langle n_{a_-}\rangle = \langle n_a\rangle. \tag{6.59}$$

The only other effect of chemisorption included in the model is the modification of the surface CP from σ_s to σ_c (while σ_b is assumed to be unchanged). One possible effect *not* included is that of chemisorption-induced changes in the concentrations c_s and c_b (see, e.g., Modrak 1997) – although potentially important, for simplicity, we ignore this phenomenon.

In light of the above comments, the effective Hamiltonian H_c for the chemisorbed system is related to the pre-chemisorption Hamiltonian H_s of (6.41) by

$$H_c = H_s + V_c. \tag{6.60}$$

The perturbation due to chemisorption has the form

$$V_c = \nu|0\rangle\langle 0| + \gamma\left(|0\rangle\langle 1| + |1\rangle\langle 0|\right) + \delta|1\rangle\langle 1|, \tag{6.61}$$

where

$$\nu = U\langle n_a \rangle \tag{6.62}$$

and

$$\delta = \sigma_c(E) - \sigma_s(E). \tag{6.63}$$

The Greenian G_c of H_c is related to G_s by the Dyson equation, i.e.,

$$G_c = G_s + G_s V_c G_c. \tag{6.64}$$

The matrix elements of G_c can be found by substituting (6.61) into (6.64). The key elements are those centered on the adatom and the surface atom. Using (6.64), the evaluation of $G_c(0,0) = \langle 0|G_c|0\rangle$ gives

$$G_c(0,0) = G_s(0,0) + \nu G_s(0,0)G_c(0,0) + \gamma G_s(0,0)G_c(1,0), \tag{6.65}$$

in which we have taken $G_s(0,1) = 0$, because there is no bond between the adatom and the surface before chemisorption. The unknown element $G_c(1,0)$ is also obtained from (6.64) as

$$G_c(1,0) = \gamma G_s(1,1)G_c(0,0) + \delta G_s(1,1)G_c(1,0), \tag{6.66}$$

where again $G_s(1,0) = 0$. Solving (6.66) for $G_c(1,0)$, and inserting the result into (6.65), yields the adatom GF

$$g_a(E) = G_c(0,0) = \left\{G_s^{-1}(0,0) - \nu - \gamma^2[G_s^{-1}(1,1) - \delta]^{-1}\right\}^{-1}. \tag{6.67}$$

Noting that the GF for the isolated adatom is

$$G_s(0,0) = (E - \varepsilon_a)^{-1}, \tag{6.68}$$

and introducing this, along with (6.62) and (6.63), into (6.67) gives

$$\begin{aligned} g_a(E) &= G_c(0,0) \\ &= \left\{E - \varepsilon_a - U\langle n_a\rangle - \gamma^2[G_s^{-1}(1,1) - \sigma_c + \sigma_s]^{-1}\right\}^{-1}, \end{aligned} \tag{6.69}$$

where $G_s(1,1) = g_s(E)$ is just the surface GF (6.49). A similar derivation, starting from (6.64), leads to the matrix element of G_c on the surface atom, viz.,

$$G_c(1,1) = \left\{G_s^{-1}(1,1) - \delta - \gamma^2[G_s^{-1}(0,0) - \nu]^{-1}\right\}^{-1}. \tag{6.70}$$

Since the adatom GF $g_a(E)$ is purely complex only within the energy band(s), the adatom DOS has the form (4.75)

$$\rho_a(E) = -\pi^{-1}\text{Im } g_a(E). \tag{6.71}$$

Outside the band, the only energies of interest are those energies E_p of any localized states of the chemisorbed system. These energies are given by the poles of $g_a(E)$ in (6.69), namely, by

$$\begin{aligned} E_p - \varepsilon_a - U\langle n_a\rangle - \gamma^2[Js(\xi^2-1)^{1/2} - (c_s - c_b)\Delta \\ - \sigma_c(E_p) + \sigma_b(E_p) - J\xi]^{-1} = 0, \end{aligned} \tag{6.72}$$

using (6.49). These energies must, of course, be calculated numerically, and are subject to an existence condition analogous to (6.56) for surface states. The condition is derived by first rearranging (6.72) as

$$Js(\xi^2-1)^{1/2} = \Gamma(E_p) + J\xi, \tag{6.73}$$

where

$$\Gamma(E_p) = \gamma^2[E_p - \varepsilon_a - U\langle n_a\rangle]^{-1} + (c_s - c_b)\Delta + \sigma_c(E_p) - \sigma_b(E_p). \tag{6.74}$$

Upon squaring, and using $s^2 = 1$ from (6.32), (6.73) can be rearranged as

$$\xi = -\Gamma(E_p)/(2J) - J/(2\Gamma(E_p)). \tag{6.75}$$

Adding (6.73) and (6.75) gives the quantity t from (6.30):

$$t \equiv \xi + s(\xi^2-1)^{1/2} = -J/\Gamma(E_p). \tag{6.76}$$

From the requirement $|t| < 1$ in (6.32), comes the *chemisorption-state existence condition*

$$|\Gamma(E_p)| > |J|. \tag{6.77}$$

6.4 Chemisorption Properties

In the previous discussion of the adatom GF, we glossed over the calculation of a couple of important quantities. The evaluation of the CP's σ_b and σ_s was discussed earlier, but that of σ_c was not. Moreover, the computation of the

adatom occupancy $\langle n_a \rangle$ has, so far, been ignored. In fact, both $\sigma_c(E)$ and $\langle n_a \rangle$ are linked together, and their simultaneous evaluation is now discussed.

The surface CP $\sigma_c(E)$ in the chemisorbed system is determined by a self-consistency condition, which is found by substituting $G_c(1,1)$ into the general CPA equation (6.39), to give

$$\sigma_c = (\Delta c_s + \sigma_c) G_c(1,1) \left[\Delta(1 - c_s) - \sigma_c\right]. \tag{6.78}$$

With the aid of (6.49), substituting (6.70) into (6.78) and simplifying leads to the self-consistency expression for σ_c:

$$\begin{aligned} \sigma_c(E) = \Delta^2 c_s (1 - c_s) \big[& Js(\xi^2 - 1)^{1/2} - (c_s - c_b)\Delta + \sigma_b - J\xi \\ & - \gamma^2 (E - \varepsilon_a - U\langle n_a \rangle)^{-1} - \Delta(1 - 2c_s) \big]^{-1}, \end{aligned} \tag{6.79}$$

which clearly shows that the value of the occupation number $\langle n_a \rangle$ must be known in order to evaluate the complex energy-dependent function $\sigma_c(E)$. However, we recall from (4.76) and (4.78) that $\langle n_a \rangle$ is given by the self-consistency condition

$$\langle n_a \rangle = \int_{\varepsilon_l}^{\varepsilon_f} \rho_a(E) dE + \sum_p \operatorname{Res} g_a(E_p), \tag{6.80}$$

ε_l being the lower band edge. The first term integrates the adatom DOS $\rho_a(E)$, given by (6.71), over the occupied part of the band, and the second term sums the residues of g_a at the occupied chemisorption states with energy E_p (6.72). The residue term is given by the general expression (4.79), from which a (complicated) explicit form can be derived, for computational purposes. However, the important thing to note about (6.80) is that the evaluation of $\langle n_a \rangle$ requires knowledge of $\sigma_c(E)$,which appears in $g_a(E)$ (6.69) (and hence in $\rho_a(E)$). Thus, the calculation of either $\langle n_a \rangle$ or $\sigma_c(E)$ requires the value of the other, whence there is a *coupling* of their self-consistency conditions (6.79) and (6.80), so these must be solved *simultaneously*. It should be noted that there is an "imbalance" between the two quantities, in that $\sigma_c(E)$ is a complex function of energy, whereas $\langle n_a \rangle$ is just a real constant. Consequently, once $\langle n_a \rangle$ has been calculated (self-consistently) for a particular set of parameters, then σ_c can be easily evaluated, for any energy, by (6.79) alone.

Once the double self-consistency equations have been solved numerically, it is trivial to calculate the charge transfer (4.102) from the surface to the

adatom. As seen earlier, the adatom initially has a single electron, but, after chemisorption, has occupancy $\langle n_a \rangle$ in each of its two orbitals, so the charge transfer is again

$$\Delta q = (2\langle n_a \rangle - 1)e. \tag{6.81}$$

The final property of interest is the chemisorption energy ΔE, given by (App. L)

$$\Delta E = 2\Delta E^{\sigma} - U\langle n_a \rangle^2 + \varepsilon_a - \varepsilon_f. \tag{6.82}$$

where the 1-electron energy change is

$$\Delta E^{\sigma} = \int_{-\infty}^{\varepsilon_f} (E - \varepsilon_f)\Delta\rho(E)dE, \tag{6.83}$$

ε_f being the FL. To evaluate ΔE^{σ}, it is necessary to derive the expression for $\Delta\rho$, the change in DOS caused by chemisorption, by means of the Dyson equation (6.64). Evaluating the general element $G_c(i,j) = \langle i|G_c|j\rangle$, from (6.61) in (6.64), gives

$$\begin{aligned} G_c(i,j) = G_s(i,j) + \nu G_s(i,0)G_c(0,j) + \gamma G_s(i,0)G_c(1,j) \\ + \gamma G_s(i,1)G_c(0,j) + \delta G_s(i,1)G_c(1,j), \end{aligned} \tag{6.84}$$

which, for $i \neq 0$, reduces to

$$G_c(i,j) = G_s(i,j) + \gamma G_s(i,1)G_c(0,j) + \delta G_s(i,1)G_c(1,j), \tag{6.85}$$

where the unknown elements $G_c(0,j)$ and $G_c(1,j)$ are found by using a pair of coupled equations from (6.84), namely, (for $j \neq 0$)

$$G_c(0,j) = \nu G_s(0,0)G_c(0,j) + \gamma G_s(0,0)G_c(1,j), \tag{6.86}$$

and

$$G_c(1,j) = G_s(1,j) + \gamma G_s(1,1)G_c(0,j) + \delta G_s(1,1)G_c(1,j). \tag{6.87}$$

The solutions to (6.86) and (6.87) are

$$G_c(0,j) = \gamma G_s(0,0)G_s(1,j)M^{-1}, \tag{6.88}$$

$$G_c(1,j) = [1 - \nu G_s(0,0)]\, G_s(1,j)M^{-1}, \tag{6.89}$$

where

$$M = [1 - \nu G_s(0,0)]\,[1 - \delta G_s(1,1)] - \gamma^2 G_s(0,0) G_s(1,1). \tag{6.90}$$

Putting (6.88) and (6.89) into (6.85), with $i = j > 0$, gives

$$G_c(i,i) - G_s(i,i) = \left\{\gamma^2 G_s(0,0) + \delta[1 - \nu G_s(0,0)]\right\} G_s^2(i,1) M^{-1}. \tag{6.91}$$

We also note that the adatom GF (6.69) can be rewritten as

$$G_c(0,0) = G_s(0,0)\,[1 - \delta G_s(1,1)]\,M^{-1}, \tag{6.92}$$

$G_s(0,0)$ and $G_s(1,1)$ being known from (6.68) and (6.49), respectively.

With the necessary GF's available, the change in DOS can be constructed as

$$\Delta\rho = -\pi^{-1}\mathrm{Im}\,\left\{G_c(0,0) - G_s(0,0) + \sum_{i=1}^{\infty}\left[G_c(i,i) - G_s(i,i)\right]\right\}. \tag{6.93}$$

Substituting (6.91) and (6.92) into (6.93) and rearranging leads to

$$\begin{aligned}\Delta\rho = -\pi^{-1}\mathrm{Im}\; M^{-1}\Big\{ & G_s(0,0)[1 - \delta G_s(1,1)] - G_s(0,0) M \\ & + \left[\gamma^2 G_s(0,0) + \delta[1 - \nu G_s(0,0)]\right] \sum_{i=1}^{\infty} G_s^2(i,1)\Big\}.\end{aligned} \tag{6.94}$$

It is fairly easy to show, from the Dyson equation (6.45), that the surface GF's satisfy

$$G_s(i,1) = t^{i-1} G_s(1,1), \quad i \geq 1, \tag{6.95}$$

because the bulk GF's $G_e(i,1)$ satisfy an analogous property [c.f. (5.3)]. So the summation in (6.94) evaluates simply as a geometric series, viz.,

$$\sum_{i=1}^{\infty} G_s^2(i,1) = G_s^2(1,1) \sum_{i=1}^{\infty} t^{2i-2} = G_s^2(1,1)(1 - t^2)^{-1} \tag{6.96}$$

with convergence guaranteed, because $|t| < 1$ from (6.32). Inserting (6.96) into (6.94), and simplifying, yields

$$\begin{aligned}\Delta\rho = -\pi^{-1}\mathrm{Im}\; M^{-1}\Big\{ & \nu G_s^2(0,0)[1 - \delta G_s(1,1)] + \gamma^2 G_s^2(0,0) G_s(1,1) \\ & + \left[\gamma^2 G_s(0,0) + \delta[1 - \nu G_s(0,0)]\right] G_s^2(1,1)/(1 - t^2)\Big\},\end{aligned} \tag{6.97}$$

which, although complicated, is a useable expression for $\Delta\rho$ in the numerical integration of (6.83).

Separating (6.83) for ΔE^σ into contributions from inside and outside the band, gives

$$\Delta E^\sigma = E_{p1} + E_{p2} - E_z - \varepsilon_a + \int_{\varepsilon_l}^{\omega} (E - \varepsilon_F)\Delta\rho(E)dE, \tag{6.98}$$

assuming an amalgamated band structure, and with

$$\omega = \min(\varepsilon_u, \varepsilon_f), \tag{6.99}$$

to deal with the two possibilities of the FL ε_f being within or above the band, ε_u being the upper band edge. The integral term of (6.98) covers the contribution from the continuous band states, while the other terms deal with the discrete localized states. As in the case for DBA surface states (Parent et al 1980), localized chemisorption states occur in *pairs* (assuming they exist). These are denoted in (6.98) by E_{p1} and E_{p2}. As a result of the chemisorption process, σ_s is changed to σ_c, creating an "intermediate" state of energy E_z, which, on completion of the adsorption process, is shifted to E_{p2}. We now know all the quantities required to compute the chemisorption energy (6.82).

6.5 H-Cu/Ni and H-Au/Pt Systems

Turning to the numerical results (Sulston et al 1986), we look at the chemisorption properties of H on Cu/Ni and Au/Pt alloys, over a range of bulk concentrations. The H parameters used are $\varepsilon_a = -14.3$ eV, measured from the vacuum level, and $U = 12.9$ eV. The pure-metal parameters (Newns 1969 and Nordlander et al 1984) are shown in Table 6.1. Following the concept of the VCA, ε_f and γ are assigned concentration dependencies, namely,

$$\varepsilon_f = c_b {\varepsilon_f}^A + (1 - c_b){\varepsilon_f}^B \tag{6.100}$$

and

$$\gamma = c_s\gamma_A + (1 - c_s)\gamma_B. \tag{6.101}$$

The negative bond energy J_{AB}, required in (6.43), is approximated by $J_{AB} \approx (J_A + J_B)/2$.

Table 6.1

Parameter	Ni	Cu	Pt	Au
ε_A	-6.26	-7.39	-8.54	-8.43
J	0.95	0.675	1.825	1.325
ε_f	-4.50	-4.46	-5.6	-4.3
γ	3.75	4.17	4.017	4.605
ΔE	-2.89	2.36	-2.47	-2.25

The system of H chemisorbed on Cu/Ni is examined both with and without surface segregation. In the case of $c_s = c_b$ (i.e., no surface segregation), the curve of ΔE vs c_b is shown in Fig. 6.3(a), and is seen to have a monotonic behaviour, which is almost linear for intermediate values of c_b. In the dilute limits (c_b close to 0 or 1), ΔE is closer to the value for the corresponding pure system than a purely linear relationship would produce, which suggests that the effect of any minority atoms, even near the surface, is cancelled by the averaging process used in the CPA.

However, surface segregation ($c_s \neq c_b$) has a radical effect on ΔE, as can clearly be seen in Fig. 6.3(b). Cu/Ni alloys are known (Kelley and Ponec 1981, Ouannasser et al 1997) to have an enriched Cu concentration in the surface layer for all bulk concentrations. As a result, the alloy shows a more Cu-like behaviour than it would if it were non-segregated. In particular, ΔE has a value significantly closer to that for pure Cu than in the case where $c_s = c_b$, and this occurs at all bulk concentrations c_b. The smallest change in ΔE occurs in Cu-rich alloys, which is understandable, because these alloys have mostly Cu in the surface layer anyway, so the effect of surface segregation is relatively small. Thus, surface segregation has a lesser effect in these alloys than in Ni-rich ones, which have mostly Ni in the bulk, but may have a Cu majority in the surface layer. Clearly, then, the concentration c_s of the surface layer is the primary parameter in determining the chemisorption properties of the DBA.

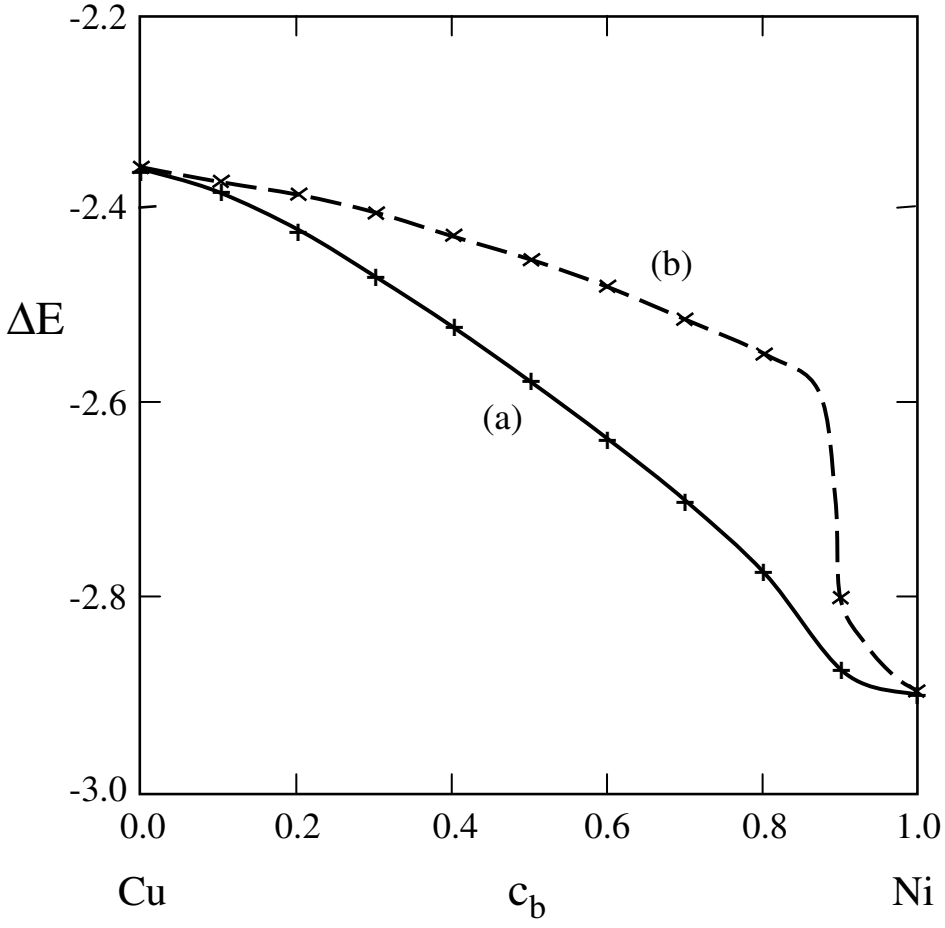

Fig. 6.3. ΔE for H-Cu/Ni versus bulk Ni concentration for (a) $c_s = c_b(+)$, (b) $c_s \neq c_b\,(\times)$. Reprinted with permission from Sulston et al (1986). Copyright 1986 by the American Physical Society.

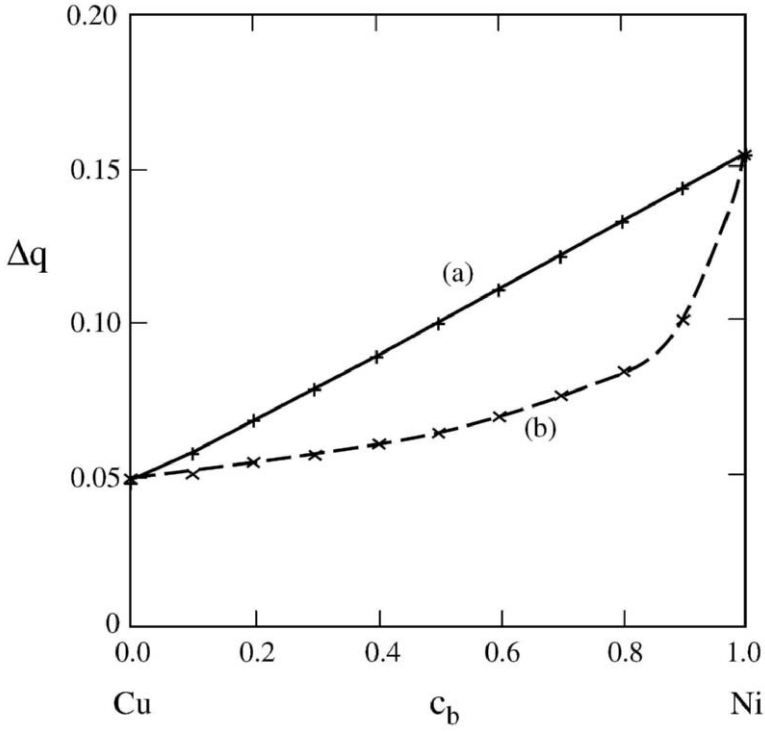

Fig. 6.4. Δq for H-Cu/Ni versus bulk Ni concentration for (a) $c_s = c_b(+)$, (b) $c_s \neq c_b(\times)$. Reprinted with permission from Sulston et al (1986). Copyright 1986 by the American Physical Society.

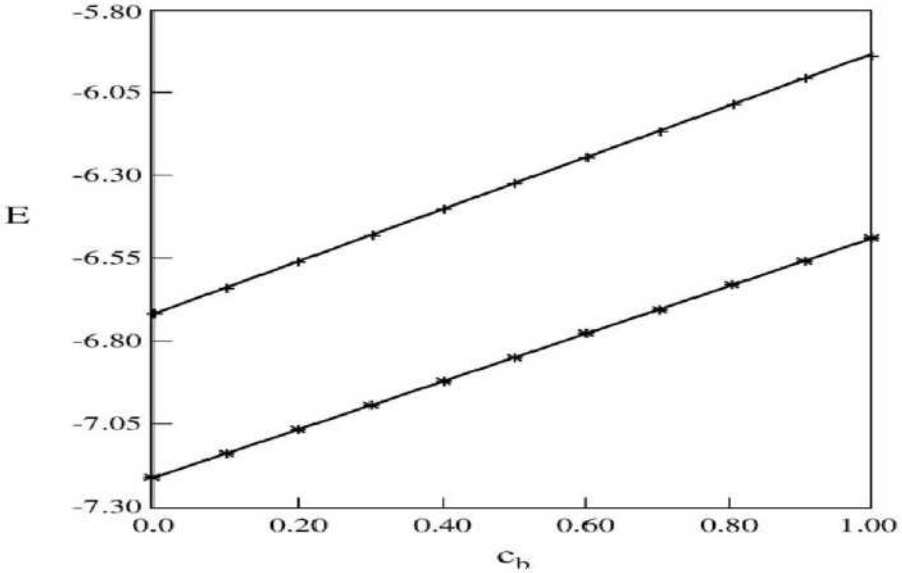

Fig. 6.5. Chemisorption-state energies for H-Cu/Ni with $c_s = c_b$. After Sulston (1986).

Charge transfer Δq to the adatom, for the case $c_s = c_b$, is displayed in Fig. 6.4(a). As is evident, the dependence of Δq on c_b is virtually linear throughout the range of concentrations. On the other hand, when surface segregation is present (Fig. 6.4b), Δq is lowered and becomes closer to the value for pure Cu (0.05), for all concentrations. Hence, in the segregated case, Δq, like ΔE, reflects the greater concentration of Cu in the surface layer.

Chemisorption-state energies (i.e., solutions of (6.72)) for $c_s = c_b$ are depicted in Fig. 6.5. Again, the dependence on c_b is virtually linear. Two states are found at all concentrations (except $c_b = 0$ and 1) with their intensities also dependent on c_b. In the dilute limits, the intensity of one state goes to zero, leaving only the state associated with the corresponding pure material. A closer study of the intensities shows that each chemisorption state is associated with one of the constituent metals: + with Ni and × with Cu. Thus, the splitting of surface states in a DBA, observed by Parent et al (1980), is also seen to occur for chemisorption states. The effect of surface segregation on the chemisorption states, as shown in Fig. 6.6, is seen to be the same as for the other chemisorption properties, namely, to produce a more Cu-like behaviour for all c_b. The chemisorption states are shifted to lower energies, with the greatest changes occurring for Ni-rich alloys.

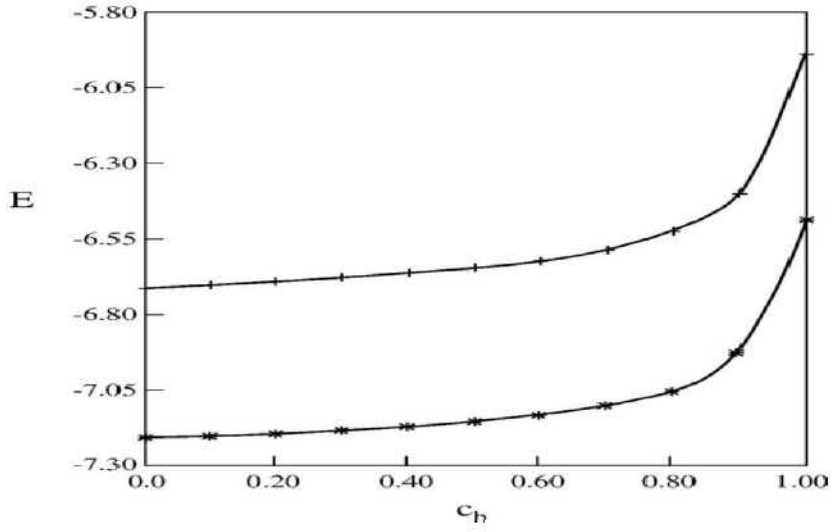

Fig. 6.6. Chemisorption-state energies for H-Cu/Ni with $c_b \neq c_s$. After Sulston (1986).

For H chemisorption on Au/Pt alloys, only the case $c_s = c_b$ was studied by Sulston et al (1986), because of a lack of consistent data on surface segregation. The curve of ΔE versus Au concentration (Fig. 6.7) has more interesting structure than the corresponding one for Cu/Ni alloy (Fig. 6.3 a). Specifically, there is an absolute minimum at $c_b \approx 0.3$, indicating that H is preferentially adsorbed on Au/Pt at the concentration ratio of 3:7. Observing (from Table 6.1) that ε_{Pt} and ε_{Au} only differ by 0.11 eV suggests that the effective electronic energy on an alloy site is not too strongly dependent on c_b. As true as this may be, here another factor comes into consideration. Calculations of the width of the occupied part of the band show it to be strongly dependent on c_b. Indeed, it turns out that band width as a function of c_b, has a maximum at $c_b \approx 0.3$ (the value at which ΔE has its minimum), indicating that for this system, the effective band width is an important parameter in the chemisorption process.

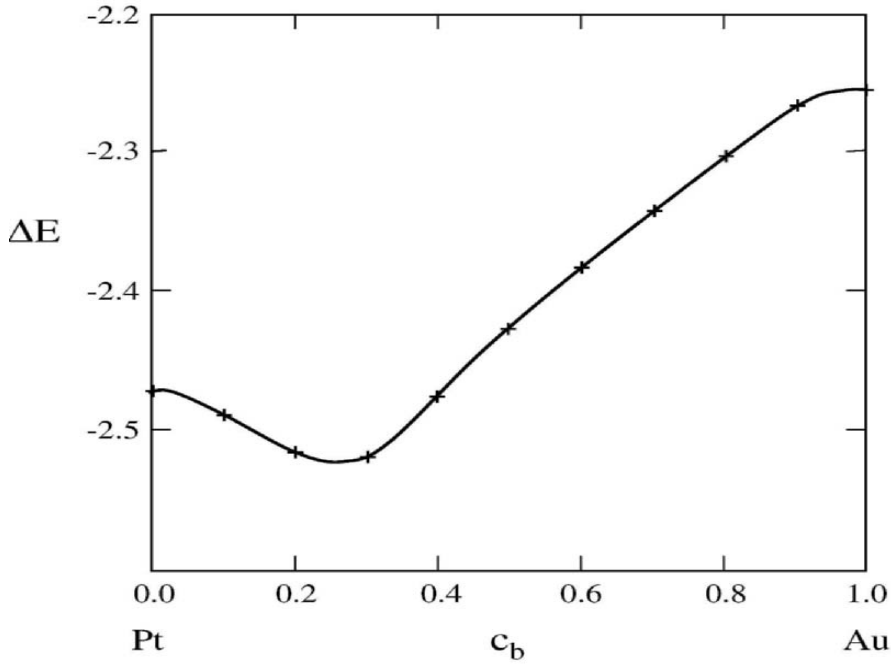

Fig. 6.7. ΔE for H-Au/Pt versus bulk Au concentration for $c_s = c_b$. Reprinted with permission from Sulston et al (1986). Copyright 1986 by the American Physical Society.

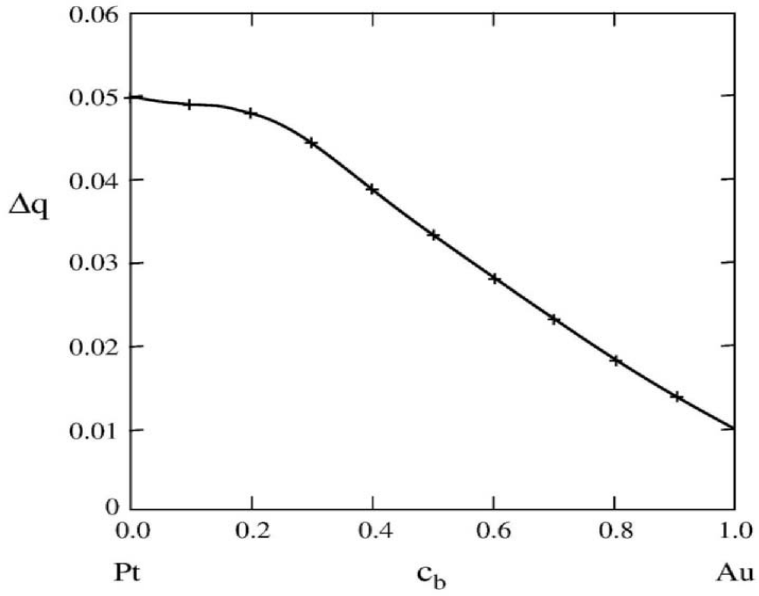

Fig. 6.8. Δq for H-Au/Pt versus bulk Au concentration for $c_s = c_b$. Reprinted with permission from Sulston et al (1986). Copyright 1986 by the American Physical Society.

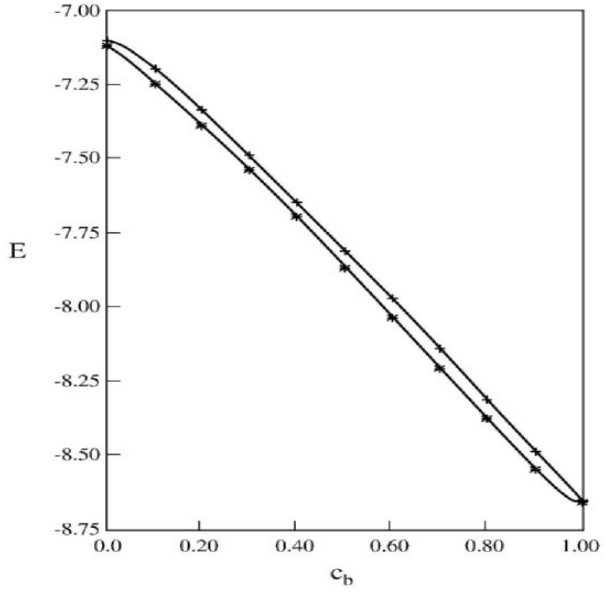

Fig. 6.9. Chemisorption-state energies for H-Au/Pt with $c_s = c_b$. After Sulston (1986).

The graph of Δq versus c_b is shown in Fig. 6.8, again for $c_s = c_b$. It displays a monotonically decreasing, but nonlinear behaviour. For concentrations less than the critical value of 0.3, the curve has a small negative slope, while for $c_b > 0.3$, the slope, though still negative, is markedly steeper. Generally speaking, one would expect smaller values of Δq (i.e., less charge transfer) to be associated with weaker chemisorption (i.e., smaller $|\Delta E|$). Such is true, in this case, only for $c_b > 0.3$. For $c_b < 0.3$, slight decreases in Δq are related to moderate increases in ΔE, contrary to expectation. However, as Fig. 6.9 shows, the chemisorption-state energies are higher (i.e., less negative) for smaller values of c_b and, hence, tend to reduce $|\Delta E|$ as c_b approaches 0. Thus, there are competing contributions to ΔE: Δq tending to raise it and E_p to lower it, as c_b increases. The result is a local minimum, occurring at $c_b \approx 0.3$, which is the concentration most favourable to chemisorption.

In conclusion, we have seen that alloys can exhibit a variety of interesting chemisorption properties. The chief parameters determining the behaviour of a system are the concentrations of the various layers, especially the surface one. Other important parameters are the effective electronic energy, the occupied band width, the adatom bond strength and the adatom position.

Chapter 7

Electrified Substrates

Why should electricity not modify the formation and properties of crystals?

— Denis Diderot

As we have seen, the chemisorption properties of the substrate depend on its electronic structure, so that changes in the latter are reflected in the former. In the case of electrified substrates, the strength of the applied electric field governs the substrate modification and, thereby, regulates the chemisorption process in a controllable manner.

7.1 Wannier-Stark Ladders

The study of the effect of electric fields on the properties of solids dates back to Zener's (1934) investigation of electrical breakdown in solid dielectrics. Further pioneering work was carried out by Houston (1940) and Slater (1949), who introduced aperiodic perturbations into the Bloch wave functions. A breakthrough came when James (1949) demonstrated the effect of a linear field on an infinite crystal, by means of the *effective-mass approximation*, and predicted that the energy spectrum would be quantized into *equally-spaced* levels. Simultaneously, and independently, Katsura et al (1950) reached the same conclusion via a one-dimensional TB model of an

infinite crystal, with wave functions shown to have *Bessel-function* (BF) coefficients, and whose energy-dependent order was required to be an integer to satisfy the normalization conditions. Although these two papers were the first to predict the discretization of the energy levels of a solid by an electric field, a more well-known article was that of Wannier (1960), so much so, that the effect is termed the *Wannier-Stark ladder* (WSL). Pursuant to Wannier's paper, a great many others were published on the topic, some of which, most notably by Zak (1967-69) and Rabinovitch (1970, 1971), cast doubt on the actual existence of a discrete WSL energy spectrum. The controversy was finally settled in favour of the WSL, when Hacker and Obermair (1970) put the results of Katsura et al and Wannier on a rigorous theoretical footing, and Koss and Lambert (1972) observed Wannier levels in their optical absorption experiments on GaAs. Nevertheless, the reservations expressed by Zak, Rabinovitch and others did possess some validity, and demonstrated the necessity for some restrictions on the existence of WSL's (Heinrichs and Jones 1972). In the ensuing years, WSL's have been investigated in a variety of contexts.

Having briefly noted the historical highlights of the WSL effect, we now examine the basic mathematical argument for its existence, namely, the idea that the energy spectrum of an infinite crystal is discretized by an applied field. For the present discussions, we assume that the applied field is linear, with its strength given by its gradient γ.

We consider an atomic chain of spacing a, within the TBA, having the usual site energies

$$\alpha = \langle n|H_0|n\rangle, \tag{7.1}$$

and bond energies

$$\beta = \langle n|H_0|n \pm 1\rangle, \tag{7.2}$$

$|n\rangle$ being the AO at site $x = na$. Thus, in terms of creation and annihilation operators, the Hamiltonian for the chain in the absence of the field is

$$H_0 = \sum_n \left[\alpha c_n^\dagger c_n + \beta(c_n^\dagger c_{n+1} + c_{n+1}^\dagger c_n)\right]. \tag{7.3}$$

Since the field-induced potential is assumed to be linear, and of the form

$$V(x) = \gamma x, \tag{7.4}$$

its matrix elements are

$$\langle n|V|n'\rangle = na\gamma\delta_{n,n'} \equiv n\Gamma\delta_{n,n'}, \quad \Gamma = \gamma a, \tag{7.5}$$

where Γ is the potential gradient. Hence, the Hamiltonian, with the applied field, can be written as

$$H = H_0 + V = \sum_n \left[(\alpha + n\Gamma) c_n^\dagger c_n + \beta (c_n^\dagger c_{n+1} + c_{n+1}^\dagger c_n) \right]. \tag{7.6}$$

Recalling that the anticommutation rules for the creation and annihilation operators are (App. C)

$$\left[c_n^\dagger, c_m \right]_+ = \delta_{nm}, \quad \left[c_n^\dagger, c_m^\dagger \right]_+ = 0, \tag{7.7}$$

we obtain a commutation relation of the form

$$\left[c_i^\dagger c_j, c_m^\dagger \right]_- = c_i^\dagger \left[c_j, c_m^\dagger \right]_+ - \left[c_i^\dagger, c_m^\dagger \right]_+ c_j = c_i^\dagger \delta_{jm}. \tag{7.8}$$

Because the creation operators $C^\dagger(E)$ for the eigenfunctions of H diagonalize the Hamiltonian, we have

$$\begin{aligned}
EC^\dagger(E) &= [H, C^\dagger(E)]_- \\
&= \left[H, \sum_m a_m(E) c_m^\dagger \right]_- \\
&= \left[\sum_n \left\{ (\alpha + n\Gamma) c_n^\dagger c_n + \beta (c_n^\dagger c_{n+1} + c_{n+1}^\dagger c_n) \right\}, \sum_m a_m(E) c_m^\dagger \right]_- \\
&= \sum_{n,m} a_m(E) \left\{ (\alpha + n\Gamma) [c_n^\dagger c_n, c_m^\dagger]_- + \beta [c_n^\dagger c_{n+1}, c_m^\dagger]_- + \beta [c_{n+1}^\dagger c_n, c_m^\dagger]_- \right\} \\
&= \sum_{n,m} a_m(E) \left[(\alpha + n\Gamma) c_n^\dagger \delta_{mn} + \beta c_n^\dagger \delta_{m,n+1} + \beta c_{n+1}^\dagger \delta_{mn} \right] \\
&= \sum_n \left[(\alpha + n\Gamma) a_n + \beta a_{n+1} + \beta a_{n-1} \right] c_n^\dagger,
\end{aligned} \tag{7.9}$$

after reindexing and summing over m. With the $c_n^\dagger$'s being independent, equating the corresponding terms on each side of (7.9) gives

$$a_{n+1} + \frac{\alpha + n\Gamma - E}{\beta} a_n + a_{n-1} = 0, \tag{7.10}$$

for each n. Equation (7.10) is recognized as the BF *recursion relation* (Abramowitz and Stegun 1972) for

$$a_n(E) = P_{n-(E-\alpha)/\Gamma}(z), \tag{7.11}$$

where $z = -2\beta/\Gamma$, and $P_\mu(z) = AJ_\mu(z) + BY_\mu(z)$ is any linear combination of BFs of the first and second kind.

The a_n's are the coefficients of the wave function, so the normalizability condition requires that

$$\sum_n |a_n(E)|^2 < \infty. \tag{7.12}$$

By referring to the properties of BFs (Abramowitz and Stegun 1972), it can be shown that condition (7.12) holds only if $B = 0$ and $\mu = n - (E - \alpha)/\Gamma$ is an integer. Thus, $(E - \alpha)/\Gamma$ is also an integer, so that

$$E \equiv E_k = \alpha + k\Gamma, \qquad k \quad \text{integer}, \tag{7.13}$$

whence,

$$a_n(E_k) = A(-1)^{n-k} J_{n-k}\left(\frac{2\beta}{\Gamma}\right). \tag{7.14}$$

Equation (7.13) demonstrates the essential point, namely, that the energy spectrum of an *infinite* chain (under a linear applied field) is not continuous, but is a WSL, exhibiting *discrete*, evenly-spaced energy levels (see Fig. 7.1).

For a *finite*, (rather than an infinite) chain under the action of an applied field, it turns out that the energy spectrum forms only an *approximate* WSL (Heinrichs and Jones 1972). To see this result, we start with the difference equations for a finite TB chain of length m:

$$(\alpha + n\Gamma - E)c_n + \beta(c_{n+1} + c_{n-1}) = 0, \quad n = 2, \ldots, m-1, \tag{7.15a}$$

$$(\alpha + \Gamma - E)c_1 + \beta c_2 = 0, \tag{7.15b}$$

$$(\alpha + m\Gamma - E)c_m + \beta c_{m-1} = 0. \tag{7.15c}$$

(Here we ignore any possible perturbation to the site energies at the ends of the chain, $n = 1$ and $n = m$.) We apply Brillouin-Wigner perturbation theory (Ohanian 1990), whereby the eigenvalue of a non-degenerate state can be expressed as

$$E_n = H_{nn} + \sum_{\ell \neq n} \frac{H_{n\ell} H_{\ell n}}{E_n - \varepsilon_{n\ell}} + \sum_{\substack{\ell,k \neq n \\ \ell \neq k}} \frac{H_{n\ell} H_{\ell k} H_{kn}}{(E_n - \varepsilon_{n\ell})(E_n - \varepsilon_{n\ell k})} + \cdots, \tag{7.16a}$$

with

$$\varepsilon_{n\ell\ldots pq} = H_{qq} + \sum_{r\neq n,\ell,\ldots,p,q} \frac{H_{qr}H_{rq}}{E_n - \varepsilon_{n\ell\ldots pqr}} + \sum_{\substack{r\neq n,\ell,\ldots,p,q \\ s\neq n,\ell,\ldots,p,q,r}} \frac{H_{qr}H_{rs}H_{sq}}{(E_n - \varepsilon_{n\ell\ldots pqr})(E_n - \varepsilon_{n\ell\ldots pqrs})} + \cdots, \tag{7.16b}$$

where the terms beyond the interaction range are identically zero. Note, we are using the NN approximation, so that only the first two terms in each of (7.16a) and (7.16b) survive. Specifically, the Hamiltonian has only the following tri-diagonal matrix elements:

$$H_{nn} = \alpha + n\Gamma, \quad n = 1, 2, \ldots, m, \tag{7.17a}$$

$$H_{nr} = H_{rn} = \beta(\delta_{r,n+1} + \delta_{r,n-1}), \quad n = 2, 3, \ldots, m-1, \tag{7.17b}$$

$$H_{1r} = \beta\delta_{r2}, \tag{7.17c}$$

$$H_{mr} = \beta\delta_{r,m-1}. \tag{7.17d}$$

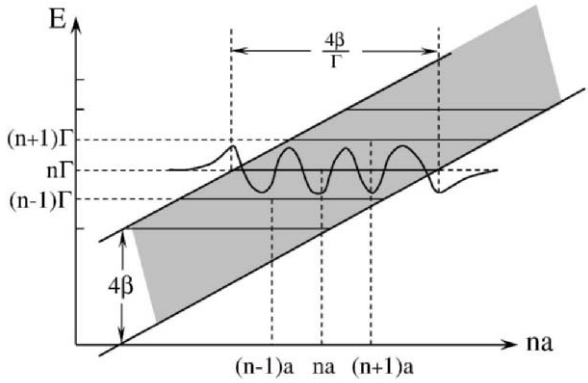

Fig. 7.1. Tilted-band picture of WSL energy spectrum showing Wannier wave functions and localization length $L = 4\beta/\Gamma$. Reprinted from Hacker and Obermair (1970) with permission from Springer.

We now let the difference between the energies of the chain and an exact WSL be

$$\Delta E_n = E_n - \alpha - n\Gamma, \tag{7.18}$$

which, on using (7.16) and (7.17), becomes

$$
\begin{aligned}
\Delta E_n &= E_n - H_{nn} \\
&= \sum_{\ell \neq n} \frac{H_{n\ell} H_{\ell n}}{E_n - \varepsilon_{n\ell}} \\
&= \frac{\beta^2}{E_n - \varepsilon_{n,n+1}} + \frac{\beta^2}{E_n - \varepsilon_{n,n-1}} \\
&= \frac{\beta^2}{\Delta E_n - \Gamma - \frac{\beta^2}{E_n - \varepsilon_{n,n+1,n+2}}} + \frac{\beta^2}{\Delta E_n + \Gamma - \frac{\beta^2}{E_n - \varepsilon_{n,n-1,n-2}}} \\
&= \cfrac{\beta^2}{\Delta E_n - \Gamma - \cfrac{}{\vdots \cfrac{}{} - \cfrac{\beta^2}{\Delta E_n - (m-1-n)\Gamma - \cfrac{\beta^2}{\Delta E_n - (m-n)\Gamma}}}} \\
&\quad + \cfrac{\beta^2}{\Delta E_n + \Gamma - \cfrac{}{\vdots \cfrac{}{} - \cfrac{\beta^2}{\Delta E_n + (n-1)\Gamma - \cfrac{\beta^2}{\Delta E_n + n\Gamma}}}}
\end{aligned}
\tag{7.19}
$$

Equation (7.19) is a self-consistent equation for ΔE_n, in the form of a sum of a pair of *continued fractions* (CFs). Although numerical solutions to (7.19) are feasible, we are only concerned with its qualitative features. In particular, we note that an exact WSL occurs when $\Delta E_n = 0$, which happens only if both CFs contain the same number of terms (apart from the trivial case $\beta = 0$). For the infinite chain, this situation is the case for every allowed energy, so an exact WSL is indeed found. But, for a finite chain, $\Delta E_n = 0$ only for the center state, which thus possesses the exact WSL energy. Therefore, the set of energies for a finite chain form only an *approximate* WSL.

As we have seen, the electronic structure of an infinite or a finite TB chain under an applied field is fundamentally different from that of the corresponding chain without the field. Consequently, the various properties of

such systems, be they chemisorption or otherwise, are an important subject of study, and can be expected to vary greatly from those of the parent system.

7.2 Recursive-Green-Function Treatment

In this section, we construct the GF for a finite chain with an applied field (Davison et al 1997), by using the CF elements of the *recursion method* (Haydock 1980) and thereby build the GF atom-by-atom, in a similar way as the causal-surface GF approach (Pendry et al 1991).

The system is defined as a linear chain of m lattice sites (labelled $n = 1, \ldots, m$), which are initially taken as isolated from each other (see Fig. 7.2(a)), so that the GF $G_{m,m}$ for this state has simple diagonal elements

$$G_{m,m}(n,n) = (E - \alpha_n)^{-1}, \quad n = 1, \ldots, m, \tag{7.20}$$

where

$$\alpha_n = \langle n|H|n\rangle, \tag{7.21}$$

and all off-diagonal elements are zero, i.e.,

$$G_{m,m}(n,\ell) = 0, \quad n \neq \ell. \tag{7.22}$$

The process used is such that, one-by-one, each atom is connected to the rest of the chain by adding a single bond between it and the neighbouring atom to its immediate right, starting at the right-hand side of the lattice, and moving to the left. Thus, we start by joining the atoms at $n = m-1$ and $n = m$ to form a 2-atom chain (with all other atoms left isolated). Then, the atom at $n = m - 2$ is bonded to the 2-chain, and so on, until all m atoms have been linked (see Fig. 7.2(b)-(d)). The notation used is to let $G_{n,m}$ be the GF for the system at the stage where atoms n to m have been joined to form a $(m - n + 1)$-atom chain, while atoms 1 to $n - 1$ remain isolated. The goal is to construct the GF $G_{1,m}$ for the entire chain or, more specifically, the element $G_{1,m}(1,1)$, which will be taken as the *surface* GF for the chemisorption studies of §7.3.

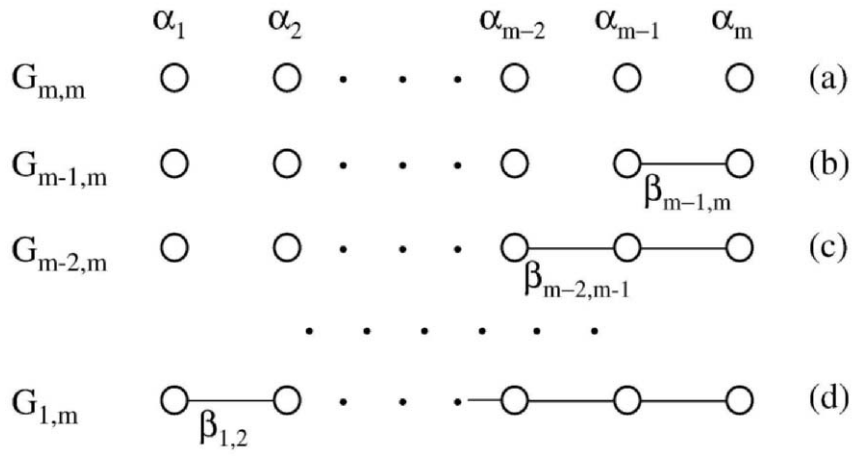

Fig. 7.2. Diagrammatic representation of process to build chain atom-by-atom. Reprinted from Davison et al (1997) with permission from the Institute of Physics.

Returning to the initial GF (7.20), we now modify the system, by adding a single bond of energy $\beta_{m-1,m}$ between sites $m-1$ and m. We can obtain the GF $G_{m-1,m}$ from $G_{m,m}$ by means of the Dyson equation (3.3)

$$G_{m-1,m} = G_{m,m} + G_{m,m} V_{m-1,m} G_{m-1,m}, \tag{7.23}$$

where

$$V_{m-1,m} = \beta_{m-1,m} \left(|m-1\rangle\langle m| + |m\rangle\langle m-1| \right). \tag{7.24}$$

Inserting (7.24) into (7.23) leads to

$$\begin{aligned} G_{m-1,m}(m-1,m-1) = {} & G_{m,m}(m-1,m-1) \\ & + G_{m,m}(m-1,m-1)\beta_{m-1,m} G_{m-1,m}(m,m-1), \end{aligned} \tag{7.25}$$

since $G_{m,m}(m-1,m)=0$ by (7.22). The right-hand side of (7.25) contains an unevaluated element of $G_{m-1,m}$, which, via (7.23), can be expressed as

$$G_{m-1,m}(m,m-1)=G_{m,m}(m,m)\beta_{m-1,m}G_{m-1,m}(m-1,m-1). \tag{7.26}$$

Substituting (7.26) into (7.25) gives

$$\begin{aligned}G_{m-1,m}(m-1,m-1)&=G_{m,m}(m-1,m-1)\\&\quad+\beta_{m-1,m}^2G_{m,m}(m-1,m-1)G_{m,m}(m,m)G_{m-1,m}(m-1,m-1),\end{aligned} \tag{7.27}$$

so that

$$G_{m-1,m}(m-1,m-1)=\frac{G_{m,m}(m-1,m-1)}{1-\beta_{m-1,m}^2G_{m,m}(m,m)G_{m,m}(m-1,m-1)}. \tag{7.28}$$

Using (7.20), we can write (7.28) as

$$G_{m-1,m}(m-1,m-1)=\frac{1}{E-\alpha_{m-1}-\beta_{m-1,m}^2\frac{1}{E-\alpha_m}}. \tag{7.29}$$

The above recursive process, for the 2-atom chain, can now be repeated for the 3-atom case. The Dyson equation analogous to (7.23) is

$$G_{m-2,m}=G_{m-1,m}+G_{m-1,m}V_{m-2,m}G_{m-2,m}, \tag{7.30}$$

where

$$V_{m-2,m}=\beta_{m-2,m-1}\left(|m-2\rangle\langle m-1|+|m-1\rangle\langle m-2|\right) \tag{7.31}$$

(see Fig. 7.2(c)). The method for finding the relevant matrix element is the same as that used to obtain (7.28), yielding

$$\begin{aligned}&G_{m-2,m}(m-2,m-2)\\&\quad=\frac{G_{m-1,m}(m-2,m-2)}{1-\beta_{m-2,m-1}^2G_{m-1,m}(m-1,m-1)G_{m-1,m}(m-2,m-2)}.\end{aligned} \tag{7.32}$$

From (7.29), and the fact that

$$G_{m-1,m}(m-2,m-2)=(E-\alpha_{m-2})^{-1}, \tag{7.33}$$

because it represents an isolated site, (7.32) can be written explicitly as

$$G_{m-2,m}(m-2,m-2) = \cfrac{1}{(E-\alpha_{m-2}) - \cfrac{\beta^2_{m-2,m-1}}{(E-\alpha_{m-1}) - \cfrac{\beta^2_{m-1,m}}{E-\alpha_m}}}, \tag{7.34}$$

which can be rearranged into the form of a rational function of E, but we prefer to leave it as a (finite) CF.

The recursive procedure can be applied repeatedly, with one more atom being bonded to the growing chain at each step, producing GF's in CF form similar to those of (7.29) and (7.34). After $(m-1)$ iterations, all m (initially isolated) atoms are joined, and the GF at the $n=1$ site has CF form

$$G_{1,m}(1,1) = \cfrac{1}{(E-\alpha_1) - \cfrac{\beta^2_{1,2}}{(E-\alpha_2) - \cfrac{\beta^2_{2,3}}{\ddots \\ - \cfrac{\beta^2_{m-2,m-1}}{(E-\alpha_{m-1}) - \cfrac{\beta^2_{m-1,m}}{E-\alpha_m}}}}}. \tag{7.35}$$

More compactly, this can be represented in standard CF notation (Lorentzen and Waadeland 1992) as

$$G_{1,m}(1,1) = \underset{n=1}{\overset{m}{\mathcal{K}}}(a_n;b_n), \tag{7.36}$$

where

$$\begin{aligned} \underset{n=1}{\overset{m}{\mathcal{K}}}(a_n;b_n) &= \cfrac{a_1}{b_1 + \cfrac{a_2}{b_2 + \ddots + \cfrac{a_{m-1}}{b_{m-1} + \cfrac{a_m}{b_m}}}} \\ &= \frac{a_1}{b_1} + \frac{a_2}{b_2} + \frac{a_3}{b_3} + \cdots, \end{aligned} \tag{7.37}$$

with

$$a_n = \begin{cases} 1, & n = 1 \\ -\beta_{n-1,n}^2, & n = 2, \ldots, m, \end{cases} \tag{7.38}$$

and

$$b_n = E - \alpha_n, \quad n = 1, \ldots, m, \tag{7.39}$$

for our particular case (7.35).

The values of the α_n's and $\beta_{n-1,n}$'s in (7.39) and (7.38), respectively, determine the physical nature of the crystal being modelled by the chain. The simplest case is to take

$$\alpha_n = \alpha, \quad \text{for all} \quad n, \tag{7.40}$$

and

$$\beta_{n-1,n} = \beta, \quad \text{for all} \quad n, \tag{7.41}$$

which yields a single-band chain with no applied field. Surface states can also be included by letting α_1 and/or α_m equal $\alpha'(\neq \alpha)$. Here, however, we are interested in modelling a solid, subject to an applied field, so that accompanying (7.41) we take (cf. (7.6))

$$\alpha_n = \alpha + n\Gamma. \tag{7.42}$$

For present purposes, we work with the GF in its CF form (7.36), which provides conceptual clarity, as well as computational convenience, due to the ease in evaluating (7.36) recursively. However, other forms for $G_{1,m}(1,1)$ are possible, because, for example, the CF in (7.36) can be rearranged as a rational function of E. Alternatively, for the case of (7.41) and (7.42) it can be shown (App. M) that $G_{1,m}(1,1)$ can be expressed, in terms of Bessel functions J and Y of the first and second kind, respectively, as

$$G_{1,m}(1,1) = \beta^{-1} \frac{J_{\nu+m+1}(x)Y_{\nu+1}(x) - J_{\nu+1}(x)Y_{\nu+m+1}(x)}{J_{\nu+m+1}(x)Y_{\nu}(x) - J_{\nu}(x)Y_{\nu+m+1}(x)}, \tag{7.43}$$

where

$$\nu = xX, \tag{7.44}$$

$$x = -F^{-1} = -2\beta/\Gamma, \tag{7.45}$$

and, as usual, the *reduced energy*

$$X = \frac{E - \alpha}{2\beta}. \tag{7.46}$$

Regardless of how we may choose to represent the GF, we should note that it is for a *finite* chain, so that there is a *discrete* spectrum of m states, whose energies are given by the poles of $G_{1,m}(1,1)$.

The energies for the finite chain are given approximately by those in (7.13) for the infinite case, so as the potential strength Γ increases, the FL

$$\varepsilon_f \approx \alpha + \frac{m}{2}\Gamma \quad \text{(for even } m\text{)} \tag{7.47}$$

moves upwards. But, to preserve the integrity of the system, at least one occupied state must remain delocalized across the entire chain, which implies that its energy must remain inside the zero-field band. This condition is guaranteed, if ε_f itself stays within the band, i.e.,

$$\alpha - 2|\beta| < \varepsilon_f < \alpha + 2|\beta|,$$

which is equivalent to

$$|mF| < 2. \tag{7.48}$$

Thus, for our purposes, the field cannot be taken as being arbitrarily strong, but is limited, according to (7.48), by the length of the chain and, in particular, the allowable strength of the field decreases in inverse proportion to the increasing length of the chain.

Because the spectrum of the chain is discrete, we can express the LDOS, at site n, as

$$\rho_n(X) = \sum_k I_k^n(X_k)\delta(X - X_k)/2\beta, \tag{7.49}$$

X_k being the k-th state reduced energy, whose intensity

$$I_k^n(X_k) = 2\beta \operatorname{Res} G_{1,m}(n,n)\Big|_{X=X_k}. \tag{7.50}$$

Plots of the LDOS at the surface ($n = 1$) site of a 100-atom chain are presented in Fig. 7.3 for various field strengths. For no field, $F = 0$ (Fig. 7.3(a)), the LDOS exhibits a discretized version of the semi-elliptical shape, familiar for a surface DOS. For small field strength (Fig. 7.3(b)), an almost-linear region appears in the lower end of the quasi-band. As the field strength increases (Fig. 7.3(c) and (d)), the region spreads across the band, with increasing intensities. In addition, there is a rigid shift in the structure to

slightly higher X_k-values, accompanied by an exponential tailing-off of the intensities above the upper band-edge at $X = 1$.

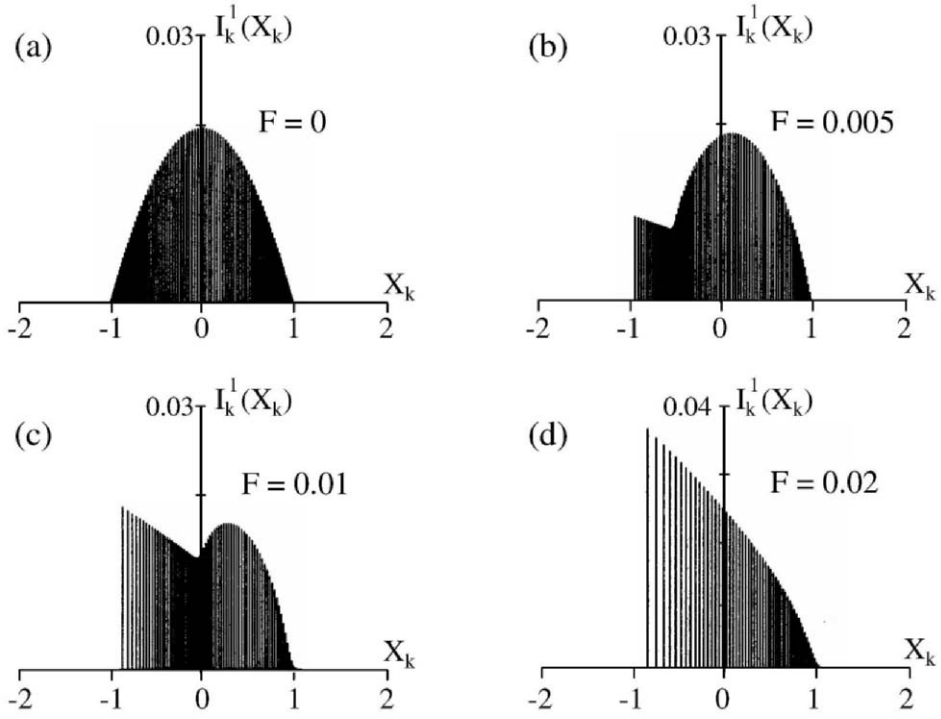

Fig. 7.3. LDOS at $n = 1$ site of 100-atom chain. As field increases, semi-elliptical shape is dominated by linear potential. Field strengths are as indicated. Reprinted from Davison et al (1997) with permission from the Institute of Physics.

7.3 Electrochemisorption

The process of chemisorbing an atom onto an electrified substrate is known as *electrochemisorption*. The initial studies, described here, employed the ANG model (English et al 1997; English and Davison 1998). Later, Davison et al (2001) incorporated the presence of surface states.

In adopting the ANG approach (Chap. 4), only a few modifications are required, which are mainly concerned with the substrate spectrum being discrete rather than continuous. The conceptual set-up is portrayed in Fig. 7.4.

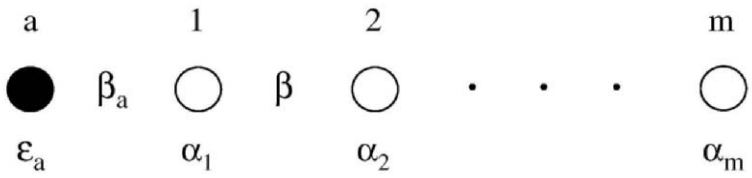

Fig. 7.4. Chemisorption of adatom of site (bond) energy $\varepsilon_a(\beta_a)$ onto electrified chain of length m. Substrate has site (bond) energy $\alpha_n(\beta)$, where $\alpha_n = \alpha + n\Gamma (n = 1, \ldots, m)$, Γ being the potential gradient.

The surface GF $g_s(1,1) \equiv G_{1,m}(1,1)$ for the m-atom chain is, of course, known from (7.36), with (7.41) and (7.42), to be

$$g_s(1,1) = \frac{1}{E-\alpha-\Gamma} - \frac{\beta^2}{E-\alpha-2\Gamma} - \cdots - \frac{\beta^2}{E-\alpha-m\Gamma}. \tag{7.51}$$

g_s is linked to the *adatom* GF g_a by the Dyson equation

$$g_a = g_s + g_s V_a g_a, \tag{7.52}$$

where

$$V_a = U\langle n_{a,-\sigma}\rangle |a\rangle\langle a| + \beta_a \left(|a\rangle\langle 1| + |1\rangle\langle a|\right), \tag{7.53}$$

$U\langle n_{a,-\sigma}\rangle$ being the averaged self-energy of the adatom, within the HFA, and β_a the adatom-surface bond energy. From (7.52), we obtain

$$\begin{aligned} g_a(a,a) = {} & g_s(a,a) + U\langle n_{a,-\sigma}\rangle g_s(a,a) g_a(a,a) \\ & + \beta_a g_s(a,a) g_a(1,a), \end{aligned} \tag{7.54}$$

since $g_s(a,1) = 0$ and, also from (7.52),

$$g_a(1,a) = \beta_a g_s(1,1) g_a(a,a). \tag{7.55}$$

Substituting (7.55) into (7.54), and using

$$g_s(a,a) = (E - \varepsilon_a)^{-1}, \tag{7.56}$$

leads to the adatom GF expression

$$g_a(a,a) = \left[E - \varepsilon_{a\sigma} - \beta_a^2 g_s(1,1)\right]^{-1} \tag{7.57}$$

where

$$\varepsilon_{a\sigma} = \varepsilon_a + U\langle n_{a,-\sigma}\rangle. \tag{7.58}$$

Now, mirroring (4.70), we can write (7.57) in the form

$$g_a(a,a) = \left[E - \varepsilon_{a\sigma} - \Lambda(E) + i\Delta(E)\right]^{-1}, \tag{7.59}$$

by virtue of the chemisorption functions

$$\Lambda(E) = \beta_a^2 \mathrm{Re}\,[g_s(1,1)], \tag{7.60}$$

$$\Delta(E) = -\beta_a^2 \mathrm{Im}\,[g_s(1,1)]. \tag{7.61}$$

The allowable energies $E_{\ell\sigma}$ of the chemisorbed system (adatom plus chain) are determined as being the (real) poles of $g_a(a,a)$, i.e., the $m+1$ solutions of

$$E_{\ell\sigma} - \varepsilon_{a\sigma} - \Lambda(E_{\ell\sigma}) = 0, \quad \sigma = + \quad \text{or} \quad -, \tag{7.62}$$

which are *discrete*, because of the finiteness of the system. Each of the corresponding eigenstates makes a contribution [cf. (4.80)]

$$\langle n_{a\sigma}\rangle_\ell = \left[1 - \Lambda'(E_{\ell\sigma})\right]^{-1} \tag{7.63}$$

to the total adatom occupancy, which from (4.76) is given by

$$\langle n_{a\sigma}\rangle = \sum_\ell \langle n_{a\sigma}\rangle_\ell, \tag{7.64}$$

where the integration in (4.76) now becomes a summation, because all energies are discrete. Equations (7.62) and (7.64) together comprise a self-consistency condition of the form of (4.81), yielding non-magnetic ~~M~~ (magnetic

M) solutions when $\langle n_{a+}\rangle$ and $\langle n_{a-}\rangle$ are equal (unequal). As always, these solutions must be found numerically, and some typical curves of $\langle n_{a\sigma}\rangle$ versus $\langle n_{a,-\sigma}\rangle$ are shown in Fig. 7.5 (cf. Fig. 4.2). For $F = 0$, both $\not{M}$ and M solutions occur, but as F increases, the M solutions are driven towards the $\not{M}$ one, eventually coalescing in a single $\not{M}$ solution in the limit as $F \to \infty$. With the adatom occupancy calculated self-consistently, the charge transfer to the adatom is once again given by (4.102).

The chemisorption energy is given by (4.85), viz.,

$$\Delta E = \sum_{\sigma} \Delta E^{\sigma} - \varepsilon_a - U\langle n_{a+}\rangle\langle n_{a-}\rangle. \tag{7.65}$$

However, because the energy spectrum is discrete, both before and after chemisorption, ΔE^{σ} does not take the form of the energy-integral (4.99), but is instead evaluated via finite sums (4.86) of the energies, i.e.,

$$\Delta E^{\sigma} = \sum_{\ell\,\mathrm{occ}} E_{\ell\sigma} - \sum_{n\,\mathrm{occ}} E^0_n, \tag{7.66}$$

the summations being over the occupied states below the FL at $\varepsilon_f = E^0_{[(m+1)/2]}$, with [ ] denoting integer value, and $(E^0_n)E_{\ell\sigma}$ being the (un)perturbed energies in the (pre-) post-chemisorption system, which are found as the poles of $(g_s(1,1))g_a(a,a)$.

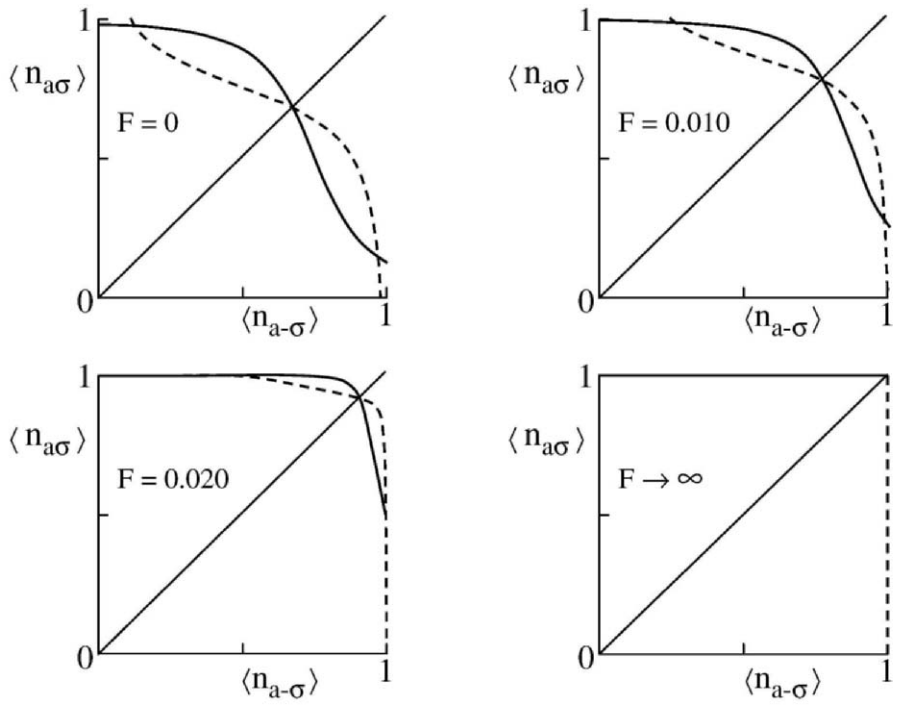

Fig. 7.5. Self-consistency curves for $\beta_a = \beta$ and F-values indicated. ($\not{M}$) M solutions occur at intersections, where $\langle n_{a\sigma}\rangle (=) \neq \langle n_{a,-\sigma}\rangle$. After English (1997).

7.4 H-Ti and H-Cr Systems

Moving on, we apply the above formalism to the system consisting of a hydrogen adatom and a metal substrate, which is taken to be either Ti or Cr. The solid chain is given a length of $m = 100$ atoms, which allows fields of strength up to $|F| = 0.02$, according to (7.48). The appropriate parameters (Newns 1969), based on experimental data, are given in Table 7.1.

Table 7.1. Parameters (in eV) for H chemisorbed on Ti and Cr, relative to vacuum level.

	Ti	**Cr**
α	-1.82	-5.25
β	2.15	1.525
$\varepsilon_f(F=0)$	-3.86	-4.56
ε_a	-13.6	-13.6
U	12.9	12.9
β_a	3.72	3.75

Looking first at the H-Ti system, the self-consistency condition (4.81) has a $\not{M}$ solution for all values of F, as well as a pair of M-solutions for all $F \neq 0$. Some typical values of $\langle n_{a+}\rangle$ and $\langle n_{a-}\rangle$ are given in Table 7.2. Hence, the charge transfer and chemisorption energy can be calculated, as shown in Fig. 7.6. The $\not{M}$ (M) solution is given by the solid (broken) curve. The initial point of reference is, of course, the zero-field situation, where Fig. 7.6 indicates a moderate charge transfer to the adatom and a consequent negative chemisorption energy (so that chemisorption does occur). The question of interest concerns whether implementation of the field serves to strengthen or weaken the chemisorption process (or, perhaps, destabilize it completely). The field modifies the adsorption through two routes: first, by moving the FL (refer to (7.47), where $\Gamma = 2\beta F$) and, second, by altering the adatom occupancy (Table 7.2). When $F > 0$, the FL is raised (tending to lower ΔE) and the $\not{M}$ -solution $\langle n_{a+}\rangle = \langle n_{a-}\rangle$ is increased, raising the effective adatom level $\varepsilon_{a\sigma}$ (cf. (7.58)), which in turn raises ΔE. Under these two competing effects, ΔE remains essentially constant, as seen in Fig. 7.6(a). However, for the M-solution, $\langle n_{a+}\rangle$ and $\langle n_{a-}\rangle$ move in opposite directions, thus effectively neutralizing the second route, so the field effect is primarily controlled by the raising of the FL, resulting in the drastic lowering of ΔE shown in Fig. 7.6(a). When $F < 0$, the situation is reversed, since the FL is now lowered, which by itself acts to raise ΔE. For the $\not{M}$ -solution, $\langle n_{a+}\rangle = \langle n_{a-}\rangle$ is again increased with increasing $|F|$, thus tending to raise ΔE via this route, too. Hence, the result is a noticeable raising of ΔE, as seen in Fig. 7.6(a). For the M-solution, the effects of $\langle n_{a+}\rangle$ and $\langle n_{a-}\rangle$ again approximately cancel each other, so, although ΔE is still lowered as F becomes more negative, the effect is much less pronounced than when $F > 0$. Because the M-solution yields a lower ΔE than the $\not{M}$ one, it is the physically desired situation.

Table 7.2. $\not{M}$ and M solutions $\langle n_{a+} \rangle$ and $\langle n_{a-} \rangle$ of H-Ti system.

F	-.020	-.015	-.010	-.005	.000	.005	.010	.015	.020
$\not{M}$	0.546	0.567	0.584	0.607	0.632	0.658	0.687	0.720	0.762
M	0.872	0.794	0.759	0.720	N/A	0.737	0.819	0.909	0.991
M	0.054	0.288	0.381	0.483	N/A	0.574	0.547	0.482	0.424

We note in Fig. 7.6 that both $\not{M}$ graphs pass smoothly through $F = 0$, whereas those for M exhibit a cusp (labelled as B), which is due to the asymmetry of the occupied levels when $F \neq 0$ (Table 7.2). States shifted above the band are also above the FL, and have only an indirect effect on ΔE, while states shifted below the band are filled, and act to produce a greater field effect.

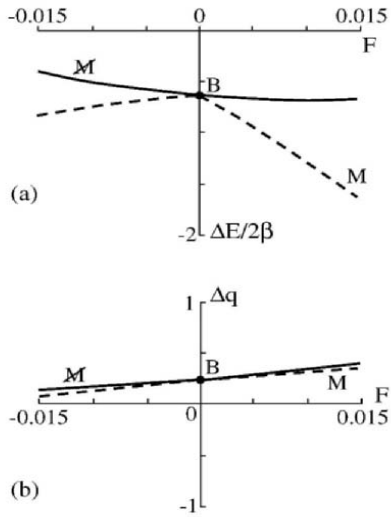

Fig. 7.6. (a) Variation of H-Ti electrochemisorption energy with field strength. Solid (broken) curve represents $\not{M}$ (M) solution. (b) Adatom charge transfer versus field strength for H-Ti. Solid (broken) line depicts $\not{M}$ (M) case. Point B locates bifurcation threshold for M-solutions. Reprinted from English and Davison (1998) with permission from Elsevier.

Turning to the H-Cr system, some representative values of $\langle n_{a+} \rangle$ and $\langle n_{a-} \rangle$ are given in Table 7.3, showing an $\not{M}$ -solution exists for all field strengths, while M ones only occur when F is greater than about 0.005. The difference from the H-Ti situation is apparently due to the fact that the Cr band is fuller, as is reflected by the value of ε_f relative to α (see Table 7.1). The corresponding graphs of Δq and ΔE are displayed in Fig. 7.7, and both exhibit a bifurcation B at the F-value, where M-solutions first appear. The F-dependence of the $\not{M}$ -solution, in both graphs, is similar to that in the H-Ti system (Fig. 7.6), and has the same physical explanation. (The exception is the ΔE curve, for $F > 0$, which shows a definite trend in ΔE to increase with F, as opposed to the corresponding part of Fig. 7.6(a). In this case, there is less cancellation between competing contributions to ΔE.) With the birth of M-solutions as F increases through 0.005, the FL is raised, which tends to lower ΔE, while the split between $\langle n_{a+} \rangle$ and $\langle n_{a-} \rangle$ maintains $\varepsilon_{a\pm}$ at roughly constant levels, resulting in the lowering of ΔE. Keeping in mind that the lower-energy solution is the physically preferred one, Fig. 7.7 reveals that, for small positive fields, the chemisorption process is slightly suppressed, while for larger field strengths, it is enhanced.

Table 7.3. $\not{M}$ and M solutions $\langle n_{a+} \rangle$ and $\langle n_{a-} \rangle$ of H-Cr system.

F	-.015	-.010	-.005	.000	.005	.010	.015
$\not{M}$	0.574	0.588	0.602	0.616	0.631	0.645	0.656
M	N/A	N/A	N/A	N/A	N/A	0.803	0.962
M	N/A	N/A	N/A	N/A	N/A	0.476	0.335

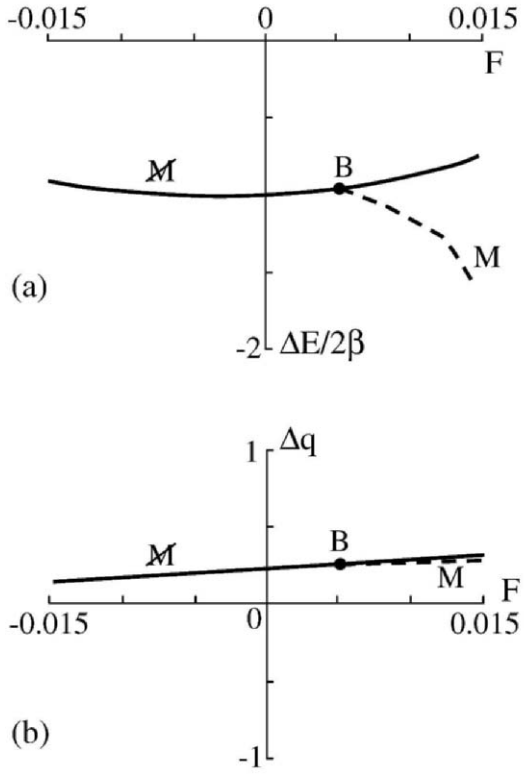

Fig. 7.7. Variation of: (a) H-Cr electrochemisorption energy; and (b) charge transfer with field strength. Solid (broken) curve depicts $\not{M}$ (M) solution. Point B locates bifurcation threshold for M-solutions. Reprinted from English and Davison (1998) with permission from Elsevier.

In conclusion, we have seen that an applied field has the ability to strongly affect the chemisorption process. One trend, clearly observable in both Fig. 7.6(b) and Fig. 7.7(b), is that the sign of F determines whether or not Δq is enhanced by the presence of the field, i.e., Δq is increased (decreased) when F is positive (negative). More variable is the dependence of ΔE on F, due to the variability in the existence (or not) of M-solutions, which, when they do occur, represent the more stable interaction. Consequently, the presence of the field may either enhance or suppress the chemisorption process.

Chapter 8

Indirect Adatom Interactions

By indirections find directions out.

— William Shakespeare

Up to now, we have investigated the situation of a *single* atom chemisorbed onto a surface. However, when *two* atoms are adsorbed onto a substrate, *direct* interactions may exist between them, provided their separation is less than a few Angstroms, so that the overlap of their orbitals is considerable. At larger separations, the direct interaction becomes negligible, but *indirect* interactions may arise between the adatoms through the substrate, because they share the same conduction band electrons. Such substrate-mediated interactions are important in many phenomena, such as the formation of adlayer structures, and can also play a significant role in applications, such as heterogeneous catalysis, where the chemical processes between the reactants take place at the surface of a catalyst.

8.1 Adatom Green Function

The occurrence of the substrate-mediated interaction between adatoms was first predicted in the seminal work by Koutecký (1958), using the resolvent technique, and was later clarified in a review by Grimley (1960), who added significantly to the theory by showing that the interaction energy is long-

range and oscillatory, in the adatom separation d, and is of the form (Grimley 1967a,b)

$$\Delta W(d) = Cd^{-n}\cos(2k_F d), \tag{8.1}$$

where C is a constant and k_F the Fermi momentum of an electron at the surface. n is an unknown integer between 2 and 5, which is believed to be determined by the effective dimensionality of the electronic states participating in the interaction. Specifically, $n = 5(2)$ for the 3(2)-dimensional situation. An extensive discussion of the status of the dimensionality problem, together with the experimental side of the question, can be found in Gumhalter and Brenig (1995a). Later, with Walker (1969), Grimley investigated the effects of the interaction on the heat of adsorption by means of the Anderson model, and with Torrini (1973) calculated the interaction between two hydrogen adatoms on W(100).

Neglecting Coulomb effects, Einstein and Schrieffer (1973) determined the interaction energy to be about an order of magnitude less than the chemisorption energy of a single adatom and confirmed Grimley's long-range behaviour. An extension of the Einstein and Schrieffer work by Burke (1976) revealed the interaction energy oscillates as a function of the Fermi energy, ε_F (adatom separation, d) for fixed d (ε_f). The inclusion of the direct adatom interaction was found to have a marked effect at small d. Besides the direct interaction, Muda and Hanawa (1974) also took account of the Coulomb repulsion between the adatoms, in their self-consistent Hartree-Fock treatment of pair-interaction effects on the adatom local DOS for H-W(100).

Correlation effects on the indirect interaction have been discussed by Schönhammer et al (1975). The chemisorption energy was found to be (in)sensitive to these effects in the (double-) single-adatom situation. Multi-adatom interactions have also been considered (Einstein 1977, Dreysée et al 1986); though insignificant for total interaction energies, they are comparable to more distant neighbour pair interactions. The asymptotic behaviour of the interaction has been established and discussed by Lau and Kohn (1978) and Einstein (1978). In a somewhat different vein, Le Bossé et al (1978, 1979, 1980) studied the indirect-interaction contribution to the binding energy of a diatomic admolecule.

In another interesting development, Gumhalter and Brenig (1995a,b) proposed that, in H-Ni(110) and H-Cu(110) systems, adatom-induced reconstruction of the surface gives rise to *quasi-one-dimensional surface states*, which mediate the indirect interaction. The greatly reduced dimensionality

of the surface electronic states gives rise to extremely long-ranged interactions. A comprehensive review of these adsorbate interactions has been given by Einstein (1996) and, more recently, by Merrick et al. (2003). Here, however, we examine the specific case of a pair of hydrogen atoms co-adsorbed on a metal surface, within the framework of the ANG model.

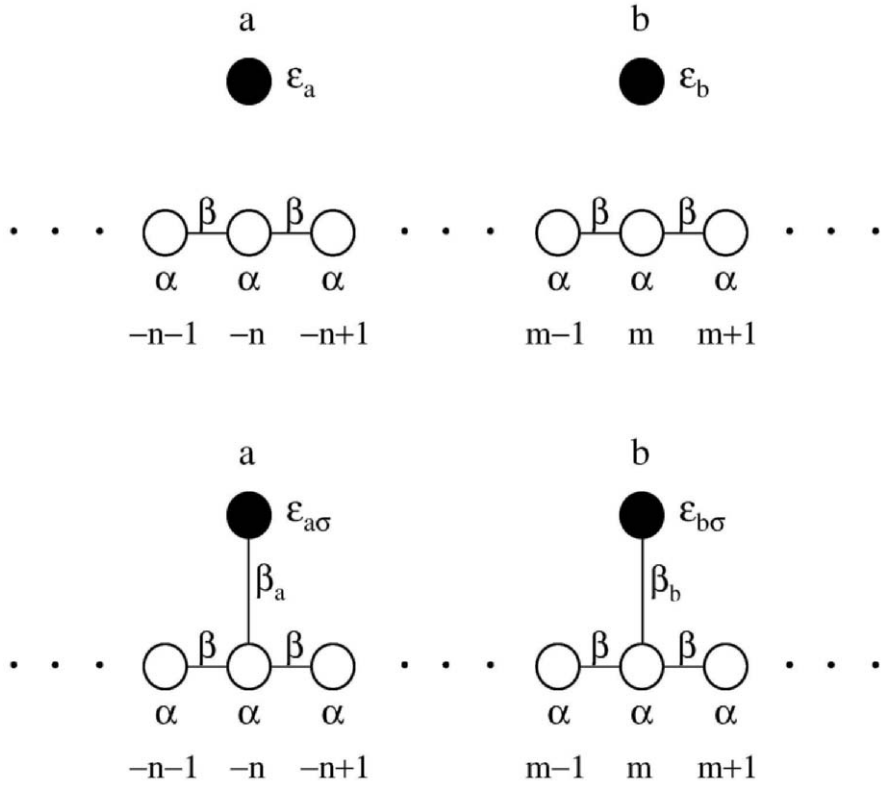

Fig. 8.1. Diagram of chemisorption process. After Schranz (1994).

Consider the situation where two isolated atoms a and b, with electronic energies ε_a and ε_b, are located above the $-n$ and m sites in a monatomic substrate, with site (bond) energy $\alpha\,(\beta)$ (see Fig. 8.1(a)). Upon chemisorption

(Fig. 8.1(b)), the electronic energies are shifted to (c.f. (4.34))

$$\varepsilon_{\lambda\sigma} = \varepsilon_\lambda + U\langle n_{\lambda,-\sigma}\rangle, \quad \lambda = a \quad \text{or} \quad b, \tag{8.2}$$

and the corresponding chemisorption bond energies are β_a and β_b. Let $H_0\,(H)$ be the Hamiltonian for the system of substrate and adatoms before (after) chemisorption. The two Hamiltonians are related by

$$H = H_0 + V, \tag{8.3}$$

where V is the perturbation potential

$$\begin{aligned} V = {} & U\langle n_{a,-\sigma}\rangle |a\rangle\langle a| + U\langle n_{b,-\sigma}\rangle |b\rangle\langle b| \\ & + \beta_a \left(|a\rangle\langle -n| + |-n\rangle\langle a|\right) + \beta_b \left(|b\rangle\langle m| + |m\rangle\langle b|\right). \end{aligned} \tag{8.4}$$

Taking $G_0(G)$ to be the GF corresponding to $H_0(H)$, the associated Dyson equation (3.3) is

$$G = G_0 + G_0 V G. \tag{8.5}$$

We need to construct the matrix elements of G on the 2 atoms; we explicitly evaluate $G(a,a)$, because the expression for $G(b,b)$ will be the same, except for the interchange of a and b and their respective bonding site indices $-n$ and m.

Substituting (8.4) into (8.5) and taking $\langle a|G|a\rangle = G(a,a)$ produces

$$G(a,a) = G_0(a,a) + \beta_a G_0(a,a)G(-n,a) + U\langle n_{a,-\sigma}\rangle G_0(a,a)G(a,a),$$

which rearranges as

$$\left[G_0^{-1}(a,a) - U\langle n_{a,-\sigma}\rangle\right] G(a,a) = 1 + \beta_a G(-n,a). \tag{8.6}$$

The unknown element $G(-n,a) = \langle -n|G|a\rangle$ is found from (8.5) to be

$$G(-n,a) = \beta_a G_0(-n,-n)G(a,a) + \beta_b G_0(-n,m)G(b,a), \tag{8.7}$$

since $G_0(-n,a) = 0$, because the sites $-n$ and a are not connected in the pre-chemisorption system (Fig. 8.1(a)). The element $G(b,a)$, required in (8.7), is determined by another application of (8.5) to be

$$G(b,a) = \beta_b G_0(b,b)G(m,a) + U\langle n_{b,-\sigma}\rangle G_0(b,b)G(b,a), \tag{8.8}$$

where $G_0(b,a)=0$. We use (8.5) again to evaluate $G(m,a)$ in (8.8),i.e.,

$$G(m,a)=\beta_a G_0(m,-n)G(a,a)+\beta_b G_0(m,m)G(b,a), \tag{8.9}$$

utilizing $G_0(m,a)=0$. Substituting (8.9) into (8.8), gives

$$\begin{aligned} G(b,a)=\beta_a\beta_b G_0(m,-n)G(a,a)\times \\ \left[G_0^{-1}(b,b)-U\langle n_{b,-\sigma}\rangle-\beta_b^2 G_0(m,m)\right]^{-1}, \end{aligned} \tag{8.10}$$

which in (8.7) leads to

$$\begin{aligned} G(-n,a)=\beta_a G(a,a)\Big\{G_0(-n,-n)+\beta_b^2 G_0(-n,m)G_0(m,-n)\times \\ \left[G_0^{-1}(b,b)-U\langle n_{b,-\sigma}\rangle-\beta_b^2 G_0(m,m)\right]^{-1}\Big\}, \end{aligned} \tag{8.11}$$

so that (8.6) becomes

$$\left[G_0^{-1}(a,a)-U\langle n_{a,-\sigma}\rangle\right]G(a,a)=1+\Omega G(a,a), \tag{8.12}$$

where the self-energy

$$\begin{aligned} \Omega=\beta_a^2\Big\{G_0(-n,-n)+\beta_b^2 G_0(-n,m)G_0(m,-n)\times \\ \left[G_0^{-1}(b,b)-U\langle n_{b,-\sigma}\rangle-\beta_b^2 G_0(m,m)\right]^{-1}\Big\}. \end{aligned} \tag{8.13}$$

Hence, (8.12) gives the desired element

$$G(a,a)=\left[G_0^{-1}(a,a)-U\langle n_{a,-\sigma}\rangle-\Omega\right]^{-1}. \tag{8.14}$$

We note that (8.14), with (8.13), shows that $G(a,a)$ (and similarly $G(b,b)$) depends on both occupancies $\langle n_{a,-\sigma}\rangle$ and $\langle n_{b,-\sigma}\rangle$ indicating (cf. (4.81)) that the occupancies $\langle n_{\lambda\sigma}\rangle$ are linked by a quartet of coupled self-consistency equations of the form (4.81). However, for simplicity, we make the reasonable approximation of ignoring this coupling by setting the term $U\langle n_{b,-\sigma}\rangle$ to 0 in (8.13). Thus, (8.14) expresses the adatom GF $G(a,a)$ entirely in terms of GF's of the pre-chemisorption system. The matrix element $G_0(\lambda,\lambda)$ ($\lambda=a$ or b) is that for the isolated atom λ, so is given very simply by

$$G_0(\lambda,\lambda)=(E-\varepsilon_\lambda)^{-1}. \tag{8.15}$$

The remaining matrix elements in (8.13) are for the as-yet-unspecified substrate. Once evaluated (see §8.2), (8.14) can be expressed in terms of the chemisorption functions (cf. (4.70))

$$\Lambda_2(E) = \mathrm{Re}(\Omega), \tag{8.16}$$
$$\Delta_2(E) = -\mathrm{Im}(\Omega), \tag{8.17}$$

as

$$G(a,a) = (E - \varepsilon_{a\sigma} - \Lambda_2(E) + i\Delta_2(E))^{-1}, \tag{8.18}$$

via (8.2) and (8.15), and with the subscript 2 referring to the fact that 2 adatoms are adsorbed on the substrate.

8.2 Chemisorption Functions

We now specify the substrate to be an infinite cyclic monatomic chain with site (bond) energy α (β) (see Fig. 8.1(a)). The GF matrix elements are (App. J)

$$G_0(\ell_1, \ell_2) = t^{|\ell_1 - \ell_2|} G_0(0,0), \tag{8.19}$$

where

$$G_0(0,0) = t/\beta(1-t^2), \tag{8.20}$$

with

$$t = \begin{cases} X \pm (X^2-1)^{1/2}, & X \lessgtr \mp 1, \\ X - i(1-X^2)^{1/2}, & |X| < 1, \end{cases} \tag{8.21}$$

and

$$X = (E-\alpha)/2\beta. \tag{8.22}$$

With this choice, (8.13) can be written as

$$\Omega = \beta_a^2 G_0(0,0) \left\{ 1 + \beta_b^2 t^{2d} G_0(0,0) \left[E - \varepsilon_b - \beta_b^2 G_0(0,0) \right]^{-1} \right\}, \tag{8.23}$$

where

$$d = m + n \tag{8.24}$$

denotes the distance between the 2 adatoms (see Fig. 8.1). The chemisorption functions are now determined via (8.16) and (8.17).

It should be noted that the single-adatom chemisorption functions (cf. (4.68) and (4.69)) are recovered by putting $\beta_b = 0$ in (8.23), namely,

$$\Lambda_1 = \mathrm{Re}[\beta_a^2 G_0(0,0)], \tag{8.25}$$

$$\Delta_1 = -\mathrm{Im}[\beta_a^2 G_0(0,0)], \tag{8.26}$$

which can also be thought of physically as the situation where the adatom separation d becomes infinite, viz.,

$$\Lambda_1 = \lim_{d\to\infty} \Lambda_2, \quad \Delta_1 = \lim_{d\to\infty} \Delta_2. \tag{8.27}$$

The *reduced* chemisorption functions

$$\Lambda_2(X) = \Lambda_2(E)/2|\beta|, \tag{8.28}$$

$$\Delta_2(X) = \Delta_2(E)/2|\beta|, \tag{8.29}$$

are depicted in Figs. 8.2 and 8.3 for the 2H-Cr system, and several values of d. $\Lambda_2(X)$ clearly has a singularity at an X-value outside the band, which is given by the zero of the [term] in (8.23). It is also apparent how the double-adatom function begins to resemble the single-adatom one, with increasing d. Inside the band, Λ_2 is an oscillatory function with $2d-1$ zeroes, and is continuous everywhere, including the band edges. However, the continuity at the band edges disappears in the limit $d \to \infty$, as the singularities initially outside the band move towards the band edges. Turning to the graphs of $\Delta_2(X)$ (Fig. 8.3), we see that the limiting case ($d = \infty$) exhibits the expected van Hove singularities (Davison and Stęślicka 1996) at the band edges. For $d < \infty$, these singularities are removed, due to the interaction between the adatoms. Within the band, Δ_2 is continuous and oscillatory, with d local maxima and $d-1$ local minima, occurring where $\Lambda_2 = 0$.

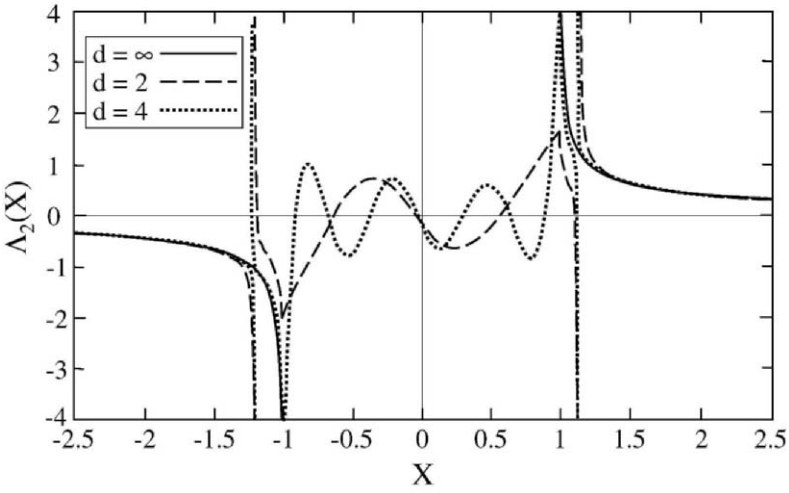

Fig. 8.2. $\Lambda_2(X)$ for 2H-Cr with $\langle n_{a\sigma} \rangle = 0.65$, for $d = 2, 4, \infty$, with $\beta_a / \mid \beta \mid = 1.5$. After Schranz(1994).

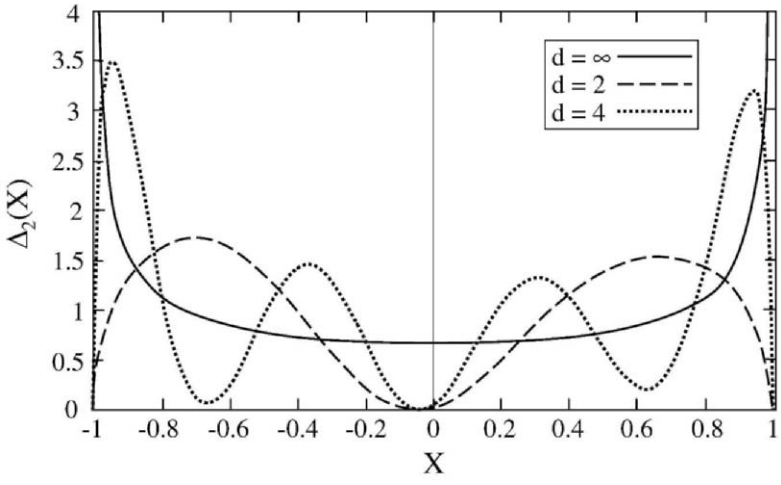

Fig. 8.3. $\Delta_2(X)$ for 2H-Cr with $\langle n_{a\sigma} \rangle = 0.65$, for $d = 2, 4, \infty$, with $\beta_a / \mid \beta \mid = 1.5$. After Schranz (1994).

The adatom DOS, within the band, is given as usual by (4.75), viz.,

$$\rho_a^\sigma(E) = \frac{\pi^{-1}\Delta_2(E)}{[E - \varepsilon_{a\sigma} - \Lambda_2(E)]^2 + \Delta_2(E)^2}, \tag{8.30}$$

while outside the band, the density is non-zero only at the localized-state energies $E_{\ell\sigma}$, which are the real poles of (8.18), namely, solutions of

$$E - \varepsilon_{a\sigma} - \Lambda_2(E) = 0, \tag{8.31}$$

with corresponding intensities (cf. (4.80))

$$\langle n_{a\sigma}\rangle_\ell = [1 - \Lambda_2'(E_{\ell\sigma})]^{-1}. \tag{8.32}$$

A typical graphical solution of (8.31), for $d = 3$, is shown in Fig. 8.4. It is noted that, in most cases of double-adsorption, there are two localized states below the band, compared to just one for single-adsorption. This pair of localized states arises due to a splitting of the doubly-degenerate single-adsorption localized state, and is the precursor to the band of such states that would emerge as more adatoms are added to the system.

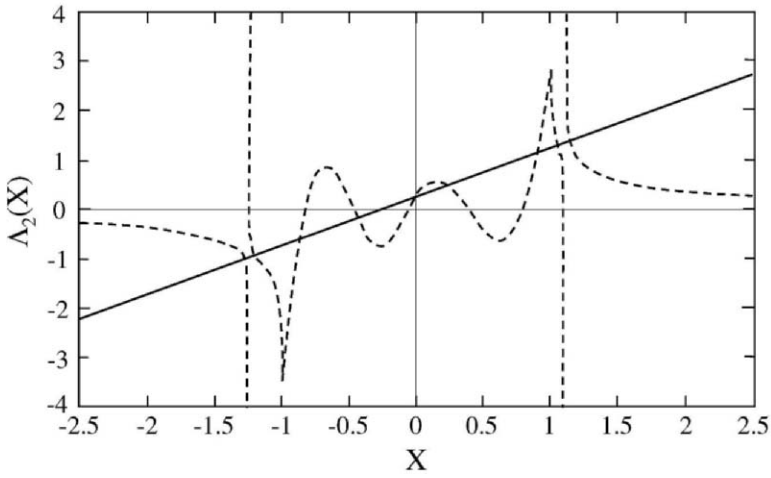

Fig. 8.4. $\Lambda_2(X)$ and $(E - \varepsilon_a - U\langle n_{a,-\sigma}\rangle)/2|\beta|$ vs X, for $d = 3$. Intersection of Λ_2 with line gives pairs of localized states. After Schranz (1994).

8.3 Self-consistency and Charge Transfer

We turn now to the issue of charge self-consistency, which utilizes the theory of §4.3, slightly modified to deal with the fact that there are now two adatoms. Specifically, the Hamiltonian (4.35) is modified to read as

$$H = \sum_{\lambda\sigma} \varepsilon_{\lambda\sigma} n_{\lambda\sigma} + \sum_{k\sigma} \varepsilon_k n_{k\sigma} + \sum_{k\lambda\sigma} (V_{\lambda k} c^\dagger_{\lambda\sigma} c_{k\sigma} + V^*_{k\lambda} c^\dagger_{k\sigma} c_{\lambda\sigma}), \tag{8.33}$$

where λ sums over the two adatoms a and b. It is important to note in (8.33) that there is *no direct* interaction term between the adatoms, so any interactions are *indirect*, occurring as a consequence of the bonding of each adatom to the substrate.

Following (4.76), the occupancy of each adatom is given by

$$\langle n_{\lambda\sigma} \rangle = \int_B \rho^\sigma_\lambda(E) dE + \sum_\ell \langle n_{\lambda\sigma} \rangle_\ell, \quad \lambda = a \text{ or } b, \tag{8.34}$$

where the integration of the adatom DOS (given by (8.30) for $\lambda = a$) is over the energy band and the summation is over the pair of localized-state intensities (8.32). Because the quantities on the right-hand side of (8.34) depend on the occupancies, they are determined by self-consistency equations of the form (4.81). For our purposes, we restrict ourselves to the non-magnetic case, so that we have

$$\langle n_{\lambda\sigma} \rangle = N(\langle n_{\lambda\sigma} \rangle), \quad \lambda = a \quad \text{or} \quad b. \tag{8.35}$$

As mentioned in §8.1, the occupancies $\langle n_{a\pm} \rangle$ and $\langle n_{b\pm} \rangle$ are in actuality coupled, but we made a simplifying approximation to uncouple them, by setting to zero the appropriate term in (8.13). Solutions to (8.35) can be calculated numerically, after which the total charge transfer is given by (cf. (4.102))

$$\Delta q = \sum_\lambda \left(\sum_\sigma \langle n_{\lambda\sigma} \rangle - 1 \right) e. \tag{8.36}$$

8.4 Change in Density of States

In order to calculate the energy changes brought about by chemisorption, we first evaluate the corresponding change in the DOS, $\Delta\rho$. We have pursued this notion earlier (in §6.4), but here we execute it differently, by relating $\Delta\rho$

to the Greenian G_0 of the pre-adsorption substrate and to the interaction potential V (8.4).

Taking the eigenenergies of the system before (after) chemisorption to be $\varepsilon_j^0\,(\varepsilon_j)$, then the change in the DOS is

$$\Delta\rho = \sum_j \left[\delta(E-\varepsilon_j) - \delta(E-\varepsilon_j^0)\right], \tag{8.37}$$

which, via (3.6) and (3.11), becomes

$$\Delta\rho = -\pi^{-1}\mathrm{Im}\sum_j \left(\frac{1}{E+is-\varepsilon_j} - \frac{1}{E+is-\varepsilon_j^0}\right). \tag{8.38}$$

Choosing the principal branch of the complex logarithm function, we can write (8.38) as

$$\Delta\rho = -\pi^{-1}\frac{\partial}{\partial E}\mathrm{Im}\,\ln\left(\prod_j \frac{E+is-\varepsilon_j}{E+is-\varepsilon_j^0}\right). \tag{8.39}$$

To proceed further, we examine the expression

$$\begin{aligned}&\det\left\{\left[(E+is)\mathbf{I}-\mathbf{H}_0\right]^{-1}\left[(E+is)\mathbf{I}-\mathbf{H}\right]\right\}\\ &\quad = \det\left[(E+is)\mathbf{I}-\mathbf{H}_0\right]^{-1}\det\left[(E+is)\mathbf{I}-\mathbf{H}\right],\end{aligned} \tag{8.40}$$

where $\mathbf{I}$ represents the identity matrix. Recalling that determinants are invariant under change of basis, it is most convenient to use the orthonormal bases of eigenvectors $\{|j_0\rangle\}$ and $\{|j\rangle\}$, corresponding to ε_j^0 and ε_j, respectively, in which $(E+is)\mathbf{I}-\mathbf{H}_0$ and $(E+is)\mathbf{I}-\mathbf{H}$ each become diagonal. Thus, (8.40) can be written as

$$\det\left\{\left[(E+is)\mathbf{I}-\mathbf{H}_0\right]^{-1}\left[(E+is)\mathbf{I}-\mathbf{H}\right]\right\} = \prod_j \frac{E+is-\varepsilon_j}{E+is-\varepsilon_j^0}, \tag{8.41}$$

so that (8.39) becomes

$$\Delta\rho = -\pi^{-1}\frac{\partial}{\partial E}\mathrm{Im}\,\ln\det\left\{\left[(E+is)\mathbf{I}-\mathbf{H}_0\right]^{-1}\left[(E+is)\mathbf{I}-\mathbf{H}\right]\right\}. \tag{8.42}$$

On noting that $G_0 = \left[(E+is)I - H_0\right]^{-1}$, and by recalling (8.3), we can write (8.42) as

$$\Delta\rho = -\pi^{-1}\frac{\partial}{\partial E}\mathrm{Im}\,\ln\det(\mathbf{I}-\mathbf{G}_0\mathbf{V}). \tag{8.43}$$

Now let us consider $\det(\mathbf{I}-\mathbf{G}_0\mathbf{V})$ in the AO basis $\{|\lambda\rangle,|\ell\rangle\}$, ordered so that the first four columns and rows are indexed by $a, b, -n$ and m. Thus, from (8.4), the matrix of V in block form is

$$\mathbf{V}=\left(\begin{array}{c|c}\mathbf{v}_1 & \mathbf{0}\\ \hline \mathbf{0} & \mathbf{0}\end{array}\right), \tag{8.44}$$

where

$$\mathbf{v}_1=\begin{pmatrix}\nu_a & 0 & \beta_a & 0\\ 0 & \nu_b & 0 & \beta_b\\ \beta_a & 0 & 0 & 0\\ 0 & \beta_b & 0 & 0\end{pmatrix}, \tag{8.45}$$

with

$$\nu_\lambda = U\langle n_{\lambda,-\sigma}\rangle, \quad \lambda = a \quad \text{or} \quad b. \tag{8.46}$$

The matrix of G_0 can also be written in block form as

$$\mathbf{G}_0=\left(\begin{array}{c|c}\mathbf{g}_1 & \mathbf{g}_2\\ \hline \mathbf{g}_3 & \mathbf{g}_4\end{array}\right), \tag{8.47}$$

whence

$$\mathbf{I}-\mathbf{G}_0\mathbf{V}=\begin{pmatrix}\mathbf{I}-\mathbf{g}_1\mathbf{v}_1 & \mathbf{0}\\ \mathbf{g}_3\mathbf{v}_1 & \mathbf{I}\end{pmatrix}, \tag{8.48}$$

so that

$$\det(\mathbf{I}-\mathbf{G}_0\mathbf{V})=\det(\mathbf{I}-\mathbf{g}_1\mathbf{v}_1). \tag{8.49}$$

The matrix $\mathbf{g}_1$ has the form

$$\mathbf{g}_1=\begin{pmatrix}G_0(a,a) & 0 & 0 & 0\\ 0 & G_0(b,b) & 0 & 0\\ 0 & 0 & G_0(-n,-n) & G_0(-n,m)\\ 0 & 0 & G_0(m,-n) & G_0(m,m)\end{pmatrix}, \tag{8.50}$$

which, with (8.45) and (8.49), leads to

$$\det(\mathbf{I}-\mathbf{G}_0\mathbf{V})=\begin{vmatrix}1-\nu_aG_0(a,a) & 0 & -\beta_aG_0(a,a) & 0\\ 0 & 1-\nu_bG_0(b,b) & 0 & -\beta_bG_0(b,b)\\ -\beta_aG_0(-n,-n) & -\beta_bG_0(-n,m) & 1 & 0\\ -\beta_aG_0(m,-n) & -\beta_bG_0(m,m) & 0 & 1\end{vmatrix}. \tag{8.51}$$

Equation (8.51) can be simplified by performing a cofactor expansion on the first row, and employing (8.13), resulting in

$$\det(\mathbf{I}-\mathbf{G}_0\mathbf{V}) = G_0(a,a)G_0(b,b)\left[G_0^{-1}(b,b)-\nu_b-\beta_b^2 G_0(m,m)\right]\times \left[G_0^{-1}(a,a)-\nu_a-\Omega\right]. \tag{8.52}$$

Here, the first factor in square brackets represents the adsorption of a single atom at site m. The second factor represents the adsorption of a second atom at site $-n$. Substituting (8.52) into (8.43), and invoking the chemisorption functions (4.68), (4.69), (8.16), (8.17), along with (8.46), results in

$$\Delta\rho = -\pi^{-1}\frac{\partial}{\partial E}\text{Im ln}\left\{[E-\varepsilon_{b\sigma}-\Lambda_1+i\Delta_1][E-\varepsilon_{a\sigma}-\Lambda_2+i\Delta_2]\right\} - \pi^{-1}\sum_\lambda \frac{\partial}{\partial E}\text{Im ln}\, G_0(\lambda,\lambda). \tag{8.53}$$

The subscripts 1 and 2 on the chemisorption functions refer to single- and double-adsorption, respectively. Note, however, that $\varepsilon_{a\sigma}$ and $\varepsilon_{b\sigma}$ are given by (8.2), where the indicated occupancies are both for the double-chemisorption situation.

Equation (8.53) can be simplified by recalling, from (8.15), that

$$G_0(\lambda,\lambda) = (E-\varepsilon_\lambda+is)^{-1},$$

so that

$$\frac{\partial}{\partial E}\ln G_0(\lambda,\lambda) = \frac{-1}{E-\varepsilon_\lambda+is}, \tag{8.54}$$

which, via (3.6) and (3.11), leads to

$$-\pi^{-1}\frac{\partial}{\partial E}\text{Im ln}\, G_0(\lambda,\lambda) = -\delta(E-\varepsilon_\lambda). \tag{8.55}$$

Also, the principal branch of the logarithm function has the property (App. F)

$$\text{Im ln}(x+iy) = \tan^{-1}\left(\frac{y}{x}\right), \tag{8.56}$$

where

$$0 < \tan^{-1}(\quad) < \pi, \tag{8.57}$$

so that

$$\text{Im ln}[E-\varepsilon_{\lambda\sigma}-\Lambda_j+i\Delta_j] = \tan^{-1}\left(\frac{\Delta_j}{E-\varepsilon_{\lambda\sigma}-\Lambda_j}\right). \tag{8.58}$$

Thus, (8.55) and (8.58) in (8.53) produce the final expression for the change in the DOS, namely,

$$\Delta\rho = -\pi^{-1}\frac{\partial}{\partial E}\left[\tan^{-1}\left(\frac{\Delta_1(E)}{E-\varepsilon_{b\sigma}-\Lambda_1(E)}\right)+\tan^{-1}\left(\frac{\Delta_2(E)}{E-\varepsilon_{a\sigma}-\Lambda_2(E)}\right)\right] - \sum_{\lambda}\delta(E-\varepsilon_\lambda). \tag{8.59}$$

8.5 Chemisorption and Interaction Energies

8.5.1 Chemisorption energy

As defined in Chap. 4, the chemisorption energy is the difference between the initial and final energies of the system. Although we could use the expression (4.85) for ΔE, it is more convenient to work with that of App. L, with a slight modification to account for double adsorption. Specifically, we have

$$\Delta E = \sum_{\sigma}\Delta E^{\sigma} + \sum_{\lambda}(-U\langle n_{\lambda+}\rangle\langle n_{\lambda-}\rangle + \varepsilon_\lambda - \varepsilon_f), \tag{8.60}$$

with the one-electron energy change given by

$$\Delta E^{\sigma} = \int_{-\infty}^{\varepsilon_f}(E-\varepsilon_f)\Delta\rho(E)dE. \tag{8.61}$$

Using (8.59) for $\Delta\rho$, we can write (8.61) as

$$\Delta E^{\sigma} = \sum_{\ell}(E_{\ell\sigma}-\varepsilon_f) - {\sum_{\lambda}}'(\varepsilon_\lambda-\varepsilon_f) + \int_B(E-\varepsilon_f)\Delta\rho(E)dE, \tag{8.62}$$

where the primed summation over λ means summing only over unperturbed isolated-atom energies *outside* the band, and B represents integration over occupied energies inside the band. The third term in (8.62) can be evaluated further, using integration by parts, to produce

$$\int_B(E-\varepsilon_f)\Delta\rho(E)dE = -{\sum_{\lambda}}''(\varepsilon_\lambda-\varepsilon_f) - \pi^{-1}(E-\varepsilon_f)\left[\tan^{-1}\left(\frac{\Delta_1(E)}{E-\varepsilon_{b\sigma}-\Lambda_1(E)}\right)+\tan^{-1}\left(\frac{\Delta_2(E)}{E-\varepsilon_{a\sigma}-\Lambda_2(E)}\right)\right]\Bigg|_{\varepsilon_L}^{\varepsilon_f} + \pi^{-1}\int_B\left[\tan^{-1}\left(\frac{\Delta_1(E)}{E-\varepsilon_{b\sigma}-\Lambda_1(E)}\right)+\tan^{-1}\left(\frac{\Delta_2(E)}{E-\varepsilon_{a\sigma}-\Lambda_2(E)}\right)\right]dE, \tag{8.63}$$

where the double-primed summation is over unperturbed isolated-atom energies *inside* the band. It can be shown that $\Delta_j(E)$ vanishes at the band edges, so that the integrated term of (8.63) vanishes. Thus, substituting (8.63) in (8.62) yields

$$\Delta E^{\sigma} = \sum_{\ell}(E_{\ell\sigma} - \varepsilon_f) - \sum_{\lambda}(\varepsilon_\lambda - \varepsilon_f) + \pi^{-1}\int_B \left[\tan^{-1}\left(\frac{\Delta_1(E)}{E - \varepsilon_{b\sigma} - \Lambda_1(E)}\right) + \tan^{-1}\left(\frac{\Delta_2(E)}{E - \varepsilon_{a\sigma} - \Lambda_2(E)}\right)\right] dE, \tag{8.64}$$

whereby (8.60) becomes

$$\Delta E = \sum_{\ell\sigma} E_{\ell\sigma} - \sum_{\lambda}(U\langle n_{\lambda+}\rangle\langle n_{\lambda-}\rangle + \varepsilon_\lambda + \varepsilon_f) + \pi^{-1}\sum_{\sigma}\int_B \left[\tan^{-1}\left(\frac{\Delta_1(E)}{E - \varepsilon_{b\sigma} - \Lambda_1(E)}\right) + \tan^{-1}\left(\frac{\Delta_2(E)}{E - \varepsilon_{a\sigma} - \Lambda_2(E)}\right)\right] dE. \tag{8.65}$$

8.5.2 Interaction energy

The interaction energy, ΔW, is the contribution (positive or negative) to ΔE, due to the (indirect) interaction between the two adatoms. In other words, ΔW is the difference between the chemisorption energy ΔE for the double-adsorption system and the sum of the chemisorption energies $\Delta E_\lambda^{(1)}(\lambda = a$ or $b)$ for the two individual single-adsorption systems, i.e.,

$$\Delta W = \Delta E - (\Delta E_a^{(1)} + \Delta E_b^{(1)}). \tag{8.66}$$

Paralleling the derivation of (8.65), we find that

$$\Delta E_\lambda^{(1)} = \sum_{\sigma} E_{\lambda\sigma}^{(1)} - (U\langle n_{\lambda+}^{(1)}\rangle\langle n_{\lambda-}^{(1)}\rangle + \varepsilon_\lambda + \varepsilon_f) + \pi^{1}\sum_{\sigma}\int_B \tan^{-1}\left(\frac{\Delta_1(E)}{E - \varepsilon_{\lambda\sigma}^{(1)} - \Lambda_1(E)}\right) dE, \tag{8.67}$$

with the superscript (1) denoting single-adsorption, and $E_{\lambda\sigma}^{(1)}$ the adsorption-state energy for that case. Substituting (8.65) and (8.67) into (8.66) gives

the interaction energy

$$\begin{aligned}\Delta W = &\sum_{\ell\sigma} E_{\ell\sigma} - \sum_{\lambda\sigma} E^{(1)}_{\lambda\sigma} + U\sum_{\lambda}(\langle n^{(1)}_{\lambda+}\rangle\langle n^{(1)}_{\lambda-}\rangle - \langle n_{\lambda+}\rangle\langle n_{\lambda-}\rangle)\\ &+ \pi^{-1}\sum_{\sigma}\int_B \tan^{-1}\left(\frac{\Delta_1(E)}{E-\varepsilon_{b\sigma}-\Lambda_1(E)}\right)dE\\ &+ \pi^{-1}\sum_{\sigma}\int_B \tan^{-1}\left(\frac{\Delta_2(E)}{E-\varepsilon_{a\sigma}-\Lambda_2(E)}\right)dE\\ &- \pi^{-1}\sum_{\lambda\sigma}\int_B \tan^{-1}\left(\frac{\Delta_1(E)}{E-\varepsilon^{(1)}_{\lambda\sigma}-\Lambda_1(E)}\right)dE. \end{aligned} \tag{8.68}$$

For the case of identical adatoms, considered here, $\varepsilon_a = \varepsilon_b$. Moreover, the non-magnetic solutions have $\langle n_{a+}\rangle = \langle n_{a-}\rangle = \langle n_{b+}\rangle = \langle n_{b-}\rangle$, so that (8.68) reduces to

$$\begin{aligned}\Delta W = 2\Bigg\{&\sum_{\ell} E_{\ell+} - 2E^{(1)}_{a+} + U(\langle n^{(1)}_{a+}\rangle^2 - \langle n_{a+}\rangle^2)\\ &+ \pi^{-1}\int_B \tan^{-1}\left(\frac{\Delta_1(E)}{E-\varepsilon_{a+}-\Lambda_1(E)}\right)dE\\ &+ \pi^{-1}\int_B \tan^{-1}\left(\frac{\Delta_2(E)}{E-\varepsilon_{a+}-\Lambda_2(E)}\right)dE\\ &- 2\pi^{-1}\int_B \tan^{-1}\left(\frac{\Delta_1(E)}{E-\varepsilon^{(1)}_{a+}-\Lambda_1(E)}\right)dE\Bigg\}, \end{aligned} \tag{8.69}$$

which is the form of the interaction energy we use here. However, many authors (e.g., Grimley 1967a, Einstein and Schrieffer 1973) use a simplified version in which the occupancies for single- and double-adsorption are assumed to be equal, i.e., $\langle n^{(1)}_{a+}\rangle = \langle n_{a+}\rangle$, so that the corresponding localized-state energies also become equal, i.e., $E_{\ell+} = E^{(1)}_{a+}$. In this scenario, (8.69) reads

$$\begin{aligned}\Delta\widehat{W} = 2\pi^{-1}\int_B\Bigg[&\tan^{-1}\left(\frac{\Delta_2(E)}{E-\varepsilon_{a+}-\Lambda_2(E)}\right)\\ &- \tan^{-1}\left(\frac{\Delta_1(E)}{E-\varepsilon_{a+}-\Lambda_1(E)}\right)\Bigg]dE, \end{aligned} \tag{8.70}$$

which, under the further assumption that $U \to 0$, and using (8.56) and the material of §8.2, can be expressed as

$$\Delta\widehat{W} = 2\pi^{-1} \int_B \text{Im ln} \left[1 - \beta_a^4 G_0(-n,m) G_0(m,-n) G_{ab}^{-1}\right] dE, \tag{8.71}$$

where

$$G_{ab} = \left[G_0^{-1}(a,a) - \beta_a^2 G_0(-n,-n)\right]^2 = \left[G_0^{-1}(b,b) - \beta_b^2 G_0(m,m)\right]^2. \tag{8.72}$$

8.6 2H-{ Ti, Cr, Ni, Cu } Systems

We now look at some results, calculated via the above theory, for a pair of H atoms chemisorbed on several d-band metals (Ti, Cr, Ni, Cu). Corresponding results for III-V and sp-hybrid semiconductor substrates have been given by Schranz and Davison (1998, 2000).

First, we describe the various system parameters, primarily adapted from Newns (1969). From the energy dispersion relation (2.32), the bulk states are distributed through a band, centered at α, and with width $W_b = 4|\beta|$. The Fermi level ε_f is taken to be at the center of this band, and is chosen to be the energy zero (so that $\varepsilon_f = \alpha \equiv 0$, for all systems). The position of ε_f, relative to the vacuum level, is given by the work function ϕ, whence the isolated H adatom level, relative to ε_f is

$$\varepsilon_\lambda = \varepsilon'_\lambda + \phi, \tag{8.73}$$

where $\varepsilon'_\lambda = -13.6$ eV is the H level relative to the vacuum. The Coulomb repulsion for H has the value $U = 12.9$ eV. These parameter values for H chemisorption on Ti, Cr, Ni and Cu are listed in Table 8.1. The difficult-to-estimate coupling parameter β_a is studied through a range of values $\beta_a = i|\beta|/3$, where $i = 1, 2, \ldots, 6$, following Einstein and Schrieffer (1973).

Table 8.1. System parameters for hydrogen chemisorption on Ti, Cr, Ni and Cu. For hydrogen, $\varepsilon'_\lambda = -13.598$ eV and $U = 12.9$ eV.

Substrate	ϕ (eV)	W_b (eV)	ε_λ (eV)
Ti	3.86	8.60	-9.74
Cr	4.56	6.10	-9.04
Ni	4.50	3.80	-9.10
Cu	4.46	2.70	-9.14

The numerical solution of the self-consistency equation (8.35) is rather difficult, so we refer readers to Schranz and Davison (1998) for a few details. However, for illustrative purposes, we present, in Fig. 8.5, a typical graph-

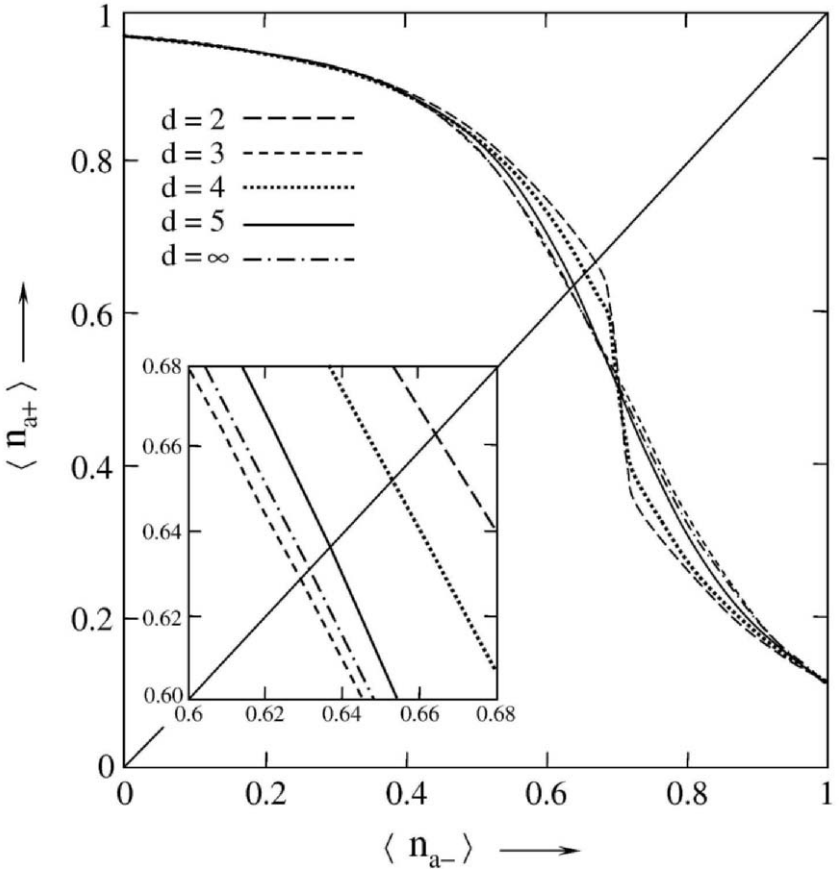

Fig. 8.5. Self-consistency plot of $\langle n_{a+}\rangle = N(\langle n_{a-}\rangle)$ for adatom spacings of $d = 2$ (long dashed), $d = 3$ (short dashed), $d = 4$ (dotted), $d = 5$ (long dash-dotted) and $d = \infty$ (short dash-dotted) for 2H-Cr with $\eta = 1.667$. Also plotted is line $\langle n_{a+}\rangle = \langle n_{a-}\rangle$ (solid line). Inset plot is above plot in range $0.60 < \langle n_{a\pm}\rangle < 0.68$. Self-consistent solutions are: $\langle n_{a+}\rangle = \langle n_{a-}\rangle = 0.664$ $(d = 2)$, $0.629\,(d = 3)$, $0.653\,(d = 4)$, $0.632\,(d = 5)$, $0.648\,(d = 6)$ and $0.637\,(d = \infty)$. After Schranz (1994).

ical solution to (8.35), for the 2H-Cr system, and various values of d. The figure shows clearly that the double-adsorption solutions, associated with even (odd) values of d, asymptotically approach the single-adsorption solution from above (below). This behaviour, as $d \to \infty$, is a reflection of the mathematical limits (8.27).

Calculations of the chemisorption energy can be examined in two ways: (i) the effect of the choice of metal for a particular β_a, and (ii) the effect of β_a for a particular metal. The former case is investigated in Fig. 8.6(a), where ΔE is plotted versus adatom separation d, for each of the 4 metals, and for $\eta = \beta_a/|\beta| = 1.667$. The most obvious feature is the damped oscillatory nature of ΔE as a function of d in agreement with Grimley's interaction law (8.1). Since adatoms tend to occupy the sites that minimize ΔE, we see that $d = 3$ is the most favourable adatom separation. Also, by referring to Table 8.1, it can be concluded that, for fixed η, ΔE decreases with increasing bandwidth, which is understandable in light of the fact that the adatom level, broadened by chemisorption (§3.3.2), has a greater overlap with the occupied band for larger W_b, leading to a stronger interaction. Turning to case (ii), Fig. 8.6(b) shows ΔE versus d for a Ti substrate and various values of η. The damped, oscillatory behaviour is observed for all η, with the greatest amplitudes occurring for the largest values of η. It is also seen that ΔE decreases as η increases, which is as expected, because the atom-surface bond is being strengthened.

To understand the oscillatory dependence of ΔE on d, it is necessary to look more closely at the interaction energy ΔW because, as (8.66) shows, ΔE is the sum of the two single-atom chemisorption energies (which are independent of d) plus ΔW. Hence, any effect of d on ΔE must arise due to ΔW. Alternatively, one may consider the situation in terms of the adatom wavefunctions, which, as they spread out from each adatom, interfere in either a constructive or destructive fashion, thus creating oscillations in the electron density that are mirrored in the interaction. Since the wavefunctions are in or out of phase, depending on d, ΔE itself becomes a function of d. As d increases, the overlap of the wavefunctions decreases, and ΔE tends towards $\Delta E_a^{(1)}$.

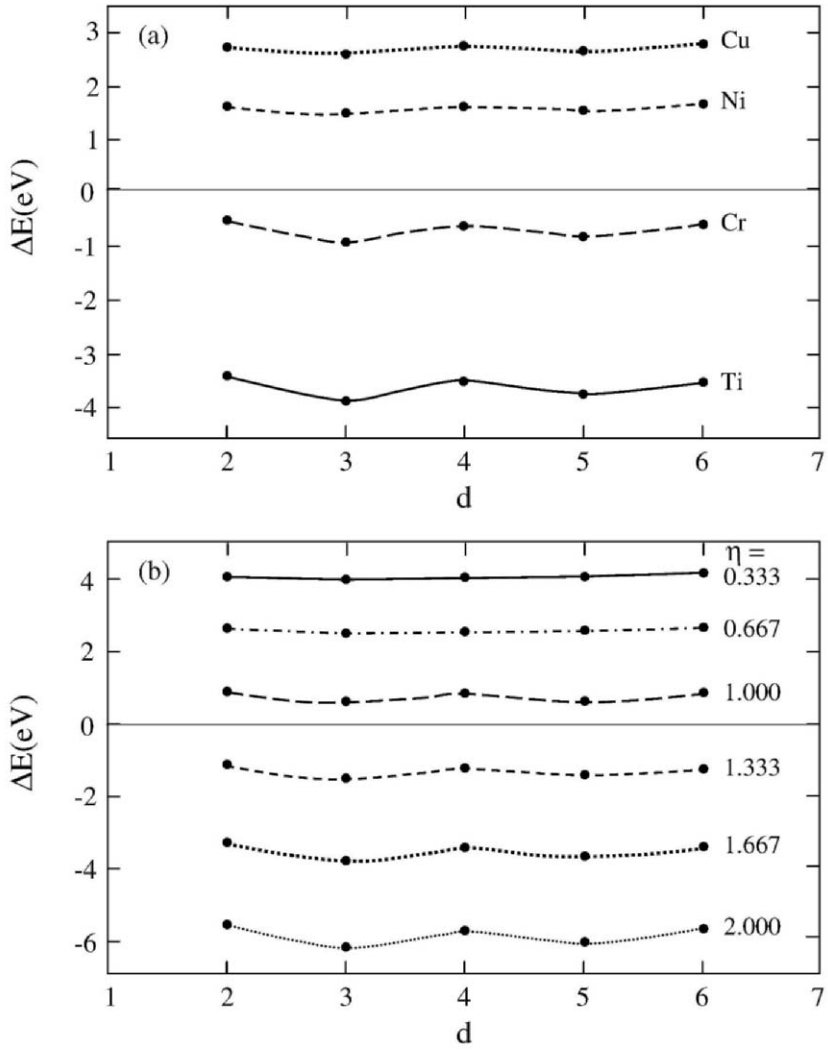

Fig. 8.6. (a) Plot of chemisorption energy (ΔE) vs adatom separation (d) for hydrogen chemisorption on Ti, Cr, Ni and Cu with $\eta = 1.667$. (b) ΔE vs d for 2H-Ti with $\eta = 0.333$, 0.667, 1.000, 1.333, 1.667 and 2.000. After Schranz (1994).

Graphs of ΔW vs d, for the 4 metals and $\eta = 1.667$, are displayed in Fig. 8.7(a). As expected, ΔW is a damped, oscillatory function of d. It is also evident that the amplitude of the oscillation increases with the bandwidth of the metal, which has a corresponding effect on ΔE, seen in Fig. 8.6(a). The effect of η on ΔW vs d is shown in Fig. 8.7(b), for a Ti substrate. We see that the amplitude of the oscillations increases with η, which can be explained as due to a stronger bond producing a greater penetration of the adatom orbitals into the substrate, thereby strengthening their interaction. Comparing Figs. 8.6 and 8.7, it is observed that ΔW is approximately an order of magnitude smaller than ΔE, which is in agreement with the finding of Einstein and Schrieffer (1973).

An analysis of the calculated values of ΔW shows that the damping factor in the indirect interaction is d^{-1}, as exemplified in Fig. 8.8, for Cr and Ti substrates and $\eta = 1.667$. "Envelope" curves of the form αd^{-1} are shown, where α is chosen, so that the curve passes through the data point corresponding to $d = 4$. The fit to d^{-1} is seen to improve as d increases, agreeing with the asymptotic nature of the interaction law.

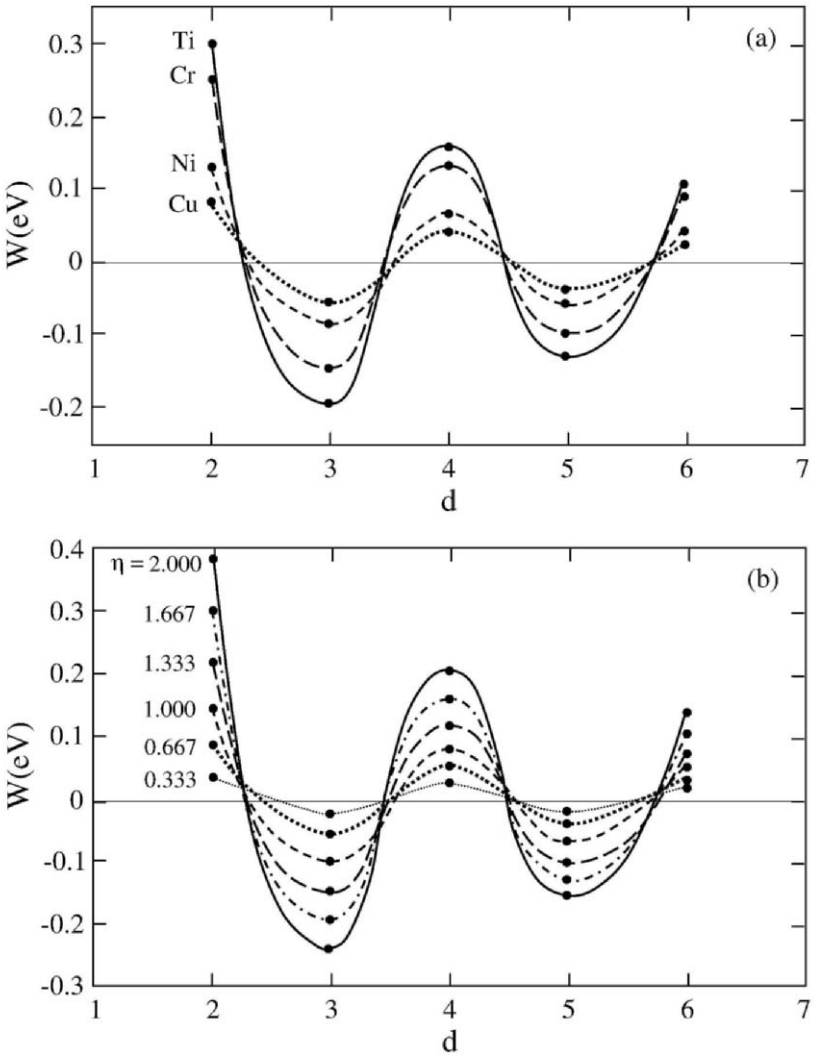

Fig. 8.7. (a) Plot of interaction energy (ΔW) vs adatom separation (d) for hydrogen chemisorption on Ti, Cr, Ni and Cu with $\eta = 1.667$. (b) ΔW vs d for 2H-Ti with $\eta = 0.333$, 0.667, 1.000, 1.333, 1.667 and 2.000. After Schranz (1994).

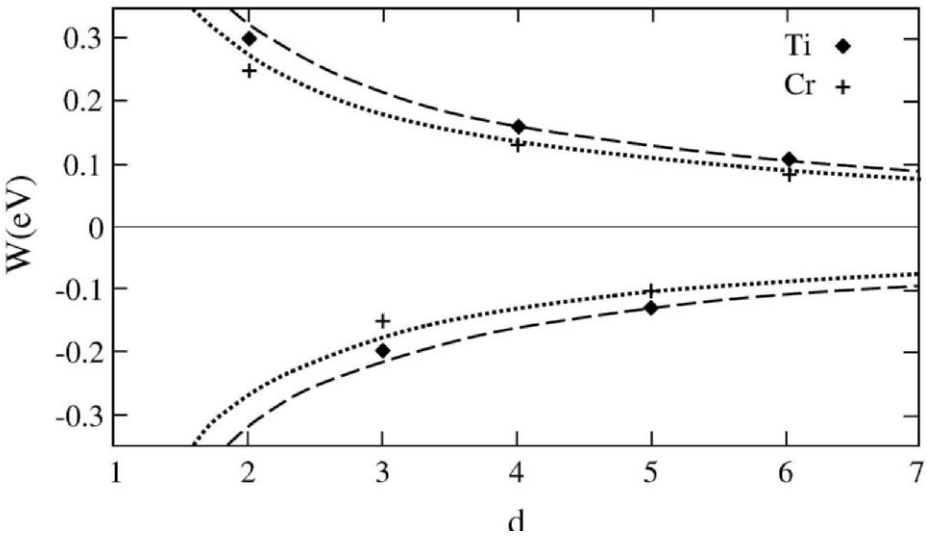

Fig. 8.8. Interaction energy ΔW vs adatom separation d for 2H-Cr and 2H-Ti with $\eta = 1.67$. Dashed lines are $\pm\alpha d^{-1}$ curves. After Schranz (1994).

The relative size of the contributions to ΔW in (8.69) can be assessed, by comparing ΔW to $\Delta\widehat{W}$ in (8.71), which neglects the effects of different occupancies and localized-state energies between the single- and double-adsorption cases. Some typical results are depicted in Fig. 8.9 for a Ti substrate and $\eta = 1.667$. The approximation $\Delta\widehat{W}$ is seen to either over- or under-estimate ΔW, at small adatom separations, with the approximation improving as d increases. Consequently, we conclude that the effect of the occupancies and localized-state energies is important only at small adatom separations.

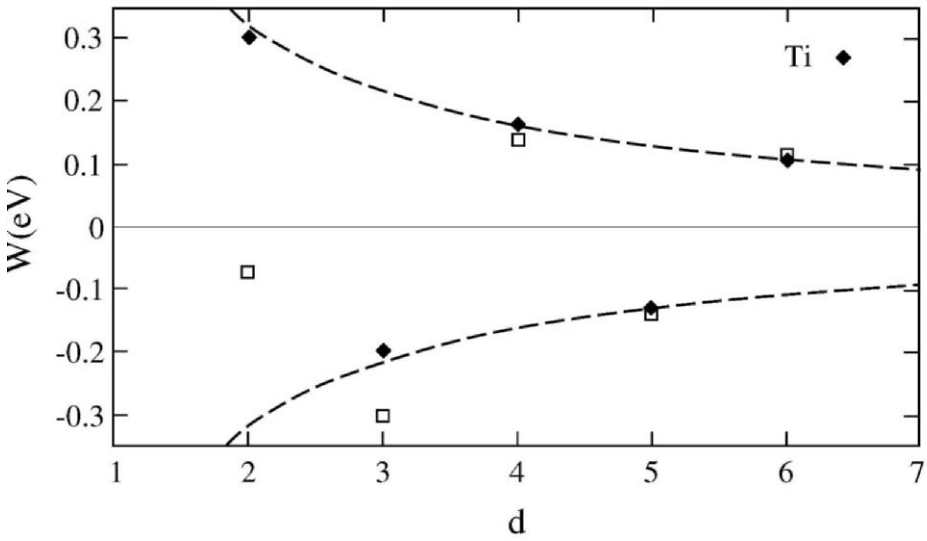

Fig. 8.9. Interaction energy ΔW vs adatom separation d for 2H-Ti with $\eta = 1.667$. Dashed lines are $\pm\alpha d^{-1}$ curves. Squares represent approximate interaction energy $\Delta\widehat{W}$, neglecting changes in occupancies and localized-state energies. After Schranz (1994).

Lastly, we turn to the charge transfer, Δq, calculated from (8.36). Fig. 8.10 provides representative graphs of Δq vs d for H adsorption on the 4 metals with $\eta = 1.667$, and for a Ti substrate with various η. The oscillation of Δq with d can be understood in terms of the solution of the self-consistency equation, which was demonstrated graphically in Fig. 8.5. Those solutions were seen to be greater (less) than the single-adsorption solution for even (odd) d, and with the double-adsorption solutions approaching that for single-adsorption, in the limit of large d. Therefore, the expectation is indeed that Δq should oscillate about its single-adsorption counterpart, and reach it as $d \to \infty$.

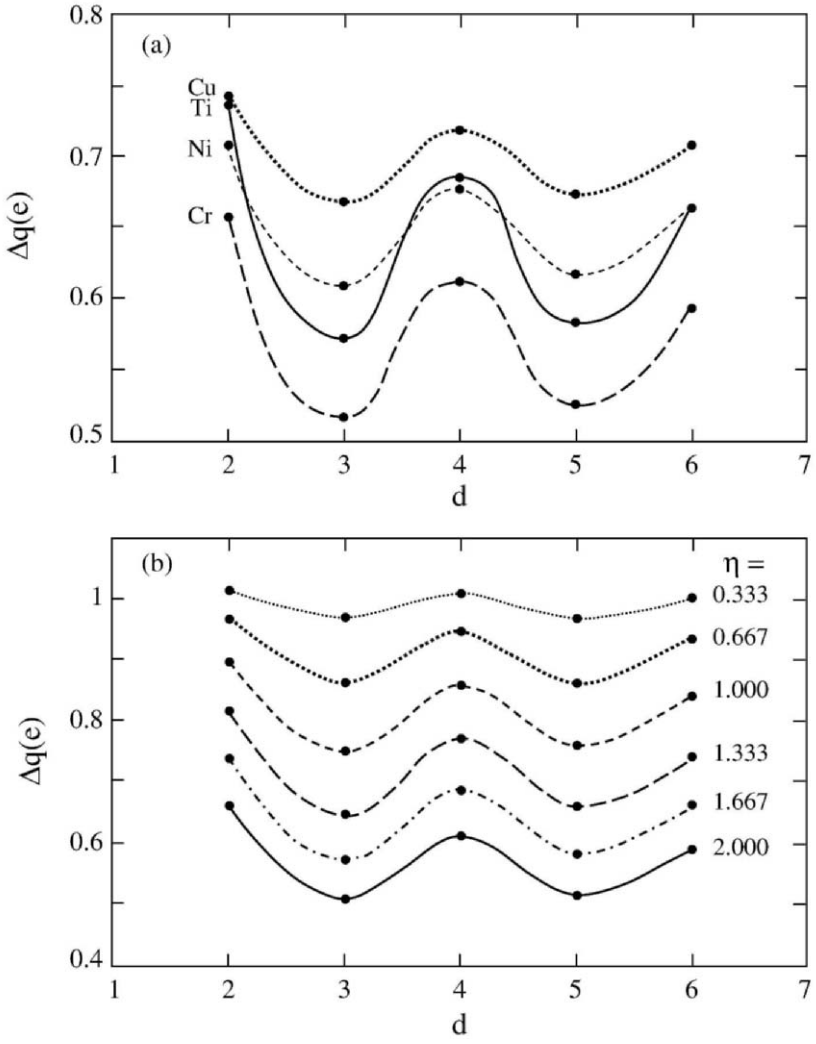

Fig. 8.10. (a) Charge transfer (Δq) vs adatom separation (d) for hydrogen chemisorption on Ti, Cr, Ni and Cu with $\eta = 1.667$. (b) Δq vs d for 2H-Ti with $\eta = 0.333$, 0.667, 1.000, 1.333, 1.667 and 2.000. After Schranz (1994).

Summarizing, it is clear that the indirect interaction between adatoms has a significant effect on the chemisorption properties of the system. Most noticeably, the chemisorption energy has a damped, oscillatory dependence on the adatom separation, as first quantified in (8.1) by Grimley. Thus, multi-atom adsorption occurs preferentially with the atoms at certain sites relative to one another.

Appendices

When you have learned what an explanation really is, then you can go on to more subtle questions.

— Richard Feynman

A. Evaluation of $J_n(b)$

For $n = 0$, evaluation of (1.86), i.e.,

$$J_n(b) = \int_{\pi/2}^{\pi} \frac{\cos n\theta}{1 + b\cos\theta} d\theta, \tag{A.1}$$

gives (Gradshteyn and Ryzhik 1980)

$$J_0(b) = \frac{2}{(1-b^2)^{1/2}} \left\{ \tan^{-1}\left[\left(\frac{1-b}{1+b} \right)^{1/2} \tan(\theta/2) \right] \right\}_{\pi/2}^{\pi},$$

which, since $b = 2(z_s + z_s^{-1})^{-1}$ by (1.85), yields

$$J_0(z_s) = 2\left(\frac{z_s + z_s^{-1}}{z_s - z_s^{-1}} \right) \left\{ \tan^{-1}\left[\left(\frac{z_s - 1}{z_s + 1} \right) \tan(\theta/2) \right] \right\}_{\pi/2}^{\pi}.$$

However, $0 \le z_s \le 1$, so

$$J_0(z_s) = -2\zeta_s \left\{ \tan^{-1}\left[-\tau_s \tan(\theta/2) \right] \right\}_{\pi/2}^{\pi}, \tag{A.2}$$

where

$$\zeta_s = (z_s^{-1} + z_s)(z_s^{-1} - z_s)^{-1},$$

and

$$\tau_s = (1 - z_s)(1 + z_s)^{-1}. \tag{A.3}$$

Thus, (A.2) gives

$$J_0(z_s) = -2\zeta_s(-\pi/2 + \tan^{-1}\tau_s). \tag{A.4}$$

If we let

$$z_s = \tan\alpha, \tag{A.5}$$

then we can write

$$\tau_s = \tan(\pi/4 - \alpha) = \tan\phi_s, \tag{A.6}$$

via (A.3), so that

$$\phi_s = \pi/4 - \alpha = \pi/4 - \tan^{-1} z_s, \tag{A.7}$$

by (A.5). Hence, (A.6) and (A.7) in (A.4), result in

$$J_0(z_s) = 2\zeta_s(\pi/4 + \tan^{-1} z_s). \tag{A.8}$$

Knowing $J_0(b)$, we can derive expressions for $J_1(b)$, and $J_2(b)$ in terms of $J_0(b)$ (Goodman 1994). From (A.1), we have

$$bJ_1 + J_0 = \int_{\pi/2}^{\pi} \frac{b\cos\theta + 1}{1 + b\cos\theta} d\theta = \frac{\pi}{2},$$

so

$$J_1(b) = b^{-1}[\pi/2 - J_0(b)]. \tag{A.9}$$

Likewise, (A.1) shows that

$$bJ_2 + 2J_1 + bJ_0 = 2\int_{\pi/2}^{\pi} \cos\theta\, d\theta = -2,$$

whence, on rearranging and using (A.9), we obtain

$$J_2(b) = -\frac{2}{b}\left[\left(1 + \frac{\pi}{2b}\right) + \left(\frac{b}{2} - \frac{1}{b}\right) J_0(b)\right]. \tag{A.10}$$

B. Slater Determinant

Providing the Hamiltonian H is a sum of 1-electron operators only, i.e.,

$$H = \sum_{i=1}^{N} H_i, \tag{B.1}$$

the total wave function Ψ can be expressed as a simple *Hartree product*

$$\Psi = \phi_1(\mathbf{r}_1)\phi_2(\mathbf{r}_2)\cdots\phi_N(\mathbf{r}_N), \tag{B.2}$$

each 1-electron function $\phi_i(\mathbf{r}_i)$ being an eigenfunction of the corresponding 1-electron operator H_i. Since any such product, with its electronic coordinates $\mathbf{r}_i$ arranged in any order, is equally acceptable and energetically equivalent, a more general solution than (B.2) can be constructed by taking a linear combination of all these products, namely,

$$\Psi = \sum_{P} c_P P[\phi_1(\mathbf{r}_1)\cdots\phi_N(\mathbf{r}_N)], \tag{B.3}$$

c_P being constants and the summation being over N permutations P of the electronic coordinates (Davison 1969).

In order to satisfy the *Pauli principle*, however, it is necessary for Ψ in (B.3) to be *antisymmetric* in the interchange of any pair of electronic coordinates (including spin), which is achieved by taking

$$c_P = (-c)^p, \tag{B.4}$$

where p is the parity of the permutation P. On separately normalizing $\phi_i(\mathbf{r}_i)$, this becomes

$$c_P = (-1)^p, \tag{B.5}$$

whence, (B.3) can be written as

$$\Psi = \sum_{P}(-1)^p P[\phi_1(\mathbf{r}_1)\cdots\phi_N(\mathbf{r}_N)], \tag{B.6}$$

i.e., the *Slater determinant*

$$\Psi = (N!)^{-1/2}\begin{vmatrix} \phi_1(\mathbf{r}_1)\cdots\phi_1(\mathbf{r}_N) \\ \cdots\cdots\cdots\cdots\cdots \\ \phi_N(\mathbf{r}_1)\cdots\phi_N(\mathbf{r}_N) \end{vmatrix}, \tag{B.7}$$

or

$$\Psi = (N!)^{-1/2} \det[\phi_k(\mathbf{r}_i)], \tag{B.8}$$

in which $(N!)^{-1/2}$ is the normalization constant and $[\phi_k(\mathbf{r}_i)]$ is the matrix of the spin-orbital elements $\phi_k(\mathbf{r}_i)$ of the determinant. It is clear that Ψ in (B.7) is antisymmetric, since interchanging any pair of $\mathbf{r}_i$'s, say $\mathbf{r}_1$ and $\mathbf{r}_2$, interchanges two columns of the determinant and thereby changes its sign. This is also true for the exchange of any two rows of ϕ_k's.

C. Anticommutation Relations

Consider a *fermion* collection, where each state is either empty or occupied, i.e., $n \in \{0, 1\}$. If the states are ordered, the total wave function can be expressed in terms of the *state occupancy* (Davydov 1991), namely,

$$|n_1, n_2, \ldots, n_k, \ldots\rangle. \tag{C.1}$$

Let us now define a *creation operator*, $c_k^\dagger$, such that, if $n_k = 0$, its operation will yield a wave function with $n_k = 1$ and, if $n_k = 1$ already, its operation will give zero, since a fermion can not be created in a state that is occupied. Hence, we have

$$c_k^\dagger |n_1, \ldots, n_k, \ldots\rangle = (-1)^{\nu_k}(1 - n_k)|n_1, \ldots, 1 - n_k, \ldots\rangle, \tag{C.2}$$

the *sign* being determined by the number of occupied states *below* k, i.e.,

$$\nu_k = \sum_{m=1}^{k-1} n_m, \tag{C.3}$$

since fermion wave functions are *antisymmetric*.

Similarly, we define the *hermitean conjugate* operator, c_k, as an *annihilation operator*, which produces a wave function with a fermion missing from the kth state, if it was occupied, or zero, if not. Thus, in this case, we have

$$c_k |n_1, \ldots, n_k, \ldots\rangle = (-1)^{\nu_k} n_k |n_1, \ldots, 1 - n_k, \ldots\rangle. \tag{C.4}$$

By combining (C.2) and (C.4), we can construct the *number operator* for the kth state, viz.,

$$n_k = c_k^\dagger c_k, \tag{C.5}$$

which returns the kth state eigenvalue via the eigenvalue equation

$$\begin{aligned} n_k|n_1,\ldots,n_k,\ldots\rangle &= n_k^2|n_1,\ldots,n_k,\ldots\rangle \\ &= n_k|n_1,\ldots,n_k,\ldots\rangle, \end{aligned} \tag{C.6}$$

since n_k is 0 or 1. Because the n_k operator has only two possible eigenvalues, it can be represented by a 2×2 matrix,

$$n_k = \begin{bmatrix} 0 & 0 \\ 0 & 1 \end{bmatrix}, \tag{C.7}$$

with the eigenvectors

$$\begin{aligned} |0\rangle_k &= |n_1,\ldots,0,\ldots\rangle = \begin{bmatrix} 1 \\ 0 \end{bmatrix}, \\ |1\rangle_k &= |n_1,\ldots,1,\ldots\rangle = \begin{bmatrix} 0 \\ 1 \end{bmatrix}. \end{aligned} \tag{C.8}$$

Hence, (C.2) becomes

$$c_k^\dagger|0\rangle_k = (-1)^{\nu_k}|1\rangle_k, \quad c_k^\dagger|1\rangle_k = 0, \tag{C.9}$$

so that

$$c_k^\dagger = (-1)^{\nu_k}\begin{bmatrix} 0 & 0 \\ 1 & 0 \end{bmatrix}. \tag{C.10}$$

Similarly, we have

$$c_k = (-1)^{\nu_k}\begin{bmatrix} 0 & 1 \\ 0 & 0 \end{bmatrix}, \tag{C.11}$$

which has the required properties

$$c_k|0\rangle_k = 0, \quad c_k|1\rangle_k = (-1)^k|0\rangle_k. \tag{C.12}$$

We can now derive the anticommutation relations.

Let us first treat the operation on a *single* state, for which the relevant four equations are

$$\left.\begin{array}{rcl} c_k c_k^\dagger|\ldots,n_k,\ldots\rangle &=& (1-n_k)|\ldots,n_k,\ldots\rangle \\ c_k^\dagger c_k|\ldots,n_k,\ldots\rangle &=& n_k|\ldots,n_k,\ldots\rangle \\ c_k c_k|\ldots,n_k,\ldots\rangle &=& n_k(1-n_k)|\ldots,n_k,\ldots\rangle = 0 \\ c_k^\dagger c_k^\dagger|\ldots,n_k,\ldots\rangle &=& 0. \end{array}\right\} \tag{C.13}$$

From these equations, we can assemble the *anticommutators* (4.13),

$$[c_k, c_k]_+ = [c_k^\dagger, c_k^\dagger]_+ = 0, \quad [c_k^\dagger, c_k]_+ = 1. \tag{C.14}$$

Next, we investigate the *two* states i and j, where $i < j$. Here, we have

$$\begin{aligned} c_i c_j |\ldots, n_i, \ldots, n_j, \ldots\rangle &= (-1)^{\nu_j} n_j c_i |\ldots n_i, \ldots, 1-n_j, \ldots\rangle \\ &= (-1)^{\nu_j+\nu_i} n_j n_i |\ldots, 1-n_i, \ldots, 1-n_j, \ldots\rangle, \end{aligned} \tag{C.15}$$

$$\begin{aligned} c_j c_i |\ldots, n_i, \ldots, n_j, \ldots\rangle &= (-1)^{\nu_i} n_i c_j |\ldots, 1-n_i, \ldots, n_j, \ldots\rangle \\ &= (-1)^{\nu_i+\nu_j-1} n_i n_j |\ldots, 1-n_i, \ldots, 1-n_j, \ldots\rangle, \end{aligned}$$

since the c_i operation first reduces ν_j by 1, but c_j leaves ν_i unchanged, whence,

$$[c_i, c_j]_+ = 0. \tag{C.16}$$

Again,

$$\begin{aligned} c_i^\dagger c_j^\dagger |\ldots, n_i, \ldots, n_j, \ldots\rangle &= (-1)^{\nu_j} (1-n_j) c_i^\dagger |\ldots, n_i, \ldots, 1-n_j, \ldots\rangle \\ &= (-1)^{\nu_j+\nu_i} (1-n_j)(1-n_i) |\ldots, 1-n_i, \ldots, 1-n_j, \ldots\rangle, \end{aligned} \tag{C.17}$$

$$\begin{aligned} c_j^\dagger c_i^\dagger |\ldots, n_i, \ldots, n_j, \ldots\rangle &= (-1)^{\nu_i} (1-n_i) c_j^\dagger |\ldots, 1-n_i, \ldots, n_j, \ldots\rangle \\ &= (-1)^{\nu_i+\nu_j-1} (1-n_i)(1-n_j) |\ldots, 1-n_i, \ldots, 1-n_j, \ldots\rangle, \end{aligned}$$

so that

$$[c_i^\dagger, c_j^\dagger]_+ = 0, \quad i < j. \tag{C.18}$$

Lastly,

$$\begin{aligned} c_i^\dagger c_j |\ldots, n_i, \ldots, n_j, \ldots\rangle &= (-1)^{\nu_j} n_j c_i^\dagger |\ldots, n_i, \ldots, 1-n_j, \ldots\rangle \\ &= (-1)^{\nu_i+\nu_j} n_j (1-n_i) |\ldots, 1-n_i, \ldots, 1-n_j, \ldots\rangle \end{aligned} \tag{C.19}$$

$$\begin{aligned} c_j c_i^\dagger |\ldots, n_i, \ldots, n_j, \ldots\rangle &= (-1)^{\nu_i} (1-n_i) c_j^\dagger |\ldots, 1-n_i, \ldots, n_j, \ldots\rangle \\ &= (-1)^{\nu_i+\nu_j-1} (1-n_i) n_j |\ldots, 1-n_i, \ldots, 1-n_j, \ldots\rangle, \end{aligned}$$

which lead to

$$[c_i^\dagger, c_j]_+ = 0, \quad i < j. \tag{C.20}$$

When $i > j$, (C.15) to (C.20) yield the same results, so we obtain

$$[c_i, c_j]_+ = [c_i^\dagger, c_j^\dagger]_+ = 0, \quad [c_i^\dagger, c_j]_+ = \delta_{ij}, \tag{C.21}$$

or any i and j.

D. Plemelj Formula

In view of (4.60), on putting

$$\varepsilon' = \varepsilon - \varepsilon_k, \tag{D.1}$$

the summands denominator in (4.66) becomes

$$\frac{1}{\varepsilon' \pm is} = \frac{\varepsilon' \mp is}{\varepsilon'^2 + s^2} = \frac{\varepsilon'}{\varepsilon'^2 + s^2} \mp \frac{is}{\varepsilon'^2 + s^2}. \tag{D.2}$$

The *first* term on the right-hand side (RHS) of (D.2) gives

$$\lim_{s\to 0^+} \int_{-\infty}^{\infty} \frac{\varepsilon' d\varepsilon'}{\varepsilon'^2 + s^2} = \lim_{s\to 0^+} \left[\int_{-\infty}^{-s} + \int_{s}^{\infty} + \int_{-s}^{s} \right] \frac{\varepsilon' d\varepsilon'}{\varepsilon'^2 + s^2}, \tag{D.3}$$

or

$$\lim_{s\to 0^+} \int_{-\infty}^{\infty} \frac{\varepsilon' d\varepsilon'}{\varepsilon'^2 + s^2} = P \int_{-\infty}^{\infty} \frac{d\varepsilon'}{\varepsilon'}, \tag{D.4}$$

where P denotes the Cauchy *principal value*, and the third term on the RHS of (D.3) is zero, because the integrand is odd.

From the *second* term on the RHS of (D.2), we have

$$\lim_{s\to 0^+} \frac{s}{\varepsilon'^2 + s^2} = 0, \quad \text{when} \quad \varepsilon' \neq 0. \tag{D.5}$$

Moreover, we can write

$$\int_{-c}^{c} \lim_{s\to 0^+} \frac{s d\varepsilon'}{\varepsilon'^2 + s^2} = \lim_{s\to 0^+} \left[\tan^{-1}\left(\frac{c}{s}\right) - \tan^{-1}\left(-\frac{c}{s}\right) \right] = \pi. \tag{D.6}$$

Contrasting this with the Dirac δ-function definition, viz.,

$$\int_{-c}^{c} \delta(\varepsilon') d\varepsilon' = 1, \tag{D.7}$$

shows that

$$\lim_{s\to 0^+} \frac{s}{\varepsilon'^2 + s^2} = \pi \delta(\varepsilon). \tag{D.8}$$

Equations (D.4) and (D.8) with (D.2) reveal that

$$\lim_{s\to 0^+} \int_{-\infty}^{\infty} \frac{d\varepsilon'}{\varepsilon' \pm is} = P \int_{-\infty}^{\infty} \frac{d\varepsilon'}{\varepsilon'} \mp i\pi \int_{-\infty}^{\infty} \delta(\varepsilon') d\varepsilon', \tag{D.9}$$

which, in shorthand form, is written as

$$\lim_{s\to 0^+} \frac{1}{\varepsilon' \pm is} = P\left(\frac{1}{\varepsilon'}\right) \mp i\pi\delta(\varepsilon'), \tag{D.10}$$

it being understood that both sides are to appear in an integrand, which may also be multiplied by a well-behaved function $f(\varepsilon')$ (Raimes 1972).

E. Residues of $g(\varepsilon)$

Consider the function

$$g(\varepsilon) = f'(\varepsilon)/f(\varepsilon), \tag{E.1}$$

where $f(\varepsilon)$ is given by (4.91) and the contour C encloses all the *zeros* (ω_+) and the *poles* (ω_-) of f corresponding to occupied *perturbed* (ε_m) and *unperturbed* (ε_k) energies, respectively.

If the *order* of the zero corresponding to ω_+ is $r = r_+$, then we can expand $f(\varepsilon)$ near $\varepsilon = \omega_+$, and write

$$f(\varepsilon) = a_r(\varepsilon - \omega_+)^r + a_{r+1}(\varepsilon - \omega_+)^{r+1} + \cdots, \tag{E.2}$$

which on differentiating gives

$$f'(\varepsilon) = ra_r(\varepsilon - \omega_+)^{r-1} + (r+1)a_{r+1}(\varepsilon - \omega_+)^r + \cdots. \tag{E.3}$$

Whence, we have

$$g(\varepsilon) = \frac{f'(\varepsilon)}{f(\varepsilon)} = \frac{ra_r(\varepsilon - \omega_+)^{r-1} + \cdots}{a_r(\varepsilon - \omega_+)^r + \cdots},$$

or

$$g(\varepsilon) \simeq r(\varepsilon - \omega_+)^{-1}, \tag{E.4}$$

so

$$Res\, g(\varepsilon)\big|_{\varepsilon=\omega_+} = r_+. \tag{E.5}$$

By the same token, if the pole ω_- has order $r = r_-$, then we have the expansion

$$f(\varepsilon) = b_{-r}(\varepsilon - \omega_-)^{-r} + b_{-r+1}(\varepsilon - \omega_-)^{-r+1} + \cdots, \tag{E.6}$$

in which case

$$f'(\varepsilon) = -rb_{-r}(\varepsilon - \omega_-)^{-r-1} + (-r+1)b_{-r+1}(\varepsilon - \omega_-)^{-r} + \cdots \tag{E.7}$$

resulting in

$$Res\, g(\varepsilon)\big|_{\varepsilon=\omega_-} = -r_-. \tag{E.8}$$

F. Logarithmic Function

Let

$$w = \ln\, z, \tag{F.1}$$

where

$$w = u \pm iv, \quad z = x \pm iy. \tag{F.2}$$

From (F.1), we find

$$z = e^w \tag{F.3}$$

so (F.1) and (F.2) in (F.3) yields

$$e^u(\cos v \pm i \sin v) = x \pm iy. \tag{F.4}$$

Thus, equating real and imaginary parts gives

$$x = e^u \cos v, \quad y = e^u \sin v, \tag{F.5}$$

which lead to

$$\tan v = y/x, \quad x^2 + y^2 = e^{2u}, \tag{F.6}$$

or

$$u = \ln(x^2 + y^2)^{1/2} = \ln\, |z|, \tag{F.7}$$

by (F.2). Substituting (F.6) and (F.7) in (F.2), using (F.1), we obtain

$$w = \ln(x \pm iy) = \ln|x \pm iy| \pm i \tan^{-1}(y/x). \tag{F.8}$$

G. Range of $\tan^{-1}$

As was pointed out by Newns (1967), for (4.99) to be complete, it is necessary to specify the range of the multi-valued function $\tan^{-1}$.

First, we note that, if the unperturbed semi-infinite metal substrate has no surface states, then $\Delta(\varepsilon) = 0$ *outside* the energy band. However, from (4.70), we see that poles may then occur in $G^{\sigma}_{aa}(\varepsilon)$ at energies given by the solutions of

$$\varepsilon - \varepsilon_{a\sigma} - \Lambda(\varepsilon) = 0, \tag{G.1}$$

which is the condition for localized states. Although (G.1) is of no significance in the band, when $\Delta(\varepsilon) \neq 0$, it does, however, imply a singularity in the argument of $\tan^{-1}$ in (4.99), if satisfied for ε in the band. Consequently, it

is necessary to consider the roots of (G.1) (Fig. G.1) in discussing the value of $\tan^{-1}$ in (4.99).

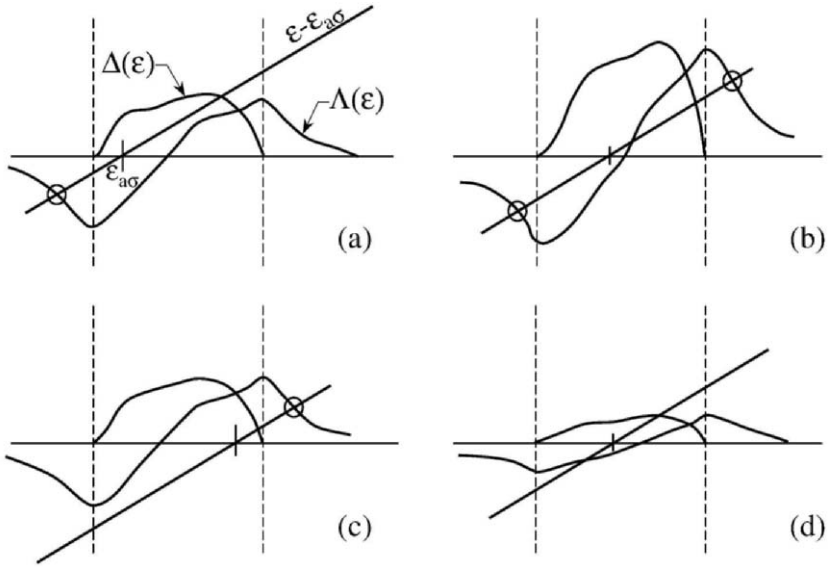

Fig. G.1. Diagrams showing $\Delta(\varepsilon)$ and $\Lambda(\varepsilon)$ curves along with localized-state solutions (o) of $\varepsilon - \varepsilon_{a\sigma} - \Lambda(\varepsilon) = 0$. After Newns (1967).

Consider the case where *no* localized (occupied) state occurs below the band, as in Fig. 4.4. As can be seen in Figs. G.1(c) and (d), the $\tan^{-1}$ argument (ξ) starts off *negative* at the bottom of the band (ε_0). If the FL is near ε_0, then ΔE^σ should be small, so that ξ is small, and must be taken in the range at and below zero. As expected, ΔE^σ is then negative. If the integrand falls below $-\pi/2$, as when no localized states exist above or below the band (Fig. G.1d), then a singularity in ξ occurs. Since no sudden change can take place in ΔE^σ as the FL crosses over a root of (G.1), $\tan^{-1}$ must be taken in the range $-\pi/2$ to $-\pi$, when ξ becomes positive. Hence, $\tan^{-1}$ in (4.99) goes smoothly away from zero in the negative direction, in the region 0 to $-\pi$, provided there is no localized state below the band.

When a localized state $\varepsilon_{\ell\sigma}$ does appear *below* the band, the contour C may be taken round all the eigenvalues between ε_f and ε_0, where the lowest

eigenvalue is now an *unperturbed* one (Fig. G.2). From its definition (4.86), ΔE^σ must include an additional term for the energy difference between $\varepsilon_{\ell\sigma}$ and an eigenvalue just outside C at ε_f, which is zero. Comparison of Figs. 4.4 and G.2 reveals that the sign of the contribution to ΔE^σ is opposite to

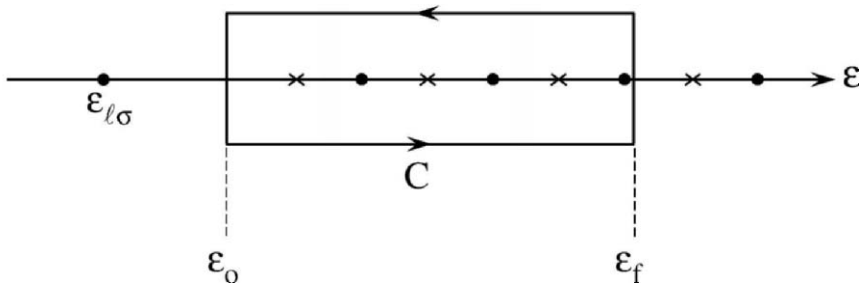

Fig. G.2. Contour C around unperturbed ($\times$) and perturbed ($\bullet$) band states with localized state at $\varepsilon_{\ell\sigma}$ below lower band edge ε_0 with ε_f being FL.

that in (4.99), whose derivation proceeds exactly as before. It is evident from Fig. G.1(a) and (b) that ξ is initially *positive* at ε_0, whence, $\tan^{-1}$ must now vary smoothly, going away from zero in the positive direction, in the range 0 to π.

H. Electronic States of Binary Chain

Solutions of (4.103) and (4.104) are sought by putting (Davison and Levine 1970)

$$c_n = u^n, \quad n \quad \text{odd}, \tag{H.1}$$

$$c_n = v^n, \quad n \quad \text{even}, \tag{H.2}$$

whereby we have

$$(X - z)u^n = v^{n-1} - v^{n+1}, \quad n \quad \text{odd}, \tag{H.3}$$

$$(X + z)v^n = u^{n+1} - u^{n-1}, \quad n \quad \text{even}. \tag{H.4}$$

From (H.4), we obtain

$$v^n = \frac{u^{n+1} - u^{n-1}}{X + z}, \tag{H.5}$$

which in (H.3) leads to the *characteristic equation* in u, viz., the quartic

$$u^4 + \gamma u^2 + 1 = 0, \tag{H.6}$$

where

$$\gamma = X^2 - z^2 - 2. \tag{H.7}$$

On choosing

$$\gamma = -2\cos 2k, \tag{H.8}$$

equation (H.7) gives

$$X = \pm(z^2 + 4\sin^2 k)^{1/2}, \tag{H.9}$$

i.e.,

$$\varepsilon_k^{\pm} = \pm(\lambda^2 + 4\beta^2 \sin^2 k)^{1/2}, \tag{H.10}$$

via (4.105) and (4.106).

Returning to (H.6), we see that the roots are given by

$$u^2 = \left[-\gamma \pm (\gamma^2 - 4)^{1/2}\right]/2, \tag{H.11}$$

which, by means of (H.8), shows that

$$u^n = e^{\pm ink}. \tag{H.12}$$

Inserting (H.12) in (H.5), we find

$$v^n = Ke^{\pm ink}, \tag{H.13}$$

where

$$K = \frac{2i\beta \sin k}{\varepsilon_k^{\pm} + \lambda}, \tag{H.14}$$

via (4.105) and (4.106).

I. Normalization Factor

The normalization of (4.108) requires that

$$\langle k|k\rangle = 1, \tag{I.1}$$

which is subject to the AO orthonormality condition

$$\langle n_i|n_j\rangle = \delta_{ij}. \tag{I.2}$$

With the aid of (I.2), inserting (4.108) in (I.1) gives

$$R^2\left(\sum_{n_1}\sin^2 n_1k + |K|^2\sum_{n_2}\cos^2 n_2k\right) = 1, \tag{I.3}$$

in which $n_1(n_2) = n$ odd (even). From (I.3), we have

$$\begin{aligned} R^2\left[\sum_{n}\sin^2 nk - \sum_{n_2}\sin^2 n_2k + |K|^2\sum_{n_2}(1-\sin^2 n_2k)\right] &= 1, \\ R^2\left[\sum_{n=1}^{2N}\sin^2 nk + |K|^2\sum_{n=1}^{N}1 - (1+|K|^2)\sum_{n_2}\sin^2 n_2k\right] &= 1. \end{aligned} \tag{I.4}$$

Since (Jolley 1961)

$$\sum_{n=1}^{2N}\sin^2 nk = N - \frac{\cos(2N+1)k\sin 2Nk}{2\sin k}, \tag{I.5}$$

(I.4) becomes

$$\begin{aligned} R^2\Bigg\{N - \frac{\cos(2N+1)k\sin 2Nk}{2\sin k} + N|K|^2 \\ - (1+|K|^2)\left[\frac{N}{2} - \frac{\cos 2(N+1)k\sin 2Nk}{2\sin 2k}\right]\Bigg\} &= 1, \\ R^2\Bigg[\frac{N}{2}(1+|K|^2) - \frac{\cos(2N+1)k\sin 2Nk}{2\sin k} \\ + (1+|K|^2)\frac{\cos 2(N+1)k\sin 2Nk}{2\sin 2k}\Bigg] &= 1. \end{aligned} \tag{I.6}$$

For (4.111), we can write (I.6) as

$$R^2\Bigg\{\frac{N}{2}(1+|K|^2)-\frac{\cos j\pi\sin[2Nj\pi/(2N+1)]}{2\sin[j\pi/2(2N+1)]} + (1+|K|^2)\frac{\cos[2(N+1)j\pi/(2N+1)]\sin[2Nj\pi/(2N+1)]}{2\sin[2j\pi/(2N+1)]}\Bigg\}=1,$$

$$R^2\Bigg\{\frac{N}{2}(1+|K|^2)-\frac{(-1)^j\sin[j\pi-j\pi/(2N+1)]}{2\sin[j\pi/(2N+1)]} + (1+|K|^2)\frac{\cos[j\pi+j\pi/(2N+1)]\sin[2Nj\pi/(2N+1)]}{2\sin[2j\pi/(2N+1)]}\Bigg\}=1,$$

which reduces to

$$R^2\Bigg\{\frac{N}{2}(1+|K|^2)+\frac{1}{2} + (1+|K|^2)(-1)^j\frac{\cos[j\pi/(2N+1)]\sin[j\pi-j\pi/(2N+1)]}{2\sin[2j\pi/(2N+1)]}\Bigg\}=1,$$

or

$$R^2\left[\frac{1}{2}N(1+|K|^2)+\frac{1}{2}-\frac{1}{4}(1+|K|^2)\right]=1,$$

whence, we find that

$$R=2\left[(1+|K|^2)(2N-1)+2\right]^{-1/2}. \tag{I.7}$$

For a *monatomic* substrate, $|K|=1$, so

$$R=N^{-1/2}, \tag{I.8}$$

as expected.

J. Green Function of Infinite Monatomic Chain

In this appendix, we rewrite the elements of the infinite GF (G_0) of the monatomic crystal in a more detailed form than Ueba (1980). It follows immediately from (2.49) and (2.37) that

$$G^c_{\ell_1-\ell_2}\equiv G_0(\ell_1,\ell_2)=t^{|\ell_1-\ell_2|}G_0(0,0). \tag{J.1}$$

Moreover, from (2.43) comes

$$G_0^c \equiv G_0(0,0) = \beta^{-1}(t_2 - t_1)^{-1} = t/\beta(1-t^2), \tag{J.2}$$

where t is chosen according to (2.40), so that $|t| < 1$. To see which specific sign is required, we must look at the different energy regions separately. To be specific, we assume that $\beta > 0$.

(i) If $E > \alpha + 2\beta$, then $X > 1$, so we see that $|t| < 1$ requires that

$$t = X - (X^2 - 1)^{1/2}, \quad \text{for} \quad X > 1. \tag{J.3}$$

(ii) Similarly, if $E > \alpha - 2\beta$, then $X < -1$, and the condition $|t| < 1$ implies that

$$t = X + (X^2 - 1)^{1/2}, \quad \text{for} \quad X < -1. \tag{J.4}$$

(iii) Inside the band, where $|X| < 1$, we take

$$X = \frac{E - \alpha}{2\beta} \to \frac{E + is - \alpha}{2\beta} = X + i\hat{s}, \tag{J.5}$$

where

$$\hat{s} = \frac{s}{2\beta} = 0^+. \tag{J.6}$$

Thus,

$$X^2 \to (X + i\hat{s})^2 \approx X^2 + 2iX\hat{s}, \quad \text{to} \quad \mathrm{O}(\hat{s}), \tag{J.7}$$

and, hence,

$$(1 - X^2)^{1/2} \to (1 - X^2 - 2iX\hat{s})^{1/2} \approx (1 - X^2)^{1/2} - i\hat{s}X(1 - X^2)^{-1/2}, \tag{J.8}$$

on performing a binomial expansion to $\mathrm{O}(\hat{s})$. Now set

$$t = X + \sigma i(1 - X^2)^{1/2}, \tag{J.9}$$

with $\sigma = \pm 1$, so that $|t| < 1$. To determine the correct value of σ, we insert (J.8) in (J.9), and obtain

$$t \approx \left[X + \sigma\hat{s}X(1 - X^2)^{-1/2}\right] + i[\sigma(1 - X^2)^{1/2} + \hat{s}]. \tag{J.10}$$

From (J.10) comes

$$|t|^2 \approx \left[X + \sigma\hat{s}X(1-X^2)^{-1/2}\right]^2 + [\sigma(1-X^2)^{1/2} + \hat{s}]^2$$
$$\approx 1 + 2\sigma\hat{s}(1-X^2)^{-1/2} + \mathrm{O}(\hat{s}^2), \tag{J.11}$$

which reveals that $|t|^2 < 1$ (and, hence, $|t| < 1$) only if $\sigma = -1$. Thus,

$$t = X - i(1-X^2)^{1/2}, \quad \text{for} \quad |X| < 1. \tag{J.12}$$

For $\beta < 0$, it is straightforward to show that the sign of t in (J.3) and (J.4) is unchanged, while it switches to "+" in (J.12).

If, in general, we write

$$t = X + \sigma(X^2-1)^{1/2}, \tag{J.13}$$

with $\sigma = \pm 1$ according to (J.3), (J.4) or (J.12) as appropriate, then

$$t^{-1} = X - \sigma(X^2-1)^{1/2}, \tag{J.14}$$

and we can recast (J.2) in the form

$$G_0(0,0) = \left[-2\beta\sigma(X^2-1)^{1/2}\right]^{-1}. \tag{J.15}$$

K. Green Function of Infinite Semiconductor

In contrast to the concise account of Bose and Foo (1974), here, a detailed derivation is provided of the matrix elements of the Greenian for an infinite semiconductor, modelled as a 1-dimensional chain, with s-orbitals on the (even) A sites and p-orbitals on the (odd) B sites (see Fig. K.1). The site energies on the even (odd) sites are taken to be $\alpha_A(\alpha_B)$ and the bond energies to be $\pm\beta_2$, resulting in a Hamiltonian of the form

$$H = \sum_k \alpha_A |2k\rangle\langle 2k| + \sum_k \alpha_B |2k+1\rangle\langle 2k+1|$$
$$+ \sum_k \beta_2 \left(|2k\rangle\langle 2k-1| + |2k-1\rangle\langle 2k|\right)$$
$$- \sum_k \beta_2 \left(|2k\rangle\langle 2k+1| + |2k+1\rangle\langle 2k|\right). \tag{K.1}$$

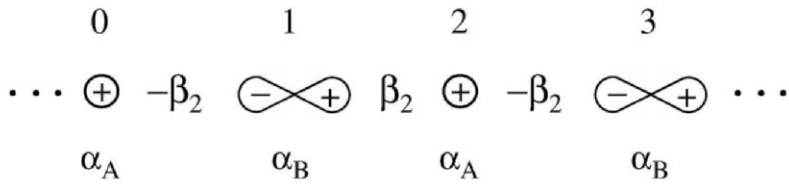

Fig. K.1. Infinite 1-dimensional chain of alternating s- and p-orbitals, with site energies α_A and α_B, respectively, and bond energies $\pm\beta_2$. Reprinted with permission from Bose and Foo (1974). Copyright 1974 by the American Physical Society.

Consequently, the Greenian matrix equation is

$$\sum_{\ell}(E\delta_{i\ell} - H_{i\ell})G(\ell, j) = \delta_{ij}, \tag{K.2}$$

where

$$H_{i\ell} = \begin{cases} \alpha_A, & \ell = i \quad \text{even}, \\ \alpha_B, & \ell = i \quad \text{odd}, \\ \beta_2, & \ell = i+1,\ i \quad \text{odd; or} \quad \ell = i-1,\ i \quad \text{even}, \\ -\beta_2, & \ell = i+1,\ i \quad \text{even; or} \quad \ell = i-1,\ i \quad \text{odd}. \end{cases} \tag{K.3}$$

Putting $i = j = 2k$ in (K.2) gives

$$(E - \alpha_A)G(2k, 2k) + \beta_2\,[G(2k+1, 2k) - G(2k-1, 2k)] = 1, \tag{K.4}$$

while $i = j = 2k - 1$ yields

$$(E-\alpha_B)G(2k-1, 2k-1)+\beta_2\,[G(2k-2, 2k-1) - G(2k, 2k-1)] = 1. \tag{K.5}$$

Also, $i = j - 1 = 2k$ provides

$$(E - \alpha_A)G(2k, 2k+1) + \beta_2\,[G(2k+1, 2k+1) - G(2k-1, 2k+1)] = 0, \tag{K.6}$$

and $i = j + 1 = 2k$ gives

$$(E - \alpha_A)G(2k, 2k-1) + \beta_2\,[G(2k+1, 2k-1) - G(2k-1, 2k-1)] = 0. \tag{K.7}$$

Similarly, $i = j - 1 = 2k - 1$ results in

$$(E - \alpha_B)G(2k-1, 2k) + \beta_2 \left[G(2k-2, 2k) - G(2k, 2k)\right] = 0, \tag{K.8}$$

and $i = j + 1 = 2k - 1$ produces

$$(E-\alpha_B)G(2k-1, 2k-2)+\beta_2 \left[G(2k-2, 2k-2) - G(2k, 2k-2)\right] = 0. \tag{K.9}$$

From translational symmetry and reflectional anti-symmetry considerations, we obtain the relationships:

$$\begin{aligned} G(2k, 2k) &= G(2k-2, 2k-2), \\ G(2k+1, 2k+1) &= G(2k-1, 2k-1), \\ G(m, m+1) &= G(m+1, m), \\ G(m, m+1) &= -G(m, m-1), \\ G(m-1, m) &= -G(m, m+1), \\ G(m-2, m) &= G(m, m+2) = G(m+2, m), \end{aligned} \tag{K.10}$$

with m either even or odd. In particular, we see that

$$G(2k+1, 2k) = -G(2k-1, 2k) = G(2k-2, 2k-1),$$

so (K.4) and (K.5) lead to

$$G(2k-1, 2k-1) = \frac{E - \alpha_A}{E - \alpha_B} G(2k, 2k). \tag{K.11}$$

Inserting (K.8) and (K.9) in (K.4), and using (K.10), we obtain

$$(E - \alpha_A)(E - \alpha_B)G(2k, 2k) + 2\beta_2^2 \left[G(2k-2, 2k) - G(2k, 2k)\right] = E - \alpha_B. \tag{K.12}$$

We now assume (and verify below) that there exists a relationship of the form

$$G(2k-2, 2k) = zG(2k, 2k) \tag{K.13}$$

for some z (presumably a function of energy E). Equation (K.13) in (K.12) yields

$$G(2k, 2k)\left[(E - \alpha_A)(E - \alpha_B) + 2\beta_2^2(z-1)\right] = E - \alpha_B. \tag{K.14}$$

Likewise, (K.6) and (K.7) in (K.5) gives

$$(E-\alpha_B)G(2k-1,2k-1) + \frac{2\beta_2^2}{E-\alpha_A}\left[G(2k+1,2k-1)-G(2k-1,2k-1)\right]=1. \quad \text{(K.15)}$$

Following (K.13), we have

$$G(2k+1,2k-1)=zG(2k-1,2k-1), \quad \text{(K.16)}$$

so that (K.15) becomes

$$G(2k-1,2k-1)\left[(E-\alpha_A)(E-\alpha_B)+2\beta_2^2(z-1)\right]=E-\alpha_A. \quad \text{(K.17)}$$

We note that (K.14) and (K.17) together are consistent with (K.11). Using (K.16) and (K.13) in (K.7) and (K.8), respectively, gives

$$(E-\alpha_A)G(2k,2k-1)+\beta_2 G(2k-1,2k-1)(z-1)=0 \quad \text{(K.18a)}$$

and

$$(E-\alpha_B)G(2k-1,2k)+\beta_2 G(2k,2k)(z-1)=0, \quad \text{(K.18b)}$$

which are seen to be equivalent from (K.10) and (K.11).

Putting $i=j-2=2k$ in (K.2) yields

$$(E-\alpha_A)G(2k,2k+2)+\beta_2\left[G(2k+1,2k+2)-G(2k-1,2k+2)\right]=0, \quad \text{(K.19)}$$

which, by (K.10), (K.13) and (K.16), results in

$$(E-\alpha_A)zG(2k,2k)+\beta_2(1-z)G(2k-1,2k)=0. \quad \text{(K.20)}$$

By eliminating $G(2k-1,2k)$ from (K.18b) and (K.20), we arrive at

$$-\frac{\beta_2 G(2k,2k)(z-1)}{E-\alpha_B}=\frac{(E-\alpha_A)zG(2k,2k)}{\beta_2(z-1)},$$

which on rearranging becomes

$$\beta_2^2(z-1)^2=-(E-\alpha_A)(E-\alpha_B)z,$$

or

$$z^2-pz+1=0, \quad \text{(K.21)}$$

where

$$p = 2 - \frac{(E-\alpha_A)(E-\alpha_B)}{\beta_2^2}. \tag{K.22}$$

Equation (K.21) is the condition determining possible values of z, in order that the assumptions (K.13) and (K.16) be consistent. Solving (K.21) leads to two possible values of z, namely,

$$z_\pm = \frac{1}{2}\left(p \pm \sqrt{p^2-4}\right), \tag{K.23}$$

which are real or complex, depending on the value of p and, hence, on the energy. We explore later which solution of (K.23) is the correct one in each energy region. But, for now, we note that, when $|p| > 2$, z is real, and consequently all the GFs are real, indicating that this regime corresponds to regions outside the energy bands. Conversely, for $|p| < 2$, z is complex and the GFs are also complex, so these energies lie inside the bands.

The forms of the various GFs can now be determined. Equation (K.14) with (K.22) and (K.23) gives

$$G(2k,2k) = (E-\alpha_B)\big/\beta_2^2(2z_\pm - p) \tag{K.24a}$$

$$= (E-\alpha_B)\big/\beta_2^2\left(\pm\sqrt{p^2-4}\right). \tag{K.24b}$$

Similarly, from (K.17), or more directly from (K.11), comes

$$G(2k-1,2k-1) = (E-\alpha_A)\big/\beta_2^2(2z_\pm - p) \tag{K.25a}$$

$$= (E-\alpha_A)\big/\beta_2^2\left(\pm\sqrt{p^2-4}\right). \tag{K.25b}$$

With the aid of (K.11), equation (K.18a) yields

$$G(2k,2k-1) = \beta_2(1-z_\pm)G(2k-1,2k-1)\big/(E-\alpha_A), \tag{K.26a}$$

$$= \beta_2(1-z_\pm)G(2k,2k)\big/(E-\alpha_B). \tag{K.26b}$$

All other GFs can be found easily using (K.10), (K.13) and (K.16). The forms (5.11) and (5.12) take $2k-1 \to n$.

Returning to the question of the correct sign of z in (K.23), we first, concentrate on the regions outside the energy bands, where (as previously pointed out) $|p| > 2$ and z is real. The correct value of z in (K.23) is the one such that $|z| < 1$, which is a requirement to guarantee that GFs of the

form $G(n, n \pm m)$ remain bounded, for large m, under repeated application of (K.13) or (K.16). Substituting (K.22) in (K.23), we examine

$$\begin{aligned} |z_{\pm}| &= \frac{1}{2}\left|p \pm \sqrt{p^2-4}\right| \\ &= \left|1 - \frac{(E-\alpha_A)(E-\alpha_B)}{2\beta_2^2}\right. \\ &\quad \left. \pm \frac{|(E-\alpha_A)(E-\alpha_B)|}{2\beta_2^2}\left[1 - \frac{4\beta_2^2}{(E-\alpha_A)(E-\alpha_B)}\right]^{1/2}\right|. \end{aligned} \tag{K.27}$$

(i) Above or below bands

Here, $|E|$ is large enough, so that either $E > \alpha_{A,B}$ or $E < \alpha_{A,B}$, and we are in the regime where $p < -2$, whence,

$$1 - \frac{(E-\alpha_A)(E-\alpha_B)}{2\beta_2^2} < -1,$$

and

$$\frac{(E-\alpha_A)(E-\alpha_B)}{2\beta_2^2} > 0.$$

Hence,

$$\begin{aligned} &1 - \frac{(E-\alpha_A)(E-\alpha_B)}{2\beta_2^2} \\ &\quad - \frac{(E-\alpha_A)(E-\alpha_B)}{2\beta_2^2}\left[1 - \frac{4\beta_2^2}{(E-\alpha_A)(E-\alpha_B)}\right]^{1/2} < -1. \end{aligned} \tag{K.28}$$

Thus, referring to (K.27) and (K.28), we see that $|z_-| > 1$, so we conclude that $|z_+| < 1$, since $z_+ z_- = 1$. Consequently, in this case,

$$z = z_+ = \frac{1}{2}\left(p + \sqrt{p^2-4}\right) \tag{K.29}$$

is the required solution to (K.21).

(ii) In band gap

The energy E now lies between the band-gap edges α_A and α_B, so that

$$\frac{(E-\alpha_A)(E-\alpha_B)}{2\beta_2^2} < 0,$$

and $p > 2$. We therefore have

$$1 - \frac{(E-\alpha_A)(E-\alpha_B)}{2\beta_2^2} + \frac{(E-\alpha_A)(E-\alpha_B)}{2\beta_2^2}\left[1 - \frac{4\beta_2^2}{(E-\alpha_A)(E-\alpha_B)}\right]^{1/2} > 1. \tag{K.30}$$

Equations (K.27) and (K.30) show that $|z_+| > 1$ and, hence, $|z_-| < 1$, giving us

$$z = z_- = \frac{1}{2}\left(p - \sqrt{p^2-4}\right), \tag{K.31}$$

as the required solution of (K.21) in this situation.

(iii) Inside bands

For energies lying within the bands, we have $p^2 - 4 < 0$, so the complex solutions for z in (K.23) take the form

$$z = \frac{1}{2}\left(p \pm i\sqrt{4-p^2}\right), \tag{K.32}$$

where the sign of the radical must be chosen so as to give a positive DOS. From (K.24b) and (K.25b), these are

$$\rho_{2k}(E) = \pm\frac{E-\alpha_B}{\pi\beta_2^2\sqrt{4-p^2}}, \tag{K.33}$$

and

$$\rho_{2k-1}(E) = \pm\frac{E-\alpha_A}{\pi\beta_2^2\sqrt{4-p^2}}. \tag{K.34}$$

The band-gap edges are at α_A and α_B, which implies that the DOS's in (K.33) and (K.34) are positive for $E > \alpha_{A,B}(E < \alpha_{A,B})$, i.e., in the upper (lower) band, where the sign is chosen to be $+(-)$, i.e., solution $z_+(z_-)$ is chosen in (K.23).

L. Alternate Expression for ΔE

The expression (4.101) is sometimes difficult to work with in practice, specifically, with regard to the integrated term. An alternate expression, which may be easier to implement, utilizes the change in DOS wrought by chemisorption. Its derivation is presented here.

The change in one-electron energy (including that on the adatom) produced by chemisorption is (c.f. (4.86))

$$\begin{aligned}\Delta E^{\sigma} &= \sum_{m} \varepsilon_m - \sum_{k'} \varepsilon_{k'}, \quad k' \in \{k, a\} \\ &= \sum_{m} \int_{-\infty}^{\varepsilon_f'} E\delta(E - \varepsilon_m)dE - \sum_{k'} \int_{-\infty}^{\varepsilon_f} E\delta(E - \varepsilon_{k'})dE \end{aligned} \tag{L.1}$$

using the definition of the Dirac δ-function, and taking $\varepsilon_f(\varepsilon_f')$ to be the FL of the pre-(post-) chemisorption system. The total DOS's for the system, before and after chemisorption, are defined as

$$\rho_0(E) = \sum_{k'} \delta(E - \varepsilon_{k'}), \quad \rho(E) = \sum_{m} \delta(E - \varepsilon_m), \tag{L.2}$$

respectively. Conservation of the number of electrons implies that

$$\int_{-\infty}^{\varepsilon_f'} \rho(E)dE = \int_{-\infty}^{\varepsilon_f} \rho_0(E)dE. \tag{L.3}$$

Using (L.2) and (L.3) in (L.1) gives

$$\begin{aligned}\Delta E^{\sigma} &= \int_{-\infty}^{\varepsilon_f'} E\rho(E)dE - \int_{-\infty}^{\varepsilon_f} E\rho_0(E)dE \\ &\qquad - \varepsilon_f \left[\int_{-\infty}^{\varepsilon_f'} \rho(E)dE - \int_{-\infty}^{\varepsilon_f} \rho_0(E)dE \right] \\ &= \int_{\varepsilon_f}^{\varepsilon_f'} (E - \varepsilon_f)\rho(E)dE + \int_{-\infty}^{\varepsilon_f} (E - \varepsilon_f)\rho(E)dE \\ &\qquad - \int_{-\infty}^{\varepsilon_f} (E - \varepsilon_f)\rho_0(E)dE \\ &\approx \int_{-\infty}^{\varepsilon_f} (E - \varepsilon_f)\Delta\rho(E)dE, \end{aligned} \tag{L.4}$$

where $\Delta\rho = \rho - \rho_0$ is the change in total DOS upon chemisorption, and $\varepsilon_f', \varepsilon_f$ are assumed close enough so that the integral with those limits can be neglected. Hence, the total chemisorption energy can be written as (c.f. (4.85))

$$\Delta E = \sum_\sigma \Delta E^\sigma - U\langle n_{a+}\rangle\langle n_{a-}\rangle + \varepsilon_a - \varepsilon_f. \tag{L.5}$$

The Fermi energy ε_f (adatom energy ε_a) appears negatively (positively) in (L.5), because it is counted twice in the first term of (L.5), via (L.1).

M. Analytic Green Function for Electrified Atomic Chain

An alternative *analytic* form of the chain GF can be found from (7.35), which with (7.41) and (7.42) can be written as (Davison et al 1997)

$$G_{1,m}(1,1) = \frac{1}{E-\alpha-\Gamma} - \frac{\beta^2}{E-\alpha-2\Gamma} - \cdots - \frac{\beta^2}{E-\alpha-m\Gamma}. \tag{M.1}$$

Dividing the top and bottom of each term in the CF by β leads to

$$G_{1,m}(1,1) = \beta^{-1}\left(\frac{1}{Z_1} - \frac{1}{Z_2} - \cdots - \frac{1}{Z_m}\right), \tag{M.2}$$

where

$$Z_n = 2(X - nF) = (E - \alpha - n\Gamma)/\beta. \tag{M.3}$$

In CF notation,

$$-\beta G_{1,m}(1,1) = \underset{n=1}{\overset{m}{\mathcal{K}}}(a_n; b_n), \tag{M.4}$$

where

$$a_n = -1, \quad b_n = Z_n. \tag{M.5}$$

For each $n = 1, \ldots, m$, we define

$$S_n(w) = \frac{a_1}{b_1} + \frac{a_2}{b_2} + \cdots + \frac{a_{n-1}}{b_{n-1}} + \frac{a_n}{b_n + w}, \tag{M.6}$$

and note that $S_m(0)$ is just the required quantity (M.4). Moreover, we have

$$S_1(w) = \frac{a_1}{b_1 + w}, \tag{M.7}$$

as well as the recursion relation

$$S_n(w) = S_{n-1}\left(\frac{a_n}{b_n + w}\right). \tag{M.8}$$

By (M.3), the TB difference equation (7.15a), i.e.,

$$(\alpha + n\Gamma - E)c_n + \beta(c_{n+1} + c_{n-1}) = 0, \tag{M.9}$$

can be rewritten as

$$Z_n c_n = c_{n+1} + c_{n-1},$$

or as

$$c_{n+1} = b_n c_n + a_n c_{n-1}, \tag{M.10}$$

via (M.5). This recursion relation motivates similar definitions for a pair of useful sequences, viz.,

$$A_n = b_n A_{n-1} + a_n A_{n-2} \quad \text{with} \quad A_{-1} = 1, A_0 = 0, \tag{M.11}$$

and

$$B_n = b_n B_{n-1} + a_n B_{n-2} \quad \text{with} \quad B_{-1} = 0,\ B_0 = 1, \tag{M.12}$$

from which we see that

$$A_1 = a_1, \quad B_1 = b_1. \tag{M.13}$$

Equations (M.12) to (M.13) show that

$$\frac{A_1 + A_0 w}{B_1 + B_0 w} = \frac{a_1}{b_1 + w} = S_1(w), \tag{M.14}$$

by reference to (M.7). We can now prove a more general relationship by induction, for suppose we have

$$\frac{A_{n-1} + A_{n-2} w}{B_{n-1} + B_{n-2} w} = S_{n-1}(w), \quad \text{for some} \quad n \geq 1, \tag{M.15}$$

then

$$\begin{aligned}
\frac{A_n + A_{n-1}w}{B_n + B_{n-1}w} &= \frac{(b_n A_{n-1} + a_n A_{n-2}) + A_{n-1}w}{(b_n B_{n-1} + a_n B_{n-2}) + B_{n-1}w} \qquad \text{by (M.11) and (M.12)} \\
&= \frac{(b_n + w)A_{n-1} + A_{n-2}a_n}{(b_n + w)B_{n-1} + B_{n-2}a_n} \\
&= \frac{A_{n-1} + A_{n-2}\frac{a_n}{b_n+w}}{B_{n-1} + B_{n-2}\frac{a_n}{b_n+w}} \\
&= S_{n-1}\left(\frac{a_n}{b_n + w}\right) \qquad \text{via (M.15)} \\
&= S_n(w) \qquad \text{using (M.8).}
\end{aligned} \tag{M.16}$$

From (M.14) and (M.16), we conclude that

$$S_n(w) = \frac{A_n + A_{n-1}w}{B_n + B_{n-1}w} \quad \forall\, n \geq 1. \tag{M.17}$$

For (M.10) to (M.12) to be expressed in the form of the BF relation (Abramowitz and Stegun 1972), viz.,

$$\mathcal{C}_{\mu-1}(x) + \mathcal{C}_{\mu+1}(x) = \frac{2\mu}{x}\mathcal{C}_\mu(x), \tag{M.18}$$

in which

$$\frac{2\mu}{x} = Z_{n+1} = 2[X - (n+1)F], \tag{M.19}$$

and $\mathcal{C}$ denotes the BF J or Y of integer order, requires

$$xF = -1, \tag{M.20}$$

and

$$xX = \nu = \text{integer}, \tag{M.21}$$

so that (M.19) reads

$$\mu = \nu + n + 1. \tag{M.22}$$

Thus, both A_n and B_n can be written as linear combinations of BFs, i.e.,

$$\begin{aligned}
A_n &= \alpha_1 J_{\nu+n+1} + \alpha_2 Y_{\nu+n+1}, \\
B_n &= \beta_1 J_{\nu+n+1} + \beta_2 Y_{\nu+n+1}.
\end{aligned} \tag{M.23}$$

Inserting (M.23) in the initial conditions (M.11), we find

$$\begin{aligned} A_0 &= \alpha_1 J_{\nu+1} + \alpha_2 Y_{\nu+1} = 0 \to \alpha_2 = -\alpha_1 \frac{J_{\nu+1}}{Y_{\nu+1}}, \\ A_{-1} &= \alpha_1 J_\nu + \alpha_2 Y_\nu = 1 \to Y_{\nu+1} = \alpha_1 (J_\nu Y_{\nu+1} - J_{\nu+1} Y_\nu). \end{aligned} \tag{M.24}$$

Because the BFs J_ν and Y_ν are linearly independent, the Wronskian

$$W = J_\nu Y_{\nu+1} - J_{\nu+1} Y_\nu \neq 0, \tag{M.25}$$

whence,

$$\alpha_1 = Y_{\nu+1}/W, \quad \alpha_2 = -J_{\nu+1}/W. \tag{M.26}$$

Similarly, (M.23) in the initial conditions (M.12) produces

$$\begin{aligned} B_{-1} &= \beta_1 J_\nu + \beta_2 Y_\nu = 0 \to \beta_2 = -\beta_1 \frac{J_\nu}{Y_\nu}, \\ B_0 &= \beta_1 J_{\nu+1} + \beta_2 Y_{\nu+1} = 1 \to Y_\nu = -\beta_1 W, \end{aligned} \tag{M.27}$$

which by (M.25) gives

$$\beta_1 = -Y_\nu/W, \quad \beta_2 = J_\nu/W. \tag{M.28}$$

The required quantity

$$S_m(0) = \frac{A_m}{B_m}, \tag{M.29}$$

in (M.17), is obtained via (M.23), (M.26) and (M.28). Hence, with the aid of (M.4), we have

$$\begin{aligned} G_{1,m}(1,1) &= -\beta^{-1} S_m(0) \\ &= \beta^{-1} \frac{J_{\nu+m+1}(x) Y_{\nu+1}(x) - J_{\nu+1}(x) Y_{\nu+m+1}(x)}{J_{\nu+m+1}(x) Y_\nu(x) - J_\nu(x) Y_{\nu+m+1}(x)}. \end{aligned} \tag{M.30}$$

Bibliography

All that mankind has done, thought, gained, or been, it is all lying in magic preservation in the pages of books.

— Thomas Carlyle

Abramowitz, A. and Stegun, I.A. (eds.) (1972), *Handbook of Mathematical Functions*, U.S. Department of Commerce, Washington, D.C.

Anderson, P.W. (1961), Phys. Rev. **124**, 41.

Bagchi, A. and Cohen, M.H. (1974), Phys. Rev. B **9**, 4103; **13**, 5351.

Baldock, G.R. (1952), Proc. Cambridge Phil. Soc., **48**, 457.

Baldock, G.R. (1953), Proc. Phys. Soc. **A66**, 2.

Bell, B. and Madhukar, A. (1976), Phys. Rev. B. **14**, 4281.

Bloch, F. (1928), Z. Physik **52**, 555.

Bose, S.M. and Foo, E.N. (1974), Phys. Rev. B. **10**, 3534.

Burke, N.R. (1976), Surf. Sci. **58**, 349.

Cannell, D.M. (1993), *George Green, Mathematician and Physicist 1793-1841*, Athlone Press, London.

Clark, A. (1974), *The Chemisorption Bond*, Academic Press, New York.

Cong, S.L. (1994), Surf. Sci. **320**, 55.

Coulson, C.A. (1961), *Valence*, Oxford University Press, London.

Davison, S.G. (1969), in *Physical Chemistry*, (eds. H. Eyring, D.J. Henderson and W. Jost), Vol. III, Academic Press, New York.

Davison, S.G. and Levine, J.D. (1970), in *Solid State Physics*, (eds. H. Ehrenreich, F. Seitz and D. Turnbull), Vol. 25, Academic Press, New York. Russian translation by A.Y. Belenky (ed. D.A. Kirzhnits) Mir, Moscow, 1973, in commemoration of Igor Tamm's death in 1971.

Davison, S.G. and Huang, Y.S. (1974), Solid State Comm. **15**, 863.

Davison, S.G., Bose, S.M. and Sulston, K.W. (1988), Surf. Sci. **200**, 265.

Davison, S.G. and Stęślicka, M. (1996), *Basic Theory of Surface States*, Clarendon Press, Oxford.

Davison, S.G., English, R.A., Mišković, Z.L., Goodman, F.O., Amos, A.T. and Burrows, B.L. (1997), J. Phys.: Cond. Matt. **9**, 6371.

Davison, S.G., Sulston, K.W., Mišković, Z.L. and Goodman, F.O. (2001), Prog. Surf. Sci. **67**, 259.

Davydov, A.S. (1991), *Quantum Mechanics*, Pergamon, Oxford.

Day, M.C. and Selbin, J. (1962), *Theoretical Inorganic Chemistry*, Reinhold, New York.

Desjonquères, M.C. and Spanjaard, D. (1993), *Concepts in Surface Physics*, Springer-Verlag, Berlin.

Dirac, P.A.M. (1958), *The Principles of Quantum Mechanics*, Oxford University Press, London.

Dreysée, H., Tomansek, D. and Bennemann, K.H. (1986), Surf. Sci. **173**, 538.

Ducastelle, F., Legrand, B. and Treglia, G. (1990), Prog. Theo. Phys. Suppl. **101**, 159.

Dyson, F.J. (1949), Phys. Rev. **75**, 1736.

Dyson, F.J. (1993), Physics World **5**, No. 8, 33.

Edwards, D.M. and Newns, D.M. (1967), Phys. Lett. A. **24**, 236.

Ehrenreich, H. and Schwartz, L.M. (1976), in *Solid State Physics*, (eds. H. Ehrenreich, F. Seitz and D. Turnbull), Vol. 31, Academic Press, New York.

Einstein, T.L. and Schrieffer, J.R. (1973), Phys. Rev. B **7**, 3629.

Einstein, T.L. (1977), Phys. Rev. B **16**, 3411.

Einstein, T.L. (1978), Surf. Sci. **75**, L161.

Einstein, T.L. (1996), in *Handbook of Surface Science*, Vol. 1 (ed. W.N. Unertl), Ch. 11.

Engel, T. and Gomer, R. (1970), J. Chem. Phys. **52**, 1832.

English, R.A. (1997), Ph.D. Thesis, University of Waterloo.

English, R.A., Davison, S.G., Mišković, Z.L., Goodman, F.O., Amos, A.T. and Burrows, B.L. (1997), Prog. Surf. Sci. **54**, 241.

English, R.A. and Davison, S.G. (1998), Surf. Sci. **397**, 251.

Faulkner, J.S. (1982), Prog. Mat. Sci. **27**, 1.

Foo, E.N., Amar, H. and Ausloss, M. (1971), Phys. Rev. B **4**, 3350.

Foo, E.N. and Davison, S.G. (1976), Surf. Sci. **55**, 274.

Friedel, J. (1958), Nuovo Cimento Suppl. [10], **7**, 287.

Gobeli, G.W. and Allen, F.G. (1966), in *Semiconductors and Semimetals*, (eds. R.F. Willardson and A.C. Beer), Vol. 2, p. 275, Academic Press, New York.

Gomer, R. and Schrieffer, J.R. (1971), Surf. Sci. **25**, 315.

Gonis, A., Stocks, G.M., Butler, W.H. and Winter, H. (1984), Phys. Rev. B **29**, 555.

Gonis, A. (1992), *Green Functions for Ordered and Disordered Systems*, North Holland, Amsterdam.

Goodman, F.O. (1994), private communication.

Goodwin, E.T. (1939a), Proc. Cambridge Phil. Soc. **35**, 474.

Goodwin, E.T. (1939b), Proc. Cambridge Phil. Soc. **35**, 221.

Gradshteyn, I.S. and Ryzhik, I.M. (1980), *Table of Integrals, Series, and Products*, Academic Press, San Diego.

Grimley, T.B. (1958), Proc. Phys. Soc. **72**, 103.

Grimley, T.B. (1960), Adv. Catalysis **12**, 1.

Grimley, T.B. (1967a), Proc. Phys. Soc. **90**, 751.

Grimley, T.B. (1967b), Proc. Phys. Soc. **92**, 776.

Grimley, T.B. (1970), J. Phys. C **3**, 1934.

Grimley, T.B. (1975), Prog. Surf. Memb. Sci. **9**, 71.

Grimley, T.B. (1983), in *The Chemical Physics of Solid Surfaces and Heterogeneous Catalysis*, (eds. D.A. King and D.P. Woodroff), Vol. 2, Chap. 5, North Holland, Amsterdam.

Grimley, T.B. and Torrini, M. (1973), J. Phys. C **6**, 868.

Grimley, T.B. and Walker, S.M. (1969), Surf. Sci. **14**, 395.

Gumhalter, B. and Brenig, W. (1995a), Prog. Surf. Sci. **48**, 39.

Gumhalter, B. and Brenig, W. (1995b), Surf. Sci. **336**, 326.

Gumhalter, B, Milun, M. and Wandelt, K. (1990), *Selected Studies of Adsorption on Metal and Semiconductor Surfaces*, Forschungszentrum Jülich GmBH.

Haberlandt, H. and Ritschl, F. (1983), J. Phys. Chem. **87**, 3244.

Hacker, K. and Obermair, G. (1970), Z. Phys. **234**, 1.

Haken, H. (1976), *Quantum Field Theory of Solids*, North Holland, Amsterdam.

Hao, Y.G. and Cooper, B.R. (1994), Surf. Sci. **312**, 250.

Haydock, R. (1980), in *Solid State Physics*, (eds. H. Ehrenreich, F. Seitz and D. Turnbull), Vol. 35, Academic Press, New York.

Heinrichs, J. and Jones, R.O. (1972), J. Phys. C **5**, 2149.

Hilsum, C. (1966), in *Semiconductors and Semimetals*, (eds. R.F. Willardson and A.C. Beer), Vol. 6, p. 6, Academic Press, New York.

Houston, W.V. (1940), Phys. Rev. **57**, 184.

James, H.M. (1949), Phys. Rev. **76**, 1611.

Jolley, L.B.W. (1961), *Summation of Series*, Dover, New York, p. 82.

Kalkenstein, D. and Soven, P. (1971), Surf. Sci. **26**, 85.

Katsura, S., Hatta, T. and Morita, A. (1950), Sci. Rep. Tôhuku Imp. Univ. **35**, 19.

Kelley, M.J. and Ponec, V. (1981), Prog. Surf. Sci. **11**, 139.

Kittel, C. (1986), *Introduction to Solid State Physics*, Wiley, New York.

Kohn, W. (1999), Rev. Mod. Phys. **71**, S59.

Korringa, J. (1958), J. Phys. Chem. Solids **7**, 252.

Koss, R.W. and Lambert, L.M. (1972), Phys. Rev. B. **5**, 147.

Koutecký, J. (1956), Z. Elektrochem. **60**, 835.

Koutecký, J. (1957), Phys. Rev. **108**, 13.

Koutecký, J. (1958), Trans. Faraday Soc. **54**, 1038.

Koutecký, J. (1965), Adv. Chem. Phys. **9**, 85.

Koutecký, J. (1976), Prog. Surf. Memb. Sci. **11**, 1.

Kranz, H. (1978), Ph.D. Thesis, University of Toronto.

Kumar, V., Anderson, O.K. and Mookerjee, A. (eds.) (1992), *Methods of Electronic Structure Calculations*, World Scientific, Singapore.

Lau, K.H. and Kohn, W. (1978), Surf. Sci. **75**, 69.

LeBossé, J.C., Lopez, J. and Rousseau-Violet, J. (1978), Surf. Sci. **72**, 125.

LeBossé, J.C., Lopez, J. and Rousseau-Violet, J. (1979), Surf. Sci. **81**, L329.

LeBossé, J.C., Lopez, J. and Rousseau-Violet, J. (1980), J. Phys. C **13**, 1139.

Lennard-Jones, J.E. (1937), Proc. Roy. Soc. A **163**, 101.

Liu, W.K. and Davison, S.G. (1988), Theo. Chim. Acta **74**, 251.

Long, D. (1968), *Energy Bands in Semiconductors*, Interscience, New York, p. 111.

Lorentzen, L. and Waadeland, H. (1992), *Continued Fractions with Applications*, North Holland, Amsterdam.

Löwdin, P.-O. (1962), J. Math. Phys. **3**, 969.

March, N.H., Young, W.H. and Sampanthar, S. (1967), *The Many-Body Problem in Quantum Mechanics*, Cambridge University Press, Cambridge.

Marsden, J.E. (1973), *Basic Complex Analysis*, Freeman, San Francisco.

Mathews, J. and Walker, R.L. (1965), *Mathematical Methods of Physics*, Benjamin, New York.

Merrick, M.L. Luo, W., and Fichthorn, K.A. (2003), Prog. Surf. Sci. **72**, 117.

Merzbacher, E. (1970), *Quantum Mechanics*, Wiley, New York.

Modrak, P. (1995), Prog. Surf. Sci. **49**, 227.

Modrak, P. (1997), Surf. Sci. **380**, L491.

Moran-Lopez, J.L., Kerker, G. and Bennemann, K.H. (1975), Surf. Sci. **57**, 540.

Muda, Y. and Hanawa, T. (1974), Japan J. Appl. Phys. Suppl. **2**, Pt. 2, 867.

Muscat, J.P. and Newns, D.M. (1978), Prog. Surf. Sci. **9**, 1.

Newns, D.M. (1967), Ph.D. Thesis, University of London.

Newns, D.M. (1969), Phys. Rev. **178**, 1123.

Newns, D.M. (1974), private communication.

Nordheim, L. (1931), Ann. Phys. (Leipzig) [5] **9**, 607, 641.

Nordlander, P. Holloway, S. and Norskov, J.K. (1984), Surf. Sci. **136**, 59.

Ohanian, H.C. (1990), *Principles of Quantum Mechanics*, Prentice-Hall, Englewood Cliffs, New Jersey.

Ouannasser, S. Wille, L.T. and Dreyssé, H. (1997), Phys. Rev. B. **55**, 14245.

Parent, L.G. Ueba, H. and Davison, S.G. (1980), Phys. Lett. A. **78**, 474.

Paulson, R.H. and Schrieffer, J.R. (1975), Surf. Sci. **48**, 329.

Pendry, J.B., Prêtre, A., Rous, P.J. and Martin-Moreno, L. (1991), Surf. Sci. **244**, 160.

Rabinovitch, A. (1970), Phys. Lett. A. **33**, 403.

Rabinovitch, A. (1971), Phys. Rev. B. **4**, 1017.

Raimes, S. (1972), *Many-Electron Theory*, North Holland, Amsterdam.

Ruckenstein, E. and Huang, Y.S. (1973), J. Catalysis **30**, 309.

Salem, L. (1966), *The Molecular Orbital Theory of Conjugated Systems*, Benjamin, New York.

Schönhammer, K. Hartung, V. and Brenig, W. (1975), Z. Phys. B. **22**, 143.

Schranz, D.W. (1994), Ph.D. Thesis, University of Waterloo.

Schranz, D.W. and Davison, S.G. (1998), Int. J. Quantum Chem. **67**, 377.

Schranz, D.W. and Davison, S.G. (2000), J. Mol. Struct. (Theo. Chem.) **501-502**, 465.

Slater, J.C. (1949), Phys. Rev. **76**, 1592.

Smith, J.R. (ed.) (1980), *Theory of Chemisorption*, Springer-Verlag, Berlin.

Soven, P. (1967), Phys. Rev. **156**, 809.

Sulston, K.W. (1986), Ph.D. Thesis, University of Waterloo.

Sulston, K.W., Davison, S.G. and Liu, W.K. (1986), Phys. Rev. B **33**, 2263.

Sulston, K.W. and Bose, S.M. (1988), Phys. Rev. B **38**, 1784.

Sun, Q., Xie, J.J. and Zhang, T. (1994a), Phys. Stat. Sol. (b) **185**, 373.

Sun, Q., Xie, J.J. and Zhang, T. (1994b), Solid State Comm. **91**, 691.

Taylor, D.W. (1967), Phys. Rev. **156**, 809.

Taylor, P.L. (1970), *A Quantum Approach to the Solid State*, Prentice-Hall, Englewood Cliffs, New Jersey.

Turek, I., Drchal, V., Kudrnovsky, J., Sob, M. and Weinberger, P. (1996), *Electronic Structure of Disordered Alloys, Surfaces and Interfaces*, Kluwer, Boston.

Ueba, H. (1980), Phys. Stat. Sol. (b) **99**, 763.

Ueba, H. and Ichimura, S. (1979a), J. Chem. Phys. **70**, 1745.

Ueba, H. and Ichimura, S. (1979b), Phys. Stat. Sol. (b) **92**, 307.

Van Santen, R.A. (1975), Surf. Sci. **53**, 35.

Van Santen, R.A. and Sachtler, W.M.H. (1977), Surf. Sci. **63**, 358.

Van Santen, R.A. (1982), Recueil **101-4**, 121.

Velický, B., Kirkpatrick, S. and Ehrenreich, H. (1968), Phys. Rev. **175**, 747.

Wannier, G. (1960), Phys. Rev. **117**, 432.

Wedler, G. (1976), *Chemisorption: An Experimental Approach*, Butterworths, London.

Whittaker, E.T. and Watson, G.N. (1965), *A Course of Modern Analysis*, Cambridge University Press, London, p. 119.

Xie, J.J., Zhang, T. and Lu, W.C. (1992), Solid State Comm. **82**, 467.

Yao, D. and Shi, J. (2000), Am. J. Phys. **68**, 278.

Yonezawa, F. (1982), in *The Structure and Property of Matter*, (ed. T. Matsubara), Springer-Verlag, New York.

Zak, J. (1967), Phys. Rev. Lett. **19**, 1385.

Zak, J. (1968), Phys. Rev. **168**, 686.

Zak, J. (1968) Phys. Rev. Lett. **20**, 1477.

Zak, J. (1969), Phys. Rev. **181**, 1366.

Zener, C. (1934), Proc. Roy. Soc. (Lond.) **145**, 523.

Zhang, T. and Wei, S.Y. (1991), Appl. Surf. Sci. **48-49**, 139.

Zhang, H. (1992a), Surf. Sci. **269-70**, 331.

Zhang, H. (1992b), J. Phys.: Cond. Matt. **4**, L529.

Ziman, J.M. (1965), *Principles of the Theory of Solids*, Cambridge University Press, Cambridge.

Author Index

Subject Index